6. CRITICALITY EVALUATION[1]

This section describes the criticality safety evaluation of the Y-12 National Security Complex (Y-12) Model ES-3100 package with highly enriched uranium (HEU) metal, or HEU oxide, or highly enriched uranyl nitrate crystals (UNX). HEU metal may be solid shapes (cylinders, bars, buttons, slugs, unirradiated TRIGA fuel) or broken metal pieces of unspecified geometric shapes. Physical testing of Type-B fissile material packages for surface transportation conducted in accordance with the physical testing requirements of 10 CFR 71 is limited to the ES-3100 packaging and non-fissile dummy contents. Consequently, analytic methods are used to demonstrate compliance of the ES-3100 package with the applicable performance requirements in 10 CFR 71. The specific requirements investigated for compliance in this evaluation are contained in 10 CFR 71.55, "General Requirements of all Fissile Material Packages," and 10 CFR 71.59, "Standards for Arrays of Fissile Material Packages." Physical testing of Type-B fissile material packages transported by air is not conducted for the ES-3100. Analytic methods are also used to demonstrate compliance of the ES-3100 package with the requirements of 10 CFR 71.55(f). This is accomplished by demonstrating compliance of the package with the more stringent requirements of the International Atomic Energy Agency (IAEA) for situations where the conditions of the fissile material package following the tests cannot be demonstrated. (TS-G-1.1, Sect. 680.2)

6.1 DESCRIPTION OF THE CRITICALITY DESIGN

6.1.1 Design Features

The principal design feature of interest in the criticality evaluation of the Model ES-3100 package is the containment/outer drum system (Drawing No. M2E801580A031, Appendix 1.4.8). The ES-3100 package uses a single containment system (Drawing No. M2E801580A011, Appendix 1.4.8) to contain the HEU contents. The containment is a high-integrity, watertight, post-load leak-testable, stainless-steel vessel (Fig. 1.2). The outer drum system (Drawing M2E801580A001, Appendix 1.4.8) is a recessed, double-compartment body with a removable top for insertion and removal of the containment vessel. The body weldment liner outer cavity and the top plug weldment contain Kaolite 1600™ (Kaolite), a thermal insulation material that protects the containment vessel from thermal absorption, shock and impact. The body weldment liner inner cavity contains a neutron poison, "277-4," which serves as a strong neutron absorber. Other sections of this report (Sects. 2, 3, and 4) demonstrate the integrity of the ES-3100 package [i.e., that this single containment vessel remains intact and watertight under the Normal Conditions of Transport (NCT) and Hypothetical Accident Conditions (HAC)].

Three 4.25-in.-diam × 10.0-in.-tall or six 4.25-in.-diam × 4.88-in.-tall convenience cans separated by can pads can be placed inside the 31-in.-tall cavity of the ES-3100 containment vessel (Fig. 1.4) Other can arrangements fit inside the containment vessel, such as three 4.25-in.-diam × 8.75-in.-tall or five 4.25-in.-diam × 4.88-in.-tall convenience cans. Both of these can arrangements include can pads and 277-4 canned spacers with overall dimensions of 4.25-in. diam × 1.82-in. height. (Drawing M2E801580A026, Appendix 1.4.8) For configurations with three Teflon or three polyethylene bottles, ~5.0 in. in diameter, the 277-4 canned spacers are not used.

Credit is not taken in this criticality analysis for fissile material spacing provided by the presence of the convenience cans or bottles inside the containment vessel. These containers are not manufactured to the *ASME Boiler and Pressure Vessel Code*, Sect. III, Subsection NG, or better.

---

[1] The calculations in this chapter have been updated. Calculational changes are not highlighted. The updated fissile loadings in Table 6.2a are highlighted.

6.1.2 Summary of the Criticality Evaluation

Testing conducted in accordance with the physical testing requirements of 10 CFR 71 demonstrated that water leakage into the containment is not a credible event under the NCT and HAC. However, credit for the high-integrity, watertight containment is not taken in this criticality evaluation, as agreed upon during discussions held at public meetings at the U.S. Nuclear Regulatory Commission. (Docket 71-9315)

10 CFR 71.55(b) requires the evaluation of water leakage into the containment vessel or leakage of liquid contents out of the containment vessel and of other conditions that produce maximum reactivity in the single package. For solid uranium contents, water leakage conditions are simulated by flooding all regions outside and inside of the containment vessel, including the sealed convenience cans. For liquid uranium contents, water leakage conditions are simulated by flooding all regions outside the containment vessel except the containment vessel well. Uranyl nitrate (UN) solution resides inside both the containment vessel well and the containment vessel, including the sealed convenience cans. For this evaluation, a flooded containment vessel under full water reflection is also analyzed. Under such leakage conditions, the calculated neutron multiplication factor ($k_{eff}+2\sigma$) for the ES-3100 package with HEU contents is lower than the upper subcritical limit (USL) for a subcritical system. Water inleakage into the containment vessel or liquid content leakage out of the containment vessel will not produce a criticality in the containment vessel of a disassembled package or an assembled single package. Therefore, the Model ES-3100 shipping package complies with all of the requirements of 10 CFR 71.55(b, d).

Credit for the high-integrity, watertight containment is not taken either in the single package analysis [10 CFR 71.55(d, e)] or in the array analysis [10 CFR 71.59(a)(1)] of undamaged packages. In the evaluation of undamaged packages under 10 CFR 71.59(a)(1) and the evaluation of damaged packages under 10 CFR 71.59(a)(2), the containment vessel is flooded with water, providing moderation to such an extent as to cause maximum reactivity of the content consistent with the chemical and physical form of the material present. Solid HEU, not solution HEU, is being shipped in the ES-3100. Consequently, in the evaluation of damaged packages under 10 CFR 71.59(a)(2), the leakage out of the containment vessel of content moderated to such an extent as to cause maximum reactivity consistent with the physical and chemical form of material is not considered credible HAC, based on results for tests specified in 10 CFR 71.73. Because credit for the high-integrity, watertight containment is not fully taken in this criticality evaluation, the fissile material mass loading limits are very conservative.

Containment vessel flooding is assumed in the criticality calculations performed for the derivation of fissile material loading limits. Even though both the NCT tests under 10 CFR 71.71 and the HAC tests under 10 CFR 71.73 demonstrate that containment is not breached, simulation of this condition in the criticality calculations produces package configurations that are more reactive than the actual package configurations. The 7.1–10.1 kg quantities of evaluation water required in both the NCT and HAC criticality calculations bound reasonable amounts of hydrogenous material and inherent moisture of fissile material (primarily HEU oxides) present inside the containment vessel. Thus, an administrative criticality control is not needed to restrict the amount of hydrogenous material normally present inside the containment vessel and other sources of moisture present in the fissile content. Nevertheless, anticipated amounts of hydrogenous materials are not expected to exceed 2,400 g. These materials include: can pads, polyethylene bags, vinyl tape; and polyethylene or Teflon bottles if used; and moisture in oxide contents.

Under NCT and HAC, three parameters that affect criticality and may vary during transport of the Model ES-3100 package are the number of packages transported, the amount of water present in the package, and the volatile (organic material) contents of the package. The number of packages transported is limited by the criticality safety index (CSI) established by this criticality evaluation. Both the amount of water present in the package and the volatile (organic material) contents of the package are parameters for the

following reasons. First, volatile materials can be driven off at the high temperatures of HAC. Second, the inherent water content of the Kaolite in NCT and the water absorption by the Kaolite in HAC are unknowns. These parameters determine a variety of competing effects that govern the fission process, including, but not limited to, mass, moderation, absorption, and reflection. To ensure that all effects are adequately included in this criticality evaluation, the range of these parameters is evaluated.

It is possible for accidents to be significantly more severe in the air transport mode than in the surface transport mode. Thus, the performance requirements for packages designed to be transported by air are more stringent. These requirements address separate aspects of the accident assessment and apply only to the criticality evaluation of an individual package under isolation. (TS-G-1.1) For a fissile material package designed to be transported by air, 10 CFR 71.55(f) requires that the criticality evaluation demonstrate that the package be subcritical assuming reflection by 20 cm (7.9 in.) of water but no water inleakage when subjected to the sequential application of the HAC free drop and crush tests of 10 CFR 71.73(c)(1 and 2) and the modified puncture and thermal tests of 10 CFR 71.55(f)(1)(iii and iv).

The ES-3100 package was not subjected to physical testing of Type-B fissile material packages transported by air. Instead, analytic methods are used to demonstrate compliance of the ES-3100 package with the requirements of 10 CFR 71.55(f). This is accomplished by demonstrating compliance of the package with the more stringent requirements imposed by the IAEA for situations where the conditions of the fissile material package following the tests cannot be demonstrated. (TS-G-1.1, Sect. 680.2) Section 680.2 of TS-G-1.1 states that worst-case assumptions regarding the geometric arrangement of the package and contents should be made in the criticality evaluation taking into account all moderating and structural components of the packaging. The assumptions should be in conformity with the potential worst-case effects of the mechanical and thermal tests, and all package orientations should be considered for the analysis. Subcriticality must be demonstrated after due consideration of such aspects as the efficiency of the moderator, loss of neutron absorbers, rearrangement of packaging components and contents, geometry changes, and temperature effects. Given that the requirements of 10 CFR 71.55(f) mirror the IAEA requirements of TS-R-1, Sect. 680, for Type B(U) fissile material packages, this approach is considered an acceptable one.

The following criticality safety evaluation shows that the Model ES-3100 package with designated content satisfies the requirements of 10 CFR 71.55 and 71.59 for surface transport, and of 10 CFR 71.55(f) for air transport. Designated contents are solid HEU metal shapes (cylinders, bars, buttons, billets, slugs, unirradiated TRIGA fuel); HEU broken metal contents of unspecified geometric shapes; HEU products or skull oxides; or UNX crystals. HEU skull oxides are distinguished from product oxides (UO_2, U_3O_8, or UO_3) as being a reside of graphite and oxidized uranium (U_3O_8) recovered in the casting process. Tables 6.1a–6.1e pertain to surface-only modes of transportation. These tables summarize the results of the evaluation for solid HEU metal shapes (Tables 6.1a and 6.1b), for HEU broken metal (Table 6.1c), for HEU product or skull oxide (Table 6.1d), and for UNX crystals or un-irradiated TRIGA fuel elements (Table 6.1e). In Table 6.1c, the fissile or the uranium masses for broken metal listed in the content headings indicate the evaluation limits of the criticality calculations. As determined by the NCT and HAC array analyses, mass loading limits may be further reduced to coincide with fissile material loadings at or below the subcritical safety limit. These reduced loading limits are identified in the "CSI" rows in bold type. Table 6.2a pertains to surface-only transport mode while Table 6.2b pertains to air-transport. The loading limit for packages under mixed-mode transportation is taken as the most restrictive limit for either mode, surface or air transport.

The criticality evaluation demonstrates that the ES-3100 packaging with the HEU content satisfies the requirements for single packages and for arrays of fissile material packages when the packages are load-limited as specified in Tables 6.2a and 6.2b (reproduced in Table 1.3) under the conditions identified in Sect. 6.2.4.

6.1.3 Criticality Safety Index

A CSI is assigned to the Model ES-3100 package on the basis of an adequate margin of subcriticality for the single package and arrays of packages for both NCT and HAC. Values for the CSI given in Tables 6.2a and 6.2b (Table 1.3) are based on the uranium and the ^{235}U mass of the content and on the presence of 277-4 canned spacers as defined in Sect. 6.2.2.

The CSI is determined from bounding calculations using KENO V.a models of the containment vessel, the single package, and arrays of packages. (SCALE, Vol. 2, Sect. F11) It is a dimensionless number used to limit the number of packages in a conveyance for nuclear criticality safety control. The CSI is the larger of the CSI values for NCT and for HAC. For NCT, the CSI is equal to 50 divided by the allowable number of packages "N" that can be shipped, where the allowable number of packages is one-fifth of the maximum array size that is calculated to be subcritical. For HAC, the CSI is equal to 50 divided by the allowable number of packages "N" that can be shipped, where the allowable number of packages is one-half of the maximum array size that is calculated to be subcritical. The CSI is a calculated number rounded up to the nearest first decimal.

The array sizes examined in this evaluation are infinite, 13×13×6, 9×9×4, 7×7×3, 5×5×2, explicit triangular pack (ETP) 27×3 for NCT, ETP 16×3 for HAC, and the degenerate single unit. For NCT, the "N" and corresponding CSI values for arrays determined to be adequately subcritical are as follows: N = ∞, CSI = 0; N = 202, CSI = 0.3; N = 64, CSI = 0.8; N = 29, CSI = 1.8; N = 10, CSI = 5.0; and N = 16, CSI = 3.2. For HAC, the "N" and corresponding CSI values for arrays determined to be adequately subcritical are as follows: N = ∞, CSI = 0; N = 507, CSI = 0.1; N =162, CSI = 0.4; N = 73, CSI = 0.7; N = 25, CSI = 2.0; and N = 24, CSI = 2.1. Absent an exact correspondence of CSI values for the NCT and HAC, the following arrays results were selected for rounded CSI values as indicated in Tables 6.1a–6.1d:

- infinite arrays evaluated for both NCT and HAC [designated as "(1,2)"], where N(1,2) = ∞ for a CSI = 0;
- 13×13×6 evaluated for NCT and 9×9×4 evaluated for HAC where N(1,2) = (202,162) for a CSI = 0.4;
- 9×9×4 evaluated for NCT and 7×7×3 evaluated for HAC where N(1,2) = (64,74) for a CSI = 0.8;
- 7×7×3 evaluated for NCT and 5×5×2 evaluated for HAC where N(1,2) = (29,25) for a CSI = 2.0; and
- 27×3 evaluated for NCT and 16×3 evaluated for HAC where N(1,2) = (16,24) for a CSI = 3.2.

Table 6.1a. Summary of criticality evaluation for solid HEU metal cylinders and bars

Conditions	cylinders (d ≤ 3.24 in.) no can spacers	cylinders (d ≤ 3.24 in.) with can spacers	square bars (l,w ≤ 2.29 in.) no can spacers	cylinders (3.24 < d ≤ 4.25 in.) no can spacers	cylinders (3.24 < d ≤ 4.25 in.) with can spacers
General requirements for each fissile package (§71.55)					
"A package used for shipment of fissile material must be so designed and constructed and its contents so limited that it would be subcritical if water were to leak into the containment system, . . . so that under the following conditions, maximum reactivity of the fissile material would be attained:" (Paragraph "b")	$k_{eff} + 2\sigma \leq 0.9228$ cvcrcyt11_21_1	$k_{eff} + 2\sigma \leq 0.8866$ cvcrcyt11_36_2	$k_{eff} + 2\sigma \leq 0.8787$ cvcrsqt11_36_1	$k_{eff} + 2\sigma \leq 0.9215$ cvcrcyct11_17_1	$k_{eff} + 2\sigma \leq 0.9202$ cvcrcyct11_32_2
(1) the most reactive credible configuration consistent with the chemical and physical form of the material,	3 stacked cylinders (d = 3.24 in.) 1 cylinder per convenience can, no can spacers, 21,000g ^{235}U	3 stacked cylinders (d = 3.24 in.) 1 cylinder per convenience can, with can spacers, 36,000g ^{235}U	3 stacked bars (l,w = 2.29 in.) 1 bar per convenience can, no can spacers, 36,000g ^{235}U	3 stacked cylinders (d = 4.25 in.) 1 cylinder per convenience can, no can spacers, 17,000g ^{235}U	3 stacked cylinders (d = 4.25 in.) 1 cylinder per convenience can, with can spacers, 32,000g ^{235}U
(2) moderation by water to the most reactive credible extent,	flooding of the containment vessel	same	same	same	same
(3) close full reflection of the containment system by water on all sides, or such greater reflection of the containment system as may be provided by the surrounding material of the packaging.	30.48 cm H_2O surrounding the containment vessel	same	same	same	same

Table 6.1a. Summary of criticality evaluation for solid HEU metal cylinders and bars

Conditions	*cylinders* (d ≤ 3.24 in.) no can spacers	*cylinders* (d ≤ 3.24 in.) with can spacers	*square bars* (l,w ≤ 2.29 in.) no can spacers	*cylinders* (3.24 < d ≤ 4.25 in.) no can spacers	*cylinders* (3.24 < d ≤ 4.25 in.) with can spacers
"A package used for shipment of fissile material must be so designed and constructed and its contents so limited under the tests specified in §71.71 (Normal Conditions of Transport) . . ." (Paragraph "d")					
(1) the contents would be subcritical,	$k_{eff} + 2\sigma \leq 0.9035$ ncsrcyt11_21_1_15	$k_{eff} + 2\sigma \leq 0.8731$ ncsrcyt11_36_2_15	$k_{eff} + 2\sigma \leq 0.8652$ ncsrsqt11_36_1_15	$k_{eff} + 2\sigma \leq 0.8941$ ncsrcyct11_17_1_15	$k_{eff} + 2\sigma \leq 0.8946$ ncsrcyct11_32_2_15
(2) the geometric form of the package contents would not be substantially altered,	3 stacked cylinders (d = 3.24 in.) 1 cylinder per convenience can, no can spacers, 21,000g ^{235}U	3 stacked cylinders (d = 3.24 in.) 1 cylinder per convenience can, with can spacers, 36,000g ^{235}U	3 stacked bars (l,w = 2.29 in.) 1 bar per convenience can, no can spacers, 36,000g ^{235}U	3 stacked cylinders (d = 4.25 in.) 1 cylinder per convenience can, no can spacers, 17,000g ^{235}U	3 stacked cylinders (d = 4.25 in.) 1 cylinder per convenience can, with can spacers, 32,000g ^{235}U
(3) there would be no leakage of water into the containment system unless, in the evaluation of undamaged packages under §71.59(a)(1), it has been assumed that moderation is present to such an extent as to cause maximum reactivity consistent with the chemical and physical form of the material,	moderation is present to such an extent as to cause maximum reactivity	same	same	same	same
(4) there will be no substantial reduction in the effectiveness of the packaging	30.48 cm H_2O surrounding the drum (d=18.37 in., h=43.5 in.)	same	same	same	same

Table 6.1a. Summary of criticality evaluation for solid HEU metal cylinders and bars

Conditions	cylinders (d ≤ 3.24 in.) no can spacers	cylinders (d ≤ 3.24 in.) with can spacers	square bars (l,w ≤ 2.29 in.) no can spacers	cylinders (3.24 < d ≤ 4.25 in.) no can spacers	cylinders (3.24 < d ≤ 4.25 in.) with can spacers
"A package used for shipment of fissile material must be so designed and constructed and its contents so limited that under the tests specified in §71.73 (Hypothetical Accident Conditions) the package would be subcritical. For this determination, it must be assumed that:" (Paragraph "e")	$k_{eff} + 2\sigma \leq 0.9044$ hcsrcyt12_21_1_15	$k_{eff} + 2\sigma \leq 0.8734$ hcsrcyt12_36_2_15	$k_{eff} + 2\sigma \leq 0.8642$ hcsrsqt12_36_1_15	$k_{eff} + 2\sigma \leq 0.8979$ hcsrcyct12_17_1_15	$k_{eff} + 2\sigma \leq 0.8977$ hcsrcyct12_32_2_15
(1) the fissile material is in the most reactive credible configuration consistent with the chemical and physical form of the contents,	3 stacked cylinders (d = 3.24 in.) 1 cylinder per convenience can, no can spacers, 21,000g ^{235}U	3 stacked cylinders (d = 3.24 in.) 1 cylinder per convenience can, with can spacers, 36,000g ^{235}U	3 stacked bars (l,w = 2.29 in.) 1 bar per convenience can, no can spacers, 36,000g ^{235}U	3 stacked cylinders (d = 4.25 in.) 1 cylinder per convenience can, no can spacers, 17,000g ^{235}U	3 stacked cylinders (d = 4.25 in.) 1 cylinder per convenience can, with can spacers, 32,000g ^{235}U
(2) water moderation occurs to the most reactive credible extent consistent with the chemical and physical form of content,	flooding of the package	same	same	same	same
(3) there is full reflection by water on all sides, as close as is consistent with the damage condition of the package.	30.48 cm H_2O surrounding the reduced diameter drum (d=17.20 in., h=43.5 in.)	same	same	same	same

Table 6.1a. Summary of criticality evaluation for solid HEU metal cylinders and bars

Conditions	cylinders ($d \le 3.24$ in.) no can spacers	cylinders ($d \le 3.24$ in.) with can spacers	square bars ($l,w \le 2.29$ in.) no can spacers	cylinders ($3.24 < d \le 4.25$ in.) no can spacers	cylinders ($3.24 < d \le 4.25$ in.) with can spacers
Standards for arrays of fissile material packages (§71.59)					
". . . the designer of a fissile material package shall derive a number "N" based on all the following conditions being satisfied, assuming packages are stacked together in any arrangement and with close reflection on all sides of the stack by water:" (Paragraph "a")					
Transport index based on nuclear criticality control, CSI = 0.0	**load-limited to 18,000g ^{235}U no can spacers**	**load-limited to 30,000g ^{235}U can spacers**	**load-limited to 30,000g ^{235}U no can spacers**	**load-limited to 15,000g ^{235}U no can spacers**	**load-limited to 25,000g ^{235}U can spacers**
(1) five times "N" undamaged packages with nothing between the packages would be subcritical,	$k_{eff} + 2\sigma \le 0.9237$ nciacyt11_18_1_3	$k_{eff} + 2\sigma \le 0.9195$ nciacyt11_30_2_3	$k_{eff} + 2\sigma \le 0.9219$ nciasqt11_30_1_3	$k_{eff} + 2\sigma \le 0.8992$ nciacyct11_15_1_3	$k_{eff} + 2\sigma \le 0.9147$ nciacyct11_25_2_3
(2) two times "N" damaged packages, if each package were subject to the tests specified in §71.73 (Hypothetical Accident Conditions) would be subcritical with optimum interspersed hydrogenous moderation,	$k_{eff} + 2\sigma \le 0.9230$ hciacyt12_18_1_3	$k_{eff} + 2\sigma \le 0.9220$ hciacyt12_30_2_3	$k_{eff} + 2\sigma \le 0.9221$ hciasqt12_30_1_3	$k_{eff} + 2\sigma \le 0.8986$ hciacyct12_15_1_3	$k_{eff} + 2\sigma \le 0.9156$ hciacyct12_25_2_3
(3) the value of "N" not <0.5.	N(1,2) = ∞	same	same	same	same
Transport index based on nuclear criticality control, CSI = 0.4	**load-limited to 18,000g ^{235}U no can spacers**	**load-limited to 30,000g ^{235}U can spacers**	**load-limited to 30,000g ^{235}U can spacers**	**load-limited to 15,000g ^{235}U no can spacers**	**load-limited to 25,000g ^{235}U can spacers**
(1) five times "N" undamaged packages	bounded by CSI=0	same	same	same	same
(2) two times "N" damaged packages, ...	bounded by CSI=0	same	same	same	same
(3) the value of "N"	N(1,2) = 202/162	same	same	same	same

Table 6.1b. Summary of criticality evaluation for solid HEU metal slugs

Conditions	slugs, no can spacers enr. ≤ 100% ≤ 18,287g ^{235}U	slugs with can spacers 80% < enr. ≤ 100% < 36,573g ^{235}U	slugs with can spacers enr. ≤ 80% < 36,573g ^{235}U
General requirements for each fissile package (§71.55)			
"A package used for shipment of fissile material must be so designed and constructed and its contents so limited that it would be subcritical if water were to leak into the containment system, . . . so that under the following conditions, maximum reactivity of the fissile material would be attained:" (Paragraph "b")	$k_{eff} + 2\sigma \leq 0.9089$ cvcr5est11_1_1	$k_{eff} + 2\sigma \leq 0.9041$ cvcr6e4st11_2	
(1) the most reactive credible configuration consistent with the chemical and physical form of the material,	cluster of 5 slugs (d = 1.5625 in., h = 2.0625 in.) per convenience can, no can spacers, 18,286g ^{235}U	cluster of 10 slugs stacked 2 high per convenience can, non-uniform content stacking, can spacers, 36,573g ^{235}U	
(2) moderation by water to the most reactive credible extent,	flooding of the containment vessel	same	
(3) close full reflection of the containment system by water on all sides, or such greater reflection of the containment system as may be provided by the surrounding material of the packaging.	30.48 cm H_2O surrounding the containment vessel	same	
"A package used for shipment of fissile material must be so designed and constructed and its contents so limited under the tests specified in §71.71 (Normal Conditions of Transport) . . ." (Paragraph "d")			
(1) the contents would be subcritical,	$k_{eff} + 2\sigma \leq 0.8704$ ncsr5est11_1_1_15	$k_{eff} + 2\sigma \leq 0.8682$ ncsr5est11_2_2_15	
(2) the geometric form of the package contents would not be substantially altered,	cluster of 5 slugs (d = 1.5625 in., h = 2.0625 in.) per convenience can, no can spacers, 18,286g ^{235}U	cluster of 10 slugs stacked 2 high per convenience can, non-uniform content stacking, can spacers, 36,573g ^{235}U	

Table 6.1b. Summary of criticality evaluation for solid HEU metal slugs

Conditions	slugs, no can spacers enr. ≤ 100% ≤ 18,287g ^{235}U	slugs with can spacers 80% < enr. ≤ 100% < 36,573g ^{235}U	slugs with can spacers enr. ≤ 80% < 36,573g ^{235}U
(3) there would be no leakage of water into the containment system unless, in the evaluation of undamaged packages under §71.59(a)(1), it has been assumed that moderation is present to such an extent as to cause maximum reactivity consistent with the chemical and physical form of the material,	moderation is present to such an extent as to cause maximum reactivity	same	
(4) there will be no substantial reduction in the effectiveness of the packaging	30.48 cm H_2O surrounding the drum (d=18.37 in., h=43.5 in.)	same	
"A package used for shipment of fissile material must be so designed and constructed and its contents so limited that under the tests specified in §71.73 (Hypothetical Accident Conditions) the package would be subcritical. For this determination, it must be assumed that:" (Paragraph "e")	$k_{eff} + 2\sigma \leq 0.8727$ hcsr5est12_1_1_15	$k_{eff} + 2\sigma \leq 0.8713$ hcsr5est12_2_2_15	
(1) the fissile material is in the most reactive credible configuration consistent with the chemical and physical form of the contents,	cluster of 5 slugs (d = 1.5625 in., h = 2.0625 in.) per convenience can, no can spacers, 18,286g ^{235}U	cluster of 10 slugs stacked 2 high per convenience can, non-uniform content stacking, 36,573g ^{235}U	
(2) water moderation occurs to the most reactive credible extent consistent with the chemical and physical form of content,	flooding of the package	same	
(3) there is full reflection by water on all sides, as close as is consistent with the damage condition of the package.	30.48 cm H_2O surrounding the reduced diameter drum (d=17.20 in., h=43.5 in.)	same	

Table 6.1b. Summary of criticality evaluation for solid HEU metal slugs

Conditions	slugs, no can spacers enr. ≤ 100% ≤ 18,287g ^{235}U	slugs with can spacers 80% < enr. ≤ 100% < 36,573g ^{235}U	slugs with can spacers enr. ≤ 80% < 36,573g ^{235}U
Standards for arrays of fissile material packages (§71.59)			
". . . the designer of a fissile material package shall derive a number "N" based on all the following conditions being satisfied, assuming packages are stacked together in any arrangement and with close reflection on all sides of the stack by water: " (Paragraph "a")			
Transport index based on nuclear criticality control, CSI = 0.0	**load-limited to 18,287g ^{235}U no can spacers**	**load-limited to 25,601g ^{235}U can spacers**	**load-limited to 29,333g ^{235}U can spacers**
(1) five times "N" undamaged packages with nothing between the packages would be subcritical,	$k_{eff} + 2\sigma \leq 0.9225$ ncia5est11_1_1_8_3	$k_{eff} + 2\sigma \leq 0.9145$ ncia70st11_2_8_3	$k_{eff} + 2\sigma \leq 0.9093$ ncia5est11_2_2_5_3
(2) two times "N" damaged packages, if each package were subject to the tests specified in §71.73 (Hypothetical Accident Conditions) would be subcritical with optimum interspersed hydrogenous moderation,	$k_{eff} + 2\sigma \leq 0.9238$ hcia5est12_1_1_8_3	$k_{eff} + 2\sigma \leq 0.9133$ hcia70st12_2_8_3	$k_{eff} + 2\sigma \leq 0.9076$ hcia5est12_2_2_5_3
(3) the value of "N" not <0.5.	N(1,2) = ∞	same	same
Transport index based on nuclear criticality control, CSI = 0.4	**load-limited to 18,287g ^{235}U no can spacers**	**load-limited to 25,601g ^{235}U can spacers**	**load-limited to 34,766g ^{235}U can spacers**
(1) five times "N" undamaged packages	bounded by CSI=0	same	$k_{eff} + 2\sigma \leq 0.9208$ ncf15est11_2_2_7_3
(2) two times "N" damaged packages, ...	bounded by CSI=0	same	$k_{eff} + 2\sigma \leq 0.9053$ hcf25est12_2_2_7_3
(3) the value of "N"	N(1,2) = 202/162	same	same

Table 6.1c. Summary of criticality evaluation for solid HEU metal of unspecified geometric shapes characterized as broken metal

Conditions	95% < enr. ≤ 100% ≤ 25,894g ^{235}U	90% < enr. ≤95% ≤ 27,252g ^{235}U	80% < enr. ≤90% ≤ 28,334g ^{235}U	70% < enr. ≤80% ≤ 28,184g ^{235}U	60% < enr. ≤70% ≤ 24,693g ^{235}U	enr. ≤60% ≤ 35,320g Uranium
General requirements for each fissile package (§71.55)						
"A package used for shipment of fissile material must be so designed and constructed and its contents so limited that it would be subcritical if water were to leak into the containment system, . . . so that under the following conditions, maximum reactivity of the fissile material would be attained:" (Paragraph "b")	$k_{eff} + 2\sigma \leq 0.9181$ cvr3lha_26_1_8_15	$k_{eff} + 2\sigma \leq 0.9206$ cvr3lha_29_1_7_15	$k_{eff} + 2\sigma \leq 0.9224$ cvr3lha_32_1_6_15	$k_{eff} + 2\sigma \leq 0.8927$ cvr3lha_36_1_5_15	$k_{eff} + 2\sigma \leq 0.8620$ cvr3lha_36_1_4_15	$k_{eff} + 2\sigma \leq 0.8289$ cvr3lha_36_1_3_15
(1) the most reactive credible configuration consistent with the chemical and physical form of the material,	A mixture of HEU metal and water is homogenized over the internal volume of an assumed content lattice, one per can location. The square footprint of the content lattice is circumscribed by the inner wall of the containment vessel. The amount of water in the flooded containment vessel is calculated on the basis that the convenience can steel is replaced with water. Can pads and spacers not used. See Appendix 6.9.3, Sect. 6.9.3.1, for justification of the content model.					
(2) moderation by water to the most reactive credible extent,	flooding of the containment vessel					
(3) close full reflection of the containment system by water on all sides, or such greater reflection of the containment system as may be provided by the surrounding material of the packaging.	30.48 cm H_2O surrounding the containment vessel					

Table 6.1c. Summary of criticality evaluation for solid HEU metal of unspecified geometric shapes characterized as broken metal

Conditions	95% < enr. ≤ 100% ≤ 25,894g ^{235}U	90% < enr. ≤95% ≤ 27,252g ^{235}U	80% < enr. ≤90% ≤ 28,334g ^{235}U	70% < enr. ≤80% ≤ 28,184g ^{235}U	60% < enr. ≤70% ≤ 24,693g ^{235}U	enr. ≤60% ≤ 35,320g Uranium
"A package used for shipment of fissile material must be so designed and constructed and its contents so limited under the tests specified in §71.71 (Normal Conditions of Transport) . . ." (Paragraph "d")						
(1) the contents would be subcritical,	$k_{eff} + 2\sigma \leq 0.8908$ (ncsrbmt11_36_1_15)					
(2) the geometric form of the package contents would not be substantially altered,	A mixture of HEU metal and water is homogenized over the internal volume of the containment vessel. The amount of water in the flooded containment vessel is calculated on the basis that the convenience can steel is replaced with water. Can pads and spacers not used.					
(3) there would be no leakage of water into the containment system unless, in the evaluation of undamaged packages under §71.59(a)(1), it has been assumed that moderation is present to such an extent as to cause maximum reactivity consistent with the chemical and physical form of the material,	moderation is present to such an extent as to cause maximum reactivity					
(4) there will be no substantial reduction in the effectiveness of the packaging	30.48 cm H_2O surrounding the drum (d = 18.37 in., h = 43.5 in.)					

Table 6.1c. Summary of criticality evaluation for solid HEU metal of unspecified geometric shapes characterized as broken metal

Conditions	95% < enr. ≤ 100% ≤ 25,894g ^{235}U	90% < enr. ≤95% ≤ 27,252g ^{235}U	80% < enr. ≤90% ≤ 28,334g ^{235}U	70% < enr. ≤80% ≤ 28,184g ^{235}U	60% < enr. ≤70% ≤ 24,693g ^{235}U	enr. ≤60% ≤ 35,320g Uranium
"A package used for shipment of fissile material must be so designed and constructed and its contents so limited that under the tests specified in §71.73 (Hypothetical Accident Conditions) the package would be subcritical. For this determination, it must be assumed that:" (Paragraph "e")	$k_{eff} + 2\sigma \leq 0.8912$ (hcsrbmt12_36_1_15)					
(1) the fissile material is in the most reactive credible configuration consistent with the chemical and physical form of the contents,	A mixture of HEU metal and water is homogenized over the internal volume of the containment vessel. The amount of water in the flooded containment vessel is calculated on the basis that the convenience can steel is replaced with water. Can pads and spacers not used.					
(2) water moderation occurs to the most reactive credible extent consistent with the chemical and physical form of content,	flooding of the package					
(3) there is full reflection by water on all sides, as close as is consistent with the damage condition of the package.	30.48 cm H_2O surrounding the reduced diameter drum (d = 17.20 in., h = 43.5 in.)					

Table 6.1c. Summary of criticality evaluation for solid HEU metal of unspecified geometric shapes characterized as broken metal

Conditions	95% < enr. ≤ 100% ≤ 25,894g ^{235}U	90% < enr. ≤95% ≤ 27,252g ^{235}U	80% < enr. ≤90% ≤ 28,334g ^{235}U	70% < enr. ≤80% ≤ 28,184g ^{235}U	60% < enr. ≤70% ≤ 24,693g ^{235}U	enr. ≤60% ≤ 35,320g Uranium
Standards for arrays of fissile material packages (§71.59)						
" . . . the designer of a fissile material package shall derive a number "N" based on all the following conditions being satisfied, assuming packages are stacked together in any arrangement and with close reflection on all sides of the stack by water: " (Paragraph "a")						
Transport index based on nuclear criticality control, CSI = 0.0	**can spacers are required**	**can spacers are required**	**can spacers are required**	**load-limited to 2,967g ^{235}U no can spacers**	**load-limited to 3,249g ^{235}U no can spacers**	**load-limited to 5,577g Uranium no can spacers**
(1) five times "N" undamaged packages with nothing between the packages would be subcritical,	Not applicable	Not applicable	Not applicable	$k_{eff} + 2\sigma \leq 0.9213$ nciabmt11_4_1_5_3	$k_{eff} + 2\sigma \leq 0.9207$ nciabmt11_5_1_4_3	$k_{eff} + 2\sigma \leq 0.9152$ nciabmt11_6_1_3_3
(2) two times "N" damaged packages, if each package were subject to the tests specified in §71.73 (Hypothetical Accident Conditions) would be subcritical with optimum interspersed hydrogenous moderation,	Not applicable	Not applicable	Not applicable	$k_{eff} + 2\sigma \leq 0.9248$ hciabmt12_4_1_5_3	$k_{eff} + 2\sigma \leq 0.9235$ hciabmt12_5_1_4_3	$k_{eff} + 2\sigma \leq 0.9127$ hciabmt12_6_1_3_3
(3) the value of "N" cannot be <0.5.	Not applicable	Not applicable	Not applicable	$N(1,2) = \infty$	same	same

Table 6.1c. Summary of criticality evaluation for solid HEU metal of unspecified geometric shapes characterized as broken metal

Conditions	95% < enr. ≤ 100% ≤ 25,894g ^{235}U	90% < enr. ≤95% ≤ 27,252g ^{235}U	80% < enr. ≤90% ≤ 28,334g ^{235}U	70% < enr. ≤80% ≤ 28,184g ^{235}U	60% < enr. ≤70% ≤ 24,693g ^{235}U	enr. ≤60% ≤ 35,320g Uranium
Transport index based on nuclear criticality control, CSI = 0.0	**load-limited to 2,774g ^{235}U can spacers**	**load-limited to 3,516g ^{235}U can spacers**	**load-limited to 3,333g ^{235}U can spacers**	**load-limited to 4,450g ^{235}U can spacers**	**load-limited to 5,198g ^{235}U can spacers**	**load-limited to 11,154g Uranium can spacers**
(1) five times "N" undamaged packages ...	$k_{eff} + 2\sigma \leq 0.9041$ nciabmt11_3_2_8_3	$k_{eff} + 2\sigma \leq 0.9199$ nciabmt11_4_2_7_3	$k_{eff} + 2\sigma \leq 0.9084$ nciabmt11_4_2_6_3	$k_{eff} + 2\sigma \leq 0.9224$ nciabmt11_6_2_5_3	$k_{eff} + 2\sigma \leq 0.9218$ nciabmt11_8_2_4_3	$k_{eff} + 2\sigma \leq 0.9181$ nciabmt11_12_2_3_3
(2) two times "N" damaged packages, ...	$k_{eff} + 2\sigma \leq 0.9050$ hciabmt12_3_2_8_3	$k_{eff} + 2\sigma \leq 0.9237$ hciabmt12_4_2_7_3	$k_{eff} + 2\sigma \leq 0.9091$ hciabmt12_4_2_6_3	$k_{eff} + 2\sigma \leq 0.9230$ hciabmt12_6_2_5_3	$k_{eff} + 2\sigma \leq 0.9209$ hciabmt12_8_2_4_3	$k_{eff} + 2\sigma \leq 0.9205$ hciabmt12_12_2_3_3
(3) the value of "N" ...	N(1,2) = ∞	same	same	same	same	same
Transport index based on nuclear criticality control, CSI = 0.4	**can spacers are required**	**can spacers are required**	**can spacers are required**	**load-limited to 5,192g ^{235}U no can spacers**	**load-limited to 5,848g ^{235}U no can spacers**	**load-limited to 14,872g Uranium no can spacers**
(1) five times "N" undamaged packages	Not applicable	Not applicable	Not applicable	$k_{eff} + 2\sigma \leq 0.9235$ ncf1bmt11_7_1_5_3	$k_{eff} + 2\sigma \leq 0.9216$ ncf1bmt11_9_1_4_3	$k_{eff} + 2\sigma \leq 0.9225$ ncf1bmt11_15_1_3_3
(2) two times "N" damaged packages, ...	Not applicable	Not applicable	Not applicable	$k_{eff} + 2\sigma \leq 0.9064$ hcf2bmt12_8_1_5_3	$k_{eff} + 2\sigma \leq 0.9118$ hcf2bmt12_12_1_4_3	$k_{eff} + 2\sigma \leq 0.9072$ hcf2bmt12_18_1_3_3
(3) the value of "N" ...	Not applicable	Not applicable	Not applicable	N(1,2) = 202/162	same	same
Transport index based on nuclear criticality control, CSI = 0.4	**load-limited to 5,549g ^{235}U can spacers**	**load-limited to 6,154g ^{235}U can spacers**	**load-limited to 7,500g ^{235}U can spacers**	**load-limited to 8,900g ^{235}U can spacers**	**load-limited to 12,996g ^{235}U can spacers**	**load-limited to 28,813g Uranium can spacers**
(1) five times "N" undamaged packages	$k_{eff} + 2\sigma \leq 0.9241$ ncf1bmt11_6_2_8_3	$k_{eff} + 2\sigma \leq 0.9220$ ncf1bmt11_7_2_7_3	$k_{eff} + 2\sigma \leq 0.9203$ ncf1bmt11_9_2_6_3	$k_{eff} + 2\sigma \leq 0.9187$ ncf1bmt11_12_2_5_3	$k_{eff} + 2\sigma \leq 0.9245$ ncf1bmt11_19_2_4_3	$k_{eff} + 2\sigma \leq 0.9235$ ncf1bmt11_29_2_3_3
(2) two times "N" damaged packages, ...	$k_{eff} + 2\sigma \leq 0.9244$ hcf2bmt12_8_2_8_3	$k_{eff} + 2\sigma \leq 0.9232$ hcf2bmt12_11_2_7_3	$k_{eff} + 2\sigma \leq 0.9192$ hcf2bmt12_12_2_6_3	$k_{eff} + 2\sigma \leq 0.8964$ hcf2bmt12_12_2_5_3	$k_{eff} + 2\sigma \leq 0.9005$ hcf2bmt12_19_2_4_3	$k_{eff} + 2\sigma \leq 0.9112$ hcf2bmt12_36_2_3_3
(3) the value of "N"	N(1,2) = 202/162	same	same	same	same	same

Table 6.1c. Summary of criticality evaluation for solid HEU metal of unspecified geometric shapes characterized as broken metal

Conditions	95% < enr. ≤ 100% ≤ 25,894g ^{235}U	90% < enr. ≤95% ≤ 27,252g ^{235}U	80% < enr. ≤90% ≤ 28,334g ^{235}U	70% < enr. ≤80% ≤ 28,184g ^{235}U	60% < enr. ≤70% ≤ 24,693g ^{235}U	enr. ≤60% ≤ 35,320g Uranium
Transport index based on nuclear criticality control, CSI = 0.8	**can spacers are required**	**can spacers are required**	**can spacers are required**	**load-limited to 8,900g ^{235}U no can spacers**	**load-limited to 13,646g ^{235}U no can spacers**	**load-limited to 28,814g Uranium no can spacers**
(1) five times "N" undamaged packages	Not applicable	Not applicable	Not applicable	$k_{eff} + 2\sigma \le 0.9216$ ncf2bmt11_12_1_5_3	$k_{eff} + 2\sigma \le 0.9234$ ncf2bmt11_20_1_4_3	$k_{eff} + 2\sigma \le 0.9205$ ncf2bmt11_29_1_3_3
(2) two times "N" damaged packages, ...	Not applicable	Not applicable	Not applicable	$k_{eff} + 2\sigma \le 0.9012$ hcf3bmt12_12_1_5_3	$k_{eff} + 2\sigma \le 0.9065$ hcf3bmt12_20_1_4_3	$k_{eff} + 2\sigma \le 0.9022$ hcf3bmt12_29_1_3_3
(3) the value of "N"	Not applicable	Not applicable	Not applicable	same	same	same
Transport index based on nuclear criticality control, CSI = 0.8	**load-limited to 9,248g ^{235}U can spacers**	**load-limited to 10,549g ^{235}U can spacers**	**load-limited to 12,500g ^{235}U can spacers**	**load-limited to 16,317g ^{235}U can spacers**	**load-limited to 20,793g ^{235}U can spacers**	**35,320g Uranium can spacers**
(1) five times "N" undamaged packages	$k_{eff} + 2\sigma \le 0.9233$ ncf2bmt11_10_2_8_3	$k_{eff} + 2\sigma \le 0.9221$ ncf2bmt11_12_2_7_3	$k_{eff} + 2\sigma \le 0.9220$ ncf2bmt11_14_2_6_3	$k_{eff} + 2\sigma \le 0.9193$ ncf2bmt11_21_2_5_3	$k_{eff} + 2\sigma \le 0.9233$ ncf2bmt11_30_2_4_3	$k_{eff} + 2\sigma \le 0.9064$ ncf2bmt11_36_2_3_3
(2) two times "N" damaged packages, ...	$k_{eff} + 2\sigma \le 0.9090$ hcf3bmt12_10_2_8_3	$k_{eff} + 2\sigma \le 0.9005$ hcf3bmt12_12_2_7_3	$k_{eff} + 2\sigma \le 0.9042$ hcf3bmt12_14_2_6_3	$k_{eff} + 2\sigma \le 0.9022$ hcf3bmt12_21_2_5_3	$k_{eff} + 2\sigma \le 0.9019$ hcf3bmt12_30_2_4_3	$k_{eff} + 2\sigma \le 0.8850$ hcf3bmt12_36_2_3_3
(3) the value of "N"	N(1,2) = 64/73	same	same	same	same	same
Transport index based on nuclear criticality control, CSI = 2.0 *	**can spacers are required**	**can spacers are required**	**can spacers are required**	**load-limited to 17,059g ^{235}U no can spacers**	**load-limited to 21,444g ^{235}U no can spacers**	**35,320g Uranium no can spacers**
(1) five times "N" undamaged packages	Not applicable	Not applicable	Not applicable	$k_{eff} + 2\sigma \le 0.9223$ ncf3bmt11_22_1_5_3	$k_{eff} + 2\sigma \le 0.9216$ ncf3bmt11_31_1_4_3	$k_{eff} + 2\sigma \le 0.9045$ ncf3bmt11_36_1_3_3
(2) two times "N" damaged packages, ...	Not applicable	Not applicable	Not applicable	$k_{eff} + 2\sigma \le 0.8852$ hcf4bmt12_22_1_5_3	$k_{eff} + 2\sigma \le 0.8858$ hcf4bmt12_31_1_4_3	$k_{eff} + 2\sigma \le 0.8705$ hcf4bmt12_36_1_3_3
(3) the value of "N"	Not applicable	Not applicable	Not applicable	N(1,2) = 29/25	same	same

Table 6.1c. Summary of criticality evaluation for solid HEU metal of unspecified geometric shapes characterized as broken metal

Conditions	95% < enr. ≤ 100% ≤ 25,894g ^{235}U	90% < enr. ≤95% ≤ 27,252g ^{235}U	80% < enr. ≤90% ≤ 28,334g ^{235}U	70% < enr. ≤80% ≤ 28,184g ^{235}U	60% < enr. ≤70% ≤ 24,693g ^{235}U	enr. ≤60% ≤ 35,320g Uranium
Transport index based on nuclear criticality control, CSI = 2.0 *	**load-limited to 13,872g ^{235}U can spacers**	**load-limited to 18,461g ^{235}U can spacers**	**load-limited to 20,000g ^{235}U can spacers**	**load-limited to 25,218g ^{235}U can spacers**	**24,692g ^{235}U can spacers**	**35,320g Uranium can spacers**
(1) five times "N" undamaged packages	$k_{eff} + 2\sigma \le 0.9204$ ncf3bmt11_14_2_8_3	$k_{eff} + 2\sigma \le 0.9239$ ncf3bmt11_20_2_7_3	$k_{eff} + 2\sigma \le 0.9213$ ncf3bmt11_23_2_6_3	$k_{eff} + 2\sigma \le 0.9216$ ncf3bmt11_32_2_5_3	$k_{eff} + 2\sigma \le 0.9035$ ncf3bmt11_36_2_4_3	$k_{eff} + 2\sigma \le 0.8745$ ncf3bmt11_36_2_3_3
(2) two times "N" damaged packages, ...	$k_{eff} + 2\sigma \le 0.8877$ hcf4bmt12_14_2_8_3	$k_{eff} + 2\sigma \le 0.8914$ hcf4bmt12_20_2_7_3	$k_{eff} + 2\sigma \le 0.8851$ hcf4bmt12_23_2_6_3	$k_{eff} + 2\sigma \le 0.8884$ hcf4bmt12_32_2_5_3	$k_{eff} + 2\sigma \le 0.8684$ hcf4bmt12_36_2_4_3	$k_{eff} + 2\sigma \le 0.8412$ hcf4bmt12_36_2_3_3
(3) the value of "N"	N(1,2) = 29/25	same	same	same	same	same
Transport index based on nuclear criticality control, CSI = 3.2 **	**can spacers are required**	**can spacers are required**	**can spacers are required**	**load-limited to 27,443g ^{235}U no can spacers**	**24,692g ^{235}U no can spacers**	**35,320g Uranium no can spacers**
(1) five times "N" undamaged packages	Not applicable	Not applicable	Not applicable	$k_{eff} + 2\sigma \le 0.9226$ ncf5bmt11_35_1_5_3	$k_{eff} + 2\sigma \le 0.9030$ ncf5bmt11_36_1_4_3	$k_{eff} + 2\sigma \le 0.8743$ ncf5bmt11_36_1_3_3
(2) two times "N" damaged packages, ...	Not applicable	Not applicable	Not applicable	$k_{eff} + 2\sigma \le 0.9052$ hcf5bmt12_35_1_5_3	$k_{eff} + 2\sigma \le 0.8819$ hcf5bmt12_36_1_4_3	$k_{eff} + 2\sigma \le 0.8542$ hcf5bmt12_36_1_3_3
(3) the value of "N"	Not applicable	Not applicable	Not applicable	N(1,2) = 16/24	same	same
Transport index based on nuclear criticality control, CSI = 3.2 **	**load-limited to 24,969g ^{235}U can spacers**	**load-limited to 26,373g ^{235}U can spacers**	**28,334g ^{235}U can spacers**	**28,184g ^{235}U can spacers**	**24,692g ^{235}U can spacers**	**35,320g Uranium can spacers**
(1) five times "N" undamaged packages	$k_{eff} + 2\sigma \le 0.9249$ ncf5bmt11_25_2_8_3	$k_{eff} + 2\sigma \le 0.9196$ ncf5bmt11_28_2_7_3	$k_{eff} + 2\sigma \le 0.9246$ ncf5bmt11_35_2_6_3	$k_{eff} + 2\sigma \le 0.8974$ ncf5bmt11_36_2_5_3	$k_{eff} + 2\sigma \le 0.8736$ ncf5bmt11_36_2_4_3	$k_{eff} + 2\sigma \le 0.8445$ ncf5bmt11_36_2_3_3
(2) two times "N" damaged packages, ...	$k_{eff} + 2\sigma \le 0.9089$ hcf5bmt12_25_2_8_3	$k_{eff} + 2\sigma \le 0.8981$ hcf5bmt12_28_2_7_3	$k_{eff} + 2\sigma \le 0.9032$ hcf5bmt12_35_2_6_3	$k_{eff} + 2\sigma \le 0.8804$ hcf5bmt12_36_2_5_3	$k_{eff} + 2\sigma \le 0.8532$ hcf5bmt12_36_2_4_3	$k_{eff} + 2\sigma \le 0.8265$ hcf5bmt12_36_2_3_3
(3) the value of "N"	N(1,2) = 16/24	same	same	same	same	same

* Neutron multiplication factors and "N" are shown for an NCT array size of 7×7×3 and an HAC array size of 5×5×2; both arrays are nearly cubic arrangements. An HAC array size is not available for CSI=1.8; therefore, CSI for NCT at 1.8 is rounded up to 2.0 as shown.

** Neutron multiplication factors and "N" are shown for an NCT array size of 27×3 and an HAC array size of 16×3; where packages in the planar dimension are in explicit triangular-pitch arrangement and stacked three high in the vertical direction. An NCT array size of 81 packages gives a CSI value of 3.12 (50/16), while an HAC array size of 48 packages gives a CSI value of 2.08 (50/24). The specified CSI value of 3.2 is the larger of the two numbers rounded up to the nearest tenth decimal place as shown.

Table 6.1d. Summary of criticality evaluation for HEU product and skull oxide

Conditions	HEU product oxide ≤ 21,125g ^{235}U	HEU skull oxide ≤ 15,673g ^{235}U and ≤ 921g C
General requirements for each fissile package (§71.55)		
"A package used for shipment of fissile material must be so designed and constructed and its contents so limited that it would be subcritical if water were to leak into the containment system, . . . so that under the following conditions, maximum reactivity of the fissile material would be attained:" (Paragraph "b")	$k_{eff} + 2\sigma \leq 0.8728$ (cvcroxt11_1_24_1)	$k_{eff} + 2\sigma \leq 0.8497$ (cvcrsk3cc_9_15_17)
(1) the most reactive credible configuration consistent with the chemical and physical form of the material,	HEU oxide at the bulk density is assumed dispersed in the containment vessel, where the oxide fills the containment vessel to a height determined by the oxide mass. The oxide is saturated with water. Water fills the void region above the oxide content, but this amount of water is reduced by an amount equivalent to the volume occupied by can spacers. The can pads, spacer can, and convenience can steel are replaced by water. See Appendix 6.9.3, Sect. 6.9.3.1, for justification of the content model.	same
(2) moderation by water to the most reactive credible extent,	flooding of the containment vessel	same
(3) close full reflection of the containment system by water on all sides, or such greater reflection of the containment system as may be provided by the surrounding material of the packaging.	30.48 cm H_2O surrounding the containment vessel	same

Table 6.1d. Summary of criticality evaluation for HEU product and skull oxide

Conditions	HEU product oxide ≤ 21,125g ^{235}U	HEU skull oxide ≤ 15,673g ^{235}U and ≤ 921g C
"A package used for shipment of fissile material must be so designed and constructed and its contents so limited under the tests specified in §71.71 (Normal Conditions of Transport) . . ." (Paragraph "d")		
(1) the contents would be subcritical,	$k_{eff} + 2\sigma \leq 0.7835$ (ncsroxt11_1_24_1_15)	$k_{eff} + 2\sigma \leq 0.7410$ (ncsrsk_9_15)
(2) the geometric form of the package contents would not be substantially altered,	HEU oxide at the bulk density is assumed dispersed in the containment vessel, where the oxide fills the containment vessel to a height determined by the oxide mass. The oxide is saturated with water. Water fills the void region above the oxide content, but this amount of water is reduced by an amount equivalent to the volume occupied by can spacers. The can pads, spacer can, and convenience can steel are replaced by water.	same
(3) there would be no leakage of water into the containment system unless, in the evaluation of undamaged packages under §71.59(a)(1), it has been assumed that moderation is present to such an extent as to cause maximum reactivity consistent with the chemical and physical form of the material,	moderation is present to such an extent as to cause maximum reactivity	same
(4) there will be no substantial reduction in the effectiveness of the packaging	30.48 cm H_2O surrounding the drum (d = 18.37 in., h = 43.5 in.)	same

Table 6.1d. Summary of criticality evaluation for HEU product and skull oxide

Conditions	HEU product oxide ≤ 21,125g ^{235}U	HEU skull oxide ≤ 15,673g ^{235}U and ≤ 921g C
"A package used for shipment of fissile material must be so designed and constructed and its contents so limited that under the tests specified in §71.73 (Hypothetical Accident Conditions) the package would be subcritical. For this determination, it must be assumed that:" (Paragraph "e")	$k_{eff} + 2\sigma \leq 0.7867$ (hcsroxt12_1_24_1_15)	$k_{eff} + 2\sigma \leq 0.7410$ (hcsrsk_9_15)
(1) the fissile material is in the most reactive credible configuration consistent with the chemical and physical form of the contents,	HEU oxide at the bulk density is assumed dispersed in the containment vessel, where the oxide fills the containment vessel to a height determined by the oxide mass. The oxide is saturated with water. Water fills the void region above the oxide content, but this amount of water is reduced by an amount equivalent to the volume occupied by can spacers. The can pads, spacer can, and convenience can steel are replaced by water.	same
(2) water moderation occurs to the most reactive credible extent consistent with the chemical and physical form of content,	flooding of the package	same
(3) there is full reflection by water on all sides, as close as is consistent with the damage condition of the package.	30.48 cm H_2O surrounding the reduced diameter drum, (d = 17.20 in., h = 43.5 in.)	same

Standards for arrays of fissile material packages (§71.59)

Table 6.1d. Summary of criticality evaluation for HEU product and skull oxide

Conditions	HEU product oxide ≤ 21,125g ^{235}U	HEU skull oxide ≤ 15,673g ^{235}U and ≤ 921g C
" . . . the designer of a fissile material package shall derive a number "N" based on all the following conditions being satisfied, assuming packages are stacked together in any arrangement and with close reflection on all sides of the stack by water: " (Paragraph "a")		
Transport index based on nuclear criticality control, CSI = 0.0	**load-limited to 21,125g ^{235}U no can spacers**	**load-limited to 15,673g ^{235}U no can spacers**
(1) five times "N" undamaged packages with nothing between the packages would be subcritical,	$k_{eff} + 2\sigma \leq 0.8908$ nciaoxt11_1_24_1_3	$k_{eff} + 2\sigma \leq 0.7562$ nciask_9_15
(2) two times "N" damaged packages, if each package were subject to the tests specified in §71.73 (Hypothetical Accident Conditions) would be subcritical with optimum interspersed hydrogenous moderation,	$k_{eff} + 2\sigma \leq 0.8877$ hciaoxt12_1_24_1_3	$k_{eff} + 2\sigma \leq 0.7599$ hciask_9_15
(3) the value of "N" cannot be <0.5.	N(1,2) = ∞	same
Transport index based on nuclear criticality control, CSI = 0.0	**load-limited to 21,125g ^{235}U can spacers**	**load-limited to 15,673g ^{235}U can spacers**
(1) five times "N" undamaged packages	$k_{eff} + 2\sigma \leq 0.8904$ nciaoxt11_1_24_2_3	bounded by no can spacers
(2) two times "N" damaged packages, ...	$k_{eff} + 2\sigma \leq 0.8883$ hciaoxt12_1_24_2_3	bounded by no can spacers
(3) the value of "N"	N(1,2) = ∞	same

Table 6.1e. Summary of criticality evaluation for UNX crystals and unirradiated TRIGA reactor fuel elements

Conditions	UNX crystals ≤ 11,303g ^{235}U	unirradiated TRIGA fuel elements ≤ 921g ^{235}U
General requirements for each fissile package (§71.55)		
"A package used for shipment of fissile material must be so designed and constructed and its contents so limited that it would be subcritical if water were to leak into the containment system, . . . so that under the following conditions, maximum reactivity of the fissile material would be attained:" (Paragraph "b")	$k_{eff} + 2\sigma \leq 0.8572$ (cvcrunhct11_9_1)	$k_{eff} + 2\sigma \leq 0.5274$ (cvcrtriga_1_15)
(1) the most reactive credible configuration consistent with the chemical and physical form of the material,	UNX crystals are homogenized with water over the internal volume of the containment vessel consistent with the high solubility properties of UNX. Maximum reactivity occurs at 415 g U/l solution concentration. Amount of water calculated for the flooded containment vessel is reduced by an amount equivalent to the volume occupied by can spacers. The can pads, spacer can, and convenience can steel are replaced by water.	Three 5-in tall sectioned pieces of $UZrH_x$ from a cylindrical TRIGA fuel element per convenience can. Sectioned pieces arranged in triangular pitch. No can spacers. Convenience can steel replaced by water.
(2) moderation by water to the most reactive credible extent,	flooding of the containment vessel	same
(3) close full reflection of the containment system by water on all sides, or such greater reflection of the containment system as may be provided by the surrounding material of the packaging.	30.48 cm H_2O surrounding the containment vessel	same

Table 6.1e. Summary of criticality evaluation for UNX crystals and unirradiated TRIGA reactor fuel elements

Conditions	UNX crystals ≤ 11,303g ^{235}U	unirradiated TRIGA fuel elements ≤ 921g ^{235}U
"A package used for shipment of fissile material must be so designed and constructed and its contents so limited under the tests specified in §71.71 (Normal Conditions of Transport) . . ." (Paragraph "d")		
(1) the contents would be subcritical,	$k_{eff} + 2\sigma \leq 0.7448$ (ncsrunhct11_9_1_15)	$k_{eff} + 2\sigma \leq 0.4950$ (ncsrtriga_1_15_15)
(2) the geometric form of the package contents would not be substantially altered,	UNX crystals are homogenized with water over the internal volume of the containment vessel consistent with the high solubility properties of UNX. Maximum reactivity occurs at 415 g U/l solution concentration. Amount of water calculated for the flooded containment vessel is reduced by an amount equivalent to the volume occupied by can spacers. The can pads, spacer can, and convenience can steel are replaced by water.	Three 5-in tall sectioned pieces of $UZrH_x$ from a cylindrical TRIGA fuel element per convenience can. Sectioned pieces arranged in triangular pitch. No can spacers. Convenience can steel replaced by water.
(3) there would be no leakage of water into the containment system unless, in the evaluation of undamaged packages under §71.59(a)(1), it has been assumed that moderation is present to such an extent as to cause maximum reactivity consistent with the chemical and physical form of the material,	moderation is present to such an extent as to cause maximum reactivity	same
(4) there will be no substantial reduction in the effectiveness of the packaging	30.48 cm H_2O surrounding the drum (d = 18.37 in., h = 43.5 in.)	same

Table 6.1e. Summary of criticality evaluation for UNX crystals and unirradiated TRIGA reactor fuel elements

Conditions	UNX crystals ≤ 11,303g ^{235}U	unirradiated TRIGA fuel elements ≤ 921g ^{235}U
"A package used for shipment of fissile material must be so designed and constructed and its contents so limited that under the tests specified in §71.73 (Hypothetical Accident Conditions) the package would be subcritical. For this determination, it must be assumed that:" (Paragraph "e")	$k_{eff} + 2\sigma \leq 0.8074$ (icsrunhct12_24_1_15)	$k_{eff} + 2\sigma \leq 0.4945$ (hcsrtriga_1_15_15)
(1) the fissile material is in the most reactive credible configuration consistent with the chemical and physical form of the contents,	Consistent with the high solubility properties of UNX, crystals and water are homogenized over the internal volume of the containment vessel and void space of the containment vessel well. Amount of water calculated for the flooded containment vessel is reduced by an amount equivalent to the volume occupied by can spacers. The can pads, spacer can, and convenience can steel are replaced by water.	Three 5-in tall sectioned pieces of $UZrH_x$ from a cylindrical TRIGA fuel element per convenience can. Sectioned pieces arranged in triangular pitch. No can spacers. Convenience can steel replaced by water.
(2) water moderation occurs to the most reactive credible extent consistent with the chemical and physical form of content,	flooding of the package	same
(3) there is full reflection by water on all sides, as close as is consistent with the damage condition of the package.	30.48 cm H_2O surrounding the reduced diameter drum, (d = 17.20 in., h = 43.5 in.)	same

Standards for arrays of fissile material packages (§71.59)

Table 6.1e. Summary of criticality evaluation for UNX crystals and unirradiated TRIGA reactor fuel elements

Conditions	UNX crystals ≤ 11,303g ^{235}U	unirradiated TRIGA fuel elements ≤ 921g ^{235}U
" . . . the designer of a fissile material package shall derive a number "N" based on all the following conditions being satisfied, assuming packages are stacked together in any arrangement and with close reflection on all sides of the stack by water: " (Paragraph "a")		
Transport index based on nuclear criticality control, CSI = 0.0	**load-limited to 3,768g ^{235}U no can spacers**	**no can spacers**
(1) five times "N" undamaged packages with nothing between the packages would be subcritical,	$k_{eff} + 2\sigma \leq 0.9191$ nciaunhct11_8_8_1_3	$k_{eff} + 2\sigma \leq 0.5254$ nciatriga_1_15_3
(2) two times "N" damaged packages, if each package were subject to the tests specified in §71.73 (Hypothetical Accident Conditions) would be subcritical with optimum interspersed hydrogenous moderation,	$k_{eff} + 2\sigma \leq 0.9216$ hciaunhct12_8_8_1_3	$k_{eff} + 2\sigma \leq 0.5261$ hciatriga_1_15_3
(3) the value of "N" cannot be <0.5.	N(1,2) = ∞	same
Transport index based on nuclear criticality control, CSI = 0.0	**load-limited to 11,303g ^{235}U can spacers**	**can spacers**
(1) five times "N" undamaged packages	$k_{eff} + 2\sigma \leq 0.8803$ nciaunhct11_8_24_2_3	$k_{eff} + 2\sigma \leq 0.4421$ nciatriga_2_15_3
(2) two times "N" damaged packages, ...	$k_{eff} + 2\sigma \leq 0.8811$ hciaunhct12_8_24_2_3	$k_{eff} + 2\sigma \leq 0.4427$ hciatriga_2_15_3
(3) the value of "N"	N(1,2) = ∞	same
Transport index based on nuclear criticality control, CSI = 0.4	**load-limited to 11,303g ^{235}U no can spacers**	**no can spacers**

Table 6.1e. Summary of criticality evaluation for UNX crystals and unirradiated TRIGA reactor fuel elements

Conditions	UNX crystals ≤ 11,303g ^{235}U	unirradiated TRIGA fuel elements ≤ 921g ^{235}U
(1) five times "N" undamaged packages	$k_{eff} + 2\sigma \leq 0.8703$ ncf1unhct11_8_24_1_3	bounded by CSI=0
(2) two times "N" damaged packages, ...	$k_{eff} + 2\sigma \leq 0.8321$ hcf2unhct12_8_24_1_3	bounded by CSI=0
(3) the value of "N"	N(1,2) = 202/162	same
Transport index based on nuclear criticality control, CSI = 0.4	**load-limited to 11,303g ^{235}U can spacers**	**can spacers**
(1) five times "N" undamaged packages	$k_{eff} + 2\sigma \leq 0.8332$ ncf1unhct11_8_24_2_3	bounded by CSI=0
(2) two times "N" damaged packages, ...	$k_{eff} + 2\sigma \leq 0.7972$ hcf2unhct12_8_24_2_3	bounded by CSI=0
(3) the value of "N"	N(1,2) = 202/162	same

Table 6.2a. HEU fissile material mass loading limits for surface-only modes of transportation

Solid HEU metal of specified geometric shapes						
Transport index based on nuclear criticality control	**cylinders (3.24 in. ≤ d)**	**cylinders (3.24 in. < d ≤ 4.25 in.)**	**bars**	**slugs enr. ≤ "N"%**	**slugs 80% < enr. ≤ 100%**	**slugs enr. ≤ 80%**
No can spacers						
CSI = 0.0	18,000g ^{235}U	15,000g ^{235}U	18,000g ^{235}U	18,286g ^{235}U [a]	-	-
With can spacers						
CSI = 0.0	30,000g ^{235}U	25,000g ^{235}U	30,000g ^{235}U	-	25,601g ^{235}U	29,333g ^{235}U
CSI = 0.4	-	-	-	34,766g ^{235}U [b]	-	-
Solid HEU metal of unspecified geometric shapes characterized as broken metal						
Transport index based on nuclear criticality control	**95% < enr. ≤ 100%**	**90% < enr. ≤95%**	**80% < enr. ≤90%**	**70% < enr. ≤80%**	**60% < enr. ≤70%**	**enr. ≤60%**
No can spacers						
CSI = 0.0	can spacers required	can spacers required	can spacers required	2,967g ^{235}U	3,249g ^{235}U	5,576g Uranium
CSI = 0.4	can spacers required	can spacers required	can spacers required	5,192g ^{235}U	5,848g ^{235}U	14,872g Uranium
CSI = 0.8	can spacers required	can spacers required	can spacers required	8,900 ^{235}U	13,646g ^{235}U	28,814g Uranium
CSI = 2.0	can spacers required	can spacers required	can spacers required	17,059g ^{235}U	21,444g ^{235}U	35,320g Uranium
CSI = 3.2	can spacers required	can spacers required	can spacers required	27,692g ^{235}U	24,692g ^{235}U	35,320g Uranium
With can spacers						
CSI = 0.0	2,774g ^{235}U	3,516g ^{235}U	3,333g ^{235}U	4,450g ^{235}U	5,198g ^{235}U	11,154g Uranium
CSI = 0.4	5,549g ^{235}U	6,154g ^{235}U	7,500g ^{235}U	8,900g ^{235}U	12,996g ^{235}U	28,813g Uranium
CSI = 0.8	9,248g ^{235}U	10,549g ^{235}U	12,500g ^{235}U	16,317g ^{235}U	20,793g ^{235}U	35,320g Uranium
CSI = 2.0	13,872g ^{235}U	18,461g ^{235}U	20,000g ^{235}U	25,218g ^{235}U	24,692g ^{235}U	35,320g Uranium
CSI = 3.2	24,969g ^{235}U	26,373g ^{235}U	28,334g ^{235}U	28,184g ^{235}U	24,692g ^{235}U	35,320g Uranium

Table 6.2a. HEU fissile material mass loading limits for surface-only modes of transportation (cont.)

HEU oxide and UNX crystals					
Transport index based on nuclear criticality control	**HEU product oxide, no can spacers**	**HEU skull oxide, no can spacers**	**UNX crystals, no can spacers**	**unirradiated TRIGA fuel elements, no can spacers [c]**	
				enr. = 20%	enr. = 70%
CSI = 0.0	21,124g ^{235}U	15,675g ^{235}U and 921g C	3,768g ^{235}U	921g ^{235}U	408g ^{235}U
CSI = 0.4	-	-	11,303g ^{235}U	-	-

[a] When can spacers **are not** used, "N" = 100 (wt % ^{235}U), and the mass limit = 18,286g ^{235}U.

[b] When can spacers **are** used, "N" = 95 (wt % ^{235}U), and the mass limit = 34,766g ^{235}U. For enrichments >95 wt % ^{235}U, the lower mass limit of 25,601g ^{235}U applies.

[c] For ground transport, TRIGA reactor fuel element content will be limited to 3 fuel sections ("meats") per loaded convenience can and up to 3 loaded cans per package. The TRIGA fuel content may also be configured as clad fuel rods, each rod derived from a single TRIGA fuel element. A ~15 inch long rod consists of the 3 fuel pellets and an exterior sheath of clad, where protruding clad at each end has been crimped in. Clad fuel rods will be packed into convenience cans, with a maximum of three fuel rods per loaded convenience can and one loaded can per containment vessel.

Table 6.2b. HEU fissile material mass loading limits for air transport mode of transportation

Solid HEU metal of specified geometric shapes				
With/without can spacers	**cylinders (d = 3.24 in.)**	**cylinders (3.24 < d ≤ 4.25 in.)**	**bars**	**slugs**
One per convenience can	700g ^{235}U	700g ^{235}U	700g ^{235}U	700g ^{235}U
Solid HEU metal of unspecified geometric shapes characterized as broken metal				
With/without can spacers	**20% < enr. ≤ 100%**		**19% < enr. ≤20%**	**Nat.U. < enr. ≤ 19%**
	not allowed		**3,500g Uranium**	**not allowed**

HEU oxide, UNX crystals, unirradiated TRIGA fuel elements					
With/without can spacers	**HEU product oxide**	**HEU skull oxide**	**UNX crystals**	**unirradiated TRIGA [a]**	
				enr. = 20%	enr. = 70%
Three per convenience can	**not allowed**	**not allowed**	**not allowed**	716g ^{235}U	408g ^{235}U

[a] For air transport, TRIGA reactor fuel element content will be limited to fuel sections or clad fuel rods as described for surface-only modes of transportation in footnote "c" of Table 6.2a and the fissile mass limit specified herein, whichever is more limiting.

6.2 PACKAGE CONTENTS

The **package content** is defined as the HEU fissile material, bottles, convenience cans, canned spacers, can pads, and the associated packing materials (plastic bags, pads, tape, etc.) inside the ES-3100 containment vessel.

6.2.1 Fissile Material Contents

The per-package HEU mass loadings considered in the criticality evaluation range from 1000 to 36,000 g for uranium metal and from 1000 to 24,000 g for uranium oxide and UNX crystals. The HEU mass may include nonradioactive contaminants and trace elements or materials in the HEU.

The bounding types of HEU content evaluated in this criticality analysis are 4.25-in.- and 3.24-in.-diam cylinders; 2.29-in.-square bars; 1.5-in.-diam × 2-in.-tall slugs; cubes ranging from 0.25 to 1 in. on a side; broken metal pieces of unspecified geometric shapes; skull oxide; uranium oxide; UNX crystals; and unirradiated TRIGA reactor fuel elements.

The term "broken metal pieces" is used to describe an HEU content without restrictions on shape or size other than a minimum size limit (spontaneous ignition), a maximum mass limit (criticality control), a minimum enrichment (the lower limit for HEU at 19 wt % ^{235}U in uranium), and the capacity limits of the convenience cans. The content geometry envelope encompasses regular, uniform shapes and sizes as well as irregular shapes and sizes.

The density of HEU metal ranges from 18.811 to 19.003 g/cm^3 for HEU metal, corresponding to enrichments ranging from 100 to 19 wt % ^{235}U. Theoretical (crystalline) densities for HEU oxide are 10.96 g/cm^3, 8.30 g/cm^3, and 7.29 g/cm^3 for UO_2, U_3O_8, and UO_3, respectively. However, bulk densities for product oxide are typically on the order of 6.54 g/cm^3; therefore, only "less-than-theoretical" mass loadings would actually be achieved. Skull oxides are a mixture of U_3O_8 and graphite, having densities on the order of 2.44 g/cm^3 for poured material and 2.78 g/cm^3 for tapped material. Combined water saturation and crystallization of the HEU oxide is not expected in the HAC because UO_2 and UO_3 are non-hygroscopic and U_3O_8 is only mildly hygroscopic. The density of UNX crystals varies depending on the degree of hydration. The most reactive form of $UO_2(NO_3)\bullet xH_2O$ is with 6 molecules of hydration, having a density of 2.79 g/cm^3. UNX crystals are highly soluble in nitric acid and mildly soluble in water. Dissolution of UNX crystals in water is assumed in this criticality evaluation. The content geometry envelope encompasses both regular, uniform clumps and densities, and irregular clumps and densities.

The approximate 40 stock items of TRIGA fuel are cataloged as one of the four basic types: a standard element, an instrumented element, a fuel follower control rod, or a cluster assembly. The active region of TRIGA element consists of three 5-in long sections "fuel meats" of uranium zirconium hydride ($UZrH_x$). The "x" in $UZrH_x$ equals 1.6 in all cases except for two stock items where x = equals 1.0 and the fissile content is < 40 g ^{235}U. The clad thickness is ~0.02 inches for a TRIGA fuel element with stainless steel cladding and ~0.03 inches for an element with aluminum cladding.

Solid form TRIGA fuel is either 20 or 70 wt % enriched in ^{235}U and has specific dimensional characteristics for its designed function. For the 20 wt % enriched TRIGA elements, the active fuel diameters are 1.44 in., 1.41 in., 1.40 in., 1.37 in., 1.34 in., or 1.31 in. The uranium weight fractions are 45 wt %, 30 wt %, 20 wt %, 12 wt %, and 8.5 wt %. The TRIGA element with a maximum fissile content of 307 g ^{235}U in 1,560 g U is 45 wt% U in $UZrH_x$ and has a computed density of ~8.6 g/cm^3

(Appendix 6.9.3.1). For the 70 wt % enriched TRIGA fuel, the active fuel diameter is 1.44 inches in the standard element and instrumented element, and 1.31 inches in the fuel follower control rod. Both the standard element and instrumented elements contain ~136 g ^{235}U in 194 g U while the fuel follower control rod contains ~113 g ^{235}U in 162 g U. The 70 wt % enriched TRIGA fuel is 8.5 wt% U in $UZrH_x$ and has a computed density of ~5.7 g/cm^3 (Appendix 6.9.3.1).

In preparation for shipment in the ES-3100, the unirradiated TRIGA fuel elements may be disassembled and the fuel sections removed from the thin-wall cladding. The TRIGA fuel may also be configured as clad fuel rods. Each clad fuel rod will be derived from a single TRIGA fuel element by removal of the stainless steel or aluminum clad beyond the plenum adjacent to the axial ends of the active fuel section. Each ~15 inch long rod consists of the 3 fuel pellets and an exterior sheath of clad, where the protruding clad at each end has been crimped in.

The 0.02 in thick sheath of stainless steel clad adds ~179 g to the mass of the active fuel for the standard element or instrumented element with 1.48 in. overall diameter, and ~163 g to active fuel mass for the fuel follower control rod with 1.35 in. overall diameter. Allowance for 1/2 in. of residual stainless steel crimped on each end of the clad fuel rod adds ~11 to 12 g stainless steel to these amounts. Likewise, the 0.03 in thick sheath of aluminum clad adds ~90 g to the mass of the active fuel for the 1.47 in. diameter standard element or instrumented element. Allowance for 1/2 in. of residual stainless steel crimped on each end of the clad fuel rod adds ~6 g aluminum.

Skull oxides, uranium alloys of aluminum or molybdenum, and unirradiated TRIGA reactor fuel elements are evaluated where composition data is for material in the as-manufactured condition. A maximum enrichment of 100 wt % is used for HEU metal, oxide and UNX crystals in the criticality calculations strictly for the purpose of maximizing reactivity, even though HEU enrichment ranges from 19 to 97.7 wt % ^{235}U. Although mass loading limits for oxide and crystals are based on 100% enrichment, the actual enrichment is expected to be less than the stated maximum, with the remainder of the uranium being primarily ^{238}U. The HEU mass may also include nonradioactive contaminants and trace elements or materials in the HEU.

No intact weapon part or component will be shipped in this package. Weapon parts or components that have been reduced to "broken metal pieces" or processed into HEU oxide and meet the additional content requirements identified in Sect. 6.2.4 can be shipped in this package.

6.2.2 Convenience Cans, Teflon and Polyethylene Bottles, and 277-4 Canned Spacers

HEU fissile material to be shipped in the ES-3100 package will be placed in stainless steel, tin-plated carbon steel, or nickel alloy convenience cans or polyethylene or Teflon bottles. Can lids may be welded, press fit, slip lid, or crimp seal types; bottle lids are screw cap type. Convenience cans and bottles are used to hold the HEU for shipment in the ES-3100 package and to assure that the inside of the containment vessel does not become contaminated with HEU under NCT. The HEU metal or oxide content may be wrapped or bagged in polyethylene, and the convenience cans may also be wrapped in polyethylene to further reduce the possibility of radioactive contamination of the packaging. Nylon straps may be use used for handling the nickel alloy cans. Masses of the convenience cans and packing materials are in addition to the fissile material mass.

Three 4.25-in.-diam × 10.0-in.-tall or six 4.25-in.-diam × 4.88-in.-tall convenience cans, separated by can pads, can be placed inside the 31-in.-tall cavity of the ES-3100 containment vessel (Fig. 1.4). The convenience cans may have press-fit or crimp-seal lids. The size of solid content placed inside a convenience can is physically limited by both the can opening and the usable height of the convenience can. Other can arrangements fit inside the containment vessel, such as three 4.25-in.-diam × 8.75-in.-tall convenience cans or five 4.25-in.-diam × 4.88-in.-tall convenience cans. Both of these can arrangements include can pads and 277-4 canned spacers. Nickel alloy cans to be used exclusively for HEU oxide content are ~3-in. diam × 4.75-in. tall. Three Teflon bottles (4.69-in. diam × 9.4-in. tall) or three polyethylene bottles (4.94-in. diam × 8.76-in. tall) fit inside the containment vessel; however, 277-4 canned spacers are not used with these configurations.

The can pad and 277-4 canned spacer have overall dimensions of 4.25-in. diam × 1.82-in. height. (Drawing M2E801580A026, Appendix 1.4.8) A stainless-steel spacer can with a lid has a usable cavity with dimensions of 4.13-in. diam × 1.37-in. height, which nominally allows for ~510 g of neutron poison material.

6.2.3 Packing Materials

Polyethylene bags may be used for contamination control. Realistically, the number of polyethylene bags used to bag content and wrap a convenience can would be six bags at most. Given that each bag weighs ~28 g, this results in a maximum of ~510 g of polyethylene per ES-3100 package. Possible additional sources of hydrogenous material inside the containment vessel include can pads, vinyl tape, and polyethylene (~85 g) or Teflon (~303 g) bottles.

For the criticality calculations, the sources of hydrogen contained in packing materials are not distinguished from other sources of hydrogen inherent in the fissile material content. Therefore, packing material mass is defined as all sources of hydrogenous packing materials inside the containment vessel plus the actual moisture in the content as constituent (the bonded hydrogen in UNX crystals or impurities in the oxide.) Given content moisture is not to exceed 6 wt %, the actual amount of hydrogenous material inside the containment vessel is not expected to exceed 2,400 g.

Normally, the H/X ratio inside the containment vessel is specified as an administrative control used to restrict both the amount of hydrogenous packing material normally used inside the containment vessel and other sources of moisture present in the fissile content. The total amount of hydrogen inside the containment vessel is used in the determination of package H/X ratio (i.e., the ratio of the number of hydrogen atoms "H" to the number of fissile atoms "X," where the hydrogen atoms are those of the content, including absorbed moisture and of the packing material both inside and outside of the convenience cans.) However, containment vessel flooding is assumed in calculations performed for the derivation of fissile material

loading limits. Even though both the NCT tests under 10 CFR 71.71 and the HAC tests under 10 CFR 71.73 demonstrate that containment is not breached, this simulated condition produces more reactive package configurations in the criticality calculations than the actual package configurations. The 7.1–10.1 kg quantities of evaluation water required in both the NCT and HAC criticality calculations bound reasonable amounts of hydrogenous material and inherent moisture of fissile material (primarily HEU oxides) present inside the containment vessel. Thus, an administrative criticality control is not needed to restrict either the amount of hydrogenous material normally present inside the containment vessel or other sources of moisture present in the fissile content.

6.2.4 Package Content Loading Restrictions

Loading restrictions based upon the results of the criticality safety calculations presented in Sects. 6.4 and 6.5 are as follows:

(1) HEU fissile material to be shipped in the ES-3100 package shall be placed in stainless steel, tin-plated carbon steel or nickel-plated carbon steel convenience cans or polyethylene or Teflon bottles. The can lids may be welded, press fit, slip lid, or crimp seal types; bottle lids are screw cap type.

(2) The content shall not exceed the "per package" fissile material mass loading limits specified in Tables 6.2a and 6.2b, and 277-4 canned spacers shall be used as indicated for criticality control.

(3) Where 277-4 canned spacers are required, not greater than one-third of the permissible package content for that category indicated in Tables 6.2a or 6.2b shall be loaded in any vacancy between or adjacent to canned spacers inside the containment vessel. The content mass loading may be further restricted based on structural, mechanical, and practical considerations (see Sects. 1 and 2).

(4) As shown in Fig. 1.4, the ES-3100 package may carry up to six loaded convenience cans. In situations where the plan for loading the containment vessel calls for the use of empty convenience cans to fill the containment vessel, the heavier cans shall be loaded into the bottom of the upright shipping container, and the empty cans shall be placed above them.

(5) The presence of uranium isotopes is limited on a weight-percent basis as follows: $^{232}U \leq 40$ ppb U, $^{234}U \leq 2.0$ wt % U, $^{235}U \leq 100.0$ wt % U, and $^{236}U \leq 40.0$ wt % U.

(6) With the exception of slug content and unirradiated TRIGA reactor fuel element content, solid HEU metal or alloy content of specified geometric shapes shall be one item per loaded convenience can. HEU bulk metal or alloy content not covered by the specified geometric shapes (cylinder, square bar, billet, slug, or unirradiated TRIGA fuel element contents) will be in the HEU broken metal category, and so limited.

(7) The package content is defined as the HEU fissile material, bottles, the convenience cans, the can spacers, and the associated packing materials (plastic bags, pads, tape, etc.) inside the ES-3100 containment vessel.

(8) The CSI is determined on the basis of the uranium enrichment and total ^{235}U mass in the package and the fissile material shape or form.

6.3 GENERAL CONSIDERATIONS

The ES-3100 packaging configuration is shown on Drawing M2E801580A031 (Appendix 1.4.8). KENO V.a modeling of this configuration with the maximum allowable contents (Sect. 6.2) for a variety of array sizes and array conditions yields bounding calculations that determine the package's CSI (Tables 6.1a–6.1e) Can spacers are used as indicated in Table 6.2a and 6.2b for the purpose of reducing neutronic interaction between the contents of the package, aiding in maintaining the $k_{eff} + 2\sigma$ below the USL for the ES-3100 package. Key input listings are provided in Appendix 6.9.7.

The HEU content of a package is in one of the following forms: metal of a specified geometric shape, metal of an unspecified shape characterized as broken metal, uranium or skull oxide, or UNX crystals, or unirradiated TRIGA reactor fuel elements. The bounding types of HEU content evaluated in this criticality analysis are: 4.25-in.- and 3.24-in.-diam cylinders; 2.29-in.-square bars; 1.5-in.-diam × 2-in.-tall slugs; cubes ranging from 0.25 to 1 in. on a side; broken metal pieces of unspecified geometric shapes; product and skull oxide; UNH crystals; and unirradiated TRIGA reactor fuel elements. Uranyl nitrate hexahydrate (UNH) has a chemical formula of $UO_2(NO_3)_2 + 6\,H_2O$. This most reactive form is used as the bounding composition for UNX crystals in the criticality evaluation. TRIGA fuel elements are 1.44-in.-diam × 15-in.-tall cylinders of $UZrH_x$ containing <310 g ^{235}U. Fuel elements are sectioned into three equal length pieces. Calculations demonstrate that these contents are bounded by 3.24-in.-diam HEU metal cylinders. Evaluation of the 3.93-in.-diam × 9.5-in.-tall U-Al cylinders is covered under the evaluation of the 4.25-in.-diam HEU metal cylinders. The evaluation of the U-Mo content is covered under the assessment of HEU contents at 95 wt % enrichment.

HEU metal shapes are distributed in an optimum arrangement in the flooded containment vessel. For the single package and the array calculations, the HEU broken metal is modeled as a homogeneous mixture of uranium metal and water filling the interior of a flooded containment vessel. This representation bounds the heterogeneous configuration of metal pieces interspersed with hydrogenous packing material inside of wrapped convenience cans. (Appendix 6.9.3., Sect. 6.9.3.1) Water soluble UNH crystalline content is modeled as a homogeneous mixture of UN and water filling the interior of the containment vessel.

No credit is taken for the fissile material spacing, neutron absorption, or free volume reduction provided by the presence of can pads, spacer can steel, and convenience cans inside the containment vessel. Water is substituted for polyethylene bagging which may be in use as packing material for both the content placed inside the convenience can and the cans themselves. Pads of steel turnings rolled up into a disk-like shape may also be present in the ES-3100 package, in use as cushioning and for reducing the free volume inside the convenience cans. This steel packing material acts as a neutron absorber and is excluded from the calculation model.

Criticality calculations are performed for the containment vessel under full water reflection whereby the water content inside the containment vessel is varied from dry to fully flooded conditions. These calculations demonstrate that the fully flooded condition is most reactive. The containment vessel is flooded in the single-unit calculation model and the infinite and finite array calculation models for both the NCT and HAC evaluations.

The KENO V.a models discussed in the following sections are the single-unit calculation model (Sect. 6.3.1.1), the infinite and finite array calculation models (Sect. 6.3.1.2), the HAC calculation models (Sect. 6.3.1.3), and the air transport models (Sect. 6.3.1.4). The single-unit calculation model is evaluated with a vacuum boundary condition and with full water reflection. The finite array calculation model is evaluated in arrays consisting of packages stacked in 13×13×6, 9×9×4, 7×7×3, 5×5×2, ETP 27×3 and

ETP 16×3 arrangements with full water reflection at the array boundary. The ETP arrangements are used specifically for defining smaller array configurations with a high CSI value.

The geometry of the ES-3100 package is depicted in Drawing No. M2E801580A001 (Appendix 1.4.8). Calculation models of this geometry for evaluating NCT and HAC must be constructed for the single-unit, infinite array and finite arrays within the constraints and capabilities of KENO V.a. As shown in the drawing, the ES-3100 geometry is complex. Given KENO V.a's constraints and capabilities, two methods may be used to evaluate these complex geometries: simplify the geometries with conservative approximations or construct accurate geometries from simple components. Both methods yield valid results; however, the latter method is chosen for this analysis in order to maximize accuracy and to eliminate unnecessary conservatism.

6.3.1 Model Configuration

A detailed ES-3100 geometry model is accurately constructed using many simple geometric shapes. The selection of these components is governed by two of KENO V.a's geometry constraints: geometry regions must be composed of uniform and homogeneous materials and exterior regions must completely enclose interior regions. It is apparent from Drawing No. M2E801580A001 (Appendix 1.4.8) that these constraints could not be simultaneously applied to the entire ES-3100 package. However, these constraints could be applied to vertical segments of the package. Segments (i.e., simple components) are defined by starting at the bottom of the package and defining geometry regions radially outward until the drum surface is reached. A vertical segment is extended upward to the point where the KENO V.a constraints are violated. This vertical position is the termination point of a segment (i.e., the interface with the adjacent segment above it). The vertical segments are constructed accordingly, ignoring the minor variations in the ES-3100 geometry (i.e., radii of curvature, beveled edges, nuts and bolts). The KENO V.a geometry model for the ES-3100 is then assembled from the vertical segments. The resulting calculation model geometry includes the HEU content, 277-4 canned spacers, the containment vessel, the stainless-steel liner, the inner-liner cavity filled with 277-4, the outer-liner cavity filled with Kaolite, the Kaolite top plug and steel shell, the silicon rubber spacers, and the stainless-steel drum.

6.3.1.1 Single-unit packaging calculation model

The single-unit packaging calculation model is comprised of the geometry model, material compositions, and boundary conditions. Figures 6.1–6.5 depict section views of the geometry model used to evaluate a single ES-3100 package. Excluding minor variations in the ES-3100 geometry (i.e., radii of curvature, beveled edges, nuts and bolts), the single-unit packaging calculation model is an accurate representation of the ES-3100 geometry.

Figure 6.1 depicts a vertical section view of an ES-3100 package with the content of three loaded convenience cans and 277-4 can spacers inside the containment vessel. The fissile material contents shown are HEU cylinders, but convenience cans are not modeled. As illustrated in Fig. 6.1, credit is not taken for fissile material spacing provided by convenience cans inside the containment vessel. Appendix 6.9.1 provides wire-frame schematic and isometric diagrams depicting other fissile material contents considered in this criticality calculation.

Figures 6.2–6.5 depict vertical section views at various elevations in the package. The dimensions and the material specifications of any element of the ES-3100 single-unit packaging model may be obtained directly from the KENO V.a input listings in Appendix 6.9.7. The vertical segments (KENO V.a geometry unit numbers) are denoted in parenthesis to the right of the dimensions. The dimensions are given in units of centimeters. Material specification data for the single-unit packaging calculation model are provided in Sect. 6.3.2.

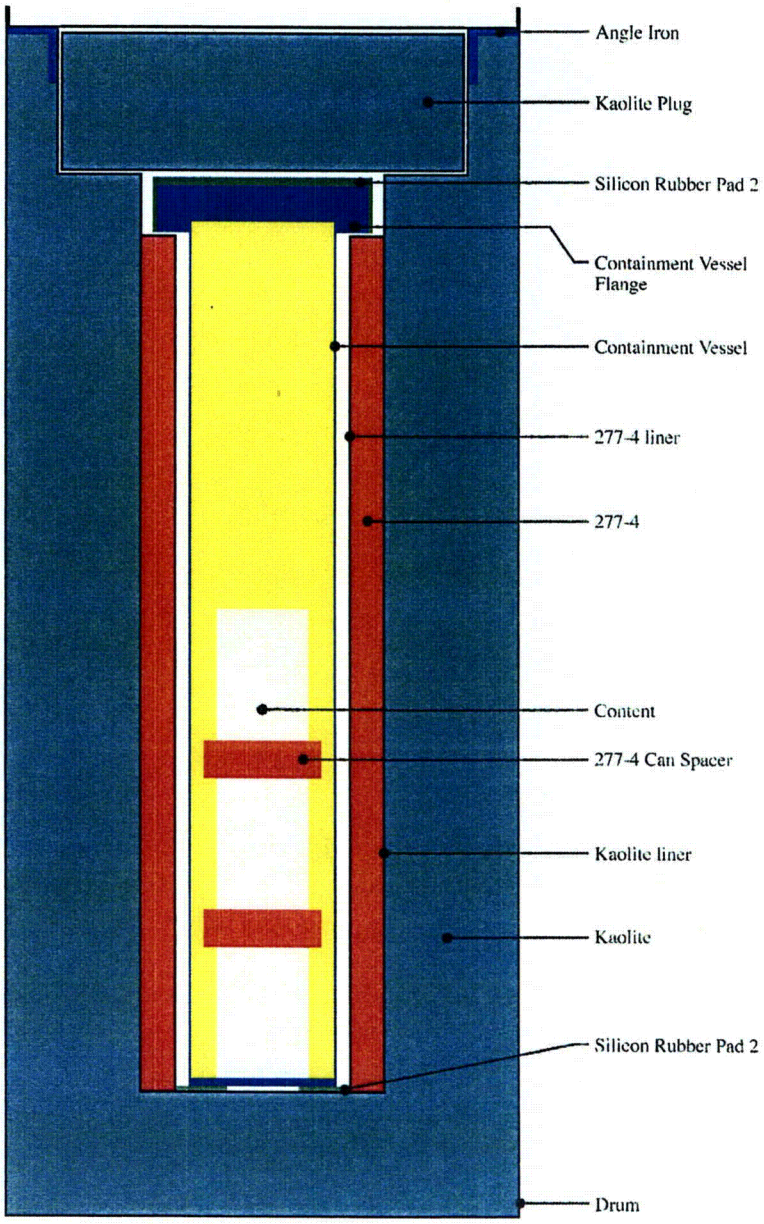

YGG 06 0182

Fig. 6.1. R/Z section view of ES-3100 single-unit packaging model.

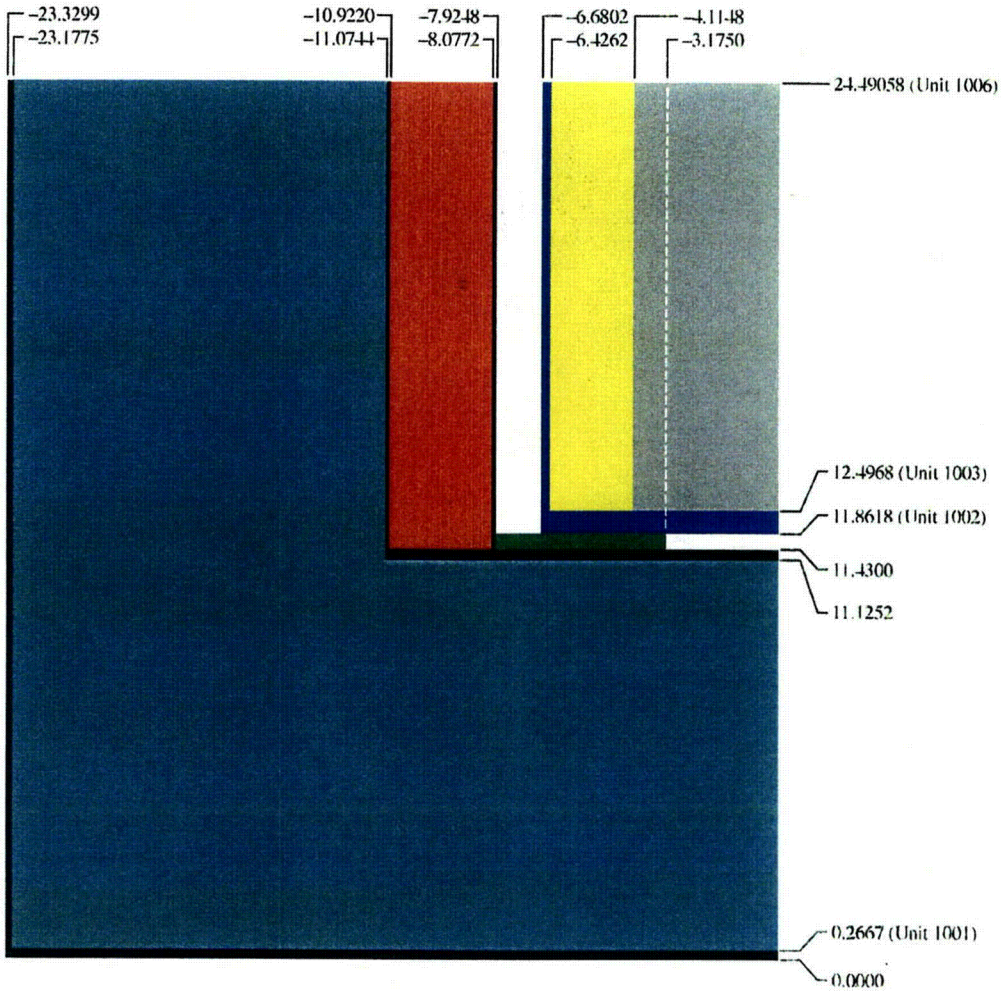

Fig. 6.2. R/Z section view at bottom of ES-3100 single-unit packaging showing KENO V.a geometry units 1001–1003, and 1006 (partial). Dimensions are in centimeters.

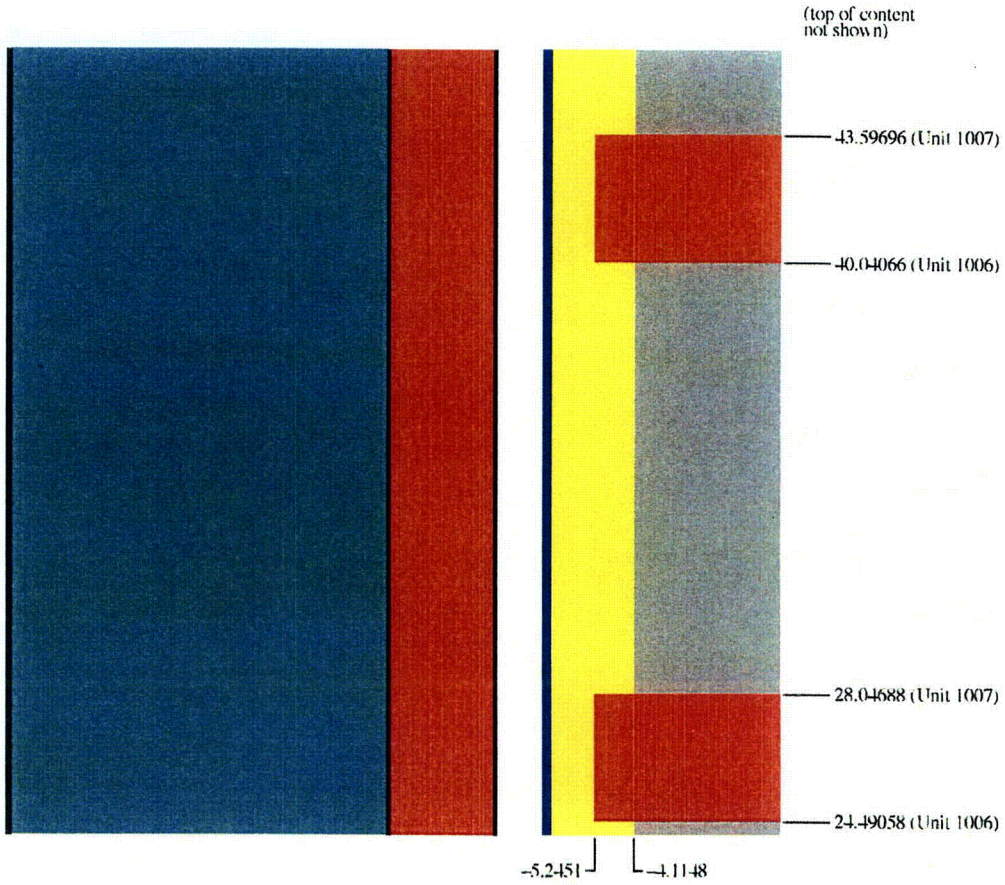

Fig. 6.3. R/Z section view at center of the ES-3100 single-unit packaging showing KENO V.a geometry units 1006 (partial), 1007, and 1008 (partial). Dimensions are in centimeters.

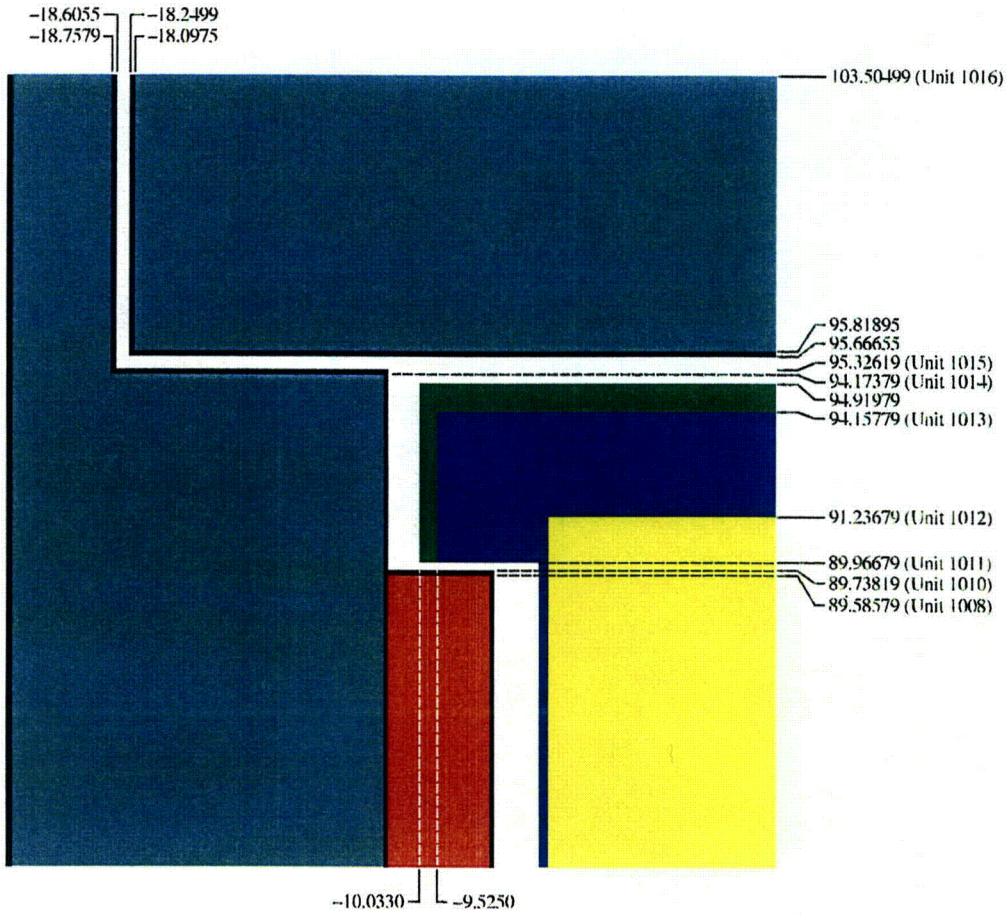

Fig. 6.4. R/Z section view of near top of the ES-3100 single-unit packaging showing KENO V.a geometry units 1008 (partial) and 1010–1016. Dimensions are in centimeters.

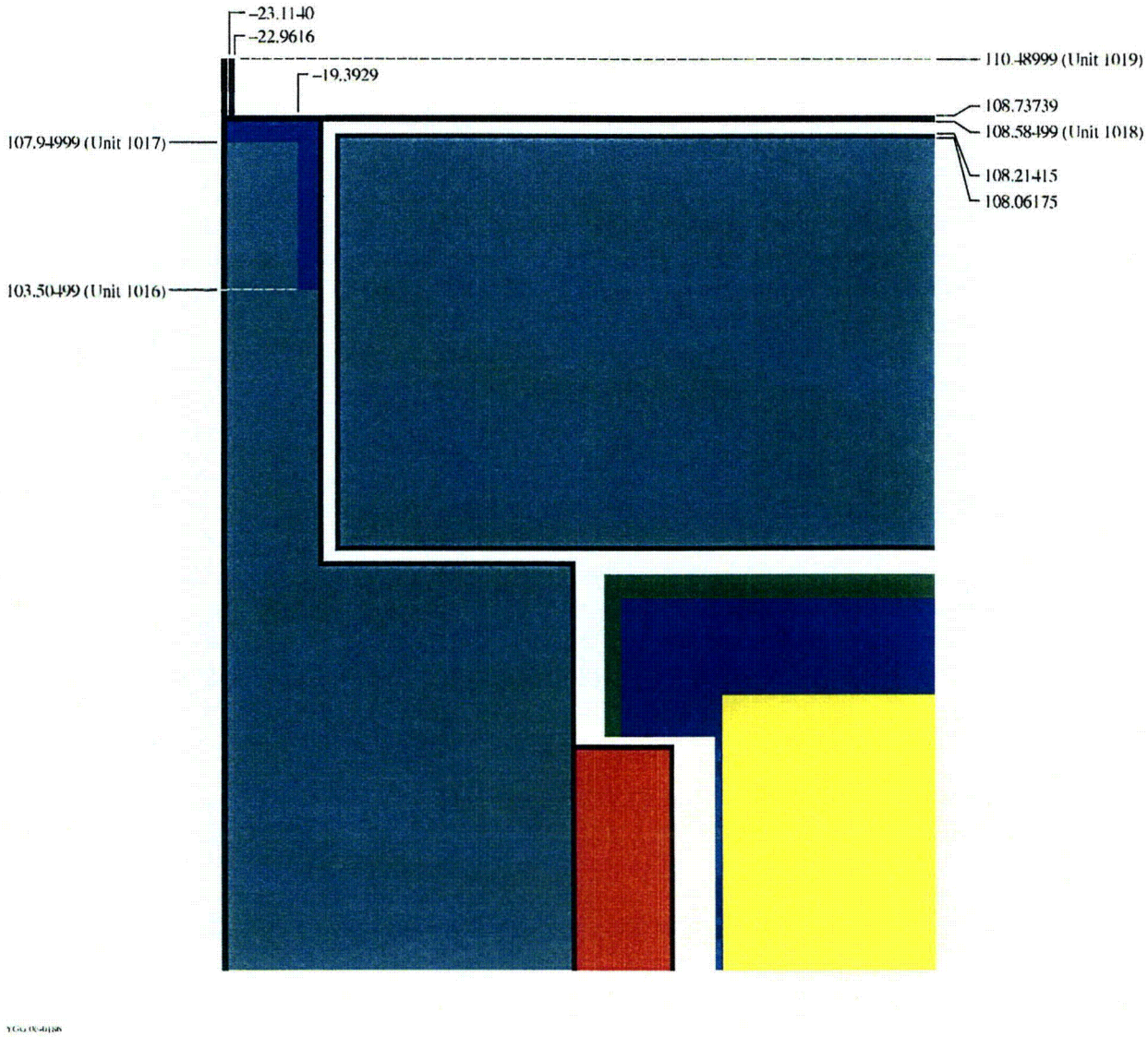

Fig. 6.5. R/Z section view at the top of the ES-3100 single-unit packaging showing KENO V.a geometry units 1016–1019. Dimensions are in centimeters.

The single-unit calculation model is evaluated as both a bare system (i.e., with a vacuum boundary condition) and as a reflected system with 30.48 cm (1 ft) of water surrounding the package for effectively infinite water reflection.

6.3.1.2 Infinite and finite array packaging calculation models

Array packaging calculation models like the single-unit packaging calculation model are comprised of geometry, material compositions, and boundary conditions. Figures 6.6–6.10 depict section views of the geometry model used to evaluate an array of ES-3100 packages. The array geometry model incorporates a 7.0% reduction in the inside diameter of the ES-3100 drum. This reduction of the drum's inside diameter produces an array density equivalent to drums in a tightly packed, triangular pitch configuration. (O'Dell and Schlesser 1991) Since all array calculations in this evaluation use a square pitch package configuration, using the 7.0% reduction in diameter of uniform-shaped packages avoids the use of a nonconservative lattice arrangement in the array analysis.

As seen in Drawings M2E801580A002 and M2E801580A003 (Appendix 1.4.8), a 7.0% reduction of the inside diameter of the ES-3100 drum affects the masses of the drum, the modified 2 × 2 × ¼ in. angle (angle iron), and the Kaolite refractory material. Also, a 7.0% reduction in diameter affects the mass of interstitial water between the ES-3100 packages of a tightly packed array. To maintain the correct mass of these materials in the array packaging calculation model, the drum's outside diameter, the density of the steel in the angle iron, the density of Kaolite, and the density of interstitial water are modified. Excluding modifications required to simulate a triangular pitch and minor variations in the ES-3100 geometry (i.e., radii of curvature, beveled edges, nuts and bolts), the array geometry model is an accurate model of the ES-3100 geometry.

In the array geometry model, the drum outside diameter is 43.444550 cm (17.104154 in.) (21.722275-cm radius used as the input value), and the drum inside diameter is 43.11015 cm (16.972500 in.) (21.555075-cm radius). This inside diameter corresponds to 93% of the inside diameter of the ES-3100 drum, and the drum outer diameter is modified to maintain drum mass. The angle iron outside diameter is identical to the drum inside diameter. To maintain mass, the angle iron steel, the liner outer-cavity Kaolite, and interstitial water densities are modified by factors of 1.25705, 1.22252, and 1.16235, respectively. Excluding the modifications to drum and angle iron dimensions, the dimensions of any element of the ES-3100 array geometry model may be obtained directly from Appendix 6.9.7. Material specification data from the array calculation models are provided in Sect. 6.3.2.

O'Dell and Schlesser equate modeling triangular arrays with square pitch arrays, provided that the outer dimension of the array is reduced by a factor of 0.9306 and that the mass of materials is maintained. The actual reduction factors (ratio of the reduced radii to the single unit radii) for the Kaolite of the body weldment and for the angle iron is slightly <0.9306. Given that the array packages are closer than required by O'Dell and Schlesser, the array models are conservative with respect to their reduced radii.

The finite array calculation model is evaluated with arrays of packages stacked in 13×13×6, 9×9×4, 7×7×3, and 5×5×2 arrangements where the arrays are surrounded with 30 cm (~1 ft) of water as a boundary condition representative of full water reflection. These arrays are nearly cubic in shape for optimum reactivity of the array, thus eliminating the need for placing limitations on array configurations in terms of stack height, width, and depth.

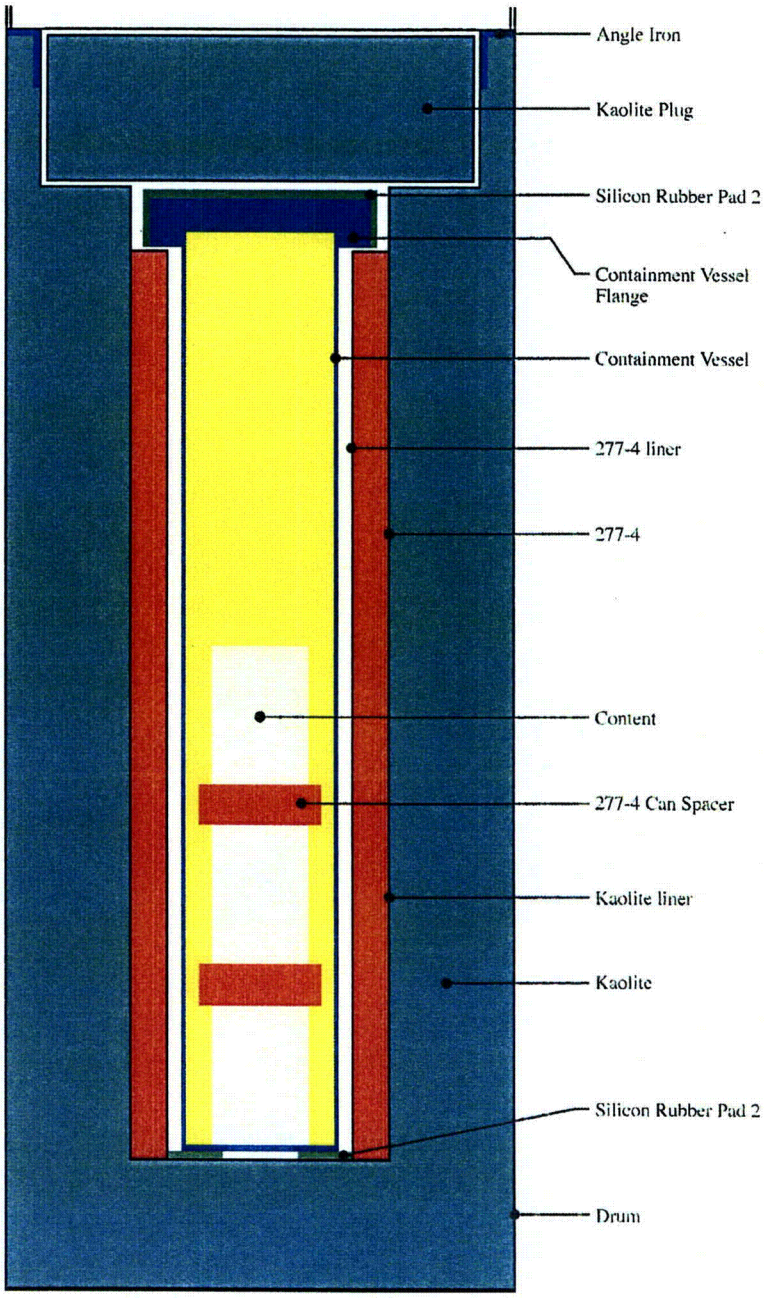

Fig. 6.6. R/Z section view of ES-3100 array packaging model with a 7% reduction in the drum's inner diameter.

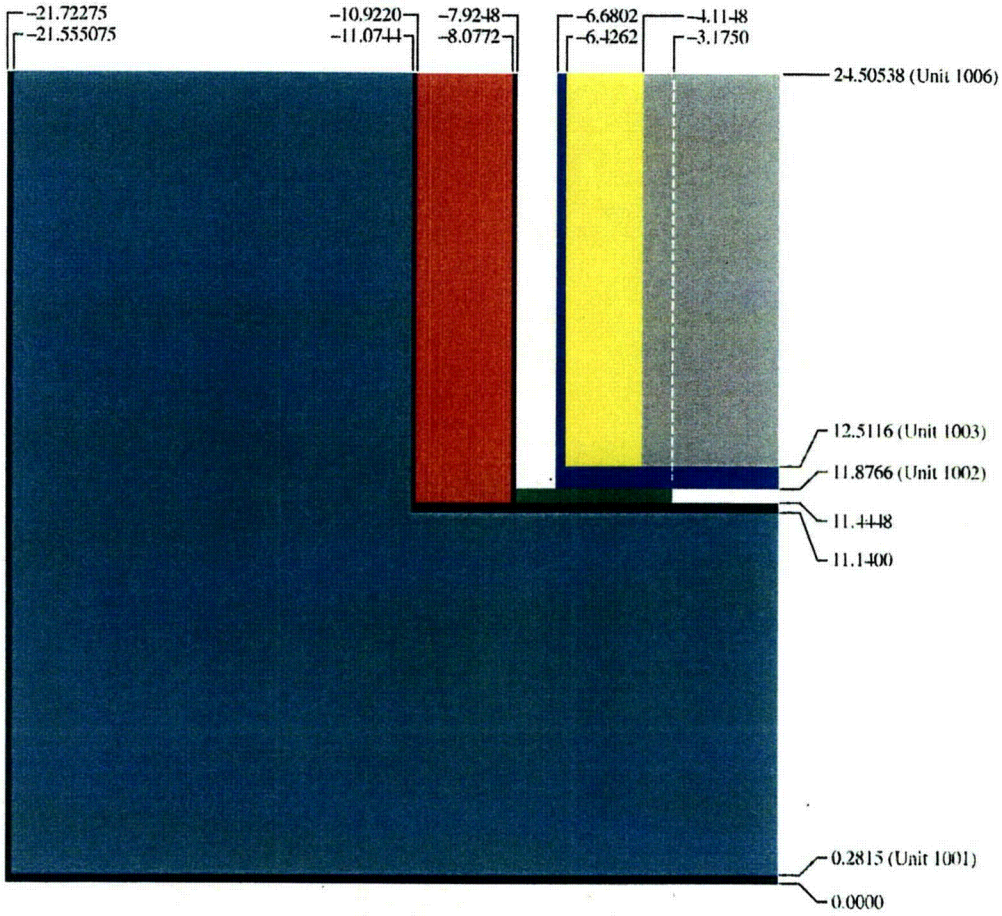

Fig. 6.7. R/Z section view at the bottom of the ES-3100 array packaging showing KENO V.a geometry units 1001–1003, and 1006 (partial). Dimensions are in centimeters.

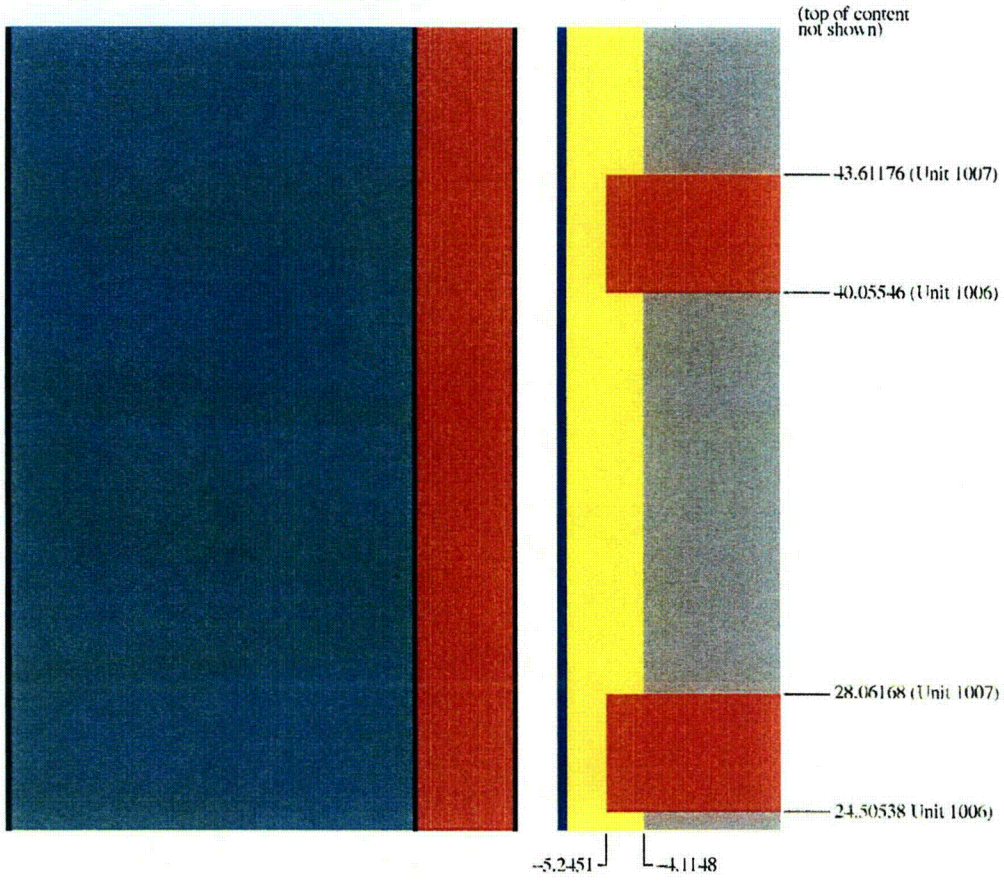

Fig. 6.8. R/Z section view at the center of the ES-3100 array packaging showing KENO V.a geometry units 1006 (partial), 1007, and 1008 (partial). Dimensions are in centimeters.

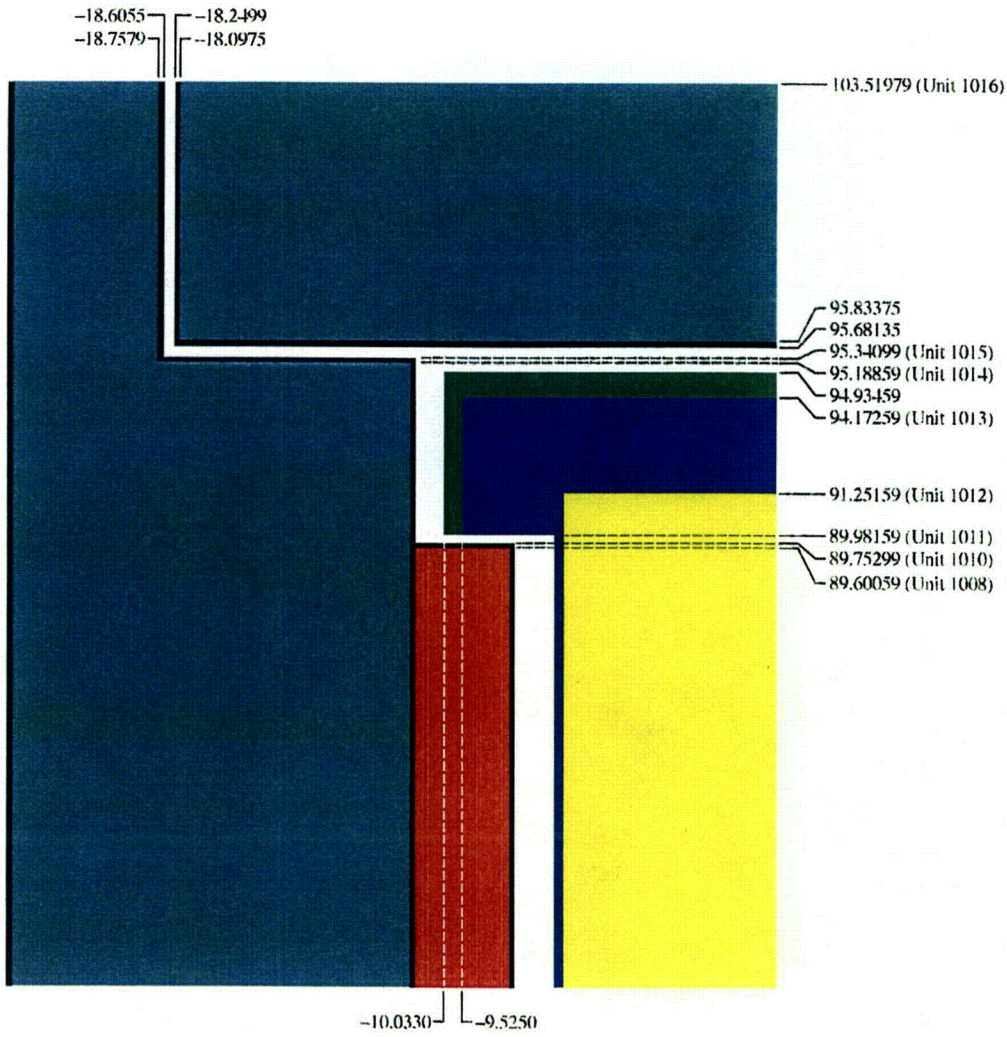

Fig. 6.9. R/Z section view of near top of the ES-3100 array packaging showing KENO V.a geometry units 1008 (partial) and 1010–1016. Dimensions are in centimeters.

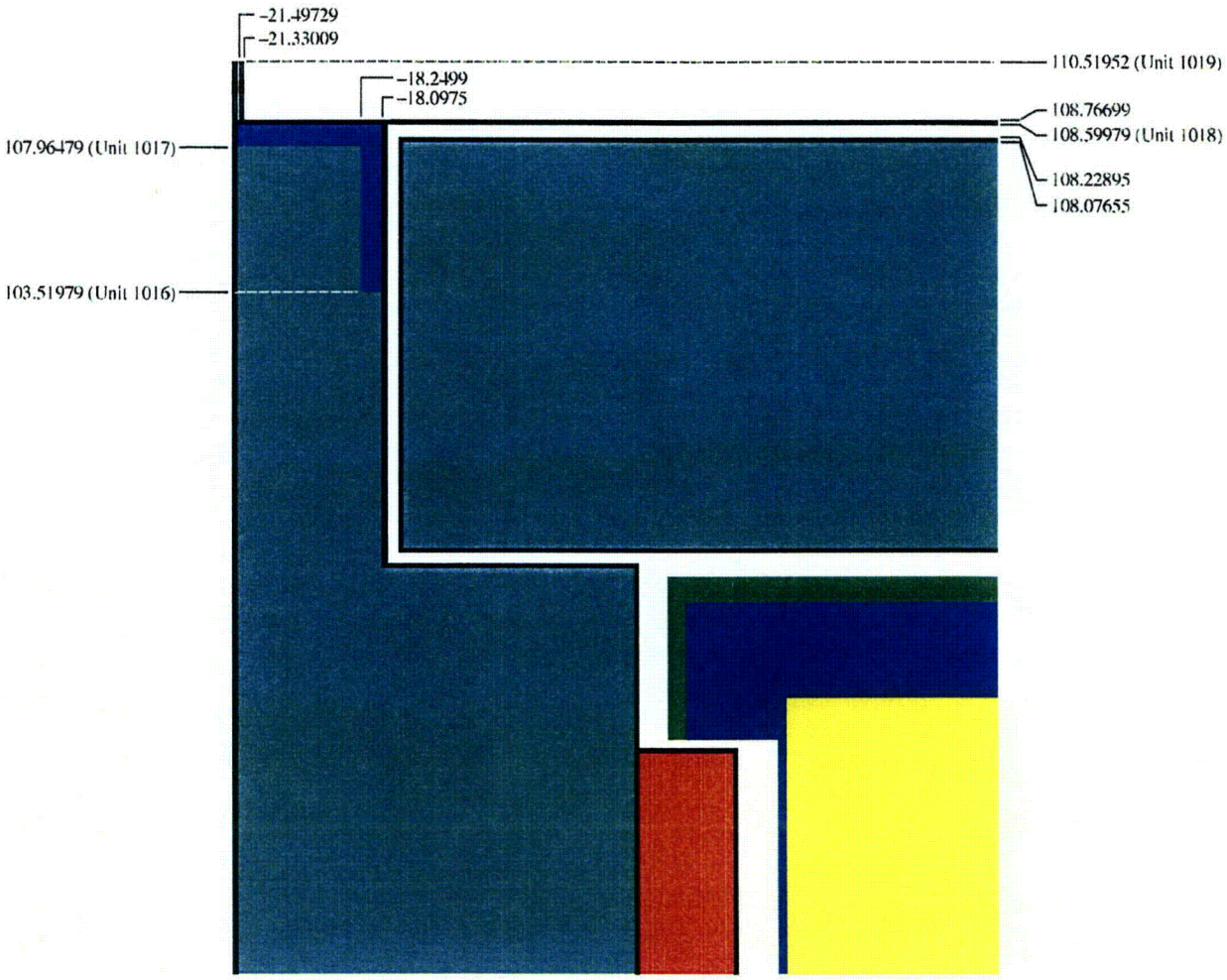

Fig. 6.10. R/Z section view at the top of the ES-3100 array packaging showing KENO V.a geometry units 1016–1019. Dimensions are in centimeters.

The KENO V.a users manual (SCALE, Vol. 2, Sect. F11) describes the input statements for an ETP model of cylinders in a close-pack array. This technique is adapted for modeling the ES-3100 in small compact array configurations. The ETP geometry model is much more complicated than the reduced-diameter approximation model described previously, but it yields smaller package configurations with correspondingly higher CSI values than the 7×7×3 and 5×5×2 package arrangements. Use of the ETP geometry specification allows for constructing compact package arrangements of 27×3 (27 packages in the horizontal plane stacked 3 packages high) and 16×3 packages.

6.3.1.3 Calculation models for damaged packages

Sections 2, 3, and 4 of this report address the overall integrity of the Model ES-3100 package in tests for NCT and HAC. (ORNL/NTRC-013) From a dimensional viewpoint, the only physical changes of interest for criticality safety occurred as a result of the 9-m (30-ft) drop test, the crush test, and the 1-m (40-in.) puncture test. There was significant crushing of the drum rim at the point of impact from the 9-m (30-ft) drop test and an indentation on the drum side from the 1-m (40-in.) puncture test. Even though significant crushing of the drum mid-section and bottom occurs, the effective center-to-center spacing of the contents actually increases under HAC. Selective rearrangement of alternating packages would be required to achieve a more compact array; however, this event is not credible.

The deformation of the outer diameters of the drum as-predicted by finite element analysis is presented in Table 6.3. These diameters measured along the 90–270° and 0–180° axes are specified at five node points located along the vertical axis of an upright package. These node points are designated in a downward direction from the top of the drum as "UR," "MUR," "MR," "MLR," and "LR." Equivalent circular diameters for representing the deformed drum in the calculation models for the HAC study (Appendix 6.9.2) are based on the assumption that the drum cross section at each deformation point is ellipsoidal.

The package water content in the void spaces external to the containment vessel and the interstitial spaces between drums is varied in the calculation model while maintaining the Kaolite in the dry condition. At a low moisture content where neutronic interaction between packages of an array is greatest, there is no statistically significant difference in the calculated neutron multiplication factor for package models based on the "MR," "MLR," and "LR" node points. At high moisture content where a statistically significant difference in the calculated neutron multiplication factor occurs, the packages of an array are nearly isolated. The slight increase in k_{eff} at the smaller diameters is not numerically significant. A calculation model based on the "MLR" node point is used to represent HAC.

As concluded in Sect. 6.9.2.3, the criticality analysis of an array of HAC packages based on the "MLR" package model (diameter = 17.20 in.) in rectangular pitch bounds the analysis of damaged packages (diameter = 17.26 in.) in close-pack array configurations. Considering both the irregular shape of the deformed drums and the fact that overall (maximum) dimensions rather than a mean or minimum dimension for a damaged package would establish array spacing—this assumption is a reasonable one, and the model is conservative.

The neutron poison, Kaolite refractory material, and stainless-steel components of the ES-3100 package were not significantly damaged during thermal testing. The principal material change of consequence that occurred during the thermal test was the loss of volatile material (Sect. 2.7.4). No loss of volatile material other than steam from the Kaolite was experienced during prototype testing of the Model ES-3100 package.

Table 6.3. Deformation of 18.37-in.-diam ES-3100 drum projected by finite element analysis Case "3100 RUN1HL Lower Bound Kaolite May 2004"

Deformation point	FEA node	Diameter at 90° (in.)	Diameter at 180° (in.)	Equivalent circular diameter (in.)
UR	098194	20.02	15.60	17.67
MUR	100238	20.74	15.07	17.68
MR	101589	20.74	14.18	17.15
MLR	103012	22.00	13.44	17.20
LR	105786	20.92	12.92	16.44

Physical damage is significant in terms of criticality safety when the amount of volatile hydrogenous material available for interstitial moderation is reduced. Conversely, the package could be saturated with water during water immersion conditions. Both possibilities affect only the amount of interstitial moderation. The representation of the changes to material composition from temperature extremes and water intrusion is addressed in Sect. 6.3.2.

In the case of broken metal content, the ETP geometry specification using the "MLR" package model (diameter = 17.20 in.) produces a 16×3 package configuration having a correspondingly higher CSI value than a 5×5×2 package arrangement. This allows for a greater fissile payload.

6.3.1.4 Calculation models for catastrophically-damaged packages (air-transport)

It is possible for accidents to be substantially more severe in the air transport mode than in the surface transport mode. Thus, the performance requirements for packages designed to be transported by air are more stringent. Regulatory Guide 7.9 states that the criticality evaluation should evaluate a single package under the expanded accident conditions specific in 10 CFR 71.55(f).

For a fissile material package designed to be transported by air, 10 CFR 71.55(f) requires the criticality evaluation demonstrate that the package be subcritical, assuming no water inleakage and reflection by 20 cm (7.9 in.) of water, when subjected to the sequential application of the HAC free drop and crush tests of 10 CFR 71.73(c)(1 and 2) and the modified puncture and thermal tests of 10 CFR 71.55(f)(1)(iii and iv).

Physical testing of Type-B fissile material packages transported by air was not conducted for the ES-3100. In lieu of testing, criticality calculations are performed using calculation models that conform to the basic requirements of 10 CFR 71.55(f) regarding both the reflection of the package by 20 cm of water and the absence of water inleakage. In addition, the air-transport calculation models incorporate features exhibiting the worst-case assumptions made regarding the geometric arrangement of the packaging and package contents. No credit is taken for the geometric form of the package content. Spherical geometry is used to represent the ultimate configuration of the ES-3100 package which undergoes catastrophic destruction.

The criticality analysis for air transport does not credit the ES-3100 for maintaining the geometry configuration of the packaged content. Fissile material is configured spherical in shape for optimization of neutron multiplication. Also, the criticality analysis does not credit the ES-3100 packaging for structural

integrity of the containment and the confinement. The reactivity "enhancing" materials of the packaging and of the accident environment may be interspersed with the fissile material content. However, selective removal of the neutron absorbing material of the package (i.e., Kaolite and stainless steel) accompanied by retention of the moderating constituents of the neutron absorbing material (i.e., bound water in the Kaolite) is not a credible condition. Moreover, a calculation model where the fissile material is homogenized with moderating material, is only an appropriate representation when the fissile material content being shipped consists of numerous solid pieces uranium ("broken metal"), oxide, or crystals. Homogenization of fissile material with moderating material is not performed with exclusive preference given to specific constituents of the moderating material.

A set of six calculation models are constructed in order to determine the worst case or most reactive configuration with consideration given to the efficiency of moderators, loss of neutron absorbers, rearrangement of packaging components and contents, geometry changes, and temperature effects. The fissile material component is dry in each case.

Model 1 (Fig. 6.11) represents the fissile material content configured into a spherical core with a 20.0-cm thick water reflector. All ES-3100 packaging material (Kaolite, stainless steel, 277-4 neutron poison, etc.) is excluded from Model 1. The fissile material content considered in the calculation model consists of a specific material form: solid HEU metal (7 – 10 kg ^{235}U); TRIGA fuel (10 kg $UZrH_x$ having 921 g ^{235}U); or broken HEU metal ($\leq$ 7 kg ^{235}U). The presence of hydrogenous packing material inside the containment vessel is also addressed in this calculation model. 513 g of polyethylene is used to represent a maximum amount of hydrogenous packing material in the ES-3100. For 7 kg ^{235}U HEU homogenized with 513 g of polyethylene, the radius of the core is 6.0547 cm. The parametric variation of both the ^{235}U mass and the enrichment in Model 1 is used to establish a reference point for the evaluation neutron reflection and absorption effects on k_{eff} provided by the stainless steel and Kaolite packaging material, addressed separately in Models 2 and 3.

Model 2 (Fig. 6.12) represents a spherical core of Model 1 blanketed by a variable-thickness shell of stainless steel, and a 20.0 cm thick water reflector external to the shell. The shell at maximum thickness corresponds to the 66,133 g stainless steel of the containment vessel and the liner and drum assembly. For 7 kg ^{235}U HEU metal, the radius of the core is 6.0547 cm while the outer radius of the stainless steel shell is 13.0264 cm.

Model 3 (Fig. 6.13) is configured the same as Model 2 with the exception that the variable-thickness shell is composed of the Kaolite instead of stainless steel. At maximum shell thickness, the 128,034 g of Kaolite corresponds to the mass of water-saturated Kaolite inside the drum body weldment and the drum top plug. The 76,819 g of saturation water corresponds to the amount of water in the Kaolite cast-slurry prior to baking. For 7 kg ^{235}U HEU metal, the radius of the core is 6.0547 cm while the outer radius of the Kaolite shell is 31.0814 cm. The parametric variation of shell thickness in Models 2 and 3 is performed for the purpose of evaluating the effect on k_{eff} of neutron reflection and absorption provided by each packaging material.

Models 1–3 are applicable for establishing loading limits for air transport packages having a single piece or several pieces of solid HEU metal where the integrity of the content can be established based on package tests or dynamic impact simulations per Type-C test criteria. Otherwise, the criticality evaluation of additional accident models is required for those situations where: (1) data is not available or is inadequate for discounting fragmentation of the fissile content in the air transport accident, or (2) the fissile material is in a physical form (crystals, oxide, or multiple pieces of solids) having the potential to blend with the other material of the package in the air transport accident.

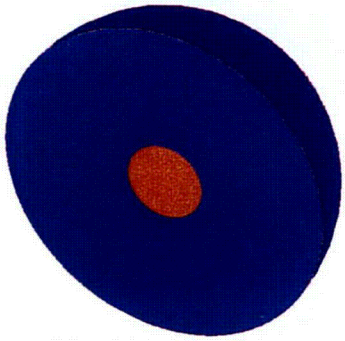

Fig. 6.11. Model 1.
7 kg ^{235}U (red) reflected by 20 cm of water (blue).

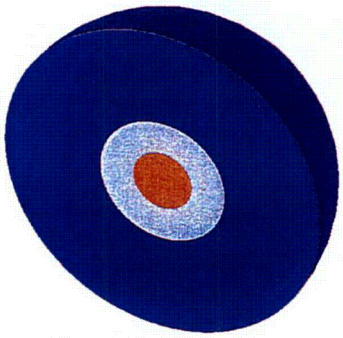

Fig. 6.12. Model 2.
7 kg ^{235}U (red) blanketed by a stainless-steel shell (gray), reflected by 20 cm of water (blue).

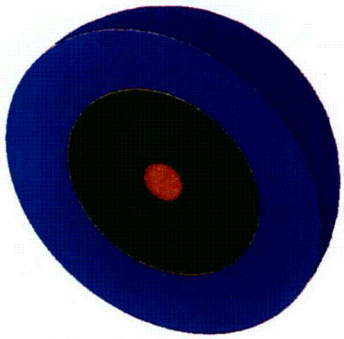

Fig. 6.13. Model 3.
7 kg ^{235}U (red) blanketed by a Kaolite shell (green), reflected by 20 cm of water (blue).

Model 4 (Fig. 6.14) depicts a spherical core of broken metal homogenized with water-saturated Kaolite and hydrogenous packing materials inside the containment vessel represented by 513 g of polyethylene. A 20-cm thick water reflector blankets the spherical core. All other ES-3100 packaging material (stainless steel, 277-4 neutron poison, etc.) is excluded from Model 4. For 25 kg of HEU (5 kg of ^{235}U), the radius of the homogenized core ranges from 31.4499 cm with dry Kaolite to 39.1608 cm with water saturated Kaolite. Model 4 also applies to TRIGA fuel content.

Model 5 (Fig. 6.15) is an extension of Model 3 applied to the case of TRIGA fuel and broken metal contents. Excess water from saturated Kaolite is homogenized with the fissile material in the core. For 25 kg of HEU where 5 kg of ^{235}U is homogenized with 513 g of polyethylene and 7,461 g of excess water from water saturated Kaolite, the radius of the spherical core is 13.0681 cm. The exterior Kaolite shell containing 69,357.9 g of water and the 51,214.9 g of vermiculite-cement constituents, has an outer radius of 31.7599 cm. At the extreme condition where the entire 74,614.0 g of excess water excess from the water saturated Kaolite is homogenized with the core, the radius of the spherical core is 26.3485 cm. The exterior shell of dry Kaolite, containing 2204.7 g of bound water and 51,214.9 g of vermiculite cement constituents, has an outer radius of 36.3668 cm. Although an unlimited amount of moderator could be imparted from the environment, the amount of moderator interspersed with pieces of fissile material does not exceed the excess moisture absorbed by the Kaolite.

Model 6 (Fig. 6.16) is configured similarly to Model 4 with the exception that only a partial amount of broken metal resides in the homogenized core. The remainder of the fissile material is modeled as a shell external to the spherical core and internal to the 20.0 cm thick water reflector. The amount of fissile material in the homogenized core is varied in 500 g increments from the full amount of Model 5 minus 500 g to a minimum amount of 500 g HEU. In the case of 25 kg of broken metal where 4.5 kg of ^{235}U is homogenized with 513 g of polyethylene and water-saturated Kaolite, the radius of the core is 39.1539 cm while the outer radius of the exterior 0.5 kg shell of ^{235}U is 39.1609 cm. In the case where 0.5 kg of ^{235}U is homogenized with 513 g of polyethylene and water-saturated Kaolite, the radius of core is 39.0992 cm while the outer radius of the exterior 4.5 kg shell of ^{235}U is 39.1609 cm. Model 6 addresses potential redistribution of fissile material consisting of multiple pieces, specifically the broken metal content. The parametric variation of shell thickness in Model 6 is performed for the purpose of evaluating the effect on k_{eff} of moderation efficiency of the core and enhanced neutron multiplication of the shell.

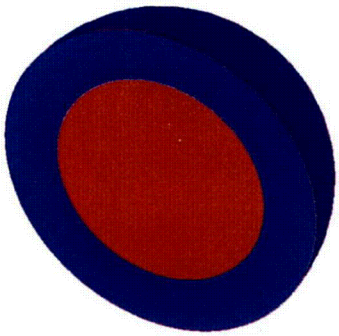

Fig. 6.14. Model 4.
Homogenized sphere of 5 kg ^{235}U, polyethylene, and water saturated Kaolite (red), reflected by 20 cm of water (blue).

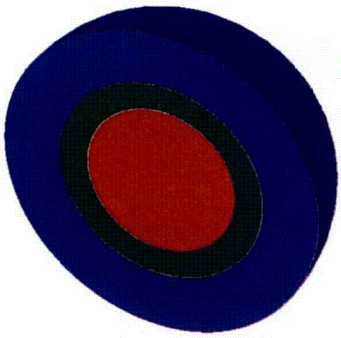

Fig. 6.15. Model 5.
Homogenized sphere of 5 kg ^{235}U and excess moisture from Kaolite (red), blanketed by Kaolite shell (lt. green), reflected by 20 cm of water (blue).

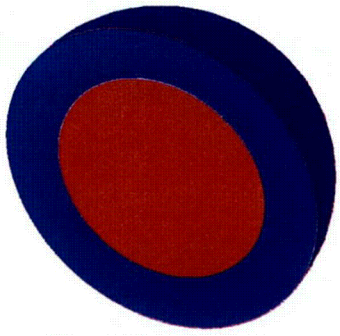

Fig. 6.16. Model 6.
Homogenized sphere of 4.5 kg ^{235}U, polyethylene, and water saturated Kaolite (red); blanketed by shell of 0.5 kg ^{235}U (not visible), reflected by 20 cm of water (blue).

Models 1–6 are applicable to air transport of the ES-3100 package given that the physical integrity of the fissile content following the air transport accident can not be established, or that the physical form of fissile material content may be multiple solid pieces or oxide.

6.3.2 Material Properties

Criticality calculation models include the definition of material compositions in the geometry model for both NCT and HAC. The materials which affect nuclear criticality safety and may be present in the ES-3100 package during these conditions are fissile material content (HEU metal, aluminum and molybdenum alloys of uranium, HEU product or skull oxide, UNX crystals, or $UZrH_x$), stainless steel, 277-4 neutron poison, Kaolite, silicon rubber, Teflon or polyethylene, and various amounts of water. Other materials are present in the package (e.g., tin-coated steel convenience cans, nylon bagging, rubber O-rings, and trace impurities). However, these other materials are not present in amounts that will significantly affect the reactivity of the package. Detailed discussion of the package content and packaging materials is contained in Appendix 6.9.3. Specific topics are summarized in this section as required to support the discussion of the criticality calculations presented in Sects. 6.4–6.6.

277-4 neutron poison is designed to maximize the hydrogen content necessary for thermalizing fast neutrons for capture in the boron constituent. 277-4 is a formulation of Thermo Electron Corporation's Cat 277-0, a boron carbide additive, and water. This mixture is cast and dried. "Loss On Drying" (LOD) tests are used to measure the amount of water in the as manufactured 277-4 casting. The as-manufactured neutron poison material at 100 lb/ft^3 and 31.8% LOD has a hydrogen concentration of 3.56 wt % and a natural boron concentration of 4.359 wt %. (DAC-PKG-801624-A001, Table 5)

The testing of 277-4 reveals that the material will dehydrate at elevated temperatures. Test specimens were dried at 250°F for 168 hours to reach the NCT state, and weight measurements were taken. These specimens where subsequently heated to 320°F for 4 hours to reach the HAC state, and weight measurements were again taken. The compositions of 277-4 at NCT and HAC states were derived by adjustment of the formulation specification for measured losses taking into account the statistical variations in the data. Conservation of mass for non-volatiles was observed in the derivation of material specifications based upon testing. Given that hydrogen presence is key to the effectiveness of the neutron poison, conservative material specifications were derived for minimum hydrogen content and minimum material density.

The NCT material specification for 277-4 at minimum density (95.39 lb/ft^3) and minimum hydrogen (25.15% LOD) is given in Table 11 of DAC-PKG-801624-A001. The average density of 277-4 in the ES-3100 package used for NCT calculations in KENO V.a is 1.52797 g/cm^3; the boron constituent is 7.31015e-2 g/cm^3; the residual base is 1.07070 g/cm^3; and the water component is 3.84169e-01 g/cm^3 (Appendix 6.9.3, Table 6.9.3.3-2). The HAC material specification at minimum density (95.32 lb/ft^3) and minimum hydrogen (25.09% LOD) is given in Table 12 of DAC-PKG-801624-A001. The average density of 277-4 used for HAC calculations in KENO V.a is 1.52680 g/cm^3; the boron constituent is 7.31015e-2 g/cm^3; the residual base is 1.07071 g/cm^3; and the water component is 3.82995e-1 g/cm^3 (Appendix 6.9.3, Table 6.9.3.3-3).

A set of 20 canned spacer assemblies as-manufactured has an average weight of 591.55 g. On average, the weight of an empty can with a lid is 86.05 g, and the 277-4 is 505.5 g. On the basis of volumetric measurements, the neutron poison is ~10.075 oz or 297.95 cm^3. The resultant 277-4 density is 1.6966 g/cm^3. The corresponding minimum mass is 473.84 g (given that the 277-4 material inside the spacer can is ≥4.07-in. diam and 1.31-in. thickness). Based on model dimensions of 4.13-in. diam × 1.37-in. height and use of composition data from Table 11 of DAC-PKG-801624-A001 (as-manufactured material at minimum density and hydrogen), the mass of neutron poison in the calculation model of the canned spacer is conservatively modeled as 457.15 g.

The density of 277-4 in the liner inner cavity is further reduced by a factor of 0.966893 because the actual volume of neutron poison is 12,831.4 cm^3 in the package, but 13,270.8 cm^3 is used in the calculation model. Also, guidance in Sect. 6.5.3.2 of NUREG-1609 requires that 75% of elemental boron be used in the material specification. Consequently, the minimum weight of 277-4 in the liner inner cavity of the calculation models is 19.37 kg (42.71 lb) for NCT and 19.36 kg (42.67 lb) for HAC, determined from the input density and the volume of the 277-4 region calculated by KENO V.a.

Kaolite is a lightweight, low thermal conductivity, refractory material that is used in the ES-3100 package between the drum and the inner liner. Kaolite is formed by mixing a dry constituent powder with water, pouring the mixture into a casting form, and curing and baking the cast. For NCT, the average density of Kaolite in the Model ES-3100 package is 0.34438 g/cm^3, and the residual water is 0.01493 g/cm^3 (Appendix 6.9.3, Sect. 6.9.3.4). The nominal weights of Kaolite in the liner outer cavity and in the top plug as determined from the input density and the region volumes calculated by KENO V.a are 49.04 kg (108.1 lb) and 4.37 kg (9.63 lb), respectively.

Kaolite is a nonvolatile refractory material, not significantly damaged by thermal excursions associated with HAC. It is assumed that upon immersion, a cured and dried casting will absorb a quantity of water equal to that required during preparation. This assumption is valid because the casting is fully saturated with water prior to curing and baking, and the casting does not change volume significantly during baking. The maximum water content of Kaolite refractory material is the water content of manufacture (1.5 g water per gram dry Kaolite) equivalent to a density of 0.51655 g/cm^3. For the single package, water saturation in the Kaolite region maximizes the effect of self-reflection in the surrounding package. This condition is assumed in the NCT single package calculations. For an array of packages, neutronic interaction between packages is maximized when the minimum amount of water is present in the Kaolite, which occurs in the as-manufactured condition. A volume fraction of 1.0 in the material specification corresponds to the water-saturated condition, while a volume fraction of 0.0289 corresponds to the dry condition.

The fissile material content packed into the containment vessel is ordinarily dry. Given that a flooded containment vessel is assumed for both NCT and HAC, the concurrent condition where the water-saturated Kaolite is baked dry beyond the as-manufactured condition while the containment vessel remains flooded is considered not credible. Therefore, the as-manufactured condition is assumed for the Kaolite water content in the HAC array analysis.

All other material compositions for HAC are identical to the material compositions for NCT. For the HAC calculation model, the densities for the Kaolite in the body weldment liner inner cavity, the stainless steel of the angle iron, and the drum steel are adjusted to correspond with changes in dimensions. However, the atomic densities do not change in the HAC calculation model because mass is conserved.

The material composition used in the calculation model for the containment vessel, the drum liner, and the drum is Type 304 stainless steel at a density of 7.94 g/cm^3. The density and composition of the 304 stainless steel for the drum is taken from the Standard Composition Library of the Standardized Computer Analysis for Licensing Evaluation (SCALE) code system. The nominal weights of these components, as determined by input density and volume calculated by KENO V.a, are 14.9 kg (32.85 lb) for the containment vessel, 15.67 kg (34.55 lb) for the drum liner, and 25.44 kg (56.1 lb) for the drum.

The amount of hydrogenous packaging material used for packing the content in the containment vessel is an unknown variable. Polyethylene with a density of 0.92 g/cm^3 and a molecular formula of CH_2 has the greatest hydrogen density of potential packing materials. Although polyethylene bags are generally used in packing for contamination control, the exact mass of the polyethylene bags used is unknown. Multiple bags may be used to package the contents and to enclose the convenience cans, or bags may be omitted altogether. Realistically, the number of polyethylene bags used to bag the contents and wrap a convenience can would be six bags at most. Given that each bag weighs ~28 g, this results in a maximum of ~510 g of polyethylene per ES-3100 package. Possibly additional sources of hydrogenous material inside the containment vessel include can pads, vinyl tape, and polyethylene (~85 g) or Teflon (~303 g) bottles.

For the criticality calculations, the sources of hydrogen contained in packing materials are not distinguished from other sources of hydrogen inherent in the fissile material content. Therefore, packing material mass is defined as all sources of hydrogenous packing materials inside the containment vessel plus the actual moisture in the content as constituent (the bonded hydrogen in UNX crystals or impurities in the oxide.) Given content moisture is not to exceed 6 wt %, the amount of hydrogenous material inside the containment vessel is not expected to exceed 2,400 g.

Containment vessel flooding is assumed in calculations performed for the derivation of fissile material loading limits. Even though both the NCT tests under 10 CFR 71.71 and the HAC tests under 10 CFR 71.73 demonstrate that containment is not breached, this simulated condition produces package

configurations in the criticality calculations that are more reactive than the actual package configurations. The 7.1–10.1 kg quantities of evaluation water required in both the NCT and HAC criticality calculations bound reasonable amounts of hydrogenous material and inherent moisture of fissile material (primarily HEU oxides) present inside the containment vessel (2,400 g).

HAC alter only the amount of volatile hydrogenous material contained in the package external to the containment vessel (Sect. 2.7.3). High temperatures may reduce the hydrogenous material content of the Kaolite. Conversely, water intrusion may increase the hydrogenous material content in the package. Thus, the package's range of possible volatile hydrogenous material content varies from none, caused by high temperatures, to the maximum possible value caused by water intrusion.

Table 6.4 lists the material, density, atomic or isotopic constituent, and atomic or isotopic weight percent as basic data for materials used in the single-unit packaging and array calculation models in this criticality safety evaluation for NCT and HAC, respectively. Appendix 6.9.3 provides the rationale, justification, or both for using the basic data for computing atomic densities listed in Table 6.4.

Table 6.4. Material compositions used in the ES-3100 calculation models

Material	Mix. No.	Theoretical density input parameter (g/cm^3)[a]	Volume fraction	Constituent	Atomic weight	Weight fraction	Atomic density (atoms/b-cm)
Fissile material contents							
Uranium (solid metal)	1	18.81109	1.0	^{235}U	235.0441	1.00	4.81970e-02
				^{238}U	238.0510	0.00	0.0
Uranium (solid metal)	1	18.82298	1.0	^{235}U	235.0441	0.95	4.58156e-02
				^{238}U	238.0510	0.05	2.38089e-03
Uranium (solid metal)	1	18.83488	1.0	^{235}U	235.0441	0.90	4.34317e-02
				^{238}U	238.0510	0.10	4.76479e-03
Uranium (solid metal)	1	18.85873	1.0	^{235}U	235.0441	0.80	3.86548e-02
				^{238}U	238.0510	0.20	9.54164e-03
Uranium (solid metal)	1	18.88264	1.0	^{235}U	235.0441	0.70	3.38659e-02
				^{238}U	238.0510	0.30	1.43306e-02
Uranium (solid metal)	1	18.90661	1.0	^{235}U	235.0441	0.60	2.90647e-02
				^{238}U	238.0510	0.40	1.91317e-02
Uranium (solid metal)	1	18.95474	1.0	^{235}U	235.0441	0.40	1.94258e-02
				^{238}U	238.0510	0.60	2.87707e-02
Uranium (solid metal)	1	19.00554	1.0	^{235}U	235.0441	0.19	9.25199e-03
				^{238}U	238.0510	0.81	3.89445e-02
Uranium oxide (UO_2)	1	6.94256	1.0	H	1.0077	0.6490	2.69208e-02
				O	15.9904	16.4340	4.29699e-02
				^{235}U	235.0441	82.9170	1.47490e-02
Uranium oxide (U_3O_8)	1	6.75167	1.0	H	1.0077	0.3510	1.41552e-02
				O	15.9904	17.6620	4.49101e-02
				^{235}U	235.0441	81.9870	1.41826e-02
Uranium oxide (UO_3)	1	6.64270	1.0	H	1.0077	0.1730	6.86795e-03
				O	15.9904	18.0650	4.51925e-02
				^{235}U	235.0441	81.7620	1.39155e-02
Skull oxide (UO_3+graphite)	1	3.34850	1.0	H	1.0077	1.9000	3.80225e-02
				C	12.0001	11.9173	2.00261e-02
				O	15.9904	25.9923	3.27786e-02

Table 6.4. Material compositions used in the ES-3100 calculation models

Material	Mix. No.	Theoretical density input parameter (g/cm^3)[a]	Volume fraction	Constituent	Atomic weight	Weight fraction	Atomic density (atoms/b-cm)
				^{235}U	235.0441	56.0976	4.81282e-03
				^{238}U	238.0510	4.0929	3.46713e-04
UNH crystals	1	2.50804	1.0	H	1.0077	2.9770	4.46274e-02
(24000.0 g)				N	14.0033	5.2570	5.66985e-03
$[UO_2(NO_3)_2+6H_2O]$				O	15.9904	47.6480	4.50055e-02
				^{235}U	235.0441	44.1180	2.83495e-03
UNH crystals	1	1.56439	1.0	H	1.0077	6.2525	5.84562e-02
(9000.0 g)				N	14.0033	3.1604	2.12620e-03
$[UO_2(NO_3)_2+6H_2O]$				O	15.9904	64.0630	3.77431e-02
				^{235}U	235.0441	26.5240	1.06311e-03
UNH crystals	1	1.50149	1.0	H	1.0077	6.6172	5.93782e-02
(8000.0 g)				N	14.0033	2.9270	1.89000e-03
$[UO_2(NO_3)_2+6H_2O]$				O	15.9904	65.8907	3.72591e-02
				^{235}U	235.0441	24.5651	9.45006e-04
UNH crystals	1	1.06111	1.0	H	1.0077	10.3811	6.58313e-02
(1000.1 g)				N	14.0033	0.5178	2.36275e-04
$[UO_2(NO_3)_2+6H_2O]$				O	15.9904	84.7556	3.38697e-02
				^{235}U	235.0441	4.3455	9.45006e-04
~20% enriched UZrH	1	8.65974	1.0	H	1.0078	0.9554	4.94386e-02
(3466.7 g)				Zr	91.2196	54.0447	3.08972e-02
				^{235}U	235.0441	8.8558	1.96487e-03
				^{238}U	238.0510	36.1441	7.91816e-03
~70% enriched UZrH	1	5.70132	1.0	H	1.0078	1.5894	5.41480e-02
(2282.4 g)				Zr	91.2196	89.9107	3.38410e-02
				^{235}U	235.0441	5.9588	8.67175e-04
				^{238}U	238.0510	2.5413	3.69825e-04
Single-unit calculation models (NCT)							
277-4	2	1.50970	1.0	H	1.0077	2.84745	2.56909e-02
canned spacer				^{10}B	10.0130	0.65907	5.98418e-04
Table 11 data: [b]				^{11}B	11.0096	2.97264	2.45475e-03
as-manufactured,				C	12.0001	1.36094	1.03107e-03
minimum density and				N	14.0033	0.01000	6.49252e-06
hydrogen				O	15.9904	53.39650	3.03592e-02
				Na	22.9895	0.08326	3.29274e-05
				Mg	24.3048	0.23957	8.96150e-05
				Al	26.9818	27.69370	9.33137e-03
				Si	28.0853	1.74979	5.66427e-04
				S	32.0634	0.21865	6.19983e-05
				Ca	40.0803	8.39267	1.90373e-03
				Fe	55.8447	0.37575	6.11714e-05
Water-flooded CV	3	0.9982	1.0	H	1.0077	11.1909	6.67536e-02
				O	15.9904	88.8091	3.33856e-02

Table 6.4. Material compositions used in the ES-3100 calculation models

Material	Mix. No.	Theoretical density input parameter (g/cm^3)[a]	Volume fraction	Constituent	Atomic weight	Weight fraction	Atomic density (atoms/b-cm)
SS304	8	7.9400	1.0	C	12.0001	0.0800	3.18772e-04
containment				Si	28.0853	1.0000	1.70252e-03
vessel body				P	30.9741	0.0450	6.94680e-05
16.60 lb				Cr	51.9957	19.0000	1.74726e-02
but 15.74 lb used				Mn	54.9379	2.0000	1.74071e-03
				Fe	55.8447	68.3750	5.85446e-02
				Ni	58.6872	9.5000	7.74020e-03
SS304	9	7.9400	0.97267	C	12.0001	0.0800	3.10060e-04
containment vessel				Si	28.0853	1.0000	1.65599e-03
lower flange				P	30.9741	0.0450	6.75695e-05
used 3.36 lb				Cr	51.9957	19.0000	1.69951e-02
				Mn	54.9379	2.0000	1.69314e-03
				Fe	55.8447	68.3750	5.69445e-02
				Ni	58.6872	9.5000	7.52866e-03
SS304	10	7.9400	0.94348	C	12.0001	0.0800	3.00755e-04
containment vessel				Si	28.0853	1.0000	1.60629e-03
upper flange				P	30.9741	0.0450	6.55417e-05
used 13.75 lb				Cr	51.9957	19.0000	1.64850e-02
				Mn	54.9379	2.0000	1.64233e-03
				Fe	55.8447	68.3750	5.52356e-02
				Ni	58.6872	9.5000	7.30272e-03
277-4	11	1.45971	1.0	H	1.0077	2.84746	2.48404e-02
filling CV				^{10}B	10.0130	0.65907	5.78606e-04
inner-liner cavity				^{11}B	11.0096	2.97265	2.37348e-03
Table 11 data: [b]				C	12.0001	1.36094	9.96935e-04
as-manufactured,				N	14.0033	0.01000	6.27756e-06
minimum density and				O	15.9904	53.39660	2.93541e-02
hydrogen				Na	22.9895	0.08326	3.18372e-05
				Mg	24.3048	0.23957	8.66479e-05
				Al	26.9818	27.69360	9.02241e-03
				Si	28.0853	1.74979	5.47673e-04
				S	32.0634	0.21865	5.99456e-05
				Ca	40.0803	8.39266	1.84069e-03
				Fe	55.8447	0.37575	5.91461e-05
Kaolite	12	(body weldment)					
Al_2O_3		0.34864	0.096	Al	26.9818	52.9390	3.95461e-04
				O	15.9904	47.0610	—
SiO_2		0.34864	0.367	Si	28.0853	46.7570	1.28281e-03
				O	15.9904	53.2430	—
Fe_2O_3		0.34864	0.067	Fe	55.8447	69.9540	1.76211e-04
				O	15.9904	30.0460	—
TiO_2		0.34864	0.012	Ti	47.8793	59.9530	3.15486e-05
				O	15.9904	40.0470	—
CaO		0.34864	0.307	Ca	40.0803	71.4810	1.14955e-03
				O	15.9904	28.5180	—

Table 6.4. Material compositions used in the ES-3100 calculation models

Material	Mix. No.	Theoretical density input parameter (g/cm^3)[a]	Volume fraction	Constituent	Atomic weight	Weight fraction	Atomic density (atoms/b-cm)
MgO		0.34864	0.131	Mg	24.3048	60.3170	6.82560e-04
				O	15.9904	39.6830	—
Na_2O		0.34864	0.020	Na	22.9895	74.1960	1.35522e-04
				O	15.9904	25.8040	—
Total O		—	—	—	15.9904	—	5.39065e-03
Water	12	0.52294	1.0	H	1.0077	11.1909	3.49711e-02
				O	15.9904	88.8091	1.74856e-02
Kaolite	13	(top plug)					
Al_2O_3		0.33241	0.096	Al	26.9818	52.9390	3.77052e-04
				O	15.9904	47.0610	—
SiO_2		0.33241	0.367	Si	28.0853	46.7570	1.22309e-03
				O	15.9904	53.2430	—
Fe_2O_3		0.33241	0.067	Fe	55.8447	69.9540	1.68008e-04
				O	15.9904	30.0460	—
TiO_2		0.33241	0.012	Ti	47.8793	59.9530	3.00799e-05
				O	15.9904	40.0470	—
CaO		0.33241	0.307	Ca	40.0803	71.4810	1.09604e-03
				O	15.9904	28.5180	—
MgO		0.33241	0.131	Mg	24.3048	60.3170	6.50785e-04
				O	15.9904	39.6830	—
Na_2O		0.33241	0.020	Na	22.9895	74.1960	1.29213e-04
				O	15.9904	25.8040	—
Total O		—	—	—	15.9904	—	5.13975e-03
Water	13	0.49860	1.0	H	1.0077	11.1909	3.33433e-02
				O	15.9904	88.8091	1.66717e-02
silicon rubber pads	14	1.21791	1.0	H	1.0077	8.1562	5.93660e-02
				C	12.0001	32.3774	1.97887e-02
				O	15.9904	21.5782	9.89729e-03
				SI	28.0853	37.8882	9.89432e-03
Water—CV well	15	0.9982	variable	H	1.0077	11.1909	variable
				O	15.9904	88.8091	variable
SS304 liner	16	7.94	1.0	C	12.0001	0.0800	3.18772e-04
				Si	28.0853	1.0000	1.70252e-03
				P	30.9741	0.0450	6.94680e-05
				Cr	51.9957	19.0000	1.74726e-02
				Mn	54.9379	2.0000	1.74071e-03
				Fe	55.8447	68.3750	5.85446e-02
				Ni	58.6872	9.5000	7.74020e-03
SS304 plug cover used 9.907 lb	17	7.94	1.06388	C	12.0001	0.0800	3.39135e-04
				Si	28.0853	1.0000	1.81128e-03
				P	30.9741	0.0450	7.39056e-05
				Cr	51.9957	19.0000	1.85887e-02
				Mn	54.9379	2.0000	1.85191e-03
				Fe	55.8447	68.3750	6.22844e-02

Table 6.4. Material compositions used in the ES-3100 calculation models

Material	Mix. No.	Theoretical density input parameter (g/cm^3)[a]	Volume fraction	Constituent	Atomic weight	Weight fraction	Atomic density (atoms/b-cm)
				Ni	58.6872	9.5000	8.23464e-03
SS304 angle iron	18	7.94	1.0	C	12.0001	0.0800	3.18772e-04
				Si	28.0853	1.0000	1.70252e-03
				P	30.9741	0.0450	6.94680e-05
				Cr	51.9957	19.0000	1.74726e-02
				Mn	54.9379	2.0000	1.74071e-03
				Fe	55.8447	68.3750	5.85446e-02
				Ni	58.6872	9.5000	7.74020e-03
SS304 steel drum	19	7.94	1.0	C	12.0001	0.0800	3.18772e-04
				Si	28.0853	1.0000	1.70252e-03
				P	30.9741	0.0450	6.94680e-05
				Cr	51.9957	19.0000	1.74726e-02
				Mn	54.9379	2.0000	1.74071e-03
				Fe	55.8447	68.3750	5.85446e-02
				Ni	58.6872	9.5000	7.74020e-03
Water—interstitial	20	0.9982	variable	H	1.0077	11.1909	variable
				O	15.9904	88.8091	variable
Water—reflector	21	0.9982	1.0	H	1.0077	11.1909	6.67536e-02
				O	15.9904	88.8091	3.33856e-02
Array calculation models (NCT)							
Kaolite	12	(body weldment)					
Al_2O_3		0.42622	0.096	Al	26.9818	52.9390	4.83460e-04
				O	15.9904	47.0610	—
SiO_2		0.42622	0.367	Si	28.0853	46.7570	1.56821e-03
				O	15.9904	53.2430	—
Fe_2O_3		0.42622	0.067	Fe	55.8447	69.9540	2.15422e-04
				O	15.9904	30.0460	—
TiO_2		0.42622	0.012	Ti	47.8793	59.9530	3.85688e-05
				O	15.9904	40.0470	—
CaO		0.42622	0.307	Ca	40.0803	71.4810	1.40535e-03
				O	15.9904	28.5180	—
MgO		0.42622	0.131	Mg	24.3048	60.3170	8.34444e-04
				O	15.9904	39.6830	—
Na_2O		0.42622	0.020	Na	22.9895	74.1960	1.65678e-04
				O	15.9904	25.8040	—
Total O		—	—	—	15.9904	—	6.58477e-03
Water	12	0.63931	0.287	H	1.0077	11.1909	1.22702e-03
				O	15.9904	88.8091	6.13510e-04
Kaolite	13	(top plug)					
Al_2O_3		0.33241	0.096	Al	26.9818	52.9390	3.77052e-04
				O	15.9904	47.0610	—
SiO_2		0.33241	0.367	Si	28.0853	46.7570	1.22309e-03
				O	15.9904	53.2430	—
Fe_2O_3		0.33241	0.067	Fe	55.8447	69.9540	1.68008e-04
				O	15.9904	30.0460	—

Table 6.4. Material compositions used in the ES-3100 calculation models

Material	Mix. No.	Theoretical density input parameter (g/cm^3)[a]	Volume fraction	Constituent	Atomic weight	Weight fraction	Atomic density (atoms/b-cm)
TiO_2		0.33241	0.012	Ti	47.8793	59.9530	3.00799e-05
				O	15.9904	40.0470	—
CaO		0.33241	0.307	Ca	40.0803	71.4810	1.09604e-03
				O	15.9904	28.5180	—
MgO		0.33241	0.131	Mg	24.3048	60.3170	6.50785e-04
				O	15.9904	39.6830	—
Na_2O		0.33241	0.020	Na	22.9895	74.1960	1.29213e-04
				O	15.9904	25.8040	—
Total O		—	—	—	15.9904	—	5.13548e-03
Water	13	0.49860	0.0287	H	1.0077	11.1909	9.56954e-04
				O	15.9904	88.8091	4.78477e-04
SS304 angle iron	18	7.94	1.25705	C	12.0001	0.0800	4.00712e-04
				Si	28.0853	1.0000	2.14015e-03
				P	30.9741	0.0450	8.73248e-05
				Cr	51.9957	19.0000	2.19639e-02
				Mn	54.9379	2.0000	2.18816e-03
				Fe	55.8447	68.3750	7.35934e-02
				Ni	58.6872	9.5000	9.72982e-03
SS304 steel drum	19	7.94	0.99981	C	12.0001	0.0800	3.18711e-04
				Si	28.0853	1.0000	1.70220e-03
				P	30.9741	0.0450	6.94548e-05
				Cr	51.9957	19.0000	1.74693e-02
				Mn	54.9379	2.0000	1.74038e-03
				Fe	55.8447	68.3750	5.85334e-02
				Ni	58.6872	9.5000	7.73873e-03
Water—reflector	21	1.16235	1.0	H	1.0077	11.1909	7.75911e-06
				O	15.9904	88.8091	3.88058e-06
Single-unit calculation models (HAC) same as NCT except as follows:							
277-4	2	1.50853	1.0	H	1.0077	2.84094	2.56124e-02
canned spacer				^{10}B	10.0130	0.65958	5.98418e-04
Table 12 data:[b]				^{11}B	11.0096	2.97494	2.45475e-03
as-manufactured,				C	12.0001	1.36193	1.03103e-03
minimum density and				N	14.0033	0.01001	6.49258e-06
hydrogen				O	15.9904	53.36920	3.03202e-02
				Na	22.9895	0.08333	3.29277e-05
				Mg	24.3048	0.23976	8.96158e-05
				Al	26.9818	27.71520	9.33140e-03
				Si	28.0853	1.75109	5.66409e-04
				S	32.0634	0.21882	6.19989e-05
				Ca	40.0803	8.39916	1.90373e-03
				Fe	55.8447	0.37604	6.11720e-05
277-4	11	1.45858	1.0	H	1.0077	2.84097	2.47645e-02
filling CV				^{10}B	10.0130	0.65959	5.78606e-04
inner-liner cavity				^{11}B	11.0096	2.97496	2.37348e-03
Table 12 data:[b]				C	12.0001	1.36193	9.96883e-04

Table 6.4. Material compositions used in the ES-3100 calculation models

Material	Mix. No.	Theoretical density input parameter (g/cm^3)[a]	Volume fraction	Constituent	Atomic weight	Weight fraction	Atomic density (atoms/b-cm)
as-manufactured, minimum density and hydrogen				N	14.0033	0.01001	6.27756e-06
				O	15.9904	53.36930	2.93162e-02
				Na	22.9895	0.08333	3.18372e-05
				Mg	24.3048	0.23976	8.66479e-05
				Al	26.9818	27.71510	9.02236e-03
				Si	28.0853	1.75109	5.47651e-04
				S	32.0634	0.21882	5.99456e-05
				Ca	40.0803	8.39913	1.84068e-03
				Fe	55.8447	0.37604	5.91461e-05
Kaolite	12	(body weldment)					
Al_2O_3		0.41898	0.096	Al	26.9818	52.9390	4.75248e-04
				O	15.9904	47.0610	—
SiO_2		0.41898	0.367	Si	28.0853	46.7570	1.54162e-03
				O	15.9904	53.2430	—
Fe_2O_3		0.41898	0.067	Fe	55.8447	69.9540	2.11763e-04
				O	15.9904	30.0460	—
TiO_2		0.41898	0.012	Ti	47.8793	59.9530	3.79136e-05
				O	15.9904	40.0470	—
CaO		0.41898	0.307	Ca	40.0803	71.4810	1.38148e-03
				O	15.9904	28.5180	—
MgO		0.41898	0.131	Mg	24.3048	60.3170	8.20270e-04
				O	15.9904	39.6830	—
Na_2O		0.41898	0.020	Na	22.9895	74.1960	1.62864e-04
				O	15.9904	25.8040	—
Total O		—	—	—	15.9904	—	6.47830e-03
Water	12	0.62843	1.0	H	1.0077	11.1909	4.20256e-02
				O	15.9904	88.8091	2.10128e-02
SS304 angle iron	18	7.94	1.23239	C	12.0001	0.0800	3.92851e-04
				Si	28.0853	1.0000	2.09817e-03
				P	30.9741	0.0450	8.56117e-05
				Cr	51.9957	19.0000	2.15330e-02
				Mn	54.9379	2.0000	2.14524e-03
				Fe	55.8447	68.3750	7.21497e-02
				Ni	58.6872	9.5000	9.53894e-03
SS304 steel drum	19	7.94	1.08401	C	12.0001	0.0800	3.45552e-04
				Si	28.0853	1.0000	1.84555e-03
				P	30.9741	0.0450	7.53040e-05
				Cr	51.9957	19.0000	1.89405e-02
				Mn	54.9379	2.0000	1.88695e-03
				Fe	55.8447	68.3750	6.34629e-02
				Ni	58.6872	9.5000	8.39045e-03
Array calculation models (HAC) same as NCT except as follows:							
Kaolite	12	(body weldment)					

Table 6.4. Material compositions used in the ES-3100 calculation models

Material	Mix. No.	Theoretical density input parameter (g/cm^3)[a]	Volume fraction	Constituent	Atomic weight	Weight fraction	Atomic density (atoms/b-cm)
Al_2O_3		0.42622	0.096	Al	26.9818	52.9390	4.83460e-04
				O	15.9904	47.0610	—
SiO_2		0.42622	0.367	Si	28.0853	46.7570	1.56821e-03
				O	15.9904	53.2430	—
Fe_2O_3		0.42622	0.067	Fe	55.8447	69.9540	2.15422e-04
				O	15.9904	30.0460	—
TiO_2		0.42622	0.012	Ti	47.8793	59.9530	3.85688e-05
				O	15.9904	40.0470	—
CaO		0.42622	0.307	Ca	40.0803	71.4810	1.40535e-03
				O	15.9904	28.5180	—
MgO		0.42622	0.131	Mg	24.3048	60.3170	8.34444e-04
				O	15.9904	39.6830	—
Na_2O		0.42622	0.020	Na	22.9895	74.1960	1.65678e-04
				O	15.9904	25.8040	—
Total O		—	—	—	15.9904	—	6.58477e-03
Water	12	0.63931	0.287	H	1.0077	11.1909	1.22702e-03
				O	15.9904	88.8091	6.13510e-04
Kaolite	13	(top plug)					
Al_2O_3		0.33241	0.096	Al	26.9818	52.9390	3.77052e-04
				O	15.9904	47.0610	—
SiO_2		0.33241	0.367	Si	28.0853	46.7570	1.22309e-03
				O	15.9904	53.2430	—
Fe_2O_3		0.33241	0.067	Fe	55.8447	69.9540	1.68008e-04
				O	15.9904	30.0460	—
TiO_2		0.33241	0.012	Ti	47.8793	59.9530	3.00799e-05
				O	15.9904	40.0470	—
CaO		0.33241	0.307	Ca	40.0803	71.4810	1.09604e-03
				O	15.9904	28.5180	—
MgO		0.33241	0.131	Mg	24.3048	60.3170	6.50785e-04
				O	15.9904	39.6830	—
Na_2O		0.33241	0.020	Na	22.9895	74.1960	1.29213e-04
				O	15.9904	25.8040	—
Total O		—	—	—	15.9904	—	5.13548e-03
Water	13	0.49860	0.0287	H	1.0077	11.1909	9.56954e-04
				O	15.9904	88.8091	4.78477e-04
SS304 angle iron	18	7.94	1.25705	C	12.0001	0.0800	4.00712e-04
				Si	28.0853	1.0000	2.14015e-03
				P	30.9741	0.0450	8.73248e-05
				Cr	51.9957	19.0000	2.19639e-02
				Mn	54.9379	2.0000	2.18816e-03
				Fe	55.8447	68.3750	7.35934e-02
				Ni	58.6872	9.5000	9.72982e-03
SS304 steel drum	19	7.94	0.99981	C	12.0001	0.0800	3.18711e-04

Table 6.4. Material compositions used in the ES-3100 calculation models

Material	Mix. No.	Theoretical density input parameter (g/cm^3)[a]	Volume fraction	Constituent	Atomic weight	Weight fraction	Atomic density (atoms/b-cm)
				Si	28.0853	1.0000	1.70220e-03
				P	30.9741	0.0450	6.94548e-05
				Cr	51.9957	19.0000	1.74693e-02
				Mn	54.9379	2.0000	1.74038e-03
				Fe	55.8447	68.3750	5.85334e-02
				Ni	58.6872	9.5000	7.73873e-03
Water—reflector	21	1.16235	1.0	H	1.0077	11.1909	7.75911e-06
				O	15.9904	88.8091	3.88058e-06

[a] The theoretical density input parameter is specified for each material such that the required (or desired) mass of material is represented in the KENO V.a calculation model. The mass of material is computed by KENO V.a as the product of the theoretical density input parameter times the volume fraction times the volume of the geometry region in which the material resides in the calculation model.

[b] DAC-PKG-801624-A001.

6.3.3 Computer Codes and Cross-Section Libraries

The Criticality Safety Analysis Sequences within the SCALE modular code system provide automated, problem-dependent, cross-section processing followed by calculation of the neutron multiplication factor (k_{eff}) for the system being modeled. (SCALE, Vol. 1, Sect. C4) Initiated by "=csas25" appearing on the first line in the user input, the CSAS module runs the CSAS25 control sequence. The cross-section processing functional modules BONAMI (SCALE, Vol. 2, Sect. F1) and NITAWL-II (SCALE, Vol. 2, Sect. F2) are activated, providing resonance-corrected cross sections to the multigroup Monte Carlo functional module, KENO V.a (SCALE, Vol. 2, Sect. F11). Using the processed cross sections, KENO V.a calculates the k_{eff} of three-dimensional system models. The geometric modeling capabilities available in KENO V.a, coupled with the automated cross-section processing, allow complex, three-dimensional systems to be easily analyzed.

The CSAS25 control sequence and the 238-group ENDF/B-V cross-section library in SCALE are used for all calculations. The control sequence, functional modules, and cross-section library are summarized in the following paragraphs.

The CSAS25 control sequence reads user-specified input data, which include the required cross-section library, specifications for mixtures, information for resonance processing of nuclides (size, geometry, and temperature), and a detailed geometry model for KENO V.a. Physical and neutronic information not specified but required by the functional modules (such as theoretical density, molecular weights, and average resonance region background cross sections) is supplied by the Standard Composition Library or calculated by the Materials Information Processor. The Standard Composition Library (SCALE, Vol. 3, Sect. M8) consists of a standard composition directory and table, an isotopic distribution directory and table, and a nuclide information table. The Materials Information Processor (SCALE, Vol. 3, Sect. M7) checks the input data pertaining to cross-section preparation and prepares binary input files for the applicable functional modules BONAMI and NITAWL-II.

The standardized automated procedures process SCALE cross sections using the Bondarenko method (via BONAMI) and the Nordheim integral method (via NITAWL-II) to provide a resonance-corrected cross-section library based on the physical characteristics of the problem being analyzed.

BONAMI performs resonance shielding through the application of the Bondarenko shielding factor method. BONAMI reads the master format library and applies the Bondarenko correction to all nuclides that have Bondarenko data. BONAMI produces a Bondarenko-corrected master format library which is read by NITAWL-II.

NITAWL-II applies the Nordheim Integral Treatment to perform neutron cross-section processing in the resonance energy range for nuclides that have ENDF/B resonance parameter data. This technique involves the numerical integration of ENDF/B resonance parameters using a calculated flux distribution, which is based on the calculated collision density across each resonance and subsequent weighing of the reaction cross section to the desired broad group structure. In the CSAS sequence, NITAWL-II assembles the group-to-group transfer arrays from the elastic and inelastic scattering components and performs other tasks to produce a problem-dependent, working cross-section library which can be used by KENO.

KENO V.a, a multigroup Monte Carlo computer code, is used to determine k_{eff} for multidimensional systems. The basic geometrical bodies allowed in KENO V.a for defining models are cuboids, spheres, cylinders, hemispheres, and hemicylinders. KENO V.a has the following major characteristics:

- enhanced geometry package that allows arrays to be defined and positioned throughout the model;
- P_n scattering treatment;
- extended use of differential albedo reflection;
- printer plots for checking the input model;
- energy-dependent data supergrouping;
- restart capability; and
- origin specifications for cuboids, spheres, cylinders, hemicylinders, and hemispheres.

The 238-group ENDF/B-V master cross-section library in SCALE is activated in the CSAS25 control sequence by specifying 238GROUPNDF5 (238GR) as the cross-section library name. The 238-GROUP ENDF/B-V library is a general-purpose criticality analysis library and the most complete library available in SCALE. The library contains data for all nuclides (more than 300) available in ENDF/B-V processed by the AMPX-77 systems. It also contains data for ENDF/B-VI evaluations of ^{14}N, ^{15}N, ^{16}O, ^{154}Eu, and ^{155}Eu. The library has 148 fast groups and 90 thermal groups (below 3 eV). Most resonance nuclides in the 238 group have resonance data (to be processed by NITAWL-II in the resolved resonance range) and Bondarenko factors (to be processed by BONAMI) for the unresolved range. The 238-group library contains resolved resonance data for s-wave, p-wave, and d-wave resonances **R** = 0, **R** = 1, and **R** = 2, respectively. These data can have a significant effect on results for under-moderated, intermediate-energy problems. Resonance structures in several light-to-intermediate mass "nonresonance" ENDF nuclides (i.e., ^{7}Li, ^{19}F, ^{27}Al, ^{28}Si) are accounted for using Bondarenko shielding factors. These structures can also be important in intermediate energy problems.

All nuclides in the 238-group library use the same weighting spectrum, consisting of:

- Maxwellian spectrum (peak at 300 K) from 10^{-5} to 0.125 eV,
- a 1/E spectrum from 0.125 eV to 67.4 keV,
- a fission spectrum (effective temperature at 1.273 MeV) from 67.4 keV to 10 MeV, and
- a 1/E spectrum from 10 to 20 MeV.

The k_{eff} values for each KENO V.a case are based on 500,000 neutron histories produced by running for 215 generations with 2,500 neutrons per generation and truncating the first 15 generations of data. The convergence of the KENO V.a calculation is related to trends in the average calculated k_{eff}. In general, the

KENO V.a output table of k_{eff} by Generation Skipped is reviewed for trends. If no trends are observed, the calculation is accepted, and the reported value of k_{eff} is the one with the most neutron histories. Usually there is no statistically significant difference between this result and the one with the smallest standard deviation.

No manual cross-section adjustment is performed for the criticality safety evaluation. Cross-section processing is performed automatically in the CSAS25 code sequence. By modeling the contents as precisely as possible, the information for correct cross-section processing is introduced into the evaluation.

The CSAS control module, the associated functional modules, cross sections, and databases used in this evaluation reside in the verified configuration control area designated **/vcc/scale4.4a** on a Hewlett Packard Series 9000 J Class workstation at the Y-12 Safety Analysis Engineering organization in Oak Ridge, Tennessee. The detailed input and computer output for the criticality safety evaluation of the ES-3100 shipping container with HEU reside in a configuration control area **/archive/ylf717_Rv2** on the workstation. Input listings of the key cases indicated in Tables 6.1a–6.1e are provided in Appendix 6.9.7.

6.3.4 Demonstration of Maximum Reactivity

10 CFR 71.55(b) requires the evaluation of water leakage into the containment vessel, leakage of liquid contents out of the containment vessel, and other conditions which produce maximum reactivity in the single package. For solid uranium contents, water leakage conditions are simulated by flooding all regions outside and inside of the containment vessel, including the sealed convenience cans. For liquid uranium contents, water leakage conditions are simulated by flooding all regions outside the containment vessel except the containment vessel well. Uranyl nitrate solution resides inside both the containment vessel, including the sealed convenience cans, and the well external to the containment vessel. According to the 10 CFR 71.55(b) requirement, a flooded containment vessel under full water reflection is also evaluated.

Credit for the high-integrity, watertight containment is not taken either in the single package analysis [10 CFR 71.55 (d, e)] or in the array analysis [10 CFR 71.59 (a)(1)] of undamaged packages. In the evaluation of undamaged packages under 10 CFR 71.59 (a)(1) and the evaluation of damaged packages under 10 CFR 71.59 (a)(2), the containment vessel is flooded with water, providing moderation to such an extent as to cause maximum reactivity of the content consistent with the chemical and physical form of the material present. Solid HEU, not solution HEU, is being shipped in the ES-3100. Consequently, in the evaluation of damaged packages under 10 CFR 71.59 (a)(2), the leakage out of the containment vessel of content moderated to such an extent as to cause maximum reactivity consistent with the physical and chemical form of the material is not considered credible HAC, based on results for tests specified in 10 CFR 71.73.

Contents are generally dry, and only small quantities of hydrogenous packing materials are used. However, credit for the high-integrity, watertight containment is not taken in this criticality evaluation. (Meeting, Docket 71-9315) Fissile material loading are restricted such that if a containment vessel were flooded, it would be adequately subcritical under full water reflection. But instead of loading limits being established in accordance with conditions of confinement and containment as demonstrated under the NCT and HAC tests, these single-unit fissile material loading limits are severely reduced on the basis of the array calculations where all of the containment vessels of the packages in an array are assumed to flooded but each packaging is dry. This has the effect of maximizing both the neutron source and neutronic interaction between packages. Because credit for the high-integrity, watertight containment is not fully taken in this criticality evaluation, and the fissile material mass loading limits developed as a result are very conservative.

Section 6.3.1 provides dimensional data for content and package models, and Sect. 6.3.2 provides material composition data used in the calculation models. Appendix 6.9.3 provides justification for the

composition data used in the evaluation. These sections and this appendix describe how the packaging dimensions and materials are optimized to produce a conservative model by reducing neutron absorbing materials and maximizing the reactivity of the fissile material content through the inclusion of water in the containment vessel.

As described in Sect. 6.3.1.1, a geometry region is defined by dimensions and the type of material contained therein. The amount of material within a region is quantified in terms of the density, material volume fraction, and the volume of the region (Sect. 6.3.2). The term "water fraction" means the fraction of the maximum specific gravity of water possible for any geometry region in the ES-3100 package. Therefore, the water content is the fraction of the maximum specific gravity of water possible in a material in the ES-3100 package when flooded.

The maximum value for the void regions (spaces external to the containment vessel) is 1.0 for both single-unit and array geometries. For the geometry regions containing Kaolite, the maximum values are 0.51655 for the single unit and 0.63931 for the array. For the geometry regions containing 277-4, the maximum value is 0.6942 for both the single-unit and array geometries. The same single-unit values are used in the array calculation models because the 277-4–bearing regions do not require adjustment for the close-pack approximation (Sect. 6.3.1.2).

In general, boundary condition specifications are not required in KENO V.a, so that calculation models analyzed using KENO V.a require no special boundary conditions. However, in this evaluation, the infinite array cases use a single package with a reduced radius modeled with spectral reflection on all faces of a surrounding cuboid. The energies and angular dependence of the neutrons are treated such that an infinite system with no neutron leakage is simulated.

For simplicity, the NCT and HAC sets of calculations were performed for selected ES-3100 array sizes by varying the water content of the ES-3100 package external to the containment vessel from zero to its maximum value. This technique bounds all NCT and HAC; however, only the relevant calculation results are used in determination of the CSI for criticality purposes.

Although four decimal places are shown for k_{eff} values in result tables, the actual accuracy of the code, for a particular calculation, may be on the order of ± 0.02–0.03 based on the spread in results for benchmark calculations. (Y/DD-896/R1, Y/DD-972/R1) Also, the standard deviation of the mean for a particular calculation is on the order of 0.001 for benchmark cases and somewhat higher for the package calculations. Therefore, numerical values are considered physically meaningful or significant to the third decimal place. The primary reason for reporting four (or five) decimal places for a calculation result is to confirm that the result reported actually originated from a given output file. A value of 0.925 is the USL used for this safety analysis report (Sect. 6.8.3).

6.4 SINGLE PACKAGE EVALUATION

The HEU content of a package is in one of the following forms: metal of a specified geometric shape; metal of an unspecified shape characterized as broken metal; uranium oxide; or UNH crystals. The bounding types of HEU content evaluated in this criticality analysis are 3.24-in. and 4.25-in.-diam cylinders; 2.29-in.-square bars; 1.5-in.-diam × 2-in.-tall slugs; cubes ranging from 0.25 to 1 in. on a side; broken metal pieces of unspecified geometric shapes; product oxide; skull oxide; UNH crystals; and unirradiated TRIGA reactor fuel elements.

Dimensions for bounding calculation models of TRIGA fuel are 1.44 inches in diameter × 5 in. tall. The 20% enrichment fuel contains more fissile mass than the 70% enrichment fuel on account of a higher uranium weight fraction and associated material density. A 20 wt % enriched TRIGA fuel element with 45 wt % U contains ≤307 g ^{235}U; whereas, a 70 wt % enriched TRIGA fuel with 8.5 wt % U contains ≤136 g ^{235}U. The physical parameters which characterize the TRIGA fuel are enrichment, uranium weight fraction, and the fuel diameter. (Appendix 6.9.3.1). These parameters are addressed in this section demonstating that the calculation models are bounding in the criticality evaluation.

Uranium-aluminum (U-Al) alloy averages 0.94 kg of uranium, 0.60 kg of ^{235}U, and 4.07 kg of aluminum. Uranium-molybdenum alloy varies from 1.5 wt % to 10 wt % molybdenum and the enrichment varies from 92.65 to 93.21 wt% ^{235}U. Where scattering media (aluminum or molybdenum) is treated as multiplying media (^{235}U), the alloy is conservatively assessed. The evaluation of the 3.93-in.-diam × 9.5-in.-tall U-Al cylinders is covered under the evaluation the 4.25-in.-diam HEU metal cylinders. Evaluation of the U-Mo content is covered under the assessment of HEU contents at 95 wt% enrichment.

6.4.1 Solid HEU Metal of Specified Geometric Shapes

For bare and reflected single packages with HEU metal content, the neutron multiplication factor increases as a function of the ^{235}U mass and the moisture fraction of the package external to the containment vessel (MOIFR). For example, consider the ES-3100 package loaded with three convenience cans for a total of 36,000 g ^{235}U. Each press-fit lid type can contains a single 3.24-in.-diam, 12,000 g cylinder of ^{235}U. The $k_{eff} + 2\sigma$ values in the bare package increase from 0.911 to 0.955 with increasing moisture fraction of the package external to the containment vessel (MOIFR), Cases **ncsbcyt11_36_1_1** through **ncsbcyt11_36_1_15** (Appendix 6.9.6, Table 6.9.6-2). The $k_{eff} + 2\sigma$ values increase from 0.918 to 0.955 with increasing MOIFR in the water-reflected package, Cases **ncsrcyt11_36_1_1** through **ncsrcyt11_36_1_15** (Appendix 6.9.6, Table 6.9.6-2). The addition of water to the package reduces the neutron leakage fraction (NLF), thereby increasing k_{eff}. Water reflection external to a flooded package is inconsequential to package reactivity as a comparison of results for Cases **ncsbcyt11_36_1_15** and **ncsrcyt11_36_1_15** indicates.

In this series of calculations using the ES-3100 package model with NCT geometry (Cases **ncsrcyt11_36_1_1** through **ncsrcyt11_36_1_15**), the MOIFR is varied uniformly over the package model with the exception of the neutron poison of the body weldment liner inner cavity and the flooded containment vessel. The single-unit case with a MOIFR = 1.0 pertains specifically to the flooded drum under conditions specified in 10 CFR 71.55(b). This pseudo-HAC condition is more reactive than either the true NCT where both the containment vessel and Kaolite are dry [10 CFR 71.55(d)] or this evaluation for NCT where the containment vessel is flooded and the Kaolite is dry (in the as-manufactured condition, MOIFR ~ 0.0289). At MOIFR = 1.0, external water reflection of the package is inconsequential to package reactivity. Moisture in the Kaolite and in the recesses of the package acts as a close reflector that decreases neutron leakage away from the package.

The single-unit case with a MOIFR = 1e-20 pertains specifically to a package under pseudo-HAC where both the Kaolite and the recesses of the package do not contain **any** water or bound hydrogen. This configuration is less reactive than the cases for Kaolite in the as-manufactured condition or water-saturated Kaolite because water in the Kaolite will provide some neutron moderation and reflection of neutrons back into the content.

Single package reactivity changes slightly between the bare and reflected conditions, while NLF changes considerably over the range of water fractions. This behavior illustrates the dependence of package reactivity on internal conditions of the package. Bare packages with low MOIFR values manifest low

reactivity (k_{eff} = 0.911) and high neutron leakage (NLF = 0.47). These parameters indicate that fast neutrons scattered in the packaging do not slow down significantly but escape the package. Consequently, neutron interaction between these packages when they are configured into an array is high. Bare packages with MOIFR values >1e-2 manifest increasing k_{eff} values (from 0.911 to 0.955) and reduced NLF values (from 0.47 to 0.18). The increase in k_{eff} occurs due to reflection of neutrons that would otherwise escape the package back into the HEU content by water present in the regions of the package external to the content.

The ES-3100 package is not as efficient a reflector as full water reflection provided to the flooded containment vessel. For the containment vessel loaded with 3.24-in.-diam cylinders, the $k_{eff} + 2\sigma$ values increase monotonically from 0.907 to 0.974 with increasing moisture fraction inside the containment vessel (MOCFR) [Cases **cvcrcyt11_36_1_1** through **cvcrcyt11_36_1_15** (Appendix 6.9.6, Table 6.9.6-1, and Appendix 6.9.1, Fig. 6.9.1-1)]. The flooded containment vessel under full water reflection is a more reactive configuration than the containment vessel inside of flooded ES-3100 packaging, Case **ncsrcyt11_36_1_15**. For this reason, calculation results for the flooded containment rather than a flooded package are reported in Tables 6.1a–6.1e for 10 CFR 71.55(b) and are taken into consideration in the determination of HEU fissile mass loading limits.

Examination of the results for Cases **cvcrcyt11_36_1** through **cvcrcyt11_18_1** indicates that an adequately subcritical loading is achieved when the mass loading is limited to 21,000 g ^{235}U (Case **cvcrcyt11_21_1**). Case **cvcrcyt11_36_2** reveals that the 277-4 canned spacers are adequate for mass loading >8,000 g ^{235}U but ≤36,000 g ^{235}U.

Case **hcsrcyt12_36_1_15** (Appendix 6.9.6, Table 6.9.6-3) represents the HAC model of the damaged ES-3100 package, where the outer dimensions of the package are reduced accordingly and the entire package is flooded with the exception of the neutron poison of the body weldment liner inner cavity. The containment vessel well is flooded with water, and the Kaolite contains maximum water content. This single-unit case with a MOIFR = 1.0 pertains specifically to the flooded drum under conditions specified in 10 CFR 71.55(e). The $k_{eff} + 2\sigma$ = 0.955 for this HAC. The changes in both the outer dimensions of the package and the compositions of the Kaolite and 277-4 due to HAC result in an ~0.002 change in the neutron multiplication factor.

Repeated for 4.25-in.-diam cylinders (Appendix 6.9.6, Tables 6.9.6-6 and 6.9.6-7); 2.29-in. -square bars (Tables 6.9.6-4 and 6.9.6-5); and 1.5-in.-diam × 2-in.-tall slugs (Tables 6.9.6-8 and 6.9.6-9), this type of analysis for the 3.24-in.-diam cylinders demonstrates that single packages with restricted fissile material (^{235}U) loading remain subcritical over the entire range of water content or MOIFR. HEU bulk metal or alloy content not covered by the specified geometric shapes (cylinder, square bar, or slug contents) will be in the HEU broken metal category, and so limited.

Each TRIGA fuel element for shipment in the ES-3100 is to be disassembled. The active fuel consisting of three 5-in.-tall cylinders of $UZrH_{1.6}$ is to be packed into a metal-type convenience can. (Section 6.2.1) The use of three loaded convenience cans in the ES-3100 is assumed in the criticality calculation models for ground transport. However, credit is only taken for vertical spacing provided by canned spacers when present. For configurations where canned spacers are not used, the TRIGA content is assumed stacked end-to-end. The three cylinders of the active fuel are modeled in triangular-pitch configuration within the radial boundary of the convenience can(s). The pitch used in the criticality calculation models for the NCT and HAC ground transport is 4.9809 cm (1.96 in.)

As shown in Table 6.9.6-19b, a set of parametric cases were run where the triangular pitch for the fuel content is varied from 1.44 in. (fuel sections touching) to 2.413 in. (fuel sections at maximum separation and touching the inner boundary of the convenience can.) As shown in Fig. 16a, the calculated $k_{eff} + 2\sigma$ values

increase slightly from 0.48 to an asymptotic value of ~ 0.53 at a pitch of 2.121 in. or a foci of 3.1106 cm. (Table 6.9.6-19b) The foci of 2.8757 cm. for the TRIGA fuel sections used in the criticality calculation models, corresponds to a 1.96 in. pitch. The calculated $k_{eff} + 2\sigma$ value is 0.527 for Case **cvcrtriga_1_15** (Table 6.9.6-19a) indicating that the configuration is in the range of optimum moderation. Moreover, the calculated $k_{eff} + 2\sigma$ value is substantially below the USL. (The foci is the distance perpendicular from the CV's vertical axis to the center of each fuel section. The value is obtained from the computer input listing on the comment line for geometry Unit 1006 which reads: " -2.875700 minus-y location lower cylinder. ")

Parametric cases were also run as a function of the moisture fraction ("mocfr") in the CV. As shown in Fig. 16b, the $k_{eff} + 2\sigma$ values decrease with decreasing water content in the CV; and content spacing has less of an effect on k_{eff} at lower at the lower fractions.

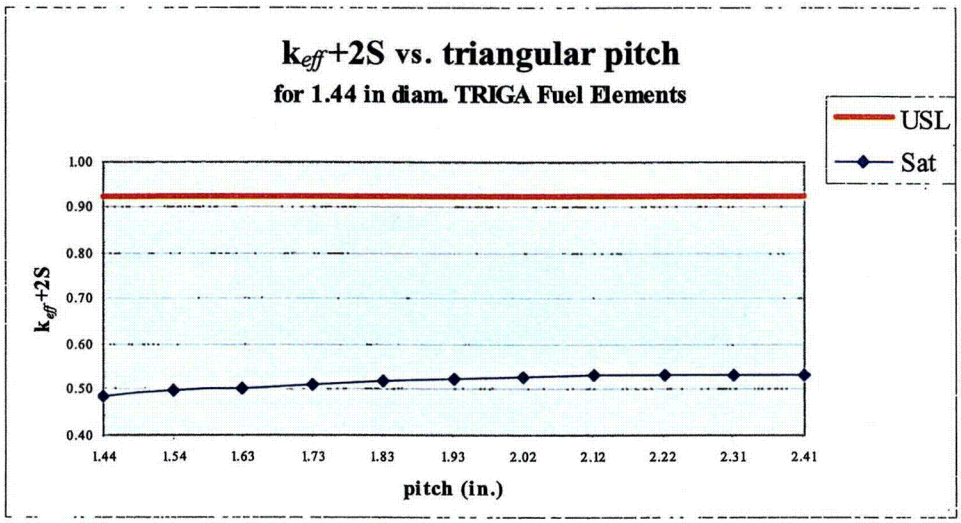

Fig. 16a $k_{eff} + 2\sigma$ versus pitch for triangular arrangement of content in CV

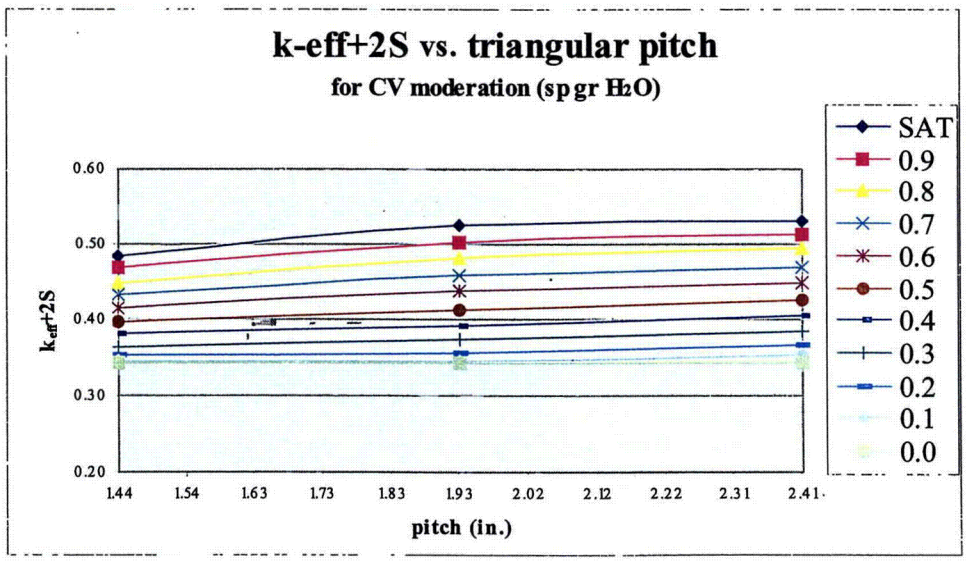

Fig. 16b $k_{eff} + 2\sigma$ versus triangular pitch over range of CV moderation

The first of the three physical parameters which characterize the TRIGA fuel is enrichment. Table 6.9.6-19a presents results for 20 % enriched and 70 % enriched TRIGA fuel where the diameter of the active fuel is 1.44 in. The calculated $k_{eff} + 2\sigma$ values for TRIGA fuel content at the lower enrichment is greater than for the fuel with the higher enrichment due to the greater quantity of fissile isotope present. The 20% enriched TRIGA fuel is considered the bounding content.

The second physical parameter which characterizes the TRIGA fuel is the uranium weight fraction. For a TRIGA fuel enriched to 20 wt % ^{235}U in U, the uranium weight fractions for the $UZrH_{1.6}$ fuel are: 45 wt %; 30 wt %; 20 wt %; 12 wt %; and 8.5 wt % U. A set of parametric cases were run where the uranium weight fraction is varied from the minimum value of 8.5 wt % to the maximum value of 45 wt %. Additionally, moderation in the containment vessel is varied from the dry to the flooded condition. As shown in Fig. 16c, the $k_{eff} + 2\sigma$ values decrease with both decreasing uranium weight fraction and decreasing water content in the CV. Details are provided in Table 6.9.6-19c.

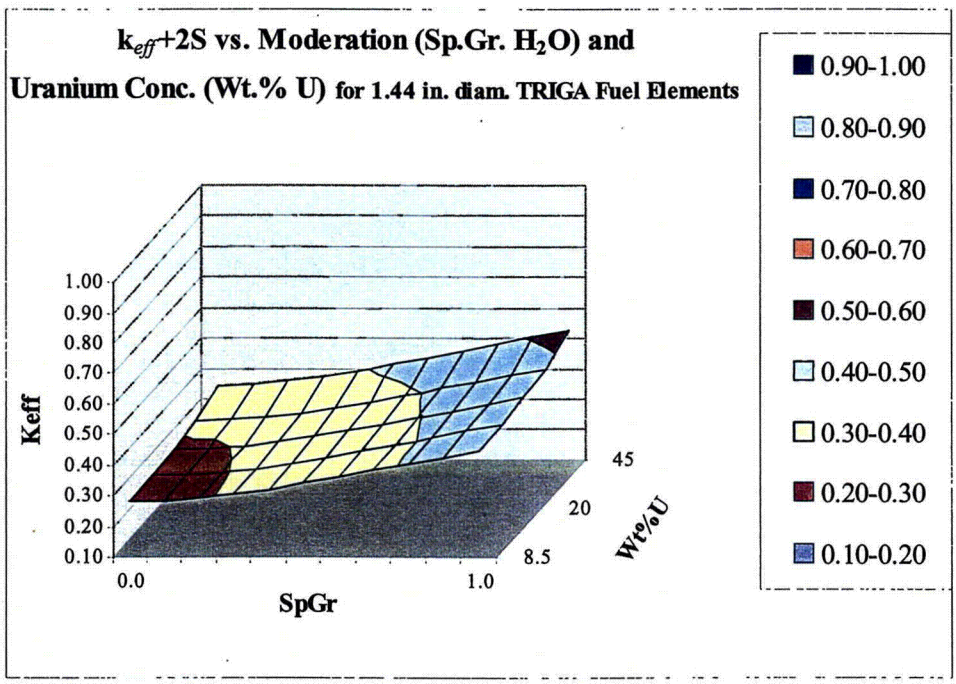

Fig. 16c $k_{eff} + 2\sigma$ as a function of uranium weight fraction and moderation

Third physical parameter which characterizes the TRIGA fuel is active fuel diameter. The active fuel diameters are: 1.44 in.; 1.41 in.; 1.40 in.; 1.37 in.; 1.34in.; and 1.31 in. The smaller the diameter, the less the amount of ^{235}U is present resulting in lower $k_{eff} + 2\sigma$ values, as demonstrated later in this section.

Cases **cvcrtriga_1_1** through **cvcrtriga_1_15** (Appendix 6.9.6, Table 6.9.6-19a) represent the TRIGA fuel content in a flooded containment vessel, reflected by 30.48 cm of water. The flooded containment vessel under full water reflection is a more reactive configuration than the containment vessel inside of flooded ES-3100 packaging, Case **ncsrtriga_1_15_15** (Appendix 6.9.6, Table 6.9.6-20a). Further examination of the results in Table 6.9.6-20a indicates the content loading is adequately subcritical loading and that 277-4 canned spacers are not required for criticality control. Comparison of results for the NCT Case **ncsrtriga_1_15_15** and the HAC **hcsrtriga_1_15_15**, both with $k_{eff} + 2\sigma = 0.495$, reveal that changes to the packaging external to the containment vessel due to the HAC do not result in an appreciable change in the neutron multiplication factor for the single package.

Cases **ncsrtriga70_1_1_1** through **ncsrtriga70_1_15_15** (Appendix 6.9.6, Table 6.9.6-20b) represent the 70 % enriched TRIGA fuel content in a flooded ES-3100 package, reflected by 30.48 cm of water. Comparison of results for these cases with results for the 20 % enriched TRIGA fuel (Cases **ncsrtriga_1_1_1** through **ncsrtriga_1_15_15**) confirm that the 20 % enriched TRIGA fuel is the bounding content.

Cases **ncsrT70_131_1_1_15** through **ncsrT70_131_1_15_15** (Appendix 6.9.6, Table 6.9.6-20c) represent the 1.31 in. diameter TRIGA fuel content in a flooded ES-3100 package, reflected by 30.48 cm of water. Comparison of results for these cases with results for the larger 1.44 in. diameter TRIGA fuel content (Cases **ncsrtriga70_1_1_1** through ncsrtriga70_1_15_15) confirm that the 1.44 in. diameter TRIGA fuel is the bounding content.

10 CFR 71.55(d)(2) requires the geometric form of a package's content not be substantially altered under the NCT. Also, 10 CFR 7155(e)(1) requires that the package be adequately subcritical under HAC with the package contents in the most reactive credible configuration. However, conclusions about damage to the fuel content can not be extrapolated from test data because a mock (test weight) content rather than actual TRIGA content is evaluated in the NCT and HAC tests of 10 CFR 71.71 and 10 CFR 71.73. Consequently, one way for addressing these requirements is to model the content in an extremely damaged condition and make a determination of subcriticality through a series of criticality calculations. Cases **ncsrt55d2_1_1_15** through **ncsrt55d2_1_15_15** (Appendix 6.9.6, Table 6.9.6-20d) represent TRIGA fuel content homogenized with variable density water over the free volume of the containment vessel, where the ES-3100 packaging is flooded and reflected by 30.48 cm of water. The variable density water ranges from the dry containment condition to the fully flooded condition. Credit for physical integrity of the content is not taken in this set of cases which model the substantially altered content. The calculation results in Table 6.9.6-20d indicate extremely damaged content (Case **ncsrt55d2_1_15_15** with $k_{eff} + 2\sigma = 0.611$) is more reactive than the unaltered configuration (Case **ncsrtriga_1_15_15** with $k_{eff} + 2\sigma = 0.403$). Nevertheless, both cases are adequately below the USL of 0.925 and the requirement of 10 CFR 71.55(d)(2) is satisfied. Given that changes external to the containment vessel due to the HAC do not result in an appreciable change in the nuetron multiplication for the single package, similar results are expected for the cases demonstrating compliance with 10 CFR 7155(e)(1).

The shipping configuration for disassembled TRIGA fuel addressed in this subsection is not the only permissible shipping configuration for TRIGA fuel in the ES-3100. TRIGA fuel may also be configured as clad fuel rods (Appendix 6.9.3.1). Each 15 in. long rod is derived from a single TRIGA fuel element. The clad fuel rod consists of the 3 fuel pellets and the exterior sheath of stainless steel or aluminum clad. Clad fuel rods are packed into stainless steel or tin-plated carbon steel convenience cans with a maximum of three fuel rods per loaded convenience can. This shipping configuration requires that only one convenience can is loaded with clad fuel rods.

Except for a 0.02 in. thick sheath of stainless steel clad added to the exterior surface of the $UZrH_{1.6}$, a calculation model for the clad fuel rod configuration is essentially the same as the NCT shipping configuration model for disassembled TRIGA fuel. A 0.02 in thickness of stainless steel is insignificant for an external reflection. As illustrated in Fig. 6.21 (Sect. 6.7.2), stainless steel up to several cm in thickness acts as a neutron absorber. Several inches in thickness are required for neutron multiplication to increase from neutron reflection by the stainless steel. The NCT shipping configuration model for disassembled TRIGA fuel is bounding. The same applies for TRIGA fuel with aluminum clad.

A clad fuel rod with 1.44 in. diameter fuel pellets contains 2,282.4 g $UZrH_x$ (Appendix 6.9.3.1) and ~179 to 191 g of stainless steel. Stainless steel tends to act as a neutron absorber; moreover, its presence as clad in the TRIGA fuel content replaces water moderator otherwise present in the geometry configuration of TRIGA fuel meats. When stainless steel is homogenized with the $UZrH_{1.6}$ as in the calculation model for

package content in the extremely damaged condition [10 CFR 71.55(d)(2) and 10 CFR 7155(e)(1)], the stainless steel acts more effectively as a neutron absorber. However, the amount of stainless steel added and water displaced is not expected to have a statistically significant affect on neutron multiplication. Thus, the HAC shipping configuration model for disassembled TRIGA fuel (bare fuel meats) is bounding.

A clad fuel rod with 1.41 in. diameter fuel pellets contains ~2,188 g $UZrH_x$ and ~90 to 96 g of aluminum. While aluminum tends to act as a neutron scatter, its presence in the TRIGA fuel content replaces water moderator otherwise present in the geometry configuration of TRIGA fuel meats. The amount of aluminum added and water displaced is not sufficient to have a statistically significant affect on neutron multiplication. Thus, the HAC shipping configuration model for disassembled TRIGA fuel is also bounding for aluminum clad TRIGA fuel content.

The TRIGA content is to be transported by air; consequently, additional discussion is included in Sect. 6.7.

The 1.5-in.-diam × 2-in.-tall slugs may be packed up to ten items per press-fit lid type convenience can and up to twelve items per crimp-lid type convenience can. With nominal dimensions, each slug weighs ~1,090 g. With +1/16 in. tolerance on both the diameter and height, each slug in the calculation model weighs ~1291 g. As described in Appendix 6.9.1, different arrangements of slugs in the convenience cans are

possible. A configuration of slugs in a flooded reflected containment vessel must be shown to be adequately subcritical and so limited either by the use of 277-4 canned spacers, by limitation of fissile mass, or by both.

For this evaluation, the slugs are modeled as 100 wt % ^{235}U but the convenience cans are not modeled. The calculation results presented in Table 6.9.6-8 (Appendix 6.9.6) for a flooded containment vessel indicate that only five slugs per convenience can (18,287 g ^{235}U per package) may be loaded without the use of 277-4 canned spacers (Cases **cvcr5st11_1_1** and **cvcr5est11_1_1**). Further evaluation of the single package and array configurations are required. Also, results highlighted in red indicate that 277-4 canned spacers are required for the slug content.

The sensitivity of k_{eff} to the space between slugs arranged in a pentagonal ring is evident in the calculation results for Cases **cvcr5st11_1_2** and **cvcr5est11_1_2,** which model content for three convenience cans, each location with two pentagonal rings (10 slugs) per can. These two configurations represent degrees of separation between adjacent neighbors in the pentagonal rings of 0.0 cm and 1.0 cm, respectively. The most reactive configuration occurs when the slugs are spaced 1.0 cm apart from direct contact with adjacent neighbors in the pentagonal rings. Because positioning devices are not used in the convenience cans to control spacing and prevent an optimal arrangement of contents from occurring, the latter calculation model for slug arrangement "**5est**" is the basis for additional calculations where spacers may not be required.

The calculation results presented in Table 6.9.1-8 for a flooded containment vessel indicate that up to 10 slugs per convenience can (36,573 g ^{235}U per package) *might* be loaded when 277-4 canned spacers are used. Conceivable arrangements are considered in Cases **cvcr5st11_2_2, cvcr5est11_2_2, cvcr6e4st11_2,** and **cvcr73st11_2,** (Table 6.9.6-8). Suitability is contingent on the results of single package and array calculations.

Cases **ncsr5est11_2_1_1** through **ncsr5est11_2_1_15** (Appendix 6.9.6, Table 6.9.6-9) model a reflected package with one pentagonal ring of slugs per content location with 277-4 canned spacers between content locations and HEU content at 100 wt % ^{235}U. The $k_{eff} + 2\sigma$ values range from a low value of 0.687 to 0.737. These results show that the most reactive configuration is the flooded condition with MOIFR=1.0.

As shown by the cylindrical content calculation models, the ES-3100 package is not as an efficient reflector as full water reflection provided to the flooded containment vessel. This is also true for content loadings of one pentagonal ring of slugs per content location without 277-4 canned spacers between locations and HEU content at 100 wt % ^{235}U. For Cases **cvcr5est11_1_1** and **ncsr5est11_1_1_15,** the $k_{eff} + 2\sigma$ values are 0.909 and 0.870, respectively. Likewise, the $k_{eff} + 2\sigma$ values are 0.903 and 0.868 for content loadings of two pentagonal rings of slugs per content location with 277-4 canned spacers between locations, Cases **cvcr5est11_2_2** and **ncsr5est11_2_2_15,** respectively.

For the flooded containment vessel under full water reflection and loaded with the slugs in a pentagonal arrangement and 277-4 canned spacers between content locations, $k_{eff} + 2\sigma = 0.904$, Case **cvcr6e4st11_2** [10 CFR 71.55(b).] This value is below the USL value of 0.925. For packages with the required 1.4-in. 277-4 canned spacers, the calculated $k_{eff} + 2\sigma$ value is 0.868 for the water-reflected package, Case **ncsr5est11_2_2_15** [10 CFR 71.55(d).] Case **hcsr5est11_02_2_15** represents the HAC model of the damaged ES-3100 package, where the outer dimensions of the package are reduced accordingly and the entire package is flooded except the neutron poison of the body weldment liner inner cavity. This single-unit case with a MOIFR = 1.0 pertains specifically to the flooded drum under conditions specified in 10 CFR 71.55(e). The $k_{eff} + 2\sigma = 0.871$ for this HAC. The changes in both the outer dimensions of the package and the compositions of the Kaolite and 277-4 due to HAC result in an ~0.003 change in the neutron multiplication factor.

6.4.2 HEU Solid Metal of Unspecified Geometric Shapes or HEU Broken Metal

Like packages with HEU metal, the neutron multiplication factor for reflected single packages with HEU broken metal increases as a function of the ^{235}U mass and the MOIFR. For example, consider the ES-3100 package loaded with three convenience cans for a total of 35,142 g ^{235}U. The $k_{eff} + 2\sigma$ values range from 0.814 to 0.891 with increasing MOIFR in the water-reflected package [Cases **ncsrbmt11_36_1_1** through **ncsrbmt11_36_1_15** (Appendix 6.9.6, Table 6.9.6-11)]. The addition of water to the package reduces the NLF, thereby increasing k_{eff}.

For the containment vessel loaded with the broken metal content but without 277-4 canned spacers between content locations, the $k_{eff} + 2\sigma$ values increase from 0.751 to 0.949 as the water content in the containment vessel increases [Cases **cvr3lha_36_1_8_1** through **cvr3lha_36_1_8_15** (Appendix 6.9.6, Table 6.9.6-10, and Appendix 6.9.3, Fig. 6.9.3.1-5)]. Cases **cvr3lha_36_1_8_15** through **cvr3lha_36_1_1_15** model the flooded containment vessel with 35 kg of broken HEU metal where the enrichment ranges from 100 to 19 wt % ^{235}U. The result for Case **cvr3lha_36_1_6_15** indicates that for an enrichment of 90 wt % ^{235}U, the mass loading cannot exceed 31,482 g in the absence of canned spacers. However, the application of this limit to higher enrichment material is non-conservative, as illustrated by the result for Case **cvr3lha_26_1_8_15**. (The results for cases highlighted in yellow indicate potential limits.) As the enrichment increases, the mass loading limit decreases (from 28,334 g to 25,894 g in this example) due to less ^{238}U for neutron absorption.

For the flooded containment vessel under full water reflection and loaded with the broken metal content and 277-4 canned spacers between content locations, the $k_{eff} + 2\sigma = 0.876$, Case **cvr3lha_36_2_8_15** [10 CFR 71.55(b)]. For packages loaded with the broken metal content and 277-4 canned spacers between content locations, the calculated $k_{eff} + 2\sigma$ value is 0.872, Case **ncsrbmt11_36_2_15** [10 CFR 71.55(d)]. Case **hcsrbmt12_36_2_15** (Appendix 6.9.6, Table 6.9.6-11) represents the HAC model of the damaged ES-3100 package, where the outer dimensions of the package are reduced accordingly and the entire package is flooded except the neutron poison of the body weldment liner inner cavity. This single-unit case with a MOIFR = 1.0 pertains specifically to the flooded drum under conditions specified in 10 CFR 71.55(e). The $k_{eff} + 2\sigma = 0.874$ for this HAC condition. The changes in both the outer dimensions of the package and the compositions of the Kaolite and 277-4 due to HAC result in an ~0.002 change in the neutron multiplication factor.

6.4.3 HEU Oxide

HEU product oxide content is non-hygroscopic or mildly hygroscopic with a bulk density over 6 times greater than water. HEU skull oxide is a less dense form of U_3O_8 intermixed with graphite. Of interest are those compositions with carbon/fissile uranium ($C/^{235}U$) ratios up to 2.3×10^5 μg $C/g^{235}U$. The quantity of fissile uranium is extremely low where even higher $C/^{235}U$ ratios are present.

HEU product oxide content is packed in polyethylene bottles; HEU skull oxide content is packed in metal-type convenience cans. While both the size and shape of the polyethylene bottles prevents the use of 277-4 canned spacers with product oxide loadings, the 10-in. height of the metal-type convenience cans eliminates the use of 277-4 canned spacers for skull oxide content packaged in these size cans. However, the convenience cans are not modeled in this criticality evaluation and this analysis is performed from the standpoint that metal-type convenience cans may be used for both oxide types.

HEU oxide content is not considered a "rigid" content like solid or broken HEU metal. Thus a different modeling approach is used to avoid having to address uncertainties regarding the location of spacers in the containment vessel. For the calculation models of HEU oxides, the 277-4 canned spacers are not

actually modeled. Instead, the evaluation water in the void region of the containment vessel is homogenized over the volume of the containment vessel that is not occupied by oxide content. (The void region of the containment vessel is defined as the containment vessel volume minus the oxide content volume minus the canned spacer volume.) Because of the differences in densities and compositions, product oxides are addressed separately from skull oxides.

Like packages with HEU metal or broken metal, the neutron multiplication factor for reflected single packages with HEU oxide increases as a function of increasing MOIFR and decreases with decreasing ^{235}U mass. For example, consider the ES-3100 package loaded with three convenience cans for a total of 24,000 g UO_2 (21,125 g ^{235}U) but lacking 277-4 canned spacers between content locations. The $k_{eff} + 2\sigma$ values range from 0.700 to 0.784 with increasing MOIFR in the reflected package [Cases **ncsroxt11_1_24_1_1** through **ncsroxt11_1_24_1_15** (Appendix 6.9.6, Table 6.9.6-13)]. The addition of water to the package reduces the NLF, thereby increasing k_{eff}. Results for Cases **ncsroxt11_2_24_1_15** and **ncsroxt11_3_24_1_15** indicate that both the U_3O_8 content ($k_{eff} + 2\sigma = 0.678$) and the UO_3 content ($k_{eff} + 2\sigma = 0.619$) are bounded by the UO_2 content ($k_{eff} + 2\sigma = 0.784$).

For the containment vessel loaded with the HEU product oxide but lacking 277-4 canned spacers between content locations, the $k_{eff} + 2\sigma$ values decrease from 0.873 to 0.846 [Cases **cvcroxt11_1_24_1** through **cvcroxt11_1_20_1** (Appendix 6.9.6, Table 6.9.6-12, and Appendix 6.9.1, Fig. 6.9.1-5)]. Canned spacers are not required for criticality control. For the containment vessel loaded with the HEU product oxide and 277-4 canned spacers between content locations, the $k_{eff} + 2\sigma$ values decrease from 0.874 to 0.848 [Cases **cvcroxt11_1_24_2** through **cvcroxt11_1_20_2** (Appendix 6.9.6, Table 6.9.6-12)]. Comparison of results for a package without spacers (Case **cvcroxt11_1_*nn*_1**) versus results for one with spacers (Case **cvcroxt11_1_*nn*_2**) reveals that the amount of water removed by the spacers has an insignificant effect on the neutron multiplication factor.

For the flooded containment vessel under full water reflection containment, the $k_{eff} + 2\sigma$ value is 0.873, Case **cvcroxt11_1_24_1**. [10 CFR 71.55(b)] The $k_{eff} + 2\sigma$ value is 0.784 for water-reflected package, Case **ncsroxt11_1_24_1_15**. [10 CFR 71.55(d)] Case **hcsroxt12_1_24_1_15** (Appendix 6.9.6, Table 6.9.6-13) represents the HAC model of the damaged ES-3100 package, where the outer dimensions of the package are reduced accordingly and the entire package is flooded except the neutron poison of the body weldment liner inner cavity. This single-unit case with a MOIFR = 1.0 pertains specifically to the flooded drum under conditions specified in 10 CFR 71.55(e). The $k_{eff} + 2\sigma = 0.787$ for this HAC condition. The changes in both the outer dimensions of the package and the compositions of the Kaolite and 277-4 due to HAC result in an ~0.002 change in the neutron multiplication factor.

Cases **cvcrsk3cc_1_15_17** through **cvcrsk3cc_10_15_17** (Appendix 6.9.6, Table 6.9.6-17) evaluate the 10 skull oxide compositions identified Table 6.9.3.1-3b, where the containment vessel is loaded with 3 convenience cans. The fissile enrichment is ~70 wt % ^{235}U for contents "**sk3cc_1**" through "**sk3cc_5**" and ~38 wt % ^{235}U for contents "**sk3cc_6**" through "**sk3cc_8**." The observed maximums of 7.1 kg skull oxide and ~93.2 wt % ^{235}U enrichment present in 292 convenience cans are the basis for the hypothetical contents "**sk3cc_9**" and "**sk3cc_10**." Content "**sk3cc_10**" differs from "**sk3cc_9**" in that 921 g of graphite in the skull oxide is replaced with 921 g ^{235}U in the form of U_3O_8. Content "**sk3cc_10**" is more representative of high enrichment skull oxides where < 85 g of graphite is present. For each of the 10 content models, 513 g of the skull oxide content is modeled as polyethylene, representing the potential use of hydrogenous packing material. The U_3O_8 content ranges from 8 to 21 kg, while the ^{235}U content ranges from 3.7 to 16.4 kg. The graphite content ranges from 0 to 921 g C, and the $C/^{235}U$ ratio ranges from 0 to 223,432 μg C/g ^{235}U. For Cases **cvcrsk3cc_1_15_17** through **cvcrsk3cc_10_15_17** at both saturation moisture and full graphite content, the $k_{eff} + 2\sigma$ values range from 0.759 to 0.855 in the flooded, water-reflected containment vessel. The results

for Cases **cvcrsk3cc_9_15_17** and **cvcrsk3cc_10_15_17** reveal that $k_{eff}+2\sigma$ increases slightly when the 921 g of carbon in the skull oxide is replaced with 921 g ^{235}U.

Cases **cvcrsk3cc_4_1_1** through **cvcrsk3cc_4_*m*_*g*** evaluate the effects of moisture and skull oxide graphite content on reactivity. The case designator "***m***" ranges from 1 to 15, signifying the variation in moisture; "***g***" ranges from 1 to 17, signifying the variation in graphite. Examination of results indicates that moisture content has a predominate effect on the neutron multiplication factor, while variation in graphite content has a minor effect. The peak $k_{eff}+2\sigma$ value occurs at saturated moisture and full graphite content.

Cases **ncsrsk_1_15** through **ncsrsk_10_15** (Appendix 6.9.6, Table 6.9.6-18a) model the 10 skull oxide compositions in a flooded containment vessel in a water reflected package. The $k_{eff}+2\sigma$ values range from 0.641 to 0.745. Likewise, Cases **hcsrsk_1_15** through **hcsrsk_10_15** (Appendix 6.9.6, Table 6.9.6-18b) evaluate infinite arrays damage packages. The $k_{eff}+2\sigma$ values ranging from 0.658 to 0.767 are not statistically significantly different from the NCT case results.

Cases **ncsrsk_9_1** through **ncsrsk_9_15** evaluate the bounding skull oxide content containing ~19.9 kg U_3O_8 and 921 g graphite, where the saturation moisture is varied from 0 to 3801 g water. Likewise, Cases **ncsrsk_10_1** through **ncsrsk_10_15** evaluate the skull oxide content containing ~20.8 kg U_3O_8 where the 921 g of graphite in the skull oxide is replaced with 921 g ^{235}U in the form of U_3O_8. The $k_{eff}+2\sigma$ values range from 0.403 to 0.741 in the former set of cases and range from 0.404 to 0.746 in the latter set of cases. The $k_{eff}+2\sigma$ values are well below the USL value of 0.925, indicating that canned spacers are not required for criticality control. Moreover, these results indicate that moisture content has a predominate effect on the neutron multiplication factor, while the graphite content has an insignificant effect.

6.4.4 UNH Crystals

Although UNH crystal content is to be packed in Teflon bottles, this criticality evaluation does not preclude use of metal-type convenience cans that the 277-4 canned spacers are designed to accommodate. Therefore, 277-4 canned spacers are considered in the evaluation of UNH crystals. UNH crystal content is not considered a "rigid" content like solid or broken HEU metal. Therefore, the same modeling technique is used for HEU oxide content and UNH crystal content. The 277-4 canned spacers are not actually modeled.

Unlike the other HEU contents, UNH crystals are soluble in water. The most reactive credible configuration for a solution occurs for a concentration at ~450 g ^{235}U/l. Fixed by the inner dimensions of the containment vessel, the near optimum solution concentration occurs at a content mass loading of 9000 g UNH crystals. This condition assumes the mixing of UNH crystals with water of the flooded containment vessel, producing a solution with a concentration on the order of 415 g ^{235}U/l.

For a flooded containment vessel loaded with the UNH crystals but without 277-4 canned spacers between content locations, the $k_{eff}+2\sigma$ values change from 0.823 to 0.609 [Cases **cvcrunhct11_24_1** through **cvcrunhct11_1_1** (Appendix 6.9.6, Table 6.9.6-14, and Appendix 6.9.1, Fig. 6.9.1-6)]. In the range of the optimal concentration (~9000 g UNH), the $k_{eff}+2\sigma = 0.857$ for Case **cvcrunhct11_9_1**. [10 CFR 71.55(b)] Where dilution of UNH crystals is confined to the containment vessel, the reported $k_{eff}+2\sigma$ value is 0.745 for a water-reflected package (Case **ncsrunhct11_9_1_15**). [10 CFR 71.55(d)]

Similar to packages loaded with HEU metal, broken metal, or oxide, the neutron multiplication factor for a reflected single package with UNH crystals increases as a function of MOIFR. Consider the ES-3100 package loaded with three convenience cans for a total of 24,000 g UNH crystals (11,303 g ^{235}U). The concentration is 1106 g ^{235}U/l in the flooded containment vessel. For Cases **ncsrunhct11_24_1_1** through **ncsrunhct11_24_1_15** (Appendix 6.9.6, Table 6.9.6-15), the $k_{eff}+2\sigma$ values range from 0.605 to 0.702 with

increasing MOIFR in the water-reflected package. However, the results for Cases **ncsrunhct11_24_1_15** through **ncsrunhct11_1_1_15** demonstrate that the optimal concentration is not reached until the mass loading is reduced to ~9000 g UNH or 415 g ^{235}U/l. For Case **ncsrunhct11_9_1_15**, the $k_{eff} + 2\sigma = 0.745$.

Unlike solid HEU metal and oxide content, which are confined to the containment vessel and only water leakage into the containment vessel need be considered, the evaluation of UNH crystal content for compliance with 10 CFR 71.55(b) also requires that the leakage of liquid HEU contents out of the containment be addressed. This is because UNH crystals are soluble in water and would dissolve in the water flooding the containment vessel and the containment vessel well. For a content loading of 24,000 g UNH, the uranium concentration drops from 1106 g ^{235}U/l to 689 g ^{235}U/l. Optimum moderation at solution concentrations in the range of 415 g ^{235}U/l to 429 g ^{235}U/l occurs for fissile mass loadings of ~15,000 g UNH.

Cases **hcsrunhct12_9_1_15** (Appendix 6.9.6, Table 6.9.6-15) and **icsrunhct12_15_1_15** (Appendix 6.9.6, Table 6.9.6-16) represent the HAC model of the damaged ES-3100 package where the outer dimensions of the package are reduced accordingly. For Case **hcsrunhct12_9_1_15**, the dilution of the UNH crystals is confined to the containment vessel, and maximum reactivity occurs at ~9000 g UNH. For Case **icsrunhct12_15_1_15**, UNH crystals are dissolved in the water flooding the containment vessel and the containment vessel well, and maximum reactivity occurs at ~15,000 g UNH. The respective solution concentrations are 415 g ^{235}U/l and 429 g ^{235}U/l. These single-unit cases with a MOIFR = 1.0 pertain specifically to the flooded drum under conditions specified in 10 CFR 71.55(e), where the $k_{eff} + 2\sigma$ values are 0.748 and 0.807 for this HAC condition. The changes in both the outer dimensions of the package and the compositions of the Kaolite and 277-4 due to HAC do not result in a significant change in the neutron multiplication factor.

6.5 EVALUATION OF PACKAGE ARRAYS UNDER NORMAL CONDITIONS OF TRANSPORT

For the NCT array evaluation of ES-3100 packages, the package content is confined within the containment vessel, consistent with the result of the tests specified in §71.71 (Normal Conditions of Transport). The array sizes examined in this evaluation are infinite, 13×13×6, 9×9×4, 7×7×3, 5×5×2, ETP 27×3, ETP 16×3, and the degenerate single unit. The "N" and corresponding CSI values for arrays determined to be adequately subcritical are as follows: $N = \infty$, CSI = 0; N = 202, CSI = 0.4; N = 64, CSI = 0.8; N = 29, CSI = 1.7; N = 10, CSI = 5.0; and N = 16, CSI = 3.2. All arrays, except the infinite array, are reflected with 30 cm (1 ft) of water. These arrays are nearly cubic in shape for optimum array reactivity, thus eliminating the need for placing criticality controls on package arrangements in terms of stack height, width, and depth of an array. The array configurations and the range of water contents (Table 6.4) evaluated bound all possible packaging arrangements and moderation conditions for NCT.

6.5.1 Solid HEU Metal of Specified Geometric Shapes

For infinite and finite arrays of packages with HEU metal, the neutron multiplication factor increases as a function of the ^{235}U mass and decreases as a function of MOIFR. For example, consider the ES-3100 package loaded with three convenience cans for a total of 36,000 g ^{235}U where each can contains a 3.24-in.-diam cylinder. For package content without 277-4 canned spacers, the $k_{eff} + 2\sigma$ values range from 1.027 to 0.963 with increasing MOIFR in the package [Cases **nciacyt11_36_1_1** through **nciacyt11_36_1_15** (Appendix 6.9.6, Table 6.9.6-3)]. For package content with 277-4 canned spacers, the $k_{eff} + 2\sigma$ values range from 0.957 to 0.880 with increasing MOIFR in the package [Cases **nciacyt11_36_2_1** through **nciacyt11_36_2_15** (Appendix 6.9.6, Table 6.9.6-3)].

The effect of increasing the water content of the array is straightforward. As interspersed water is added to the packages of an array, two reactivity effects occur in series. The first effect is the tendency for reactivity to remain constant due to controlled neutron interaction between the packages of the array. For an infinite array where neutrons cannot escape from the system, neutrons are scattered about the array. In the MOIFR range of 1e-20 to 1e-02, both the interspersed moderator inside the packages of the dry array and the interstitial moderator between the package drums of the array are not sufficient for neutron thermalization and absorption to occur in the adjacent packaging materials. However, hydrogen in the 277-4 provides moderation, and neutrons are absorbed in the interspersed boron of this neutron poison. This results in a subcritical system with near constant neutron multiplication factors over the range of MOIFR. The second effect is the tendency for reactivity to decrease due to internal moderation in packages of the array. The introduction of water above ~0.01 MOIFR shows the effect of isolating the individual array units from each other. The neutron multiplication factor approaches k_{eff} for the single, water-reflected unit at a full-content water fraction (MOIFR = 1.0).

The array case with a water fraction of MOIFR = 1e-04 pertains specifically to packages under NCT where the Kaolite and recesses of the package external to the containment vessel do not contain any residual moisture. This NCT case is more reactive than all other NCT cases where more moisture is present in the Kaolite and recesses of the package. Interspersed water between the containment vessels in the array will reduce neutronic interaction between the flooded contents because neutrons are absorbed in the hydrogen of the water. As more water is added, the packages of the array become isolated, and array reactivity ($k_{eff} + 2\sigma = 0.880$, Case **nciacyt11_36_2_15**) approaches the reactivity of the single unit ($k_{eff} + 2\sigma = 0.873$, Case **ncsrcyt11_36_2_15**).

Repeated for 4.25-in.-diam cylinders (Appendix 6.9.6, Table 6.9.6-7); 2.29-in. -square bars (Table 6.9.6-5); and 1.5-in.-diam × 2-in.-tall slugs (Table 6.9.6-9), this type of analysis for the 3.24-in.-diam cylinders demonstrates that arrays of packages with restricted fissile material (^{235}U) loading remain subcritical over the entire range of water content or MOIFR. HEU bulk metal or alloy content not covered by the specified geometric shapes (cylinder, square bar, or slug contents) will be in the HEU broken metal category, and so limited.

Cases **nciatriga_1_1_3** through **nciatriga_1_15_3** (Appendix 6.9.6, Table 6.9.6-20a) represent infinite arrays of packages containing the bounding TRIGA fuel content (20 % enrichment with 45 wt % U containing 307 g ^{235}U), without 277-4 canned spacers. The MOIFR is set at 1.0e-04 such that neutronic interaction between packages is maximized. For these cases, the $k_{eff} + 2\sigma$ values increase from 0.218 to 0.525 as MOIFR increases. The $k_{eff} + 2\sigma = 0.525$ for Case **nciatriga_1_15_3** is substantially below the below the USL value of 0.925, indicating that canned spacers are not required for criticality control.

As stated in Sect. 6.4.1, 10 CFR 71.55(d)(2) requires the geometric form of a package's content not be substantially altered under the NCT. Similarly, 10 CFR 7155(e)(1) requires that the package be adequately subcritical under HAC with the package contents in the most reactive credible configuration. Even though visible signs of damage to the metal convenience can have not been observed resulting from the regulatory tests, conclusions about damage to the TRIGA fuel content are not extrapolated from test data. The regulatory requirements are addressed by modeling the TRIGA fuel content in an extremely damaged condition. A series of criticality calculations is performed for making a determination of subcriticality. Cases **nciat55d2_1_1_3** through **ncia55d2_1_15_3** (Appendix 6.9.6, Table 6.9.6-20d) represent TRIGA fuel content homogenized with variable density water over the free volume of the containment vessel. The packaging is flooded in each ES-3100 package of the infinite array. The variable density water ranges from the dry containment condition to the fully flooded condition. Credit for physical integrity of the content is not taken in this set of cases which model the subtantially altered content. The calculation results in Table 6.9.6-20d indicate extremely damaged content (Case **nciat55d2_1_15_3** with $k_{eff} + 2\sigma = 0.716$) is more reactive than the unaltered

configuration (Case **nciatriga_1_15_3** with $k_{eff}+2\sigma = 0.442$). Nevertheless, both cases are adequately below the USL of 0.925 and the requirement of 10 CFR 71.55(d)(2) is satisfied. Given that changes external to the containment vessel due to the HAC do not result in an appreciable change in the neutron multiplication for the an array of packages, similar results are expected for the cases demonstrating compliance with 10 CFR 7155(e)(1).

For TRIGA fuel content as clad fuel rods, the amount of clad added (stainless steel as a neutron absorber or aluminum as a neutron scatter) and corresponding amount of water moderator displaced by the clad is not expected to have a statistically significant affect on the calculated k_{eff}. Thus, the NCT shipping configuration model for disassembled TRIGA fuel (bare fuel meats) bounds shipping configuration model forTRIGA fuel configured as clad fuel rods (Appendix 6.9.3.1).

The array results for three slug configurations presented in Table 6.9.6-9 (Appendix 6.9.6) are for 5 or 10 slugs spaced apart in a pentagonal ring (**ncia5est11**) and for 7 slugs formed by a hexagonal ring of slugs with one slug in the center of the ring (**ncia70st11**). These cases are used to establish the mass loading limitations, which in turn limit the number of slugs in the package to less than the number required to assemble a critical configuration.

Cases **ncia5est11_1_1_8_3** through **ncia5est11_1_1_1_3** (Appendix 6.9.6, Table 6.9.6-9) represent infinite arrays of packages containing 18,287 g U without 277-4 canned spacers. For these cases, the $k_{eff}+2\sigma$ values increase from 0.550 to 0.923 as the enrichment is increased from 19.0 wt % to 100.0 wt % ^{235}U. The $k_{eff}+2\sigma = 0.923$ for Case **ncia5est11_1_1_8_3** is below the USL of 0.925.

Cases **ncia5est11_2_1_8_3** through **ncia5est11_2_1_1_3** (Appendix 6.9.6, Table 6.9.6-9) represent infinite arrays of packages containing 36,573 g ^{235}U without 277-4 canned spacers. For these cases, the $k_{eff}+2\sigma$ values increase from 0.452 to 0.806 as the enrichment is increased from 19.0 wt % to 100.0 wt % ^{235}U. The $k_{eff}+2\sigma = 0.806$ value for Case **ncia5est11_1_2_8_3** does not exceed the USL of 0.925.

At 60 wt % ^{235}U, the $k_{eff}+2\sigma = 0.905$ value for Case **ncia5est11_1_2_3_3** is below the USL. However, a restriction placed upon mass that requires that values must be ≤18,287 g ^{235}U still applies to satisfy the subcriticality requirement for the reflected containment vessel.

Cases **ncia70st11_1_8_3** through **ncia70st11_1_1_3** (Appendix 6.9.6, Table 6.9.6-9) represent infinite arrays of packages containing 25,601 g U without 277-4 canned spacers. For these cases, the $k_{eff}+2\sigma$ values increase from 0.530 to 1.025 as the enrichment is increased from 19.0 wt % to 100.0 wt % ^{235}U. The $k_{eff}+2\sigma = 1.025$ for Case **ncia70st11_1_8_3** exceeds the USL of 0.925.

At 70 wt % ^{235}U, the $k_{eff}+2\sigma = 0.884$ value for Case **ncia70st11_1_4_3** is below the USL. The 17,989 g ^{235}U falls within the restriction placed upon mass that requires that values must be ≤18,287 g ^{235}U to satisfy the subcriticality requirement for the reflected containment vessel.

Cases **ncia5est11_2_2_8_3** through **ncia5est11_2_2_1_3** (Appendix 6.9.6, Table 6.9.6-9) represent infinite arrays of packages containing 36,573 g ^{235}U with 277-4 canned spacers. For these cases, the $k_{eff}+2\sigma$ values increase from 0.582 to 0.983 as the enrichment is increased from 19.0 wt % to 100.0 wt % ^{235}U. At 80 wt % ^{235}U, the $k_{eff}+2\sigma = 0.909$ value for Case **ncia5est11_2_2_5_3** is just below the USL. Therefore, a restriction on mass and enrichment for slug content is that for ≤80 wt % ^{235}U, the mass of ^{235}U in the package must not exceed 29,333 g as a prerequisite for the shipment of the package slug content and with 277-4 canned spacers under a CSI = 0.0.

Cases **ncia70st11_2_8_3** through **ncia70st11_2_1_3** (Appendix 6.9.6, Table 6.9.6-9) represent infinite arrays of packages containing 25,601 g ^{235}U with 277-4 canned spacers. The $k_{eff}+2\sigma$ values increase from 0.473 to 0.914 as the enrichment is increased from 19.0 wt % to 100.0 wt % ^{235}U. Therefore, the restriction placed on mass and enrichment for slug content is that for between 80 and 100 wt % ^{235}U, the mass of ^{235}U in the package must not exceed 25,601 g as a prerequisite for the shipment of the package with slug content and 277-4 canned spacers under a CSI = 0.0.

Cases **ncf15est11_2_2_8_3** through **ncf15est11_2_2_1_3** (Appendix 6.9.6, Table 6.9.6-9) represent a 13 × 13 × 6 array of packages for which the corresponding rounded CSI = 0.4. The $k_{eff}+2\sigma = 0.941$ for Case **ncf15est11_2_2_8_3** at 100 wt % ^{235}U exceeds the USL of 0.925. Case **ncf15est11_2_2_7_3** at 95 wt % ^{235}U with $k_{eff}+2\sigma = 0.921$ is below the USL of 0.925 to permit increasing the limit on enrichment for mass loadings of ≤34.7 kg uranium metal. These CSI determinations are contingent upon satisfactory results under the HAC evaluation (Sect. 6.6.1).

6.5.2 HEU Solid Metal of Unspecified Geometric Shapes or HEU Broken Metal

Like packages with HEU metal, the neutron multiplication factor for arrays of packages with HEU broken metal decreases as a function of MOIFR and increases as a function of the ^{235}U mass. For example, consider the ES-3100 package loaded with three convenience cans for a total of 35,142 g ^{235}U and no canned spacers between content locations. The $k_{eff}+2\sigma$ values range from 1.138 to 0.913 with increasing MOIFR [Cases **nciabmt11_36_1_8_1** through **nciabmt11_36_1_8_15** (Appendix 6.9.6, Table 6.9.6-11)]. The introduction of water above ~0.01 MOIFR shows the effect of isolating the individual array units from each other. Array reactivity ($k_{eff}+2\sigma = 0.913$) approaches the reactivity of the water-saturated, water-reflected single package Case **ncsrbmt11_36_1_15** ($k_{eff}+2\sigma = 0.891$).

In the series of calculations using the ES-3100 package model with NCT geometry (Cases **nciabmt11_1_*n*_*m*_3** through **nciabmt11_*36*_*n*_*m*_3**), the enrichment of the content is varied from 19 wt % to 100 wt % ^{235}U. These array cases with a water fraction of MOIFR = 1e-04 pertain specifically to NCT packages where both the neutron poison of the body weldment liner inner cavity and the Kaolite are dry (in the as-manufactured condition) and both the recesses of the package external to the containment vessel and the interstitial space between the drums of the array do not contain any residual moisture. As stated before, this NCT case is more reactive than all other NCT cases where more moisture is present in the Kaolite and recesses of the package. Increased interspersed water between the containment vessels in the array will reduce neutronic interaction between the flooded contents to a point where the packages of the array become isolated.

Ranges of enrichment are specified in Table 6.1b (10 CFR 71.59) for identifying fissile mass loading limits for HEU broken metal. Consider specifically enrichments >95 wt % ^{235}U. The containment vessel calculations (Case **cvr3lha_36_1_8_15** versus Case **cvr3lha_36_2_8_15**) indicate that 277-4 canned spacers are required in this enrichment range, where the maximum evaluated fissile mass loading of 35,142 g ^{235}U is possible. However, the fissile mass loading must be limited to 2,774 g ^{235}U (Case **nciabmt11_3_2_8_3**) in order for the $k_{eff}+2\sigma$ value (= 0.904) to be below the USL of 0.925. This fissile mass limit is conservative when applied to enrichments only slightly greater than 95 wt % ^{235}U. A reduction in the enrichment within the range of 80 to 95 wt % ^{235}U (Cases **nciabmt11_4_2_7_3** and **nciabmt11_4_2_6_3**) does not result in a sufficient reduction in the $k_{eff}+2\sigma$ from neutron absorption in ^{238}U to allow for increased mass loadings. Therefore, the uranium mass limit remains at ~2774 g, while the fissile mass loading limit decreases with the reduction in enrichment as illustrated in Table 6.1b. As stated previously, these fissile mass loading limits for a CSI = 0 are contingent upon the infinite array of damaged packages also being adequately subcritical for HAC (Sect. 6.6.2).

This evaluation technique for determination of mass loading limits for enrichment intervals is repeated over the range of HEU enrichments identified in Table 6.1b. At HEU enrichment <60 wt % ^{235}U, the evaluated package mass loading limit of 35 kg uranium is achieved, so further delineation of fissile mass loading limits is not required.

6.5.3 HEU Oxide

Like packages with HEU metal or broken metal, the neutron multiplication factor for an array of packages with product oxide decreases as a function of decreasing ^{235}U mass [Cases **nciaoxt11_1_24_1_3** through **nciaoxt11_1_16_1_3** (Appendix 6.9.6, Table 6.9.6-13)]. The $k_{eff} + 2\sigma$ values are below the USL of 0.925.

Cases **nciask_1_15** through **nciask_10_15** (Appendix 6.9.6, Table 6.9.6-18) evaluate infinite arrays of packages having the 10 skull oxide compositions described in Sect. 6.4.3. The MOIFR is set at 1.0e-04 such that neutronic interaction between packages is maximized. The $k_{eff} + 2\sigma$ values, ranging from 0.656 to 0.764, are substantially below the below the USL value of 0.925, indicating that canned spacers are not required for criticality control.

The CSI = 0.0 for an infinite array of packages having product oxide content with a maximum of 21,125 g ^{235}U or having skull oxide content with a maximum of 16,399 g ^{235}U and 921 g graphite. The suitability of this determination is contingent upon satisfactory results under the HAC evaluation (Sect. 6.6.3.)

6.5.4 UNH Crystals

Unlike HEU metal, broken metal or oxide content, UNH crystal is soluble in water (Sect. 6.4.4). Near optimum solution concentration occurs at content mass loadings of ~9000 g UNH crystals or 415 g ^{235}U/l. Like packages with HEU metal, broken metal, or oxide, the neutron multiplication factor for an array of packages with UNH crystals decreases as a function of increasing MOIFR. Cases **nciaunhct11_8_24_1_1** through **nciaunhct11_8_24_1_15** (Appendix 6.9.6, Table 6.9.6-15) reveal the effect of isolating the individual array units from each other with the introduction of water above ~0.01 MOIFR. Array reactivity ($k_{eff} + 2\sigma = 0.721$) approaches the reactivity of the water-saturated, water-reflected unit single package ($k_{eff} + 2\sigma = 0.702$).

The difference between Cases **nciaunhct11_8_*nn*_1_3** and **nciaunhct11_8_*nn*_2_3** is the absence of 277-4 canned spacers in the former case and the presence of 277-4 canned spacers in the latter case. The 277-4 canned spacers are not actually modeled in the NCT package calculation models for UNH crystals content. Instead, the amount of solution content distributed over the entire containment vessel is reduced proportionally by the free volume of the containment vessel not occupied by canned spacers.

In a series of NCT calculations (Cases **nciaunhct11_8_*nn*_1_3**), the $k_{eff} + 2\sigma$ values are above the USL of 0.925 for mass loadings between 9,000 and 21,000 g UNH crystals. Although mass loadings above 21,000–24,000 are adequately subcritical, credit is not taken for water tightness that is demonstrated by the NCT (and HAC) tests. Therefore, mass loading are restricted to <8 kg UNH crystals. The CSI = 0.0 [10 CFR 71.59(a)(1) and 10 CFR 71.59(b)] for ES-3100 packages having a maximum of 3789g ^{235}U. The suitability of this determination depends upon satisfactory results under the HAC evaluation of Sect. 6.6.4. [10 CFR 71.59(a)(2) and 10 CFR 71.59(b)]

The $k_{eff} + 2\sigma$ values are expected to range from subcritical to critical for array configurations where UNH crystals are dissolved in the water flooding the containment vessel and the containment vessel well. It requires intrusion of water into the containment vessel, dissolving of UNH crystals in the influent, and leakage of solution out of the containment vessels in each package of an array. This condition is an accident condition, not credible for NCT.

For Cases **ncf1unhct12_8_*nn*_1_3**, the $k_{eff} + 2\sigma$ values are below the USL of 0.925. Given that the results for NCT (Sect. 6.5.4) and HAC are adequately subcritical, packages may be shipped under a CSI = 0.4

for packages with a maximum of UNH crystals. The CSI = 0.4 [10 CFR 71.59(a)(1) and 10 CFR 71.59(b)] for ES-3100 packages having a maximum of 24,000 g UNH crystal. Likewise, the suitability of this determination depends upon satisfactory results under the HAC evaluation of Sect. 6.6.4.

6.6 EVALUATION OF PACKAGE ARRAYS UNDER HYPOTHETICAL ACCIDENT CONDITIONS

Except for UNH crystals, the package content is confined within the containment vessel for the HAC array evaluation of ES-3100 packages, consistent with the result of the tests specified in 10 CFR 71.73 (Hypothetical Accident Conditions). The array sizes examined in this evaluation are infinite, 13×13×6, 9×9×4, 7×7×3, 5×5×2, and the degenerate single unit. The "N" and corresponding CSI values for arrays determined to be adequately subcritical are as follows: N = ∞, CSI = 0; N = 507, CSI = 0.1; N =162, CSI = 0.4; N = 73, CSI = 0.7; N = 25, CSI = 2.0; and N = 19, CSI = 2.7. All arrays, except the infinite array, are reflected with 30 cm (1 ft) of water. These array are nearly cubic in shape for optimum reactivity of the array, thus eliminating the need for placing criticality controls on package arrangements in terms of stack height, width, and depth of an array. The array configurations and the range of water contents (Table 6.4) evaluated bound all possible packaging arrangements and moderation conditions for HAC.

For the single damaged package, and for infinite and finite arrays of damaged packages with HEU metal, HEU oxide, or UNH crystal content, the neutron multiplication factor changes as a function of the ^{235}U mass, MOIFR, or applicable solution concentration in the same manner as in an array of undamaged packages.

6.6.1 Solid HEU Metal of Specified Geometric Shapes

For infinite and finite arrays of damaged packages with HEU metal, the neutron multiplication factor increases as a function of the ^{235}U mass and decreases as a function of MOIFR. For example, consider the ES-3100 package loaded with three convenience cans that contain a 3.24-in.-diam cylinder with 12,000 g ^{235}U for a total of 36,000 g ^{235}U. For package content without 277-4 canned spacers, the $k_{eff}+2\sigma$ values range from 1.027 to 0.967 with increasing MOIFR in the damaged packages [Cases **hciacyct12_36_1_1** through **hciacyt12_36_1_15** (Appendix 6.9.6, Table 6.9.6-3)]. For package content with 277-4 canned spacers, the k_{eff} + 2σ values range from 0.956 to 0.884 with increasing MOIFR in the damaged package [Cases **hciacyt12_36_2_1** through **hciacyt12_36_2_15** (Appendix 6.9.6, Table 6.9.6-3)].

The introduction of water above ~0.01 MOIFR shows the effect of isolating the individual array units from each other. The neutron multiplication factor approaches k_{eff} for the single, water-reflected unit at a full content-water fraction (MOIFR = 1.0). Comparison of these results with the corresponding NCT cases (Sect. 6.5.1.) indicates no significant differences. This result is as expected given that the neutron multiplication in an infinite array is independent of pitch between fissile contents but is dependent on changes in mass and moderation in the array. The changes in both the outer dimensions and the compositions of the Kaolite and 277-4 of the ES-3100 package due to HAC result in changes to the neutron multiplication factor on the order of ~0.001 to 0.002.

Repeated for 4.25-in.-diam cylinders (Appendix 6.9.6, Table 6.9.6-7); 2.29-in.-square bars (Table 6.9.6-5); and 1.5-in.-diam × 2-in.-tall slugs (Table 6.9.6-9), this type of analysis for the 3.24-in.-diam cylinders demonstrates that arrays of damaged packages with restricted fissile material (^{235}U) loading remain subcritical over the entire range of water content or MOIFR. HEU bulk metal or alloy content not covered by the specified geometric shapes (cylinder, square bar, or slug contents) will be in the HEU broken metal category, and so limited.

Cases **hciatriga_1_1_3** through **hciatriga_1_15_3** (Appendix 6.9.6, Table 6.9.6-20) represent infinite arrays of damaged packages containing the bounding TRIGA fuel content (20 % enrichment with 45 wt % U containing 307 g ^{235}U), without 277-4 canned spacers. For these cases, the $k_{eff}+2\sigma$ values increase from 0.218 to 0.526 as MOIFR increases. The $k_{eff}+2\sigma = 0.526$ for Case **hciatriga_1_15_3** is substantially below the USL of 0.925, indicating that canned spacers are not required for criticality control. Given that the results for NCT (Sect. 6.5.2) and HAC are adequately subcritical, packages with TRIGA fuel content ≤921 g ^{235}U may be shipped under a CSI = 0.

As stated in Sect. 6.5.1, calculation results presented in Table 6.9.6-20d for an infinite array of ES-3100 packages (NCT packaging with extremely damaged TRIGA fuel content) is substantially below the USL of 0.925. Similar results are expected for an infinite array of ES-3100 packages (HAC packaging with extremely damaged TRIGA fuel content) given that changes external to the containment vessel due to the HAC do not result in an appreciable change in the neutron multiplication for the an array of packages. Therefore, the 10 CFR 7155(e)(1) requirement that the package be adequately subcritical under HAC with the package contents in the most reactive credible configuration is satisfied.

Consider the ~1090 g, 1.5-in.-diam x 2-in.-tall slugs that may be packed ten per convenience can. Cases **hcf25est11_2_2_8_3** through **hcf25est11_2_2_1_3** (Appendix 6.9.6, Table 6.9.6-9) represent a 9×9×4 array of packages for which the corresponding rounded CSI = 0.4. Case **hcia5est12_2_2_8_3** at 100 wt % with $k_{eff} + 2\sigma = 0.923$ is below the USL. Therefore, the restriction upon enrichment under the NCT evaluation, which requires values be ≤80 wt % as prerequisite for shipment of the package under a CSI = 0, need not change. Likewise, the fissile mass loading limit must be reduced to 18,287 g ^{235}U for eliminating the restriction on enrichment.

Case **hcf25est12_2_2_8_3** at 100 wt % ^{235}U (Appendix 6.9.6, Table 6.9.6-9) represents a 9 × 9 × 4 array of packages for which the corresponding rounded CSI = 0.4. Although Case **ncf25est12_2_2_7_3** at 95 wt % ^{235}U with $k_{eff}+2\sigma = 0.905$ is below the USL of 0.925, the fissile mass loading limit is conservatively set by the NCT result, which requires that the enrichment not exceed 80 wt % ^{235}U for 36 kg uranium mass loadings. The $k_{eff}+2\sigma$ decreases sufficiently when the array size is reduced to permit increasing the limit on enrichment to ≤95 wt % ^{235}U for mass loadings of 34.7 kg uranium metal. These CSI determinations are contingent upon satisfactory results under the HAC evaluation (Sect. 6.6.1).

The changes in both the outer dimensions of the package and the compositions of the Kaolite and 277-4 due to HAC result in an ~0.001 change in the neutron multiplication factor.

6.6.2 HEU Solid Metal of Unspecified Geometric Shapes or HEU Broken Metal

Consider the ES-3100 package loaded with three convenience cans for a total of 35,142 g ^{235}U with no canned spacers between content locations. The $k_{eff}+2\sigma$ values range from 1.14 to 0.939 with increasing MOIFR, Cases **hciabmt12_36_1_8_1** through **hciabmt12_36_1_8_15** (Appendix 6.9.6, Table 6.9.6-11). The introduction of water above ~0.01 MOIFR shows the effect of isolating the individual array units from each other. Array reactivity ($k_{eff}+2\sigma = 0.939$) approaches the reactivity of the water-saturated, water-reflected single package ($k_{eff}+2\sigma = 0.891$, Case **hcsrbmt12_36_1_15**, Table 6.9.6-11).

Cases **hciabmt12_1_*nn_mm*_3** through **hciabmt12_36_*nn_mm*_3** model the ES-3100 with the reduced-diameter HAC package model where the enrichment of the content is varied from 60 wt % to 100 wt % ^{235}U. These array cases with MOIFR = 1e-04 pertain specifically to HAC packages where the neutron poison of the body weldment liner inner cavity is at 90% moisture content, but the Kaolite is dry (in the as-manufactured condition), and neither recess of the package external to the containment vessel and the interstitial space between the drums of the array contains any residual moisture. As stated before, this HAC

case is more reactive than all other HAC cases where more moisture is present in the Kaolite and recesses of the package. Increasing the interspersed water between the containment vessels in the array will reduce neutronic interaction between the flooded contents to a point where the packages of the array become isolated.

Ranges of enrichment are specified in Table 6.1b (10 CFR 71.59) for identifying fissile mass loading limits for HEU broken metal. Consider specifically enrichments >95 wt % ^{235}U. The containment vessel calculations (Case **cvr3lha_36_1_8_15** versus Case **cvr3lha_36_2_8_15**, Appendix 6.9.6, Table 6.9.6-10) indicate that 277-4 canned spacers are required in this enrichment range, where the maximum evaluated mass loading of 35,142 g ^{235}U is possible. However, the fissile mass loading must be limited to 2774 g ^{235}U (Case **hciabmt12_3_2_8_3**) in order for the $k_{eff} + 2\sigma$ value (= 0.905) to be below the USL of 0.925. This fissile mass limit is conservative when applied to enrichments only slightly greater than 95 wt % ^{235}U. Given that the results for NCT (Sect. 6.5.2) and HAC are adequately subcritical, packages ≤2774 g ^{235}U and enrichment >95 wt % ^{235}U may be shipped under a CSI = 0.

This evaluation technique for determination of mass loading limits for enrichment intervals is repeated over the range of HEU enrichments. At HEU enrichment <60 wt % ^{235}U, the package mass loading limit is achieved, so no further delineation is required.

6.6.3 HEU Oxide

Like packages with HEU metal or broken metal, the neutron multiplication factor for an array of packages with HEU oxide decreases as a function of decreasing ^{235}U mass [Cases **hciaoxt12_1_24_1_3** through **hciaoxt12_1_16_1_3** (Appendix 6.9.6, Table 6.9.6-13)]. The $k_{eff} + 2\sigma$ values are below the USL of 0.925. Given that the results for NCT (Sect. 6.5.3) and HAC are adequately subcritical, packages may be shipped under a CSI = 0.0 for an infinite array of packages having product oxide with a maximum of 21,125 g ^{235}U.

Cases **hciask_1_15** through **hciask_10_15** (Appendix 6.9.6, Table 6.9.6-18b) evaluate infinite arrays of damaged packages having the 10 skull oxide compositions described in Sect. 6.4.3. The differences between the HAC case results and the NCT case results are not statistically significant. The $k_{eff} + 2\sigma$ values, ranging from 0.658 to 0.767, are substantially below the USL value of 0.925. Given that the results for NCT (Sect. 6.5.3) and HAC are adequately subcritical, packages may be shipped under a CSI = 0.0 for an infinite array of packages having skull oxide content with a maximum of 16,399 g ^{235}U and 921 g graphite.

6.6.4 UNH Crystals

Unlike HEU metal, broken metal or oxide content, UNH crystal is soluble in water, as mentioned in Sect. 6.4.4. Near optimum solution concentration occurs at content mass loadings of 9000 g UNH crystals or 415 g ^{235}U/l. Like packages with HEU metal, broken metal, or oxide, the neutron multiplication factor for an array of damaged packages with UNH crystals decreases as a function of increasing MOIFR. Cases **hciaunhct12_8_24_1_1** through **hciaunhct12_8_24_1_15** (Appendix 6.9.6, Table 6.9.6-15) reveal the effect of isolating the individual array units from each other with the introduction of water above ~0.01 MOIFR. Array reactivity ($k_{eff} + 2\sigma$ = 0.729) approaches the reactivity of the water-saturated, water-reflected unit single package ($k_{eff} + 2\sigma$ = 0.705).

Like the NCT evaluation, the difference in the HAC package calculation model represented by Cases **hciaunhct12_8_*nn*_1_3** and **hciaunhct12_8_*nn*_2_3** is the absence of 277-4 canned spacers in the former case and the presence of 277-4 canned spacers in the latter case. For the HAC package calculation models with of UNH crystal content, the 277-4 canned spacers are not actually modeled. Instead, the amount

of solution content distributed over the entire containment vessel is reduced proportionally by the free volume of the containment vessel not occupied by canned spacers.

In a series of HAC calculations, Cases **hciaunhct11_8_*nn*_1_3**, the calculated $k_{eff} + 2\sigma$ values are below the USL of 0.925 for loading with <9000 g UNH crystals. Given that the results for NCT (Sect. 6.5.4) and HAC are adequately subcritical, the CSI = 0.0 [10 CFR 71.59(a)(2) and 10 CFR 71.59(b)] for packages having a maximum of 3789g ^{235}U crystal.

The $k_{eff} + 2\sigma$ values are expected to range from subcritical to critical for array configurations where UNH crystals are dissolved in the water flooding the containment vessel and the containment vessel well. It requires intrusion of water into the containment vessel, dissolving of UNH crystals in the influent, and leakage of solution out of the containment vessels in each package of an array. The leakage out of the containment vessel of content moderated "to such an extent as to cause maximum reactivity consistent with the physical and chemical form of material" is not considered credible HAC based on results for tests specified in 10 CFR 71.73.

In a series of HAC calculations, Cases **hcf2unhct121_8_*nn*_1_3**, the calculated $k_{eff} + 2\sigma$ values are below the USL of 0.925 for loading with <9000 g UNH crystals. Given that the results for NCT (Sect. 6.5.4) and HAC are adequately subcritical, packages may be shipped under a CSI = 0.4 for packages with a maximum of 24,000 g UNH crystals.

6.7 FISSILE MATERIAL PACKAGES FOR AIR TRANSPORT

A series of calculations are performed for determining the most reactive configuration of the content and surrounding packaging material in an ES-3100 package that undergoes catastrophic destruction. Fissile content mass loadings that remain under the USL for these catastrophic events are identified. Subcriticality is demonstrated after due consideration of such aspects as the efficiency of moderator, loss of neutron absorbers, rearrangement of packaging components and contents, geometry changes and temperature effects. The seven calculation models used in this evaluation are described in Sect 6.3.1.4. Key model dimensions and parameters are tabulated in Tables 6.9.6-21 through 6.9.6-23, Appendix 6.9.6.

6.7.1 Results for Solid HEU, One Piece per Convenience Can

Cases **atdmr_10_8** through **atdmr_7_1** (Table 6.9.6-21, Appendix 6.9.6) pertain to Model 1 (Fig. 6.11, Section 6.3.1.4). HEU solid or broken metal of three convenience cans is homogenized with 513 g of polyethylene, representing the potential use of hydrogenous packing materials in the ES-3100. The fissile core is configured into a spherical shape with an exterior 20 cm water reflector. As shown in Fig. 6.17 and Table 6.9.6-21, the $k_{eff} + 2\sigma$ values decrease as a function of both enrichment and ^{235}U mass. The $k_{eff} + 2\sigma$ values are substantially below the USL of 0.925. The $k_{eff} + 2\sigma$ value for 7 kg of HEU at 100 % enrichment is 0.792.

Cases **atdmsr_7_8_11** through **atdmsr_7_1_1** (Table 6.9.6-21, Appendix 6.9.6) pertain to Model 2 (Fig. 6.12, Section 6.3.1.4). The fissile core of Model 1 is blanketed with a variable thickness stainless steel shell and an exterior 20 cm water reflector. As shown in Fig 6.18 and Table 6.9.6-21, the maximum $k_{eff} + 2\sigma$ values occur at zero stainless steel thickness. The $k_{eff} + 2\sigma$ value for 7 kg of HEU at 100% enrichment and zero stainless steel thickness is 0.793. The $k_{eff} + 2\sigma$ values decrease to minimum values for steel thicknesses of 0.99 cm at 100 % enrichment and thicknesses of 1.47 cm at 19 % enrichment while the NLF decreases from ~ 0.07 to 0.06. The NLF continues to decrease to a value of 0.03 as stainless steel is added up to the 66,133 g amount of the containment vessel and the liner and drum assembly. At maximum stainless steel thickness, the $k_{eff} + 2\sigma$ values increase to within 0.02 of the values for zero stainless steel thickness. The stainless steel

of the ES-3100 packaging is not as effective a reflector as the 20 cm water surrounding the core. The overall effect of adding the stainless steel of the ES-3100 packaging to the configuration is the reduction in the neutron multiplication factor for the system. The $k_{eff} + 2\sigma$ values are substantially below the USL of 0.925.

Cases **atdmkr_7_8_11** through **atdmkr_7_1_1** (Table 6.9.6-21, Appendix 6.9.6) pertain to Model 3 (Fig. 6.13, Section 6.3.1.4). The fissile core of Model 1 is blanketed with a variable thickness Kaolite shell and an exterior 20 cm water reflector. As shown in Fig. 6.19 and Table 6.9.6-21, the maximum $k_{eff} + 2\sigma$ values occur at a Kaolite shell thickness of zero. For 7 kg of HEU at 100 % enrichment, the $k_{eff} + 2\sigma$ value is 0.793. $K_{eff} + 2\sigma$ values decrease to asymptotic values at shell radii of ~14.74 cm (Kaolite thicknesses of ~ 8.66 cm) while the NLF decreases from ~ 0.07 to 0.03. The NLF continues to decrease to a value of 0.006 as water-saturated Kaolite is added up to the 128,034 g pre-bake amount inside the body weldment outer liner and the drum top plug. The asymptotic values for $k_{eff} + 2\sigma$ are ~ 0.043 below maximum $k_{eff} + 2\sigma$ values which occur at zero Kaolite thickness.

Cases **atdmdkr_7_8_11** through **atdmdkr_7_8_1** (Table 6.9.6-21, Appendix 6.9.6) pertain to Model 3 (Fig. 6.13, Section 6.3.1.4), where dry Kaolite is being evaluated consistent with test results of 10 CFR 71.55(d). Only 7 kg of HEU at 100 % enrichment is evaluated in these cases. As shown in Fig. 6.20 and Table 6.9.6-21, the $k_{eff} + 2\sigma$ value decreases to a minimum value at a shell radius of 31.08 cm (dry Kaolite thickness of 25.03 cm). The NLF decreases gradually from ~ 0.07 to 0.05 as NCT Kaolite is added up to the amount contained inside the body weldment outer liner and the drum top plug. Neutron leakage from a configuration with the NCT Kaolite of the ES-3100 packaging is much greater than leakage from one with water-saturated Kaolite. Over the range of moisture content, the Kaolite of the ES-3100 packaging is not as effective a reflector as the 20 cm water surrounding the core. The overall effect of adding Kaolite to the system is the reduction in neutron multiplication in the system. The $k_{eff} + 2\sigma$ values are substantially below the USL of 0.925.

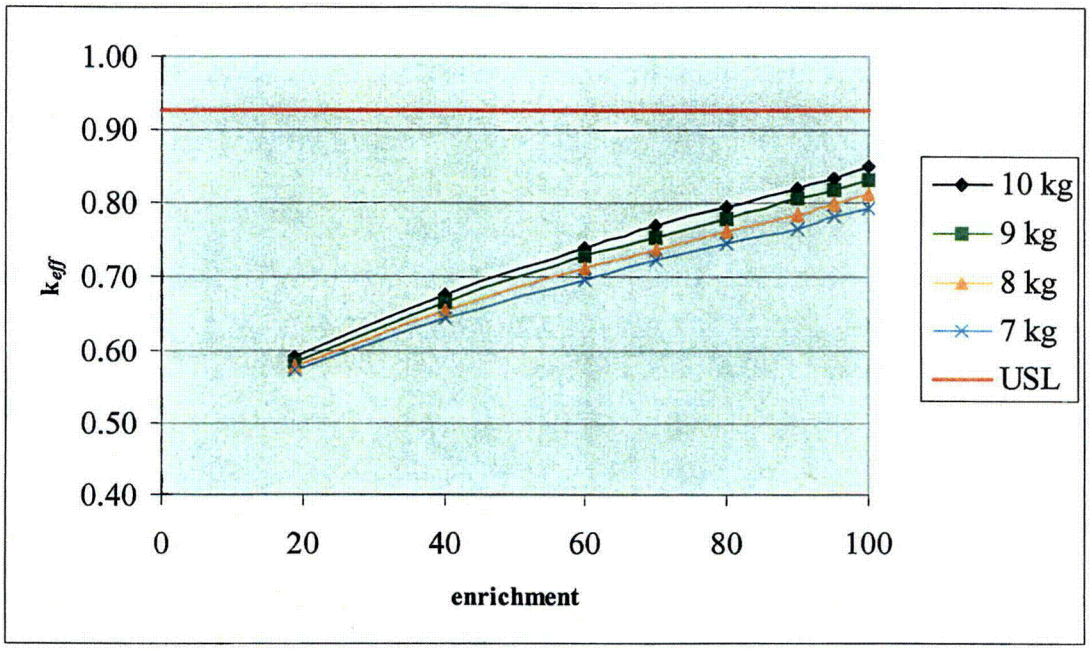

Fig. 6.17. K_{eff} vs. enrichment (wt % ^{235}U) for HEU ranging from 7 to 10 kg.

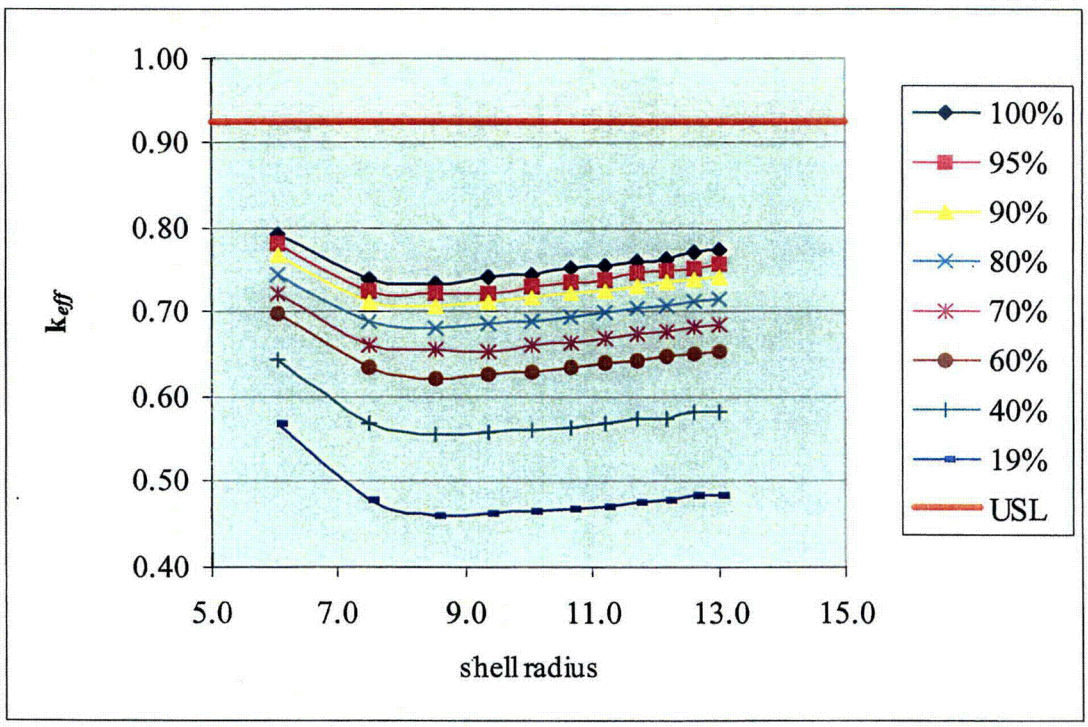

Fig. 6.18. K_{eff} vs. stainless steel shell radius (cm) for 7 kg HEU with enrichments ranging from 19 to 100 wt % ^{235}U.

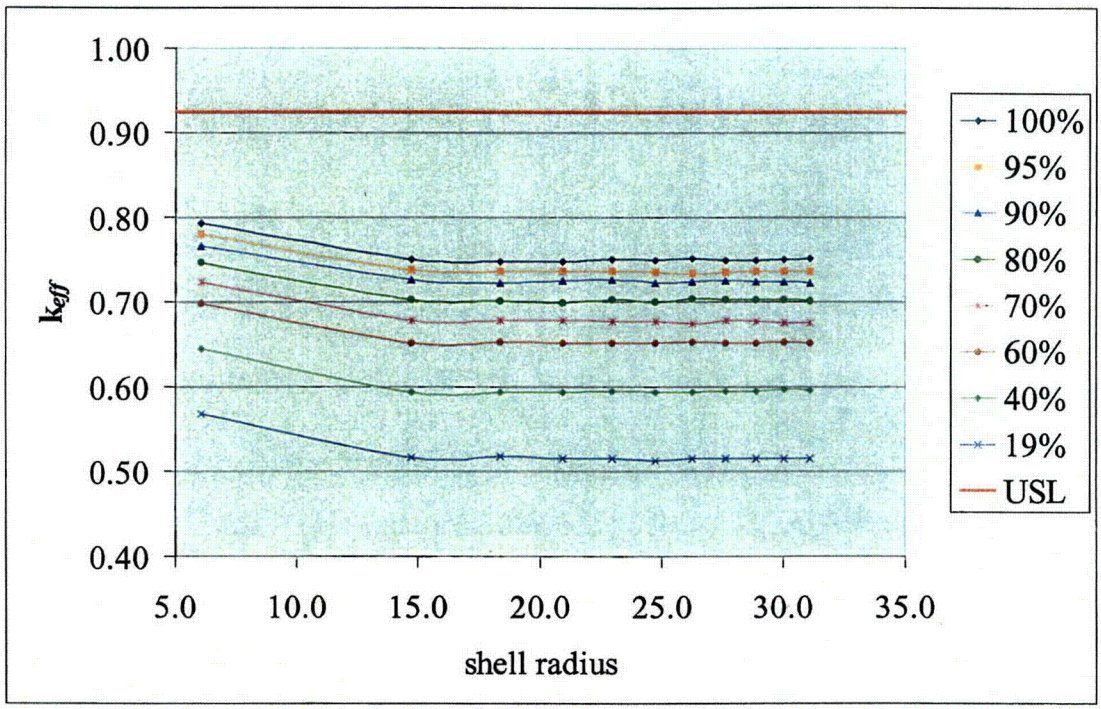

Fig. 6.19. K_{eff} vs. Kaolite shell radius (cm) for 7 kg HEU with enrichments ranging from 19 to 100 wt % ^{235}U.

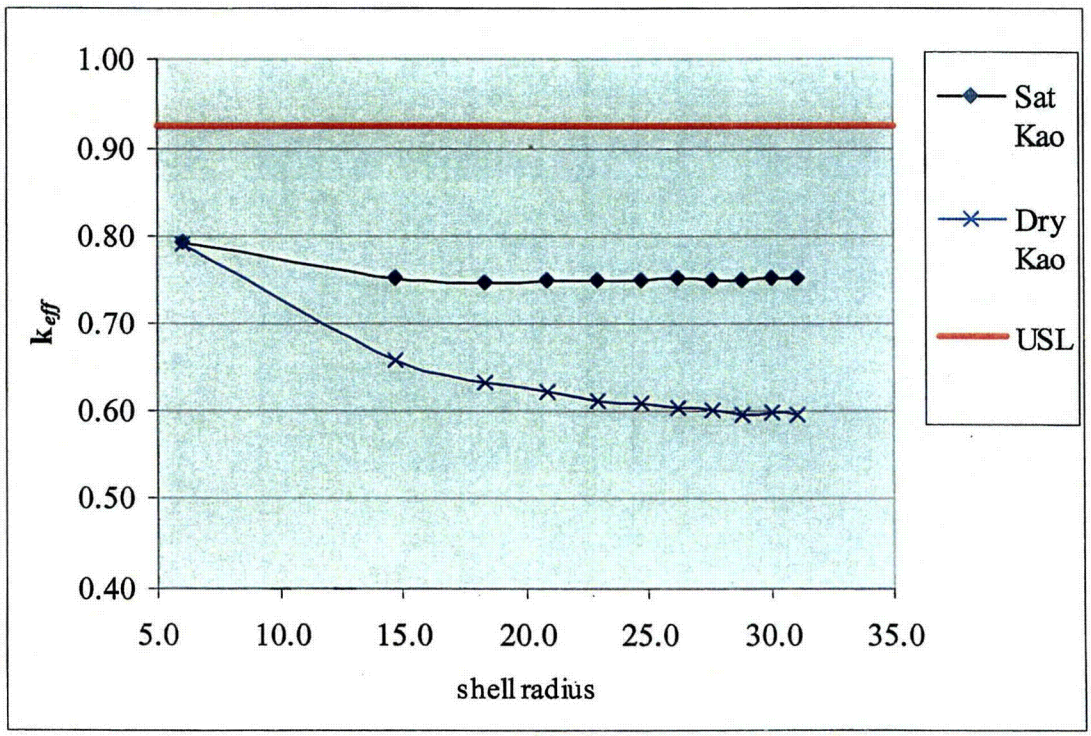

Fig. 6.20. K_{eff} vs. shell radius (cm) for dry and water-saturated Kaolite for 7 kg HEU at 100% enrichment.

6.7.2 Results for TRIGA Fuel Elements, Three Pieces per Convenience Can

Case **atdzr** pertains to Model 1 (Fig. 6.11, Section 6.3.1.4), in which 10.4 kg of $UZrH_x$ (921 g ^{235}U) of three TRIGA fuel elements is homogenized with 513 g polyethylene. The fissile core is configured into a spherical shape with an exterior 20 cm water reflector. The $k_{eff} + 2\sigma$ value of 0.679 (Table 6.9.6-22, Appendix 6.9.6) is substantially below the USL of 0.925.

Cases **atdzsr_11** through **atdzsr_1** pertain to Model 2 (Fig. 6.12, Section 6.3.1.4). The fissile core of Model 1 is blanketed with a variable thickness stainless steel shell with an exterior 20 cm water reflector. As shown in Fig 6.21 and Table 6.9.6-22 (Appendix 6.9.6), the $k_{eff} + 2\sigma$ value decreases to minimum value for a stainless steel thickness of 1.87 cm while the NLF decreases from ~ 0.06 to 0.05. The NLF decreases to 0.03 as stainless steel is added up to the 66,133 g amount of the containment vessel and the liner and drum assembly. At maximum stainless steel thickness, the $k_{eff} + 2\sigma$ values increase to within 0.058 of the values for zero stainless steel thickness. The overall effect of adding stainless steel to the system is the reduction in neutron multiplication in the system. The $k_{eff} + 2\sigma$ values are substantially below the USL of 0.925.

Cases **atdzkr_11** through **atdzkr_1** pertain to Model 3 (Fig. 6.13, Section 6.3.1.4). The fissile core

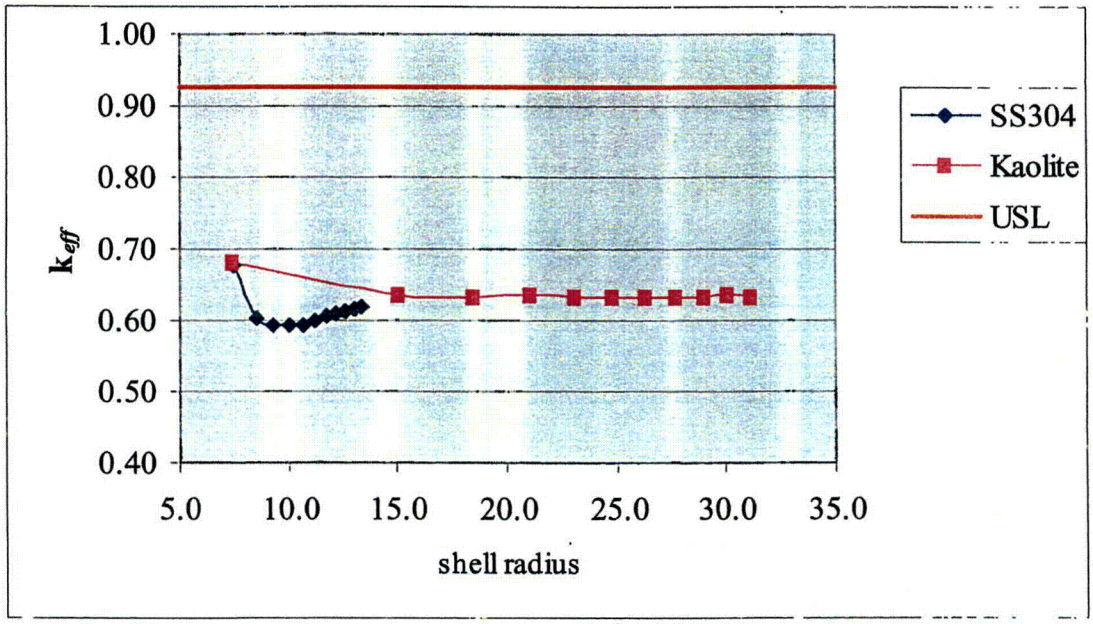

Fig. 6.21. K_{eff} vs shell radius (cm) for 10.4 kg core of $UZrH_x$ with stainless steel or Kaolite shell.

of Model 1 is blanketed with a variable thickness Kaolite shell with an exterior 20 cm water reflector. As shown in Fig. 6.21 and Table 6.9.6-22 (Appendix 6.9.6), the $k_{eff} + 2\sigma$ values decrease to an asymptotic value at a shell radius of 18.54 cm (Kaolite thickness of 11.08 cm.) The NLF decreases from ~ 0.06 to 0.02. The NLF continues to decrease to a value of 0.006 as water-saturated Kaolite is added up to the 128,034 g pre-bake amount contained inside the body weldment outer liner and the drum top plug. The asymptotic value for $k_{eff} + 2\sigma$ is ~ 0.048 below the maximum $k_{eff} + 2\sigma$ value at zero Kaolite thickness. The overall effect of adding water-saturated Kaolite to the system is the reduction in neutron multiplication in the system. The $k_{eff} + 2\sigma$ values are substantially below the USL of 0.925.

Cases **athzpkr_11** through **athzpkr_1** pertain to Model 4 (Fig. 6.14, Section 6.3.1.4). The homogenized core of Model 4 consists of $UZrH_x$, 500 g of polyethylene, and Kaolite. For this set of

parametric cases, the Kaolite water content ranges from the water-saturated (maximum radius) to the dry condition (minimum radius) [Table 6.9.6-22, Appendix 6.9.6]. As shown in Fig. 6.22 and Table 6.9.6-22, the $k_{eff}+2\sigma$ value remains constant at ~0.468 until the moisture content drops to 60% at a core radius of 37.17 cm. The $k_{eff}+2\sigma$ value decreases to a minimum value of 0.306 at the dry Kaolite condition. The homogenization of the Kaolite shell and the fissile material core from Model 3 produces two competing effects in Model 4:

- addition of Kaolite expands the fissile material core, reducing neutron multiplication (evident in the comparison of results for Cases **athzphr_11** and **atdzkr_11**), and
- the addition of the water in the Kaolite increases neutron multiplication.

Consequently, the scenario of water penetration of fissile material core requires evaluation.

Cases **athzpwskr_9_11** through **athzpwskr_9_1** pertain to Model 5 (Fig. 6.15, Section 6.3.1.4). Model 5 is a variation of Model 3, which represents a fissile material core blanketed with water-saturated

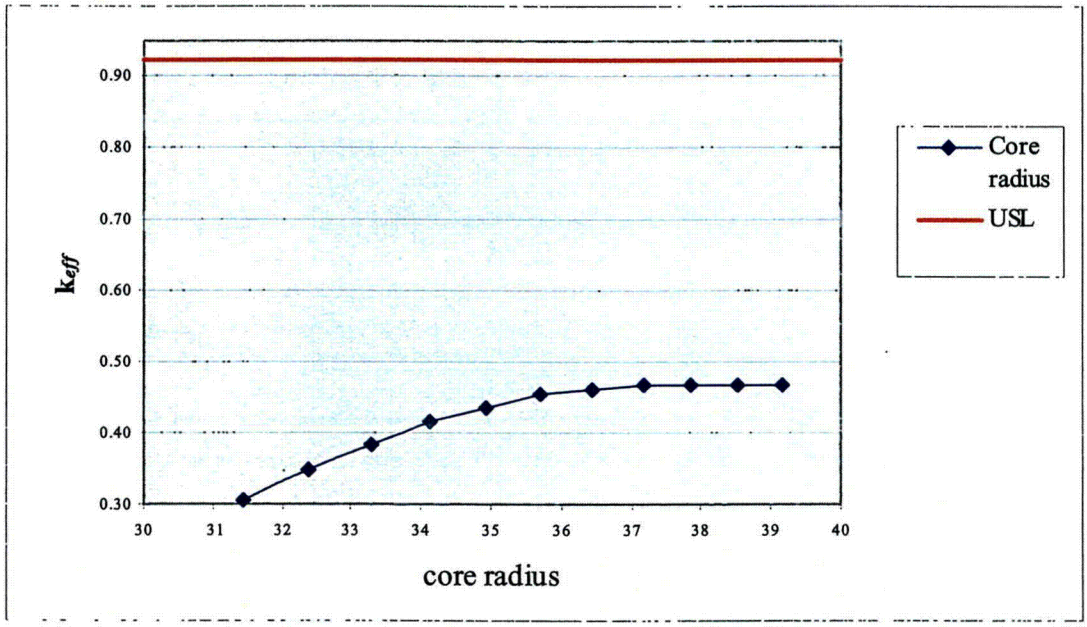

Fig. 6.22. K_{eff} vs. core radius (cm) for homogenized core of $UZrH_x$, 500 g polyethylene, and Kaolite where the Kaolite water content ranges from the dry to the water-saturated condition.

Kaolite and reflected by 20 cm of water. In Model 5, excess water from the Kaolite shell is assumed to penetrate the core. As shown in Fig. 6.23 and Table 6.9.6-22a (Appendix 6.9.6), the $k_{eff}+2\sigma$ value increases to a maximum of 0.962 with the addition of 14,922 g of excess water into the fissile material core. As more water is added to the core, the core becomes overmoderated and the $k_{eff}+2\sigma$ value decreases below the subcritical limit.

In the absence of Part 7155(f) Test data or dynamic impact simulations per Type-C test criteria, the assumption of water penetration of the fissile material core is valid under the severe air transport evaluation criteria. Models 5 is applicable to air transport of the ES-3100 package given that the geometric form of the TRIGA fuel content following the air transport accident can not be established.

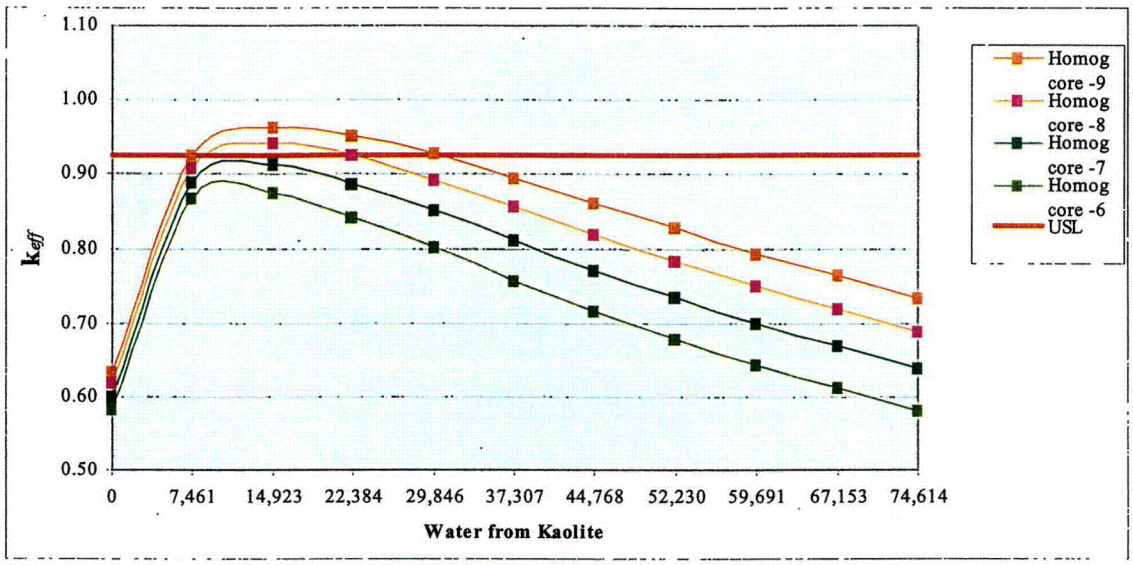

Fig. 6.23 k_{eff} vs. excess water from Kaolite for fissile core blanketed with a variable thickness Kaolite shell.

Additional case results are presented in Table 6.9.6-22a (Cases **athzpwskr_8_11** through **athzpwskr_6_1**) where the number of fuel segments is reduced from 9 items in a package to 6 items where the content remains subcritical over the entire range of moderation. As shown in Fig. 6.23 and Table6.9.6-22a (Appendix 6.9.6), the $k_{eff}+2\sigma$ value increases to a maximum of 0.911with the addition of 14,922 g of excess water into the fissile material core for a package loading of 716 g ^{235}U. As more water is added to the core, the core becomes overmoderated and the $k_{eff}+2\sigma$ value decreases to 0.601.

Model 6 (Fig. 6.16, Section 6.3.1.4) pertains to the case where fissile material from the homogenized core of Model 4 forms a shell external to the core. Given that the total amount of fissile material is limited to 716 g ^{235}U, the quantity is not sufficient to form a critical configuration. As shown in Section 6.7.3, this apparent even if kilogram quantities of additional fissile material were located in the shell adjacet to the core.

6.7.3 Results for HEU Broken Metal, More Than One Piece per Convenience Can

The results for Models 1–3 are presented in Sect. 6.7.1. Cases **athmpkr_12_8_11** through **athmpkr_8_8_1** (Table 6.9.6-23, Appendix 6.9.6) pertain to Model 4 (Fig. 6.14, Section 6.3.1.4) for broken metal loadings in the range of 4–7 kg ^{235}U for uranium at 100% enrichment and Kaolite water content from dry to water saturation values. Cases **athmpkr_12_1_11** through **athmpkr_10_1_1** pertain to loadings in the range of 5–7 kg ^{235}U for uranium at 20% enrichment and Kaolite water content from dry to water saturation values. The $k_{eff}+2\sigma$ values are adequately below the USL of 0.925 for mass loadings up to 4,000 g ^{235}U at 100% enrichment and up to 6,000 g ^{235}U at 20% enrichment.

Cases **athmpwskr_12_8_11** through **athmpwskr_2_8_1** (Table 6.9.6-23, Appendix 6.9.6) pertain to Model 5 (Fig. 6.15, Section 6.3.1.4) for mass loadings in the range of 1–7 kg ^{235}U for uranium at 100% enrichment and for core water content over the range of excess water from the Kaolite shell. As shown in Fig. 6.24 and Table 6.9.6-23 (Appendix 6.9.6), the $k_{eff}+2\sigma$ values are significantly above the USL.

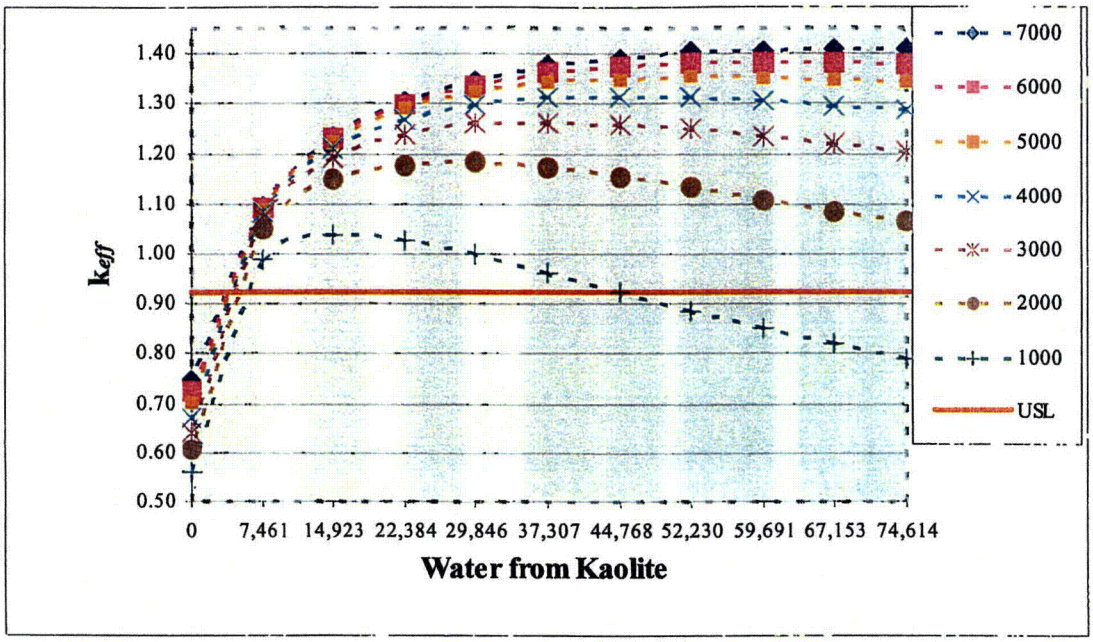

Fig. 6.24. K_{eff} vs. excess water from Kaolite for core of 1–7 kg enriched HEU broken metal at 100% enrichment, core blanketed with a variable thickness Kaolite shell.

Cases **athmpwskr_12_1_11** through **athmpwskr_2_1_1** and Cases **athm2pwskr_5_1_11** through **athm2pwskr_2_1_1** pertain to mass loadings in the range of 7–0.6 kg ^{235}U for uranium at 20% enrichment and core water content over the range of excess water from the Kaolite shell. As shown in Fig. 6.25 and Table 6.9.6-23 (Appendix 6.9.6), the $k_{eff} + 2\sigma$ values are adequately below the USL of 0.925 for mass loadings up to 700 g ^{235}U at 20% enrichment. This signifies the fissile mass loading limit for HEU broken metal content to be shipped by air transport. Therefore, the evaluation of Model 6 is focused on this limit.

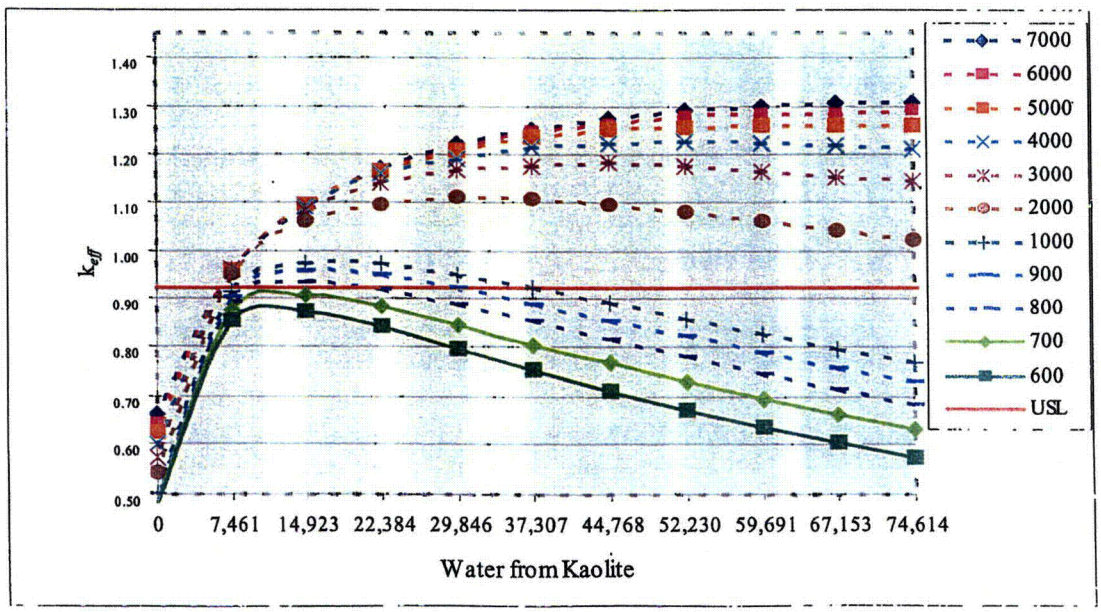

Fig. 6.25. K_{eff} vs. excess water from Kaolite for core 20% enriched HEU broken metal (0.6–7 kg ^{235}U), core blanketed with a variable thickness Kaolite shell.

Cases **athmpkmr_6_1_1_11** through **athmpwskr_1_6_1_1** (Table 6.9.6-23, Appendix 6.9.6) pertain to Model 6 (Fig. 6.16, Section 6.3.1.4), where fissile material from the homogenized core of Model 4 forms a shell external to the core. Cases **athmpkmr_6_1_1_11** through **athmpkmr_6_1_1_1** represent 3 kg ^{235}U in the core and 0.5 kg ^{235}U in the shell (17.5 kg total HEU at 20% enrichment) with the water content of the Kaolite ranging from the water-saturated to the dry condition. In the subsequent series of cases, the $k_{eff} + 2\sigma$ values decrease as HEU is moved from the core to the shell in 2.5 kg increments. Although the total HEU of 17.5 kg greatly exceeds the 3.5 kg limit identified in the evaluation of Model 5, all $k_{eff} + 2\sigma$ values are adequately below the USL of 0.925.

6.7.4 Conclusions

Given that the results for catastrophic damage are adequately subcritical, ES-3100 packages may be shipped via air transport with:

- Solid or broken HEU metal with up to 700 g ^{235}U, or
- 3 fuel sections ("meats") of $UZrH_x$ per loaded convenience can and up to 3 loaded cans per package where the ^{235}U does not exceed 716 g at 20% enrichment or 408 g ^{235}U at 70%.
- ~15 inch long clad fuel rods, each rod derived from a single TRIGA fuel element, and where per package ^{235}U does not exceed 716 g at 20% enrichment or 408 g ^{235}U at 70%.

6.8 BENCHMARK EXPERIMENTS

6.8.1 Applicability of Benchmark Experiments

The criticality validation is specific to uranium, plutonium, and uranium-233 systems encompassing a substantial subset of the database used to prepare the Organization for Economic Cooperation and Development (OECD) Handbook, Volumes I–VI. The benchmark specifications are intended for use by criticality safety engineers to validate the application of criticality calculation techniques such as SCALE 4.4a. Example calculations presented in the handbook do not constitute a validation of the codes or cross-section data sets by themselves, but the Handbook information can be and has been used to validate SCALE 4.4a by competent nuclear criticality safety persons.

The data from the benchmark experiments involving uranium represent a sufficiently wide range of enrichments and physical and chemical forms to cover many existing or presently planned activities for Y-12. These include enriched uranium with ^{235}U only and natural and depleted uranium, as well as highly enriched uranium, intermediate enriched uranium, and low enriched uranium. Data analyzed from critical experiments in this validation include systems having fast, intermediate, and thermal neutron energy spectra, and they include materials in various physical and chemical forms such as uranium metals, solutions, and oxide compounds. With the benchmark experiments that are directly applicable to uranium systems, there is a high level of confidence that the calculated results presented in this evaluation are sufficiently accurate to establish the safety of the package under both NCT and HAC. This conclusion is based on the validation of the code and cross-section library described in Sect. 6.3.3.

6.8.2 Details of Benchmark Calculations

The validation of CSAS25 control module of SCALE 4.4a with the 238-group ENDF/B-V cross-section library is documented in Y/DD-896/R1 and Y/DD-972/R1. Y/DD-896/R1 addresses the establishment of bias, bias trends, and uncertainty associated with the use of SCALE 4.4a for performance

of criticality calculations. This evaluation is directed at uranium systems consisting of fissile and fissionable material in metallic, solution, and other physical forms, as well as plutonium and ^{233}U systems, as described in the OECD Handbook. [NEA/NSC/DOC(95)03] The focus is on comparison of k_{eff} with the associated experimental results for establishment of bias, bias trends, and uncertainty as a final step. Compiled data for 1217 critical experiments are used as the basis for the calculation models. The calculated results from SCALE 4.4a using the 238-group ENDF/B-V cross-section library have been compared with reported results for the benchmark experiments. Comparison of results demonstrates that SCALE 4.4a run on the SAE HP J-5600 unclassified workstation (CMODB) produces the same results within the statistical uncertainty of the Monte Carlo calculations as reported by the OECD for the experiments.

Y/DD-972/R1 addresses determining USL and for incorporating uncertainty and margin into this USL. Y/DD-972/R1 establishes subcritical limits determined through an evaluation of statistical parameters of calculation results for critical experiments. The correlating parameters (i.e., mass, enrichment, geometry, absorption, moderation, reflection) and values for applying additional margin to the subcritical limits are application dependent. The determination of correlating parameters and additional margin is an integral part of the process analysis for a particular application. For the critical experiment results, no correlation between calculation results and neutron energy causing fission was found. As such, this document does not specify "final" USL values as has been done in the past.

6.8.3 Bias Determination

The USL is based on the non-parametric statistics-based lower tolerance limit (LTL) for greater than 0.99/99% where there is a probability of greater than 0.99 that 99% of the population is greater than a specified result, reduced by additional margin. From Table 1 of Y/DD-972R1, the LTL combining bias and bias uncertainty is 0.975 for uranium systems, including HEU metal, indicating a bias value of 0.025. Ordinarily the USL would be 0.955 where an additional margin of subcriticality of 0.02 is subtracted from the LTL of 0.975. However, guidance provided by NUREG/CR-5661 requires that the bias value of 0.025 be subtracted from 0.95 for determination of the USL, giving a value of 0.925.

6.9 APPENDICES

Appendix	Description
6.9.1	FISSILE CONTENT MODELS
6.9.2	HAC PACKAGE MODEL
6.9.3	PACKAGE MATERIAL COMPOSITIONS
6.9.4	QUALIFICATION OF A NEUTRON ABSORBER MATERIAL FOR THE ES-3100
6.9.5	MISCELLANEOUS INFORMATION AND DATA
6.9.6	ABRIDGED SUMMARY TABLES OF CRITICALITY CALCULATION RESULTS
6.9.7	INPUT LISTINGS OF ES-3100 CALCULATION MODELS FOR SELECT CASES IDENTIFIED IN TABLES 6.1a-e

APPENDIX 6.9.1

FISSILE CONTENT MODELS

APPENDIX 6.9.1

FISSILE CONTENT MODELS

Figure 6.9.1-1 depicts the wire-mesh view of the 3.24-in.-diam highly enriched uranium (HEU) cylindrical content configuration inside the containment vessel. The interstitial water has been removed for illustration purposes. As can be seen from Fig. 6.9.1-1, the cylindrical content model contains one cylinder per convenience can and 1.4-in.-thick 277-4 canned spacers between the can locations. Cylinders are at the maximum diameter that will fit through the opening of a press-fit lid type convenience can. The cylindrical content shown is at the maximum mass loading; the height of the cylinders may change depending upon the mass loading.

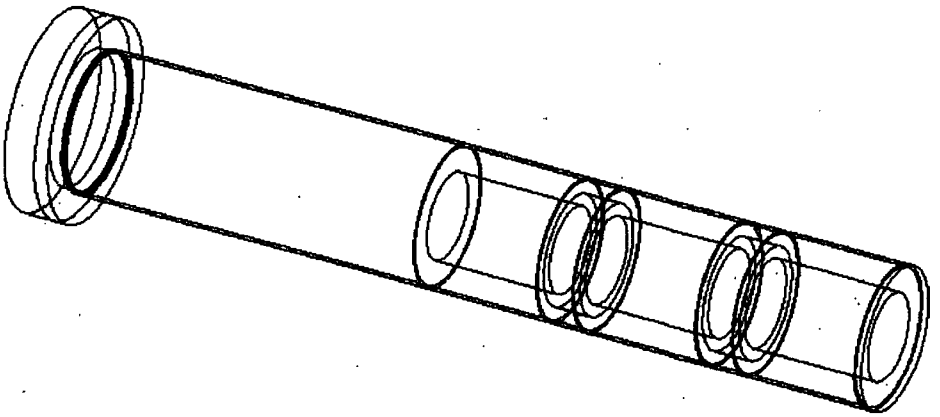

Fig. 6.9.1-1. Containment vessel containing 3.24-in.-diam cylinders and 1.4-in.-thick 277-4 canned spacers.

Figure 6.9.1-2 depicts the wire-mesh view of the 4.25-in.-diam HEU cylindrical content configuration inside the containment vessel. The interstitial water has been removed for illustration purposes. As can be seen from Fig. 6.9.1-2, the cylindrical content model contains one cylinder per convenience can and 1.4-in.-thick 277-4 canned spacers between the can locations. Cylinders are at the maximum diameter that will fit through the opening of a crimp-seal lid type convenience can. The cylindrical content shown is at the maximum mass loading; the height of the cylinders may change depending upon the mass loading.

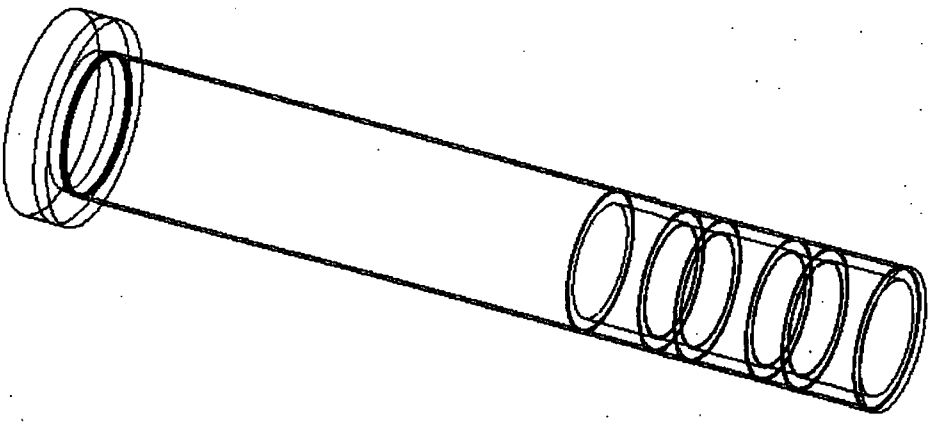

Fig. 6.9.1-2. Containment vessel containing 4.25-in.-diam cylinders and 1.4-in.-thick 277-4 canned spacers.

Figure 6.9.1-3 depicts the wire-mesh view of the 2.29-in.-square HEU bar content configuration inside the containment vessel. The interstitial water inside the containment vessel has been removed for illustration purposes. The square bar content model contains one bar per convenience can and 1.4-in.-thick 277-4 canned spacers between the can locations. The 2.29-in.-square bar is the largest size that will fit through the 3.24-in.-diam opening of a press-fit lid type convenience can. Similar to the cylindrical model, the height of the square bar is dependent upon the HEU mass.

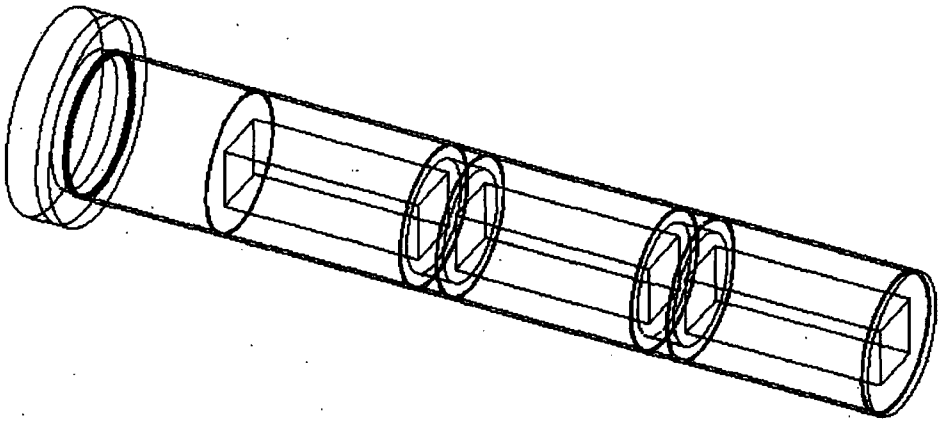

Fig. 6.9.1-3. Containment vessel containing 2.29-in.-square bars and 1.4-in.-thick 277-4 canned spacers.

Figure 6.9.1-4 depicts the wire-mesh view of a pentagonal ring configuration of the 1.5-in.-diam × 2.0-in.-tall slugs inside the containment vessel. The axial centerline of each slug is located 1.27598 in. from the origin of the pentagon such that a tight fitting configuration of slugs is modeled (i.e., there are no gaps between adjacent slugs). The slug content model contains two rings of the 1.5-in.-diam × 2.0-in.-tall slugs per convenience can and the 277-4 canned spacers between the convenience cans locations. The interstitial water inside the containment vessel has been removed for illustration purposes. Figure 6.9.1-4b depicts typical slug configurations that were evaluated.

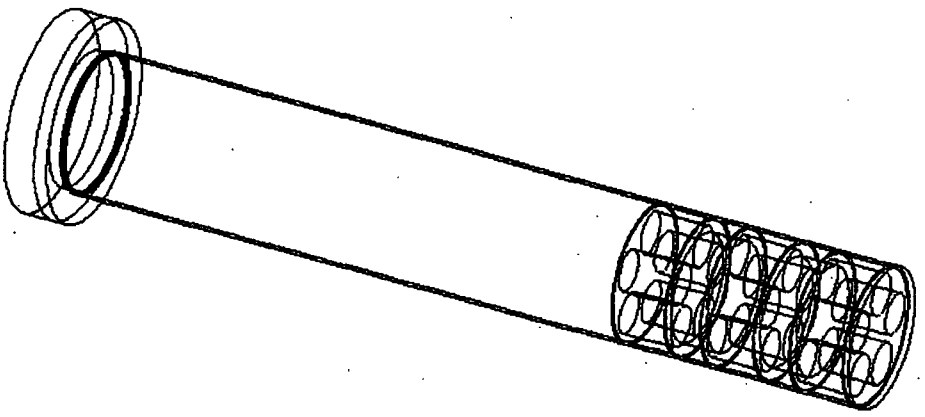

Fig. 6.9.1-4. Containment vessel containing the 1.5-in.-diam × 2.0-in.-tall slugs in a pentagonal ring configuration with 0.0-cm spacing between slugs and 1.4-in.-thick 277-4 canned spacers.

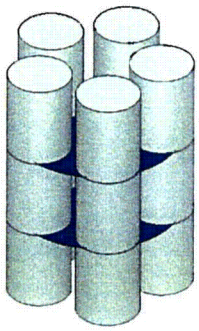

cvcr5est11_1_1
18,287 g ^{235}U
no canned spacers

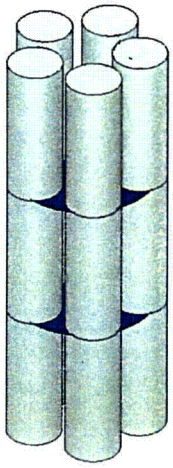

cvcr5est11_1_2
36,573 g ^{235}U
no canned spacers

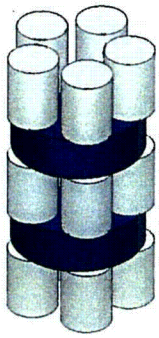

cvcr5est11_2_1
18,287 g ^{235}U
canned spacers

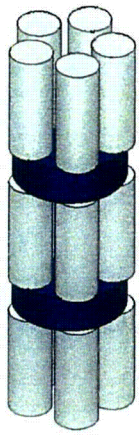

cvcr5est11_2_2
36,573 g ^{235}U
canned spacers

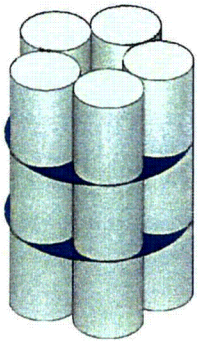

cvcr5st11_1_1
18,287 g ^{235}U
no canned spacers

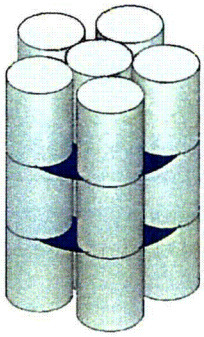

cvcr6e0t11_1_1
21,944 g ^{235}U
no canned spacers

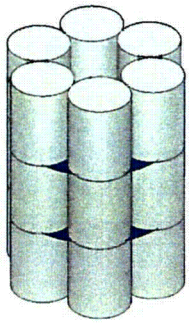

cvcr6st11_1_1
21,944 g ^{235}U
no canned spacers

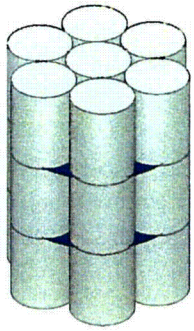

cvcr70st11_1_1
25,601 g ^{235}U
no canned spacers

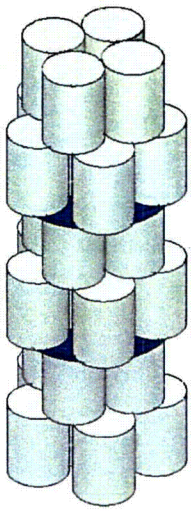

cvcr6e4t11_1_1
36,573 g ^{235}U
no canned spacers

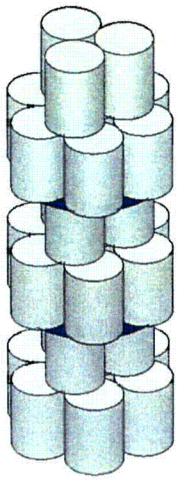

cvcr73t11_1_1
36,573 g ^{235}U
no canned spacers

Fig. 6.9.1-4b. Typical slug configurations. Blue marker depicted for configurations without 1.4-in.-thick 277-4 canned spacers.

Figure 6.9.1-5 depicts the wire-mesh view of the HEU oxide content inside the containment vessel. The interstitial water inside the containment vessel has been removed for illustration purposes. The HEU oxide mixture at bulk density is located at the bottom of the containment vessel and fills the space to the wall of the containment vessel. The height of the HEU oxide mixture is dependant upon the mass loading.

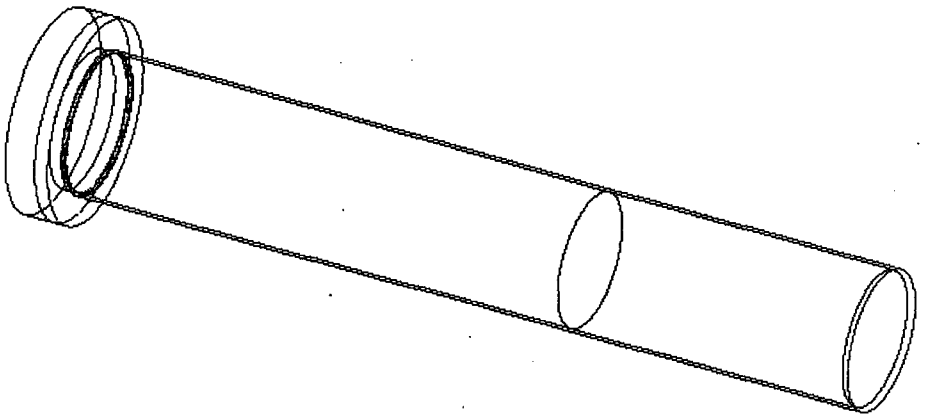

Fig. 6.9.1-5. Wire-mesh view of the containment vessel containing the HEU oxide mixture.

Figure 6.9.1-6 depicts the wire-mesh view of the UNH crystal content inside the containment vessel. A solution of UNH crystals dissolved in water fills the entire volume of the containment vessel.

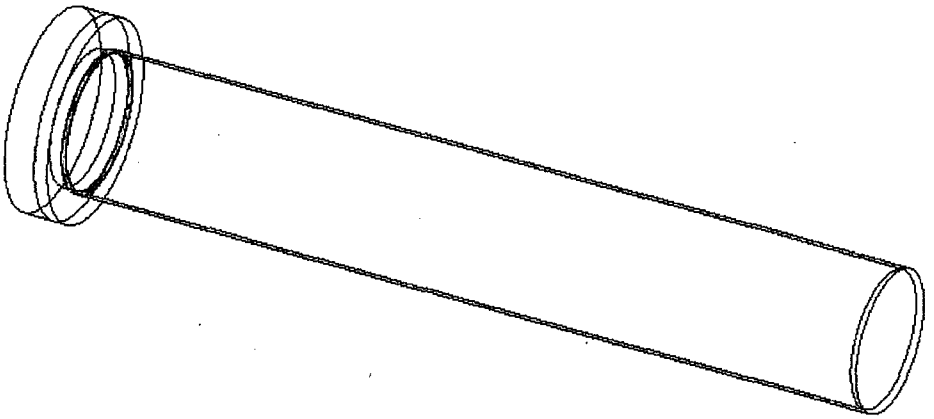

Fig. 6.9.1-6. Wire-mesh view of the containment vessel containing the UNH crystal mixture.

Wire-frame figures for the HEU broken metal models are presented in Appendix 6.9.3 (Figs. 6.9.3.1-4, 6.9.3.1-4b, 6.9.3.1-5, and 6.9.3.1-6).

APPENDIX 6.9.2

HAC PACKAGE MODEL

APPENDIX 6.9.2

HAC PACKAGE MODEL

6.9.2.1 PREDICTION OF HAC DAMAGE IN THE ES-3100 PACKAGE

Finite element analysis of an ES-3100 package under Hypothetical Accident Conditions (HAC) is used to predict the deformed outer diameters of the drum at node points along the vertical axis of an upright package. Selected node points are designated in a downward direction from the top of the drum as "UR," "MUR," "MR," "MLR," and "LR." Table 6.9.2.1-1 lists diameters at the five node points measured along the 90–270° and 0–180° axes. These dimensions represent major and minor axes at each deformation point on the assumption that the drum cross section is ellipsoidal. A corresponding equivalent circular diameter is also listed for each node point in Table 6.9.2.1-1.

A set of KENO V.a calculation models based on reduced package diameters at the "MR," "MLR," and "LR" deformation points are derived from the Normal Conditions of Transport (NCT) geometry model. These geometry models are evaluated for the purpose of establishing a bounding geometry model for representing the ES-3100 package under HAC. The primary changes made to the KENO V.a geometry input statements in the NCT model are reductions in the drum's radii. The change to the drum's inner radius also affects the outer radius of both the angle iron and the Kaolite located inside the containment vessel outer liner. The volume fractions for these materials are adjusted in the KENO V.a calculation models so that material masses of the affected package components are conserved. Table 6.9.2.1-2 provides data for transforming the KENO V.a calculation model from an NCT model into an HAC model.

Table 6.9.2.1-1. Deformation of the ES-3100 drum at five node points, projected by finite element analysis "Case 3100 RUN1HL Lower Bound Kaolite May 2004"

Deformation point	FEA node	Diameter at 90° (in.)	Diameter at 180° (in.)	Equivalent circular diameter	
				(in.)	(cm)
UR	098194	20.02	15.60	17.6724	44.8878
MUR	100238	20.74	15.07	17.6791	44.9050
MR	101589	20.74	14.18	17.1492	43.5588
MLR	103012	22.00	13.44	17.1954	43.6762
LR	105786	20.92	12.92	16.4404	41.7586

Table 6.9.2.1-2. Parameter changes for converting an NCT package model into an HAC package model

Parameter	Reference NCT package model	HAC model at MR node point of package	HAC model at MLR node point of package	HAC model at LR node point of package
Package Model Dimension				
OR_{Drum} (cm)	23.32990	21.77942	21.83809	20.87929
IR_{Drum} (cm)	23.17750	21.62702	21.68569	20.72689
$th_{Drum\ wall}$ (cm)	0.15240	0.15240	0.15240	0.15240
OR_{Lid} (cm)	23.11400	21.56352	21.62219	20.66339
IR_{Lid} (cm)	22.96160	21.41112	21.46979	20.51099
$th_{Kaolite}$ (cm)	12.10310	10.55262	10.61129	9.65249
Kaolite of the Body Weldment Inner Liner				
Mass (g)	117563.0	97080.4	97829.7	85839.8
Volume (cm^3)	134888.0	111387.0	112246.0	98489.5
Volume fraction multiplier [a]	–	1.21099	1.20171	1.36956
VF for water component of Kaolite	0.52294	0.63327 [b]	0.62843 [b]	0.71620 [b]
VF for dry mix component of Kaolite	0.34864	0.42220 [b]	0.41897 [b]	0.47749 [b]
Angle Iron				
Mass (g)	5621.76	4521.40	4561.66	3917.54
Volume (cm^3)	708.030	569.446	574.516	493.393
VF	1.0	1.24337	1.23239	1.43502
Drum Steel				
Mass (g)	25446.3	23397.6	23474.2	22231.2
Volume (cm^3)	3204.82	2946.80	2956.50	2799.90
VF	1.0	1.08756	1.08401	1.14462

[a] Volume fraction multiplier is an NCT density multiplier for conserving mass in components having modified volumes in the HAC calculation models.

[b] Volume Fraction (VF) for Kaolite components calculated by multiplying the VF used in the NCT model by volume fraction multiplier for the HAC model.

6.9.2.2 CRITICALITY CALCULATIONS

Sets of criticality calculations are performed for the "MR," "MLR," and "LR" models at five different package water contents over the range of HAC. The five package water contents of the void spaces external to the containment vessel and the interstitial space between drums are as follows: 1e-20 spg water, 1e-04 spg water, 0.1 spg water, 0.3 spg water, and 1.0 spg water. The water content in the Kaolite corresponds to the dry condition (VF= 0.0287) where neutronic interaction between the packages of an array is maximized.

An infinite array of packages is evaluated in order to eliminate any biases arising from spectral leakage effects in the reflector of the finite array. The k_{eff} values for each KENO V.a case are based on

500,000 neutron histories produced by running for 215 generations with 2,500 neutrons per generation and truncating the first 15 generations of data. Each package modeled has 36 kg of 100% enriched uranium in the form of broken metal content.

Each case is rerun using a different starting random number in order to produce sets of computed k_{eff} values that are statistically independent. The random starting number, the mean value (k_{eff}), and the corresponding standard error (s_i) computed for ten individual runs are shown in Tables 6.9.2.2-1, -2, and -3. The same statistical method (described in DAC-FS-900000-A014) used in the evaluation of Kaolite models (Appendix 6.9.3, Sect. 6.9.3.4) is also used here for determining whether or not differences in neutronic performance between the package models are statistically significant.

Table 6.9.2.2-1. Neutron multiplication factors with standard deviations for the ES-3100 package models at the "MR" and "MLR" node points

moifr	Random Number	"A" cases	k_{eff}	s	"B" cases	k_{eff}	s
1.0e-20	109E77866CF6	mrandnum_01_01	1.04965	0.00119	lrrandnum_01_01	1.05093	0.00133
1.0e-20	16AA4A58735C	mrandnum_01_02	1.05132	0.00131	lrrandnum_01_02	1.05009	0.00118
1.0e-20	1814171B652A	mrandnum_01_03	1.05368	0.00123	lrrandnum_01_03	1.05057	0.00118
1.0e-20	1A423B9472C7	mrandnum_01_04	1.05165	0.00145	lrrandnum_01_04	1.05066	0.00120
1.0e-20	20E876D82248	mrandnum_01_05	1.05344	0.00106	lrrandnum_01_05	1.04882	0.00129
1.0e-20	3F6E65CA7440	mrandnum_01_06	1.05188	0.00157	lrrandnum_01_06	1.05316	0.00127
1.0e-20	479D21DB7509	mrandnum_01_07	1.05149	0.00148	lrrandnum_01_07	1.05229	0.00134
1.0e-20	55D4371D3A23	mrandnum_01_08	1.05083	0.00113	lrrandnum_01_08	1.05186	0.00131
1.0e-20	6E1A14672B8F	mrandnum_01_09	1.04910	0.00106	lrrandnum_01_09	1.05236	0.00113
1.0e-20	77A0308C0E44	mrandnum_01_10	1.05254	0.00106	lrrandnum_01_10	1.05098	0.00120
moifr	**Random Number**	**"A" cases**	**k_{eff}**	**s**	**"B" cases**	**k_{eff}**	**s**
1.0e-04	109E77866CF6	mrandnum_03_01	1.04994	0.00132	lrrandnum_03_01	1.05122	0.00123
1.0e-04	16AA4A58735C	mrandnum_03_02	1.05023	0.00118	lrrandnum_03_02	1.05324	0.00121
1.0e-04	1814171B652A	mrandnum_03_03	1.05090	0.00139	lrrandnum_03_03	1.05143	0.00123
1.0e-04	1A423B9472C7	mrandnum_03_04	1.05072	0.00115	lrrandnum_03_04	1.05048	0.00121
1.0e-04	20E876D82248	mrandnum_03_05	1.05052	0.00119	lrrandnum_03_05	1.05095	0.00137
1.0e-04	3F6E65CA7440	mrandnum_03_06	1.05383	0.00131	lrrandnum_03_06	1.05029	0.00119
1.0e-04	479D21DB7509	mrandnum_03_07	1.05205	0.00153	lrrandnum_03_07	1.05124	0.00108
1.0e-04	55D4371D3A23	mrandnum_03_08	1.05343	0.00106	lrrandnum_03_08	1.05080	0.00116
1.0e-04	6E1A14672B8F	mrandnum_03_09	1.04831	0.00132	lrrandnum_03_09	1.05074	0.00122
1.0e-04	77A0308C0E44	mrandnum_03_10	1.05353	0.00111	lrrandnum_03_10	1.05094	0.00111
moifr	**Random Number**	**"A" cases**	**k_{eff}**	**s**	**"B" cases**	**k_{eff}**	**s**
0.10	109E77866CF6	mrandnum_06_01	0.97948	0.00120	lrrandnum_06_01	0.98315	0.00118
0.10	16AA4A58735C	mrandnum_06_02	0.98104	0.00125	lrrandnum_06_02	0.98605	0.00124
0.10	1814171B652A	mrandnum_06_03	0.98056	0.00134	lrrandnum_06_03	0.98690	0.00120
0.10	1A423B9472C7	mrandnum_06_04	0.97895	0.00114	lrrandnum_06_04	0.98347	0.00126
0.10	20E876D82248	mrandnum_06_05	0.98058	0.00113	lrrandnum_06_05	0.98770	0.00124
0.10	3F6E65CA7440	mrandnum_06_06	0.97966	0.00119	lrrandnum_06_06	0.98734	0.00140
0.10	479D21DB7509	mrandnum_06_07	0.97953	0.00145	lrrandnum_06_07	0.98417	0.00133
0.10	55D4371D3A23	mrandnum_06_08	0.97993	0.00130	lrrandnum_06_08	0.98712	0.00136
0.10	6E1A14672B8F	mrandnum_06_09	0.97972	0.00138	lrrandnum_06_09	0.98533	0.00142
0.10	77A0308C0E44	mrandnum_06_10	0.98157	0.00134	lrrandnum_06_10	0.98412	0.00116

Table 6.9.2.2-1. Neutron multiplication factors with standard deviations for the ES-3100 package models at the "MR" and "MLR" node points

moifr	Random Number	"A" cases	k_{eff}	s	"B" cases	k_{eff}	s
0.30	109E77866CF6	mrandnum_08_01	0.93412	0.00118	lrrandnum_08_01	0.93910	0.00146
0.30	16AA4A58735C	mrandnum_08_02	0.93227	0.00138	lrrandnum_08_02	0.93757	0.00117
0.30	1814171B652A	mrandnum_08_03	0.93390	0.00131	lrrandnum_08_03	0.93940	0.00146
0.30	1A423B9472C7	mrandnum_08_04	0.93252	0.00144	lrrandnum_08_04	0.93676	0.00130
0.30	20E876D82248	mrandnum_08_05	0.93334	0.00132	lrrandnum_08_05	0.93851	0.00111
0.30	3F6E65CA7440	mrandnum_08_06	0.93168	0.00132	lrrandnum_08_06	0.93914	0.00149
0.30	479D21DB7509	mrandnum_08_07	0.93514	0.00123	lrrandnum_08_07	0.94011	0.00131
0.30	55D4371D3A23	mrandnum_08_08	0.93564	0.00132	lrrandnum_08_08	0.93900	0.00139
0.30	6E1A14672B8F	mrandnum_08_09	0.93597	0.00136	lrrandnum_08_09	0.93781	0.00117
0.30	77A0308C0E44	mrandnum_08_10	0.93525	0.00128	lrrandnum_08_10	0.93965	0.00118
moifr	**Random Number**	**"A" cases**	**k_{eff}**	**s**	**"B" cases**	**k_{eff}**	**s**
1.00	109E77866CF6	mrandnum_15_01	0.93103	0.00139	lrrandnum_15_01	0.93344	0.00126
1.00	16AA4A58735C	mrandnum_15_02	0.93082	0.00131	lrrandnum_15_02	0.93281	0.00121
1.00	1814171B652A	mrandnum_15_03	0.92890	0.00148	lrrandnum_15_03	0.93468	0.00132
1.00	1A423B9472C7	mrandnum_15_04	0.93062	0.00145	lrrandnum_15_04	0.93592	0.00126
1.00	20E876D82248	mrandnum_15_05	0.93055	0.00125	lrrandnum_15_05	0.93251	0.00143
1.00	3F6E65CA7440	mrandnum_15_06	0.92950	0.00117	lrrandnum_15_06	0.93374	0.00121
1.00	479D21DB7509	mrandnum_15_07	0.92952	0.00116	lrrandnum_15_07	0.93572	0.00138
1.00	55D4371D3A23	mrandnum_15_08	0.92805	0.00154	lrrandnum_15_08	0.93498	0.00145
1.00	6E1A14672B8F	mrandnum_15_09	0.93117	0.00140	lrrandnum_15_09	0.93224	0.00114
1.00	77A0308C0E44	mrandnum_15_10	0.93218	0.00120	lrrandnum_15_10	0.93158	0.00131

Table 6.9.2.2-2.Neutron multiplication factors with standard deviations for the ES-3100 package models at the "MLR" and "LR" node points

moifr	Random Number	"A" cases	k_{eff}	s	"B" cases	k_{eff}	s
1.0e-20	109E77866CF6	mlrrandnum_01_01	1.05024	0.00139	lrrandnum_01_01	1.05093	0.00133
1.0e-20	16AA4A58735C	mlrrandnum_01_02	1.05051	0.00135	lrrandnum_01_02	1.05009	0.00118
1.0e-20	1814171B652A	mlrrandnum_01_03	1.05121	0.00128	lrrandnum_01_03	1.05057	0.00118
1.0e-20	1A423B9472C7	mlrrandnum_01_04	1.04954	0.00120	lrrandnum_01_04	1.05066	0.00120
1.0e-20	20E876D82248	mlrrandnum_01_05	1.05249	0.00110	lrrandnum_01_05	1.04882	0.00129
1.0e-20	3F6E65CA7440	mlrrandnum_01_06	1.04924	0.00132	lrrandnum_01_06	1.05316	0.00127
1.0e-20	479D21DB7509	mlrrandnum_01_07	1.05105	0.00111	lrrandnum_01_07	1.05229	0.00134
1.0e-20	55D4371D3A23	mlrrandnum_01_08	1.05039	0.00129	lrrandnum_01_08	1.05186	0.00131
1.0e-20	6E1A14672B8F	mlrrandnum_01_09	1.05161	0.00125	lrrandnum_01_09	1.05236	0.00113
1.0e-20	77A0308C0E44	mlrrandnum_01_10	1.05041	0.00129	lrrandnum_01_10	1.05098	0.00120
moifr	**Random Number**	**"A" cases**	**k_{eff}**	**s**	**"B" cases**	**k_{eff}**	**s**
1.0e-04	109E77866CF6	mlrrandnum_03_01	1.05108	0.00151	lrrandnum_03_01	1.05122	0.00123
1.0e-04	16AA4A58735C	mlrrandnum_03_02	1.05245	0.00116	lrrandnum_03_02	1.05324	0.00121
1.0e-04	1814171B652A	mlrrandnum_03_03	1.05169	0.00138	lrrandnum_03_03	1.05143	0.00123
1.0e-04	1A423B9472C7	mlrrandnum_03_04	1.05303	0.00102	lrrandnum_03_04	1.05048	0.00121
1.0e-04	20E876D82248	mlrrandnum_03_05	1.05191	0.00115	lrrandnum_03_05	1.05095	0.00137
1.0e-04	3F6E65CA7440	mlrrandnum_03_06	1.05017	0.00110	lrrandnum_03_06	1.05029	0.00119

Table 6.9.2.2-2.Neutron multiplication factors with standard deviations for the ES-3100 package models at the "MLR" and "LR" node points

moifr	Random Number	"A" cases	k_{eff}	s	"B" cases	k_{eff}	s
1.0e-04	479D21DB7509	mlrrandnum_03_07	1.05232	0.00128	lrrandnum_03_07	1.05124	0.00108
1.0e-04	55D4371D3A23	mlrrandnum_03_08	1.05100	0.00144	lrrandnum_03_08	1.05080	0.00116
1.0e-04	6E1A14672B8F	mlrrandnum_03_09	1.05046	0.00145	lrrandnum_03_09	1.05074	0.00122
1.0e-04	77A0308C0E44	mlrrandnum_03_10	1.05130	0.00134	lrrandnum_03_10	1.05094	0.00111
moifr	**Random Number**	**"A" cases**	**k_{eff}**	**s**	**"B" cases**	**k_{eff}**	**s**
0.1	109E77866CF6	mlrrandnum_06_01	0.98071	0.00129	lrrandnum_06_01	0.98315	0.00118
0.1	16AA4A58735C	mlrrandnum_06_02	0.98006	0.00110	lrrandnum_06_02	0.98605	0.00124
0.1	1814171B652A	mlrrandnum_06_03	0.98043	0.00116	lrrandnum_06_03	0.98690	0.00120
0.1	1A423B9472C7	mlrrandnum_06_04	0.98253	0.00109	lrrandnum_06_04	0.98347	0.00126
0.1	20E876D82248	mlrrandnum_06_05	0.98256	0.00135	lrrandnum_06_05	0.98770	0.00124
0.1	3F6E65CA7440	mlrrandnum_06_06	0.98093	0.00127	lrrandnum_06_06	0.98734	0.00140
0.1	479D21DB7509	mlrrandnum_06_07	0.97959	0.00127	lrrandnum_06_07	0.98417	0.00133
0.1	55D4371D3A23	mlrrandnum_06_08	0.98033	0.00111	lrrandnum_06_08	0.98712	0.00136
0.1	6E1A14672B8F	mlrrandnum_06_09	0.97940	0.00117	lrrandnum_06_09	0.98533	0.00142
0.1	77A0308C0E44	mlrrandnum_06_10	0.98318	0.00134	lrrandnum_06_10	0.98412	0.00116
moifr	**Random Number**	**"A" cases**	**k_{eff}**	**s**	**"B" cases**	**k_{eff}**	**s**
0.3	109E77866CF6	mlrrandnum_08_01	0.93254	0.00147	lrrandnum_08_01	0.93910	0.00146
0.3	16AA4A58735C	mlrrandnum_08_02	0.93186	0.00142	lrrandnum_08_02	0.93757	0.00117
0.3	1814171B652A	mlrrandnum_08_03	0.93200	0.00135	lrrandnum_08_03	0.93940	0.00146
0.3	1A423B9472C7	mlrrandnum_08_04	0.93197	0.00150	lrrandnum_08_04	0.93676	0.00130
0.3	20E876D82248	mlrrandnum_08_05	0.93601	0.00124	lrrandnum_08_05	0.93851	0.00111
0.3	3F6E65CA7440	mlrrandnum_08_06	0.93249	0.00118	lrrandnum_08_06	0.93914	0.00149
0.3	479D21DB7509	mlrrandnum_08_07	0.93299	0.00128	lrrandnum_08_07	0.94011	0.00131
0.3	55D4371D3A23	mlrrandnum_08_08	0.93500	0.00133	lrrandnum_08_08	0.93900	0.00139
0.3	6E1A14672B8F	mlrrandnum_08_09	0.93201	0.00122	lrrandnum_08_09	0.93781	0.00117
0.3	77A0308C0E44	mlrrandnum_08_10	0.93238	0.00153	lrrandnum_08_10	0.93965	0.00118
moifr	**Random Number**	**"A" cases**	**k_{eff}**	**s**	**"B" cases**	**k_{eff}**	**s**
1.0	109E77866CF6	mlrrandnum_15_01	0.93180	0.00126	lrrandnum_15_01	0.93344	0.00126
1.0	16AA4A58735C	mlrrandnum_15_02	0.93020	0.00159	lrrandnum_15_02	0.93281	0.00121
1.0	1814171B652A	mlrrandnum_15_03	0.92956	0.00117	lrrandnum_15_03	0.93468	0.00132
1.0	1A423B9472C7	mlrrandnum_15_04	0.92837	0.00165	lrrandnum_15_04	0.93592	0.00126
1.0	20E876D82248	mlrrandnum_15_05	0.93220	0.00120	lrrandnum_15_05	0.93251	0.00143
1.0	3F6E65CA7440	mlrrandnum_15_06	0.93177	0.00141	lrrandnum_15_06	0.93374	0.00121
1.0	479D21DB7509	mlrrandnum_15_07	0.93217	0.00144	lrrandnum_15_07	0.93572	0.00138
1.0	55D4371D3A23	mlrrandnum_15_08	0.92921	0.00125	lrrandnum_15_08	0.93498	0.00145
1.0	6E1A14672B8F	mlrrandnum_15_09	0.92980	0.00177	lrrandnum_15_09	0.93224	0.00114
1.0	77A0308C0E44	mlrrandnum_15_10	0.93070	0.00126	lrrandnum_15_10	0.93158	0.00131

Table 6.9.2.2-3.Neutron multiplication factors with standard deviations for the ES-3100 package models at the "MR" and "LR" node points

moifr	Random Number	"A" cases	k_{eff}	s	"B" cases	k_{eff}	s
1.0e-20	109E77866CF6	mrandnum_01_01	1.04965	0.00119	lrrandnum_01_01	1.05093	0.00133
1.0e-20	16AA4A58735C	mrandnum_01_02	1.05132	0.00131	lrrandnum_01_02	1.05009	0.00118
1.0e-20	1814171B652A	mrandnum_01_03	1.05368	0.00123	lrrandnum_01_03	1.05057	0.00118
1.0e-20	1A423B9472C7	mrandnum_01_04	1.05165	0.00145	lrrandnum_01_04	1.05066	0.00120
1.0e-20	20E876D82248	mrandnum_01_05	1.05344	0.00106	lrrandnum_01_05	1.04882	0.00129
1.0e-20	3F6E65CA7440	mrandnum_01_06	1.05188	0.00157	lrrandnum_01_06	1.05316	0.00127
1.0e-20	479D21DB7509	mrandnum_01_07	1.05149	0.00148	lrrandnum_01_07	1.05229	0.00134
1.0e-20	55D4371D3A23	mrandnum_01_08	1.05083	0.00113	lrrandnum_01_08	1.05186	0.00131
1.0e-20	6E1A14672B8F	mrandnum_01_09	1.04910	0.00106	lrrandnum_01_09	1.05236	0.00113
1.0e-20	77A0308C0E44	mrandnum_01_10	1.05254	0.00106	lrrandnum_01_10	1.05098	0.00120
moifr	**Random Number**	**"A" cases**	**k_{eff}**	**s**	**"B" cases**	**k_{eff}**	**s**
1.0e-04	109E77866CF6	mrandnum_03_01	1.04994	0.00132	lrrandnum_03_01	1.05122	0.00123
1.0e-04	16AA4A58735C	mrandnum_03_02	1.05023	0.00118	lrrandnum_03_02	1.05324	0.00121
1.0e-04	1814171B652A	mrandnum_03_03	1.05090	0.00139	lrrandnum_03_03	1.05143	0.00123
1.0e-04	1A423B9472C7	mrandnum_03_04	1.05072	0.00115	lrrandnum_03_04	1.05048	0.00121
1.0e-04	20E876D82248	mrandnum_03_05	1.05052	0.00119	lrrandnum_03_05	1.05095	0.00137
1.0e-04	3F6E65CA7440	mrandnum_03_06	1.05383	0.00131	lrrandnum_03_06	1.05029	0.00119
1.0e-04	479D21DB7509	mrandnum_03_07	1.05205	0.00153	lrrandnum_03_07	1.05124	0.00108
1.0e-04	55D4371D3A23	mrandnum_03_08	1.05343	0.00106	lrrandnum_03_08	1.05080	0.00116
1.0e-04	6E1A14672B8F	mrandnum_03_09	1.04831	0.00132	lrrandnum_03_09	1.05074	0.00122
1.0e-04	77A0308C0E44	mrandnum_03_10	1.05353	0.00111	lrrandnum_03_10	1.05094	0.00111
moifr	**Random Number**	**"A" cases**	**k_{eff}**	**s**	**"B" cases**	**k_{eff}**	**s**
0.10	109E77866CF6	mrandnum_06_01	0.97948	0.00120	lrrandnum_06_01	0.98315	0.00118
0.10	16AA4A58735C	mrandnum_06_02	0.98104	0.00125	lrrandnum_06_02	0.98605	0.00124
0.10	1814171B652A	mrandnum_06_03	0.98056	0.00134	lrrandnum_06_03	0.98690	0.00120
0.10	1A423B9472C7	mrandnum_06_04	0.97895	0.00114	lrrandnum_06_04	0.98347	0.00126
0.10	20E876D82248	mrandnum_06_05	0.98058	0.00113	lrrandnum_06_05	0.98770	0.00124
0.10	3F6E65CA7440	mrandnum_06_06	0.97966	0.00119	lrrandnum_06_06	0.98734	0.00140
0.10	479D21DB7509	mrandnum_06_07	0.97953	0.00145	lrrandnum_06_07	0.98417	0.00133
0.10	55D4371D3A23	mrandnum_06_08	0.97993	0.00130	lrrandnum_06_08	0.98712	0.00136
0.10	6E1A14672B8F	mrandnum_06_09	0.97972	0.00138	lrrandnum_06_09	0.98533	0.00142
0.10	77A0308C0E44	mrandnum_06_10	0.98157	0.00134	lrrandnum_06_10	0.98412	0.00116
moifr	**Random Number**	**"A" cases**	**k_{eff}**	**s**	**"B" cases**	**k_{eff}**	**s**
0.30	109E77866CF6	mrandnum_08_01	0.93412	0.00118	lrrandnum_08_01	0.93910	0.00146
0.30	16AA4A58735C	mrandnum_08_02	0.93227	0.00138	lrrandnum_08_02	0.93757	0.00117
0.30	1814171B652A	mrandnum_08_03	0.93390	0.00131	lrrandnum_08_03	0.93940	0.00146
0.30	1A423B9472C7	mrandnum_08_04	0.93252	0.00144	lrrandnum_08_04	0.93676	0.00130
0.30	20E876D82248	mrandnum_08_05	0.93334	0.00132	lrrandnum_08_05	0.93851	0.00111
0.30	3F6E65CA7440	mrandnum_08_06	0.93168	0.00132	lrrandnum_08_06	0.93914	0.00149
0.30	479D21DB7509	mrandnum_08_07	0.93514	0.00123	lrrandnum_08_07	0.94011	0.00131
0.30	55D4371D3A23	mrandnum_08_08	0.93564	0.00132	lrrandnum_08_08	0.93900	0.00139
0.30	6E1A14672B8F	mrandnum_08_09	0.93597	0.00136	lrrandnum_08_09	0.93781	0.00117
0.30	77A0308C0E44	mrandnum_08_10	0.93525	0.00128	lrrandnum_08_10	0.93965	0.00118

Table 6.9.2.2-3.Neutron multiplication factors with standard deviations for the ES-3100 package models at the "MR" and "LR" node points

moifr	Random Number	"A" cases	k_{eff}	s	"B" cases	k_{eff}	s
1.00	109E77866CF6	mrandnum_15_01	0.93103	0.00139	lrrandnum_15_01	0.93344	0.00126
1.00	16AA4A58735C	mrandnum_15_02	0.93082	0.00131	lrrandnum_15_02	0.93281	0.00121
1.00	1814171B652A	mrandnum_15_03	0.92890	0.00148	lrrandnum_15_03	0.93468	0.00132
1.00	1A423B9472C7	mrandnum_15_04	0.93062	0.00145	lrrandnum_15_04	0.93592	0.00126
1.00	20E876D82248	mrandnum_15_05	0.93055	0.00125	lrrandnum_15_05	0.93251	0.00143
1.00	3F6E65CA7440	mrandnum_15_06	0.92950	0.00117	lrrandnum_15_06	0.93374	0.00121
1.00	479D21DB7509	mrandnum_15_07	0.92952	0.00116	lrrandnum_15_07	0.93572	0.00138
1.00	55D4371D3A23	mrandnum_15_08	0.92805	0.00154	lrrandnum_15_08	0.93498	0.00145
1.00	6E1A14672B8F	mrandnum_15_09	0.93117	0.00140	lrrandnum_15_09	0.93224	0.00114
1.00	77A0308C0E44	mrandnum_15_10	0.93218	0.00120	lrrandnum_15_10	0.93158	0.00131

6.9.2.3 STATISTICAL EVALUATION

A evaluation of KENO V.a calculation results is made to determine if there is a statistically significant difference between the mean k_{eff} for the "MR" and "MLR" models, for the "MLR" and "LR" models, and for the "MR" and "LR" models. Cases are classified into five groups based on the amount of water assumed to be present in the shipping package. The symbol "I" is used to specify the case. The mean difference and standard deviation for each of the five sets of pair-wise differences are defined as follows:

(a) $d_i = (k_{effBi} - k_{effAi})/n$ and
(b) $s_{di} = \sqrt{[\, n\Sigma d_i^{\,2} - (\Sigma d_i)^2 \,] / n(n-1)}$ (conservatively defined for the t-test appropriate for small sample sizes),

where A_i and B_i denote the model types, and n denotes the sample size of ten. It is reasonable to assume that the paired differences have been randomly selected from a normally distributed population of paired differences with mean (μ_d) and standard deviation (σ_d), then the sampling distribution of

$$(d - \mu_d) / (s_d/\sqrt{n})$$

is a *t* distribution having n-1 degrees of freedom.

The evaluation of the mean differences (d_i) for the 10 set of cases is accomplished through hypothesis testing, a statistical tool used to provide evidence that a difference exists or does not exist. The t_i values are given in Table 6.9.2.3-1. A value of 3.25 is obtained from the standard table for critical values for the t distribution from which the decision to accept or reject the null hypothesis H_0 is made with a Type I error probability (α) of 0.01.

Table 6.9.2.3-1. T-test values for establishing the statistical significance of the differences in calculated k_{eff} values for the ES-3100 package models at the "MR," "MLR," and "LR" node points

moifr	"MR" cases (k_{eff})	"MLR" cases (k_{eff})	d_i	S_{di}	t[a]
1.0E-20	1.05154	1.05075	0.00089	1.58991e-03	1.77
1.0E-04	1.05146	1.05165	-0.00019	2.17840e-03	-0.28
0.1	0.98008	0.98091	-0.00087	1.33870e-03	-2.06
0.3	0.93404	0.93300	0.00106	1.88912e-03	1.77
1.0	0.93030	0.93067	-0.00034	1.68664e-03	-0.65
moifr	**"MLR" cases (k_{eff})**	**"LR" cases (k_{eff})**	**d_i**	**S_{di}**	**t**
1.0E-20	1.05075	1.05116	-0.00050	1.92087e-03	-0.83
1.0E-04	1.05165	1.05113	0.00041	9.36819e-04	1.38
0.1	0.98091	0.98546	-0.00456	2.28535e-03	-6.31
0.3	0.93300	0.93863	-0.00578	1.59574e-03	-11.45
1.0	0.93067	0.93369	-0.00318	2.30797e-03	-4.36
moifr	**"MR" cases (k_{eff})**	**"LR" cases (k_{eff})**	**d_i**	**S_{di}**	**t**
1.0E-20	1.05154	1.05116	0.00039	2.35840e-03	0.52
1.0E-04	1.05146	1.05113	0.00021	2.19813e-03	0.31
0.10	0.98008	0.98546	-0.00543	1.66324e-03	-10.33
0.30	0.93404	0.93863	-0.00472	1.46294e-03	-10.21
1.00	0.93030	0.93369	-0.00353	2.50750e-03	-4.45

[a] critical value = 3.25 for 10 cases

For $|t| < 3.25$, the H_o hypothesis is not rejected. Acceptance of the null hypothesis is the result of insufficient evidence to reject it. Thus, it can be concluded that the mean estimates of the difference in k_{eff} between the "MR" and "MLR" calculation models, between the "MLR" and "LR" calculation models, and between the "MR" and "LR" calculation models are not statistically significant for the dry condition where neutronic interaction between packages is significant. Also, the mean estimate of the difference in k_{eff} between the "MR" and "MLR" calculation models is not statistically significant for wet or flooded conditions where the packages of the array become isolated.

For $|t| > 3.25$, the H_o hypothesis is rejected. Therefore, it can be concluded that the mean estimate of the difference in k_{eff} between the "MLR" and "LR" calculation models, and between the "MR" and "LR" calculation models, is statistically significant for wet or flooded conditions where the packages of the array become isolated. The negative t-values indicate that the calculated k_{eff} value for the "LR" model is slightly higher than for the "MR" and "MLR" models. This result is consistent with an expected increase in k_{eff} due to "tighter or closer" water reflector surrounding the package content.

Although flattening of the side of the package represents a reduction in the diameter of the drum, the points at which minimum flattening occurs provide an indication of the reduction of lattice spacing between packages of an array under HAC. The composite of the minimum deformation points at perpendicular axes

(90–270° and 0–180°) represents the modified lattice spacing in an array of ES-3100 packages. As illustrated in Table 6.9.2.3-2, the equivalent diameter of the package for "composite" lattice spacing is not significantly different from the 18.37-in. diameter of the pre-test package. Even though significant crushing of the drum midsection and bottom occurs, the effective center-to-center spacing of the contents actually increases under HAC. Selective rearrangement of alternating packages would be required to achieve a more compact array; however, this event is not credible.

As described in Sect. 6.3.1.2, a close-pack (triangular-pitch) array of packages would be represented by a reduced package in a rectangular-pitch configuration. For HAC, the 17.26-in. reduced diameter for the "composite close-pack" package is slightly larger than the 17.20-in. diameter of the "MLR" calculation model used in the HAC calculations of Sect. 6.6. Therefore, packages evaluated with the "MLR" calculation model of packages in a rectangular-pitch configuration are deemed adequate for the HAC criticality evaluation. Considering both the irregular shape of the deformed drums and that array spacing is determined by overall (maximum) dimensions rather than by mean or minimum dimensions of a damaged package, the use of the "MLR" model for representing the ES-3100 package under HAC is conservative and bounding.

Table 6.9.2.3-2. Deformation of the ES-3100 drum projected by finite element analysis "Case 3100 RUN1HL Lower Bound Kaolite May 2004"

	FEA node	Diameter at 90° (in.)	Diameter at 180° (in.)	Equivalent circular diameter (in.)
Composite	103012/098194	22.00	15.60	18.56
Pre-test drum	-	18.37	18.37	
Pre-test, close-pack	-	17.08	17.08	
Composite, close-pack	103012/098194	-	-	17.26

APPENDIX 6.9.3

PACKAGE MATERIAL COMPOSITIONS

APPENDIX 6.9.3

PACKAGE MATERIAL COMPOSITIONS

Table 6.4 (Sect. 6.3.2) provides basic information for deriving the compositions for the ES-3100 package (Figs. 6.1 and 6.2). The atomic densities presented in Table 6.4 can be verified using additional information provided in Appendix 6.9.5. The following sections provide the rationale, the justification, or both for the material compositions used in the criticality calculations.

6.9.3.1 HEU AND UNIRRADIATED TRIGA REACTOR FUEL

HEU considered for shipment in the ES-3100 is categorized into the following material forms: highly enriched uranium (HEU) solid or broken metal; HEU oxide; uranyl nitrate hexahydrate (UNH) crystals. In the interest of adding conservatism, uranium is modeled as ^{235}U and ^{238}U, while the ^{234}U and ^{236}U isotopes are excluded. Any positive change in neutron multiplication represented by the presence of the ^{234}U is covered by the higher than actual ^{235}U content. (Rothe et al. 1978) The theoretical density of 100 wt % ^{235}U HEU is 18.8111 g/cm^3. This value is determined by adjusting the density of natural uranium included in the SCALE Standard Composition Library with 100 wt % weight factors. The theoretical density of HEU oxide types are 10.96 g/cm^3 for UO_2, 8.30 g/cm^3 for U_3O_8, and 7.29 g/cm^3 for UO_3. The theoretical density of UNH crystals is 2.79 g/cm^3. Table 6.9.3.1-1 provides details of the calculated weight percentages input to KENO V.a calculated on the basis of the stoichiometric formula of $UO_2(NO_3)_2+6H_2O$ and crystalline density. The maximum enrichment considered in the analysis is 100 wt % ^{235}U, although actual material enrichments are lower. The unirradiated solid form TRIGA fuel is uranium zirconium hydride ($UZrH_x$) where "x" is ≤2, having a density of 8.65 g/cm^3.

Table 6.9.3.1-1. Calculation of constituent weight-percentage values for uranyl nitrate hexahydrate crystals used in KENO V.a calculation models

Avogadro No. (N_o)	6.0221370E+23					
UNH						
$UO_2(NO_3)_2+6H_2O$	Atoms/Molecule	At. wt [a]	Mole. wt.	wt %	calc. Ni	NiAi
Hydrogen	12	1.0078	12.0936	2.4233	4.0401e+22	4.0716e+22
Nitrogen	2	14.0031	28.0062	5.6117	6.7333e+21	9.4286e+22
Oxygen	14	15.9949	223.9286	44.8690	4.7132e+22	7.5388e+23
U-235		235.0441		100.0000		
U-238		238.0510		0.0000		
Uranium	1	235.0441	235.0441	47.0962	3.3666e+21	7.9130e+23
			499.0725	100.0002		
summations				100.0002	9.7633e+22	1.6802e+24
At. Wt. material						
assumed density	2.7900					
den.=($\sum N_i A_i$)/No						2.7900

[a] *Source*: *Nuclides and Isotopes*, 14th ed., General Electric Company, 1989.

HEU broken metal. The critical mass of fissile material is dependent on factors such as the form and shape of the material, bulk density if the material is broken into pieces, and the enrichment. Broken metal can be compared to the minimum critical mass of submerged metal lattices of regular-shaped fissile material. Using experimental data, the approximation of a heterogeneous mixture of fissile material and moderator to a homogenous mixture is justified as follows.

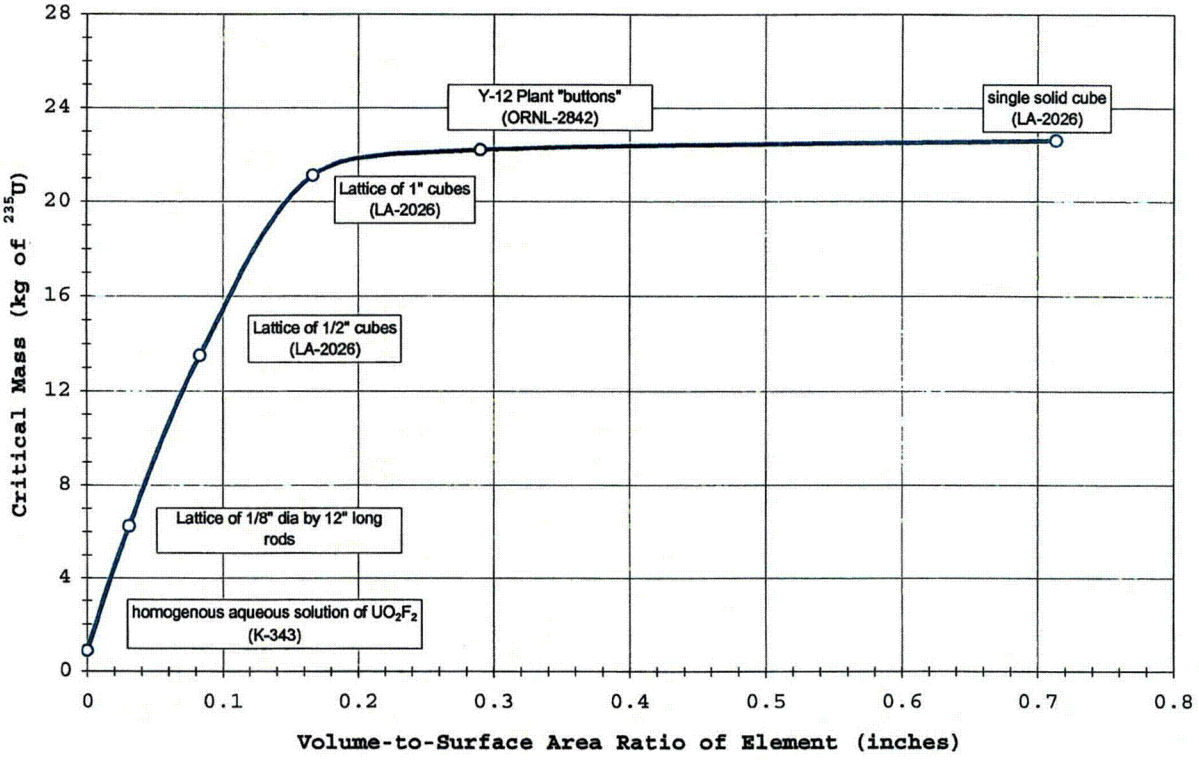

Fig. 6.3.9.1-1. Experimentally determined minimum critical mass U(~94) metal lattices immersed in water as a function of volume-to-surface area ratio of fissile material. *Source*: H. C. Paxton et al., *Critical Dimensions of Systems Containing 235U,* TID-7028, Los Alamos Scientific Lab. and Oak Ridge Natl. Lab., June 1964, Fig. 19. Y-12 data have been added.

Figure 6.3.9.1-1 depicts the experimentally determined minimum critical mass of U (~ 94) lattices immersed in water as a function of the volume-to-surface area ratio of the fissile element. (TID-7028). The critical mass is shown to increase from 850 g to 21 kg over the range of volume-to-surface ratios from 0 to 0.18 in. The critical mass is nearly constant in the range of volume-to-surface ratios from 0.18 to 0.8 in. For pieces greater than 1-in. cubes, the minimum critical mass will not be less than 21 kg. For smaller pieces, the minimum critical mass is a nearly linear function of the volume-to-surface-area ratio of the fissile element.

Figure 6.3.9.1-2 depicts the experimentally determined minimum critical mass of U (~ 94) metal water and solution systems as a function of the concentration of ^{235}U. The figure with added data reveals that: (1) a minimum critical mass exists for each metal lattice system plotted, and (2) as the bulk density of uranium or the uranium concentration increases, the curves for the critical mass of metal lattice systems converge with the curve for highly enriched solution experiments or the curve for calculated homogenous metal water mixtures. Conversely stated, the critical mass is greater for a heterogenous system than for a homogenous system, and this difference increases as the H/X ratio increases. Therefore, the practice of approximating a heterogeneous mixture of fissile material and moderator as a homogenous mixture is justifiable and also conservative at the higher H/X ratios.

Approximating broken metal as a homogenous mixture of uranium and water requires a defined space within which masses of the components are conserved. This space is generally characterized by a lattice constructed of unit cells and defined by the dimensions of the fissile material being approximated.

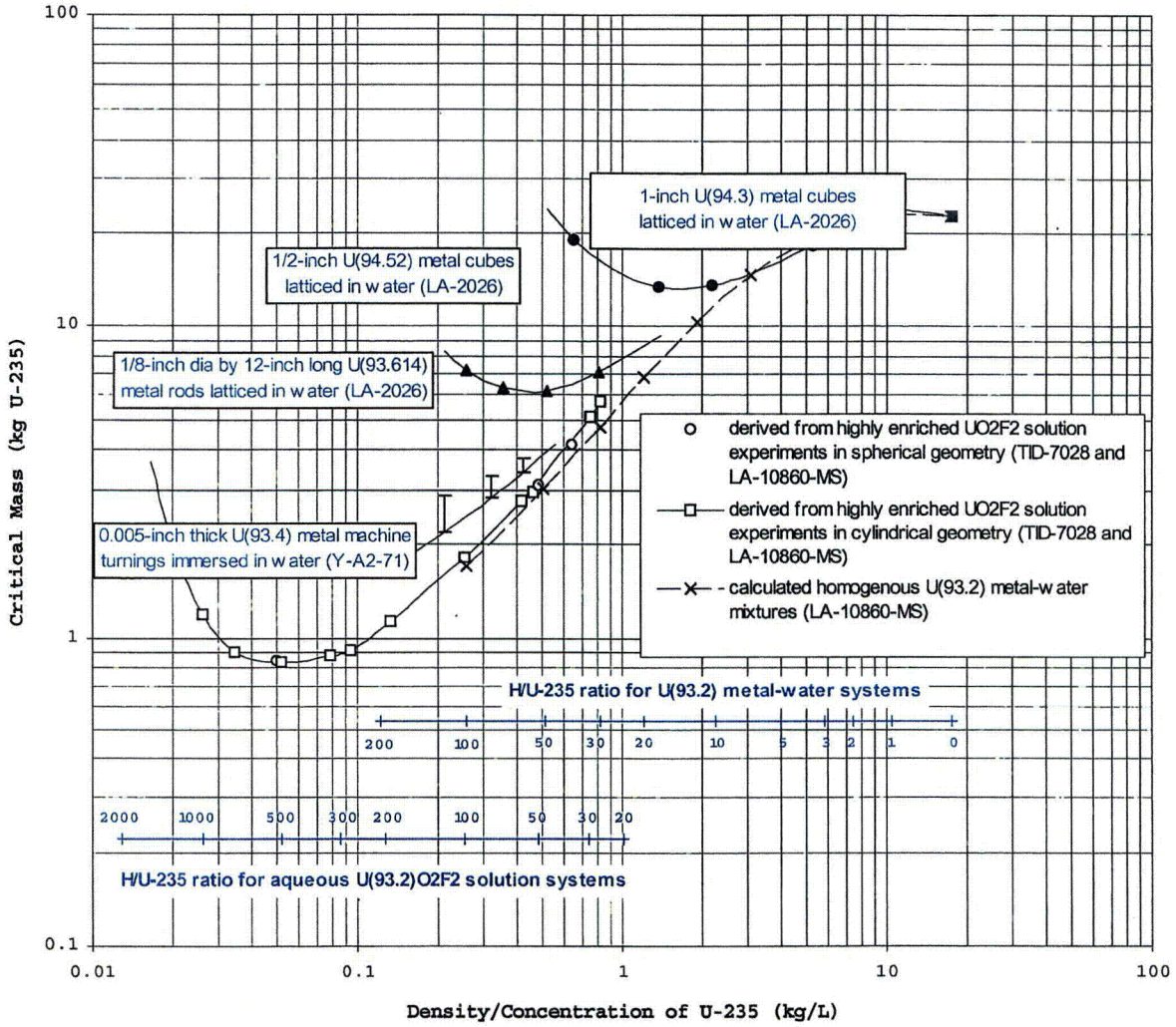

Fig. 6.3.9.1-2. Experimentally determined minimum critical mass of U(~94) metal water and solution systems as a function of the concentration of ^{235}U. *Sources*: A. W. Krass, *Survey of Experimental Data Concerning the Critical Mass of Highly Enriched Uranium–Water Systems*, CCG-365, Lockheed Martin Energy systems, Inc., Oak Ridge Y-12 Plant, July 13, 2000, Fig. 1. Y-12 data added.

The broken HEU metal consists of large, irregular pieces ranging from 0.5 in. to several inches on a side as shown in Fig. 6.9.3.1-3. A lattice of cubes is chosen to represent broken metal inside the ES-3100 containment vessel. Due to the constraints of KENO V.a, an idealized configuration is defined by a square lattice circumscribed by the inner wall of the containment vessel. Water fills the truncated cylindrical regions between the inner wall of the containment vessel and the vertical faces of the lattice. Two additional models are developed to evaluate conservatism at various stages of model approximations for broken metal.

Together, these models include an explicit arrangement of HEU metal cubes forming a compact rectangular lattice inside the containment vessel, HEU metal homogeneously mixed with water within the rectangular lattice formed by the unit cells, and HEU metal homogeneously mixed with water within the volume of the containment vessel.

Parameters varied in each of these three models include (1) the cube size in the explicit model from 1.0 in. to 0.25 in. on a side, (2) water moderation inside the containment vessel from dry to the fully flooded

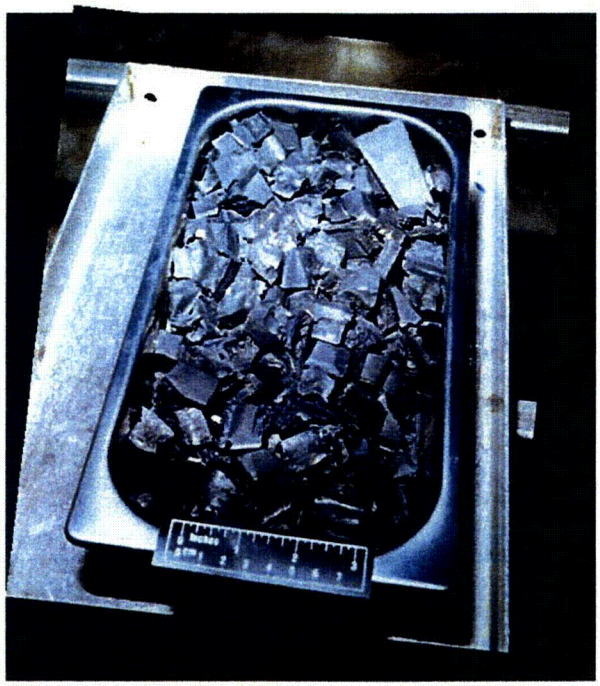

Fig. 6.9.3.1-3. Pan of HEU broken metal.

condition, (3) enrichment from 100.0 wt % ^{235}U to 20.0 wt % ^{235}U, (4) thickness of the 277-4 canned spacers located between each convenience can, and (5) the mass of the uranium metal at each content location. One-quarter inch, 0.5-in., and 1.0-in. cubes are selected to evaluate "approach-to-homogeneity" of broken metal in this idealized form. The corresponding array configurations for 0.25-in., 0.5-in., and 1.0-in. cubes are 12 × 12 × N, 6 × 6 × N, and 3 × 3 × N. The N-th layer of unit cells for a given mass loading may not all contain HEU metal; the empty cells are filled with water. Nevertheless, a slight variation still arises in the total mass of HEU metal between these array configurations given whole cubes are contained in the calculation models.

The results for the calculation models representing the various configurations of broken uranium metal are shown in the Table 6.9.3.1-2. As the explicitly modeled cubes become smaller in size, the calculated k_{eff} values for the explicit "sqa" models approach values for the "lha" models where HEU metal cubes are homogenized with water within the rectangular lattice formed by the unit cells of the array. A representative or converged k_{eff} value is 0.87 for increasing by smaller cubes based on calculation results for the "lha" models. The "lha" results indicate a slight difference between the k_{eff} values for the three array sizes; these differences are attributed to the difference in the HEU for the arrays of whole cubes.

Calculation results for the "cha" models, where arrays of cubes are fully homogenized with the water for the flooded containment vessel, indicate the highest k_{eff} values. The neutron multiplication factor jumps from 0.87 to 0.95. This model is deemed to be overly conservative when applied to broken metal for the following reasons.

- HEU metal does not dissolve in water.
- HEU metal is not in an oxide or powder form that will absorb moisture or readily mix and become homogenized with the water inside the flooded containment vessel.
- Because HEU metal is much denser than water, it will not float and become distributed throughout a flooded containment vessel; instead it will gravitate toward the bottom of the containment vessel.

Table 6.9.3.1-2. Summary for evaluation of HEU broken metal models (95 wt % ^{235}U) in a flooded containment vessel, 1.4-in. canned spacers and full water reflection of containment vessel

Array type	U (g)	^{235}U (g)	H_2O (g)	h/x	k_{eff}	σ	$k_{eff}+2\sigma$
discrete array of cubes ("sqa" cases)							
3 × 3 × *n*	35,164	33,406	7,719	6.03	0.8352	0.0012	0.84
6 × 6 × *n*	35,973	34,175	7,676	5.86	0.8559	0.0011	0.86
12 × 12 × *n*	35,988	34,188	7,765	5.86	0.8603	0.0012	0.86
cubes homogenized within footprint of lattice ("lha" cases)							
3 × 3 × *n*	35,164	33,406	7,719	6.03	0.8586	0.0011	0.86
6 × 6 × *n*	35,988	34,188	7,675	5.86	0.8650	0.0012	0.87
12 × 12 × *n*	35,988	34,188	7,675	5.86	0.8677	0.0010	0.87
cubes homogenized within containment vessel ("cha" cases)							
3 × 3 × *n*	35,164	33,406	7,719	6.03	0.9427	0.0013	0.95
6 × 6 × *n*	35,973	34,175	7,676	5.86	0.9495	0.0015	0.95
12 × 12 × *n*	35,988	34,188	7,675	5.86	0.9517	0.0016	0.95

The calculation results for the homogeneous mixture model of HEU metal and water within a rectangular lattice bound results for the explicit model. Also, the homogenization over the entire volume of the containment vessel is deemed overly conservative. For these reasons, the "lha" model is chosen to represent HEU broken metal inside the flooded containment vessel under full water reflection. For conservatism, the "cha" model is chosen to represent broken metal in single packages and the array of packages under NCT and HAC. Details about the calculation models follow.

Explicit model of HEU metal cubes forming an array of unit cells. HEU metal cubes ranging from 1.0 in. to 0.25 in. are explicitly modeled, correspondingly arranged in a 3 × 3, 6 × 6, or 12 × 12 (horizontal plane) lattice, with *N* layers vertically. The height of the lattice or the number of layers is determined by the HEU mass loading. HEU cubes are centered in the individual unit cells.

Figure 6.9.3.1-4 depicts an isometric cutaway view of the containment vessel and lid with three 12 × 12 × 18 arrays of HEU content separated by 277-4 canned spacers. The water surrounding the HEU has been removed for the purpose of the illustration. Convenience cans are not modeled; therefore, the corner unit cells nearly touch the inside wall of the containment vessel. Spacing between cubes is limited by the inner diameter of the 5.06-in. (12.8524-cm) containment vessel. The footprint of the lattice is 3.57796 in. (9.08802 cm) square. The 277-4 canned spacers are modeled as cylindrical disks with dimensions of 4.13-in. diameter × 1.37 in. height.

The HEU mass is varied in a series of calculations; however, the enrichment and density are maintained constant. The uranium mass is reduced by removing one or more cubes from the array, and the created vacancies are filled with water. Because convenience cans are not included in the calculation models, the location of the 277-4 canned spacers between the arrays decreases as complete layers of cubes are removed. The volume of the containment vessel above the top layer of the top array of cubes is filled with full-density water.

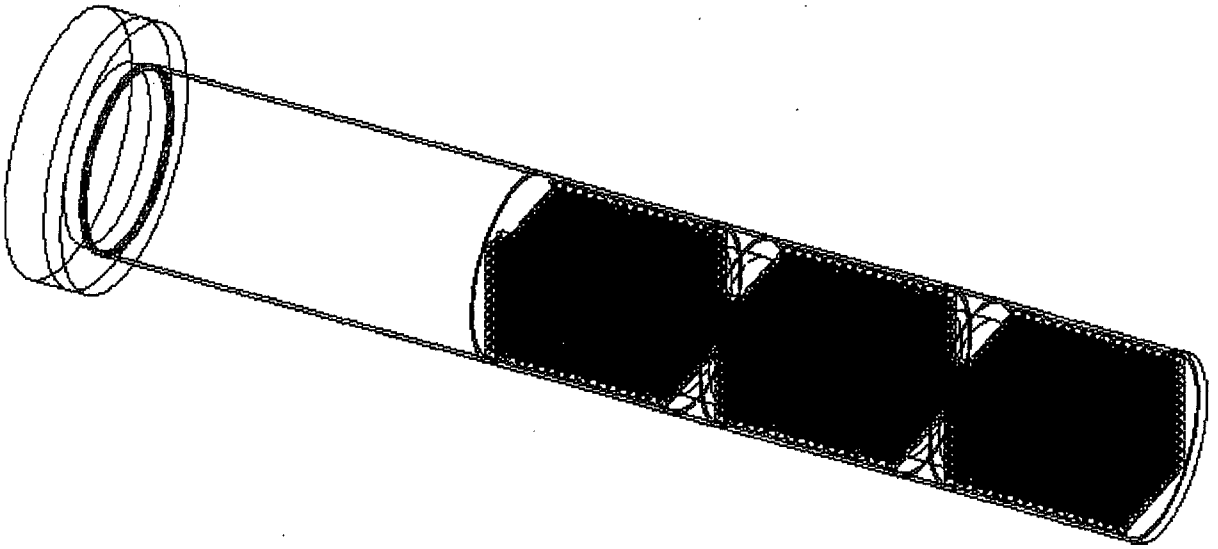

Fig. 6.9.3.1-4. Isometric view of the "sqa" model with three 12 × 12 × 18 lattices of HEU contents.

HEU metal homogeneously mixed with water within the rectangular lattice formed by the units cells. The HEU in the $3 \times 3 \times N$, $6 \times 6 \times N$, and $12 \times 12 \times N$ unit cells of the explicit model are homogeneously mixed with water in the rectangular lattice. Figure 6.9.3.1-5 depicts an isometric view of the homogenous "lha" model with HEU homogeneously mixed with water within the rectangular lattices formed by the unit cells. The dimensions of each rectangular lattice are defined by the 12 × 12 × 18 array of unit cells of the explicit model. Each lattice location contains the same mass of HEU and water that the respective explicit cube models contain. The volume outside the rectangular lattices is filled with full density water.

HEU metal homogeneously mixed with water within the volume of the containment vessel. The HEU in the $3 \times 3 \times N$, $6 \times 6 \times N$, and $12 \times 12 \times N$ unit cells of the explicit model are homogeneously mixed with water in the volume of the containment vessel. Figure 6.9.3.1-6 depicts an isometric cutaway view of the containment vessel and lid with HEU content homogenized with water in the containment vessel. The three rectangular lattices are used to position the 277-4 canned spacers for similarity with the "sqa" and "lha" models. The dimensions of each rectangular lattice are defined by the 12 × 12 × 18 array of unit cells of the explicit model. The mass of HEU and water of the explicit cube model is preserved.

HEU Oxide. Theoretical (crystalline) densities for HEU oxide are 10.96 g/cm^3, 8.30 g/cm^3, and 7.29 g/cm^3 for UO_2, U_3O_8, and UO_3, respectively. However, bulk densities for product oxide with enrichments ranging from 19 to 100 wt % ^{235}U are typically on the order of 6.54 g/cm^3. Therefore, only less-than-theoretical mass loadings would actually be achieved. Skull oxides are a mixture of graphite and U_3O_8 with densities on the order of 2.44 g/cm^3 for poured material and 2.78 g/cm^3 for tapped material. The combined water saturation and crystallization of the HEU oxide are not expected in the HAC, given that UO_2 and UO_3 are non-hygroscopic while U_3O_8 is only mildly hygroscopic. Table 6.9.3.1-3 provides summary data for 292 samples of canned skull oxide.

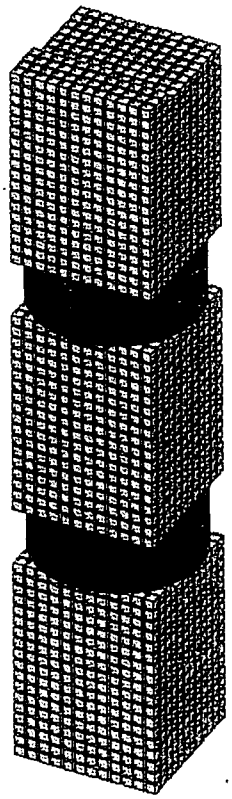

Fig. 6.9.3.1-4b. Detailed isometric view of the explicit "sqa" model for HEU broken metal. Three 12 × 12 × 18 lattices of 1-in. cubes separated by 1.4-in. 277-4 spacers are shown.

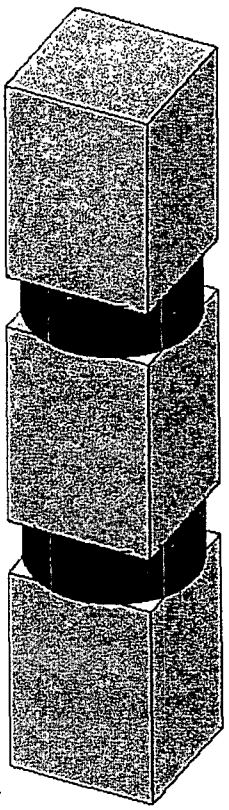

Fig. 6.9.3.1-5. Isometric view of the homogeneous "lha" model with HEU homogeneously mixed with water within the rectangular lattices formed by the units cells.

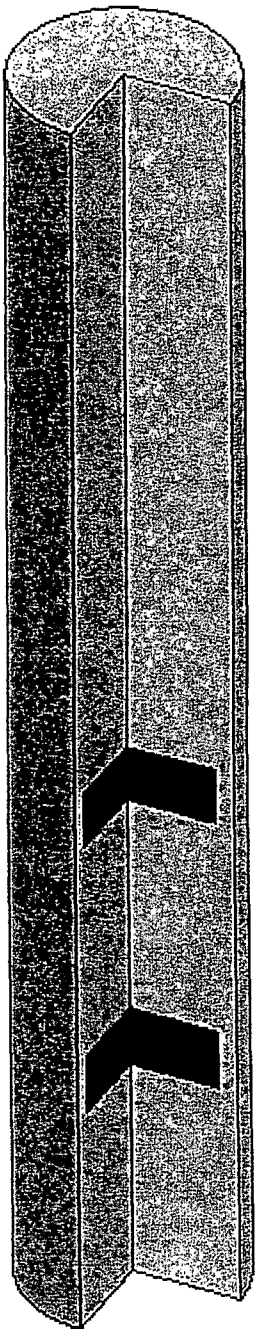

Fig. 6.9.3.1-6. Isometric view of the homogeneous "cha" model with HEU homogeneously mixed with water within the interior of the containment vessel.

Table 6.9.3.1-3. Summary data for 292 samples of skull oxide

Statistic	wt % U	wt % ^{235}U	µg C/g U	µg C /g ^{235}U	Net Wt (g)	U Wt (g)	^{235}U Wt (g)
Maximum	84.52	93.19	171,000	252,861	7,072	5,938	4,165
Minimum	12.93	20.28	13	17	442	312	221
Median	81.66	37.62	5,590	13,910	4,448	3,541	1,414
Mean	79.64	45.02	16,968	41,333	4,419	3,532	1,563
Std Dev	6.87	16.40	24,304	59,027	745	698	606

Values of wt % U, wt % ^{235}U, µg C/g U, etc. for a given statistic (maximum, minimum, medium, or mean) do not occur simultaneously in a specific sample. Inspection of sample data reveals the following characteristics:

(1) the fissile material content is ≤221 g ^{235}U in samples with concentrations up to 252,861 µg C/g^{235}U,
(2) the enrichment is 93.2 wt % ^{235}U for samples with concentrations in the range of 12,600 to 18,600 µg C/gU,
(3) the enrichment ranges from 60 to 70.2 wt % ^{235}U for samples with concentrations in the range of 3,231 to 87,720 µg C/gU, and
(4) the enrichment ranges from 37 to 38 wt % ^{235}U for samples with concentrations in the range of 400 to 233,366 µg C/gU.

Eight samples were selected and two additional ones created for establishing a bounding content calculation model. Details are provided in Table 6.9.3.1-3b.

Table 6.9.3.1-3b. Canned skull oxide (SO) content for ES-3100 calculation models, assuming 513 g polyethylene present and can spacers absent.

Content	SO (g)	UOx (g)	Sat. H_2O (g)	SO h/x	U (g)	^{235}U (g)	C (g)	µg C/ g ^{235}U	CV H_2O (g)	CV h/x	Unident (g)
sk_01	11,589	8,063	4,468	28.09	6,828	4,765	417	87,518	4,105	50.58	2,596[a]
sk_02	14,934	11,665	4,015	17.79	9,879	6,858	504	73,492	4,105	33.41	2,252[a]
sk_03	13,821	11,876	4,893	20.62	10,058	7,028	372	52,930	3,233	32.62	1,060[a]
sk_04	15,246	14,900	4,599	15.52	12,619	8,842	60	6,786	3,235	25.07	-227[b]
sk_05	21,216	21,036	3,869	9.49	17,815	12,455	27	2,168	3,235	16.27	-360[b]
sk_06	15,111	12,933	3,765	28.02	10,960	4,122	921	223,432	4,105	54.01	744[a]
sk_07	13,155	11,666	3,989	32.68	9,886	3,712	609	164,054	4,106	61.55	367[a]
sk_08	13,650	11,689	4,068	33.01	9,906	3,737	261	69,834	4,106	61.69	1,187[a]
sk_09	21,300	19,865	3,801	7.43	16,816	15,673	921	58,764	3,235	12.82	1
sk_10	21,300	20,786	3,905	7.27	17,596	16,399	0	0	3,235	12.41	1

[a] Positive value specifies grams of miscellaneous neutron absorber elements in content, modeled as water.
[b] Negative value specifies grams of excess polyethylene included in the content model.

Unirradiated TRIGA reactor fuel. TRIGA fuel is uranium zirconium hydride ($UZrH_x$), an alloy of uranium metal homogeneously dispersed as fine particles in a zirconium hydride matrix. The fuel is stable because uranium hydride does not form to any considerable extent. Moreover, uranium hydride has never been detected in the photomicrographic evaluations of TRIGA fuel.

The General Atomics catalog of stock items lists approximately 40 TRIGA fuel elements classified into four basic types: standard element, instrumented element, fuel-follower control rod, or cluster assembly. The TRIGA element active fuel region consists of three 5-in long sections "fuel meats" of $UZrH_x$. The H/Z atom ratio "x" in $UZrH_x$ equals 1.6 in all cases except for two stock items. For these cases, x = equals 1.0 and the fissile content is < 40 g ^{235}U. The unirradiated solid form TRIGA fuel is identified as either 20 % enriched or 70 % enriched, and has dimensions and material properties specific to its design function. Table 1.4 provides a summary description.

The fuel diameter for the 20 % enriched TRIGA elements is either 1.44 in., 1.41 in., 1.40 in., 1.37 in., 1.34 in., or 1.31 in. The uranium composition of the fuel is 45 wt %, 30 wt %, 20 wt %, 12 wt %, and 8.5 wt %. As illustrated in Table 6.9.3.1.4-a, the TRIGA element with a maximum fissile content of 307 g ^{235}U in 1,560 g U, 45 wt% U in $UZrH_x$, and a H/Zr atom ratio of 1.6 has a computed fuel density of ~8.66 g/cm^3. The calculated number density (N_i) for each element or isotope is also given. The TRIGA fuel element with a fuel diameter of 1.44 inches contains 3,466.7 g $UZrH_x$. Further evaluation of the manufacturers data reveals that fuel density is proportional to the uranium weight fraction. Calculated density values are: 8.6597 g/cm^3 for 45 wt% U in $UZrH_x$, 6.8995 g/cm^3 for 30 wt% U in $UZrH_x$, 6.2825 g/cm^3 for 20 wt% U in $UZrH_x$, 5.9328 g/cm^3 for 12 wt% U in $UZrH_x$, and 5.7895 g/cm^3 for 8.5 wt% U in $UZrH_x$.

The active fuel diameter for 70 % enriched TRIGA fuel is 1.44 inches in both the standard element and instrumented element, and 1.31 inches in the fuel follower control rod. The uranium composition of the fuel is 8.5 wt %. The standard element and instrumented elements contain ~136 g ^{235}U in 194 g U while the fuel follower control rod contains ~113 g ^{235}U in 162 g U. As the calculation in Table 6.9.3.1.4-b illustrates, the 70 wt % enriched TRIGA fuel has a computed density of ~5.70 g/cm^3. The TRIGA fuel element with a fuel diameter of 1.44 inches contains 2,282.4 g $UZrH_x$ while the element with a fuel diameter of 1.31 inches contains 1,888.9 g $UZrH_x$.

The clad thickness is ~0.02 inches for a TRIGA fuel element with stainless steel cladding and ~0.03 inches for an element with aluminum cladding. In preparation for shipment in the ES-3100, a TRIGA fuel element is disassembled, the fuel meats are removed from the thin cladding and packed into convenience cans.

Table 6.9.3.1-4a. Calculation of constituent weight-percentage values for 20 wt % enriched uranium-zirconium hydride content in KENOV.a calculation models

Avogadro No. (N_o) = 6.0221370e+23

$U(ZrH_x)$

atom	wt %	x	mass g	at. wt.		calc. N_i	N_iA_i
Hydrogen	0.9554	1.6		1.00780	1.6125	4.9439e+22	4.9824e+22
Zirconium	54.0447	1		91.21960	91.2196	3.0897e+22	2.8184e+24
u-235	19.6795		307.0	235.04410			
u-238	80.3205			238.05099			
uranium	45.0000		1560.0	237.45318	75.9535	9.8830e+21	2.3468e+24
	100.0001				168.7856		
summations	100.0001					9.0219e+22	5.2150e+24
At. wt molecule							
Volume (cm^3)	400.3200						
Mass (g)	3466.66667						
density (g/cm^3)	8.65974						
den.=($\sum$NiAi)/No							8.6597

Table 6.9.3.1-4b. Calculation of constituent weight-percentage values for 70 wt % enriched uranium-zirconium hydride content in KENOV.a calculation models

Avogadro No. (N_o) = 6.0221370e+23

$U(ZrH_x)$ atom	wt %	x	mass	at. wt		calc. N_i	N_iA_i
Hydrogen	1.5894	1.6		1.00780	1.6125	5.4148e+22	5.4571e+22
Zirconium	89.9107	1		91.21960	91.2196	3.3841e+22	3.0870e+24
u-235	70.1031		136.0	235.04410			
u-238	29.8969			238.05099			
uranium	8.5000		194.0	235.93508	8.6237	1.2370e+21	2.9184e+23
	100.0001				101.4558		
summations	100.0001					8.9227e+22	3.4334e+24
At. wt molecule							
Volume (cm^3)	400.3200						
Mass (g)	2282.35294						
density (g/cm^3)	5.70132						
den.=(∑NiAi)/No							5.7013

The TRIGA fuel may also be configured as clad fuel rods. Each clad fuel rod will be derived from a single TRIGA fuel element by removal of the stainless steel or aluminum clad extending beyond the plenum adjacent to the axial ends of the active fuel section. Each ~15 inch long rod consists of the 3 fuel pellets and an exterior sheath of stainless steel or aluminum clad, where the protruding clad at each end has been crimped in. The fuel rods will be packed into stainless steel or tin-plated carbon steel convenience cans, with a maximum of three fuel rods per loaded convenience can. This shipping configuration requires a minimum of two convenience cans; where only one convenience can is loaded with clad fuel rods. The loaded can is 17.5 inches tall while the empty one is 8.75 inches tall. Although can spacers are not required for criticality control, can spacers or stainless steel pads may be used to take up free volume over the 31 in. internal height of the containment vessel. The maximum quantity of fissile material per package is 408 g ^{235}U.

The clad fuel rod with 1.44 inch diameter fuel pellets contains 2,282.4 g $UZrH_x$ while rod with the 1.31 inch diameter fuel pellets contains 1,888.9 g $UZrH_x$. The 0.02 in thick sheath of stainless steel clad adds ~179 g to the mass of the active fuel for the 1.48 in. diameter standard element or instrumented element, and ~163 g to active fuel mass for the 1.35 in. diameter fuel follower control rod. Allowance for 1/2 in. of residual stainless steel crimped on each end of the clad fuel rod adds ~11 - 12 g stainless steel to these amounts. Likewise, the 0.03 in thick sheath of aluminum clad adds ~90 g to the mass of the active fuel for the 1.47 in. diameter standard element or instrumented element. Allowance for 1/2 in. of residual stainless steel crimped on each end of the clad fuel rod adds ~6 g aluminum.

6.9.3.2 TYPE 304 STAINLESS STEEL

The metallic components of the ES-3100 package are composed of type 304 stainless steel. These include the containment vessel, the convenience cans, the drum liner, and the drum. Type 304 stainless steel with a density of 7.9400 g/cm^3 is included as a material in the SCALE Standard Composition Library.

6.9.3.3 277-4 NEUTRON ABSORBER

Catalog No. 277 dry mix is a proprietary mixture of Thermo Electron Corporation for producing a heat-resistant shielding material which combines the most effective shielding components into a single homogeneous composite. The shielding composite material is designed to maximize the hydrogen content necessary for thermalizing fast neutrons for capture in the boron constituent. Widely used in nuclear power plant applications, the heat-resistant shielding material is capable of retaining a significant portion of its shielding properties up to 230°C (450°F). The recommended operating limit is 350°F, which is well above HAC temperatures expected inside the body weldment liner inner cavity and canned spacers.

The 277-4 neutron absorber material used in the ES-3100 is a formulation of Cat 277-0 dry mix, a boron carbide additive, and water. 277-4 is produced through a quality-controlled batch process of dry blending, wet mixing, vibration casting, and timed cure. (Equipment Specification JS-YMN3-801580-A005, Appendix 1.4.5) "Loss On Drying" (LOD) tests are used to measure the amount of water in the as-manufactured 277-4 casting. The as-manufactured 277-4 at 100 lb/ft^3 and 31.8 % LOD has a hydrogen concentration of 3.56 wt % and a natural boron concentration of 4.359 wt %. (DAC-PKG-801624-A001, Table 5)

The ability of 277-4 to perform its function depends upon the masses of hydrogen and ^{10}B locked inside the high alumina borated cement cast into the body weldment liner inner cavity and the spacer cans. A calculated amount of boron carbide is added to Cat 277-0 dry mix for producing as-manufactured 277-4 material with a volumetric isotopic concentration >7.621×10^{20} at/cm^3 of ^{10}B. The additive is boron carbide (B_4C) with small amount of a frit-like compound and trace amounts of unaccounted elements (0.17 wt %). Boron carbide has a theoretical density from 2.45 to 2.52 g/cm^3. The boron carbide grit partical sizes used are also small after passing through mesh sizes of 200 and 40 (63 to 355 μm). 277-4 contains a large amount of hydrated alumina, also known as aluminum trihydrate [$Al(OH)_3$]. It is a nonabrasive powder with a specific gravity of 2.42. Given that both materials are of like density and similar partial size, separation and in homogeneity of 277-4 material is not expected during the controlled vibration casting process.

Table 6.9.3.3-1 provides detailed elemental composition data derived for as-manufactured neutron absorber material at 100 lb/ft^3 and 31.8% LOD. This material description allows for clear specification of reduced boron and water contents required in the evaluation of NCT and HAC. As shown in Table 6.9.3.3-1, both the water and boron components are extracted from the material specification for the neutron absorber, and the constituent weight percents are recalculated accordingly (green box). 277-4 is specified in KENO V.a as three arbitrary materials: **arbmnpmx** with a density of 1.02276 g/cm^3, **arbmnph2o** with a density of 0.509253 g/cm^3, and **arbmboron** with a density of 6.98257e-02 g/cm^3. Model densities for 277-4 inside the body weldment liner inner cavity are reduced by a factor of 0.966893 to account for a material gap at the top of the liner. This material description allows for clear specification of reduced boron and water contents required in the evaluation of NCT and HAC.

The testing of 277-4 reveals that the material will dehydrate at elevated temperatures. Test specimens were dried at 250°F for 168 hours to reach the NCT state, and weight measurements were taken. These specimens where subsequently heated to 320°F for 4 hours to reach the HAC state, and weight measurements were again taken. The compositions of 277 at NCT and HAC states were derived by adjustment of the formulation specification for measured losses taking into account the statistical variations in the data. Conservation of mass for nonvolatile materials was observed in the derivation of material specifications based upon testing. Given that hydrogen must be present for the neutron absorber to be effective, conservative material specifications were derived for minimum hydrogen content and minimum material density.

Tables 6.9.3.3-2 and 6.9.3.3-3 respectively provide NCT and HAC composition data for as-manufactured 277-4 material at minimum density and hydrogen content. Respectively, Tables 6.9.3.3-4 and 6.9.3.3-5 provide NCT and HAC composition data or as-manufactured neutron absorber material at minimum density and boron content. Because the amount of ^{10}B present in the neutron absorber material is near saturation, a change in the hydrogen concentration has a major effect on the neutron multiplication factor, while a change in the amount of boron has a minor effect.

Table 6.9.3.3-1. Calculation of constituent weight-percentage values used in KENO V.a calculation models for as-manufactured 277-4 at minimum acceptable density and boron content [a]

			arbmboron	arbmnpmx	arbmnph2o			arbmboron	arbmnpmx	arbmnph2o
31.8% LOD	At. wt	lb/ft^3	lb/ft^3	lb/ft^3	lb/ft^3		NID	Wt %	Wt %	Wt %
H	1.0078	3.5579			3.5579	**H**	1001			11.1913%
B10	10.0129	0.7911	0.7911			**B10**	5010	18.1482%		
B11	11.0093	3.5680	3.5680			**B11**	5011	81.8518%		
C	12.0000	1.2251		1.2251		**C**	6012		1.9187%	
N	14.0031	0.0090		0.0090		**N**	7014		0.0141%	
O	15.9949	55.9620		27.7281	28.2339	**O**	8016		43.4275%	88.8087%
Na	22.9895	0.0750		0.0750		**Na**	11023		0.1175%	
Mg	24.3051	0.2156		0.2156		**Mg**	12000		0.3377%	
Al	26.9818	24.9306		24.9306		**Al**	13027		39.0461%	
Si	28.0853	1.5752		1.5752		**Si**	14000		2.4671%	
S	32.0636	0.1969		0.1969		**S**	16000		0.3084%	
Ca	40.0803	7.5553		7.5553		**Ca**	20000		11.8331%	
Fe	55.8447	0.3383		0.3383		**Fe**	24000		0.5298%	
Totals		100.0000	4.3591	63.8491	31.7918			100.00%	100.00%	100.00%
H_2O	18.0105									
density (g/cm^3)		1.601838e+00	6.982572e-02	1.022759e+00	5.092532e-01	spacer density (g/cm^3)	1.601838e+00	6.98257e-02	1.02276e+00	5.09253e-01
						liner density (g/cm^3)	1.548806e+00	6.75140e-02	9.88899e-01	4.92393e-01
						liner den. multiplier	0.966893			

a *Source*: G. A. Byington, *Mixing Weights and Elemental Composition of 277-4 Neutron Poison Used in the ES-3100*, DAC-PKG-801624-A001, BWXT Y-12, Y-12 National Security Complex, Jan. 25, 2006, Table 5.

Table 6.9.3.3-2. Calculation of constituent weight-percentage values used in KENO V.a calculation models for NCT as-manufactured 277-4 at minimum density and hydrogen content[a]

			arbmboron	arbmnpmx	arbmnph2o
	At. wt	lb/ft³	lb/ft³	lb/ft³	lb/ft³
H	1.0078	2.6840			2.6840
B10	10.0129	0.8282	0.8282		
B11	11.0093	3.7354	3.7354		
C	12.0000	1.2826		1.2826	
N	14.0031	0.0094		0.0094	
O	15.9949	50.3252		29.0262	
O	15.9949				21.2990
Na	22.9895	0.0785		0.0785	
Mg	24.3051	0.2258		0.2258	
Al	26.9818	26.1004		26.1004	
Si	28.0853	1.6491		1.6491	
S	32.0636	0.2061		0.2061	
Ca	40.0803	7.9098		7.9098	
Fe	55.8447	0.3541		0.3541	
Totals		95.3886	4.5636	66.8420	23.9830
H_2O	18.0105				
density (g/cm³)		1.527971e+00	7.310148e-02	1.070700e+00	3.841692e-01

		arbmboron	arbmnpmx	arbmnph2o
	NID	**Wt %**	**Wt %**	**Wt %**
H	1001			11.1913%
B10	5010	18.1479%		
B11	5011	81.8520%		
C	6012		1.9189%	
N	7014		0.0141%	
O	8016		43.4251%	
O	8016			88.8087%
Na	11023		0.1174%	
Mg	12000		0.3378%	
Al	13027		39.0479%	
Si	14000		2.4672%	
S	16000		0.3083%	
Ca	20000		11.8336%	
Fe	24000		0.5298%	
		100.00%	100.00%	100.00%
spacer density (g/cm³)	1.527971e+00	7.31015e-02	1.07070e+00	3.84169e-01
liner density (g/cm³)	1.477385e+00	7.06813e-02	1.03525e+00	3.71451e-01
liner den. multiplier	0.966893			

a *Source*: G. A. Byington, *Mixing Weights and Elemental Composition of 277-4 Neutron Poison Used in the ES-3100*, DAC-PKG-801624-A001, BWXT Y-12, Y-12 National Security Complex, Jan. 25, 2006, Table 11.

Table 6.9.3.3-3. Calculation of constituent weight-percentage values used in KENO V.a calculation models for HAC as-manufactured 277-4 at minimum density and hydrogen content [a]

			arbmboron	arbmnpmx	arbmnph2o
	At. wt	lb/ft^3	lb/ft^3	lb/ft^3	lb/ft^3
H	1.0078	2.6758			2.6758
B10	10.0129	0.8282	0.8282		
B11	11.0093	3.7354	3.7354		
C	12.0000	1.2826		1.2826	
N	14.0031	0.0094		0.0094	
O	15.9949	50.2605		29.0265	
O	15.9949				21.2340
Na	22.9895	0.0785		0.0785	
Mg	24.3051	0.2258		0.2258	
Al	26.9818	26.1004		26.1004	
Si	28.0853	1.6491		1.6491	
S	32.0636	0.2061		0.2061	
Ca	40.0803	7.9098		7.9098	
Fe	55.8447	0.3541		0.3541	
Totals		95.3157	4.5636	66.8423	23.9098
H_2O	18.0105				
density (g/cm^3)		1.52680e+00	7.31015e-02	1.07071e+00	3.82995e-01

		arbmboron	arbmnpmx	arbmnph2o
	NID	**Wt %**	**Wt %**	**Wt %**
H	1001			11.1913%
N10	5010	18.1479%		
N11	5011	81.8520%		
V	6012		1.9188%	
N	7014		0.0141%	
O	8016		43.4254%	
O	8016			88.8087%
Na	11023		0.1174%	
,g	12000		0.3378%	
Al	13027		39.0477%	
Si	14000		2.4671%	
S	16000		0.3083%	
Ca	20000		11.8335%	
Fe	24000		0.5298%	
		100.00%	100.00%	100.00%
spacer density (g/cm^3)	1.52680e+00	7.31015e-02	1.07071e+00	3.82995e-01
liner density (g/cm^3)	1.47626e+00	7.06813e-02	1.03526e+00	3.70316e-01
liner den. multiplier	0.966893			

a *Source*: G. A. Byington, *Mixing Weights and Elemental Composition of 277-4 Neutron Poison Used in the ES-3100*, DAC-PKG-801624-A001, BWXT Y-12, Y-12 National Security Complex, Jan. 25, 2006, Table 12.

Table 6.9.3.3-4. Calculation of constituent weight-percentage values used in KENO V.a calculation models for NCT as-manufactured 277-4 at minimum density and boron content [a]

			arbmboron	arbmnpmx	arbmnph2o
	At. wt	lb/ft^3	lb/ft^3	lb/ft^3	lb/ft^3
H	1.0078	2.9617			2.9617
B10	10.0129	0.7911	0.7911		
B11	11.0093	3.5680	3.5680		
C	12.0000	1.2251		1.2251	
N	14.0031	0.0090		0.0090	
O	15.9949	51.2291		27.7264	
O	15.9949				23.5027
Na	22.9895	0.0750		0.0750	
Mg	24.3051	0.2156		0.2156	
Al	26.9818	24.9306		24.9306	
Si	28.0853	1.5752		1.5752	
S	32.0636	0.1969		0.1969	
Ca	40.0803	7.5553		7.5553	
Fe	55.8447	0.3383		0.3383	
Totals		94.6709	4.3591	63.8474	26.4644
H2O	18.0105				
density (g/cm^3)		1.516474e+00	6.982572e-02	1.022731e+00	4.239172e-01

		arbmboron	arbmnpmx	arbmnph2o
	NID	Wt %	Wt %	Wt %
H	1001			11.1913%
B10	5010	18.1482%		
B11	5011	81.8517%		
C	6012		1.9188%	
N	7014		0.0141%	
O	8016		43.4260%	
O	8016			88.8087%
Na	11023		0.1175%	
Mg	12000		0.3377%	
Al	13027		39.0472%	
Si	14000		2.4671%	
S	16000		0.3084%	
Ca	20000		11.8334%	
Fe	24000		0.5299%	
		100.00%	100.00%	100.00%
spacer density (g/cm^3)	1.516474e+00	6.98257e-02	1.02273e+00	4.23917e-01
liner density (g/cm^3)	1.466269e+00	6.75140e-02	9.88872e-01	4.09883e-01
liner den. multiplier	0.966893			

a *Source*: G. A. Byington, *Mixing Weights and Elemental Composition of 277-4 Neutron Poison Used in the ES-3100*, DAC-PKG-801624-A001, BWXT Y-12, Y-12 National Security Complex, Jan. 25, 2006, Table 13.

Table 6.9.3.3-5. Calculation of constituent weight-percentage values used in KENO V.a calculation models for HAC as-manufactured 277-4 at minimum density and boron content [a]

			arbmboron	arbmnpmx	arbmnph2o
	At. wt	lb/ft^3	lb/ft^3	lb/ft^3	lb/ft^3
H	1.0078	2.9524			2.9524
B10	10.0129	0.7911	0.7911		
B11	11.0093	3.5680	3.5680		
C	12.0000	1.2251		1.2251	
N	14.0031	0.0090		0.0090	
O	15.9949	51.1551		27.7262	
O	15.9949				23.4289
Na	22.9895	0.0750		0.0750	
Mg	24.3051	0.2156		0.2156	
Al	26.9818	24.9306		24.9306	
Si	28.0853	1.5752		1.5752	
S	32.0636	0.1969		0.1969	
Ca	40.0803	7.5553		7.5553	
Fe	55.8447	0.3383		0.3383	
Totals		94.5876	4.3591	63.8472	26.3813
H_2O	18.0105				
density (g/cm^3)		1.515140e+00	6.982572e-02	1.022728e+00	4.225861e-01

		arbmboron	arbmnpmx	arbmnph2o
	NID	Wt %	Wt %	Wt %
H	1001			11.1913%
B10	5010	18.1482%		
B11	5011	81.8517%		
C	6012		1.9188%	
N	7014		0.0141%	
O	8016		43.4258%	
O	8016			88.8087%
Na	11023		0.1175%	
Mg	12000		0.3377%	
Al	13027		39.0473%	
Si	14000		2.4671%	
S	16000		0.3084%	
Ca	20000		11.8334%	
Fe	24000		0.5299%	
		100.00%	100.00%	100.00%
spacer density (g/cm^3)	1.515140e+00	6.98257e-02	1.02273e+00	4.22586e-01
liner density (g/cm^3)	1.464979e+00	6.75140e-02	9.88869e-01	4.08596e-01
liner den. multiplier	0.966893			

a *Source*: G. A. Byington, *Mixing Weights and Elemental Composition of 277-4 Neutron Poison Used in the ES-3100*, DAC-PKG-801624-A001, BWXT Y-12, Y-12 National Security Complex, Jan. 25, 2006, Table 14.

The neutron absorbing material used in the ES-3100 Shipping Package will perform as analyzed. The analysis of 277-4 with criticality calculations is adequate in lieu of neutron transmission testing for the demonstration of acceptable performance by experimental means. Criticality calculations show boron content is adequate and k_{eff} is not dependent on absolute (microscopic) homogeneity. Geometry characteristics of the ES-3100 system preclude the need for uniformity in boron areal density as a prerequisite for criticality safety control. The neutron absorbing material will be fabricated under strict quality control and accepted for use under an NQA-1 compliant quality assurance (QA) program. A QA-approved mixing process provides a method for creating an exact mix for the neutron absorber during ES-3100 fabrication. An important part of this QA-approved process is a 277-4 material verification and acceptance testing program. The following discussion elaborates on these key points:

The analysis of 277-4 with criticality calculations is adequate in lieu of neutron transmission testing for the demonstration of acceptable performance. Early on in the licensing process, Borobond 4 was selected as the neutron absorber material for use in the ES-3100 package. The decision to use Borobond 4 in the ES-3100 was made because of favorable experience with its use in the Highly Enriched Uranium (HEU) Rackable Can Storage Box (RCSB), an element of the new state-of-the art HEU storage facility at the Y-12 National Security Complex (Y-12). From an economic standpoint, however, Borobond 4 proved not to be a viable option for the small quantities needed for the ES-3100 project. 277-4 neutron absorber material, which has very similar nuclear material properties to Borobond 4, was then selected as an alternative.

Both the RCSB and the ES-3100 are fast systems in the normal condition when the HEU fissile material is essentially unmoderated. A key factor for an effective neutron absorber is that hydrogen should be present for moderation, and it should be interspersed with boron-10 (^{10}B), thus promoting neutron capture. The potential for neutron streaming through an absorber is significant when a hydrogenous moderator is absent, as in the case of an aluminum boron-carbide matrix (a Boral alloy).

Borobond 4 is a ceramicrete material with slightly greater than 4 wt % boron carbide (B_4C). The boron carbide powder is micro encapsulated by the crystalline matrix of the ceramic; therefore, leaching out the boron is not feasible. In Borobond 4, 100 wt % of the B_4C has a particle size <500 μm; 90 wt % of the other constituents range from <164 μm to <36 μm. Given the differences in particle size, the potential for separation in the mixing process is real.

Some of the questions regarding the use of 277-4 as a neutron poison in the ES-3100 were previously addressed regarding the use of Borobond 4 in the RCSB. Radiography was performed on Borobond 4 samples ranging in thickness from 1.0 to 1.5 in. Inspections revealed little or no visual differences, indicating uniformity of the Borobond 4. For 277-4 where the B_4C grit is on the order of 200 μm, the potential for separation is reduced.

Measurements from neutron transmission tests on Borobond 4 for determination of areal density indicated greater boron content than was physically present. This is due to the presence of elements besides the aluminum and boron (principally hydrogen, oxygen and other low and intermediate-Z elements). From these measurements, credit for 90 wt % boron in a criticality calculation was established as an adequate adjustment. Given the similarity of 277-4 to Borobond 4 (a ceramic-cement composite shielding material, with a similar elemental composition, more uniform particle size, and the same boron content), the 75% credit for boron content applied in the ES-3100 criticality calculations is an adequate enough correction for the efficiency of the material.

Criticality calculations show boron content is adequate and k_{eff} is not dependent on absolute (microscopic) homogeneity. The boron concentration calculations presented here model an infinite array of ES-3100 packages with the boron concentration of Cat 277-4 uniformly varied inside the body weldment inner liner. While the Cat 277-4 described herein is an earlier formulation of the neutron absorber material, the behavior characteristics being demonstrated for Cat 277-4 apply to the revised formulation, 277-4.

Credit for only 75% of the boron is taken in the specification of Cat 277-4. Each package in the array contains 2.774 kg of ^{235}U in broken metal form uniformly distributed inside the containment vessel. The presence of just the hydrogenous cement matrix in the inner liner reduces k_{eff} to 1.132 from a value of 1.35 without the cement matrix. As an initial 1 wt % natural boron is added to the high alumina cement system (Table 6.9.3.3-6), the calculated k_{eff} based on 75% of the boron present drops significantly. Cat 277-4 with 4.2284 wt % natural boron in the minimum cast density of 100 lb/ft^3 (1.60 g/cc) has an acceptable mixture concentration, generating a k_{eff} of 0.88. The saturation value for boron content is reached at ~8 wt %. This near doubling of the boron content results in ~4% decrease in k_{eff} to an asymptotic value of ~0.85.

The density of Cat 277-4 is the sum of constituent densities: the boron density, the base-material density, and the water density. In the calculation model, the density of water in Cat 277-4 is 0.48210 g/cm^3 (not shown in Table 6.9.3.3-6). Canned spacers are omitted from the calculation model. Credit for only 75% of the boron is taken in each parametric calculation. The volume of the 277-4 in the body weldment inner liner cavity is 1.32708×10^4 cm^3.

Table 6.9.3.3-6. Effect of boron concentration on array neutron multiplication

100%B (wt %)	Boron density (g/cm^3)	Base material density (g/cm^3)	NP277-4 mass (g)	Case name	$k_{eff} \pm 2\sigma$ (@75% B)
0.01	0.00016	1.11775	21232.6	nbiabm_kvsb_1	1.13199 +/- 0.00138
0.1	0.0016	1.11631	2.12279e+04	nbiabm_kvsb_2	1.07944 +/- 0.00145
1	0.016	1.10191	2.11801e+04	nbiabm_kvsb_3	0.95564 +/- 0.00129
2	0.032	1.08591	2.11270e+04	nbiabm_kvsb_4	0.91708 +/- 0.00135
3	0.048	1.06991	2.10739e+04	nbiabm_kvsb_5	0.89396 +/- 0.00117
4.2284	0.068614	1.04930	2.10056e+04	nbiabm_kvsb_6	0.87985 +/- 0.00145
6	9.6000e-02	1.02191.	2.09147e+04	nbiabm_kvsb_7	0.86029 +/- 0.00151
8	1.2800e-01	0.98991	2.08085e+04	nbiabm_kvsb_8	0.84769 +/- 0.00150
10	0.16	0.95791	2.07024e+04	nbiabm_kvsb_9	0.84086 +/- 0.00142

NUREG 1609 recommended that only 75% of the minimum boron density be credited in criticality evaluation in order to address the issue of non-homogeneity of ^{10}B in the neutron absorber material. The boron non-homogenity calculations presented here model an infinite array of ES-3100 packages with the boron concentration of Cat 277-4 varying along the vertical height of the body weldment inner liner. However, the total amount of boron in each package is fixed. Each package in the array contains 2.774 kg of ^{235}U in broken metal form uniformly distributed inside the containment vessel. Two sets of calculations are evaluated with this model to address the effects of boron distribution in the ES-3100 inner liner.

In one set of cases, the inner cavity is divided vertically into three equal-volume regions. The density in one region is increased to 95% of the minimum boron density, while the boron density in the other two regions is decreased to 65%, thus preserving the amount of neutron absorber material in the package. In the other set of cases, the inner cavity is divided vertically into four equal volume regions, but two regions are combined. This creates two quarter-sized regions and one half-size region. The density in the half-size region is increased to 95% of the minimum boron density, while the density in the quarter-sized regions is decreased to 55%, thus preserving the amount of neutron absorber in the package. In both sets of calculations, the high-density region was shifted upward in the package to examine the effect of boron distribution.

As shown in Figures 6.9.3.3-2 and 6.9.3.3-3, the effect of non-homogeneity of boron in the ES-3100 liner on k_{eff} is not statistically significant. The "65% - 95% - 65%" nonhomogeneous boron distributionnon represents a relative standard deviation of 23.1% in boron concentration. Given the controls on method of

manufacture and installation of the neutron absorber material, these calculated conditions bound the expected physical distribution of boron with a large degree of conservatism.

Geometry characteristics of the ES-3100 system preclude the need for uniformity in boron areal density as a prerequisite for criticality safety control. The ISG-15 provides crucial guidance for controlling areal density in a geometry configuration where one-dimensional effects are significant, such as a distributed source separated by thin Boral sheets (aluminum and boron carbide) which range in thickness from 0.075 to 0.4 in. In this example, Boral aluminum sheets are placed between fissile fuel rods just a few inches away and only become efficient when the low-enriched fissile material is placed in a sea of hydrogenous moderator. The cylindrical thickness of the ES-3100 cast neutron absorber material (Cat 277-4) is 1.12 in., which is about three times thicker than the largest Boral sheet. Its purpose in the ES-3100 is to provide criticality safety control for arrays of packages.

In the ES-3100, the proposed fissile mass loads are separated by at least one drum diameter (19.36 in.). Drawing M2E801580A031 in Appendix 1.4.8 shows the cross-section view of the many different layers of materials that are between the fissile mass loads in adjacent packages in an array. The direct neutron transport path between dispersed fissile material (assuming a neutron passes through the following thickness of materials at a normal angle to the closest neighboring package) is:

- fissile material,
- 0.100 in. 304 stainless-steel containment vessel wall,
- air gap,
- 0.06 in. 304 stainless-steel inner liner wall,
- 1.12 in. of 277-4 neutron absorber material,
- 0.06 in. 304 stainless-steel outer liner wall,
- 4.77 in. of Kaolite,
- 0.06 in. 304 stainless-steel outer drum wall, and
- air gap,

followed by the reverse:

- 0.06 in. stainless-steel outer drum wall,
- 4.77 in. of Kaolite,
- 0.06 in. 304 stainless-steel outer liner wall,
- 1.12 in. of 277-4 neutron absorber material,
- 0.06 in. 304 stainless-steel inner liner wall,
- air gap,
- 0.100 in. 304 stainless-steel containment vessel wall, and
- back into a fissile material.

At the shortest distance between fissile materials, neutrons travel through the 1.12 in. (2.8448 cm) of 277-4 neutron absorber material and 0.28 in. (0.7112 cm) of 304 stainless steel at least twice, with the high probability of several neutron scattering collisions along the way. Thus, the mean free path in the package is much smaller than the separation between the fissile material of adjacent packages.

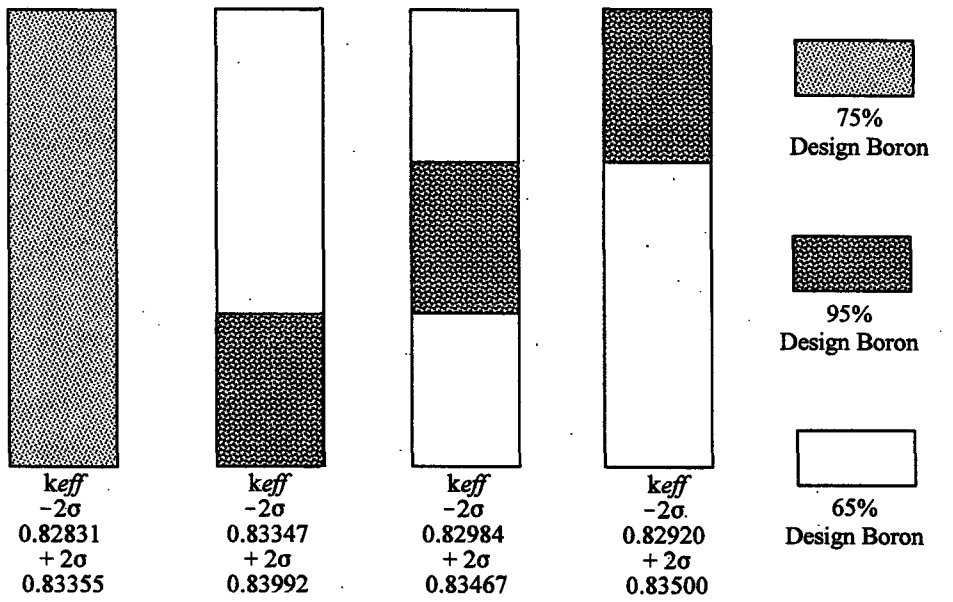

Fig. 6.9.3.3-2. Three equal-region models for evaluation of non-homogeneity in the boron distribution.

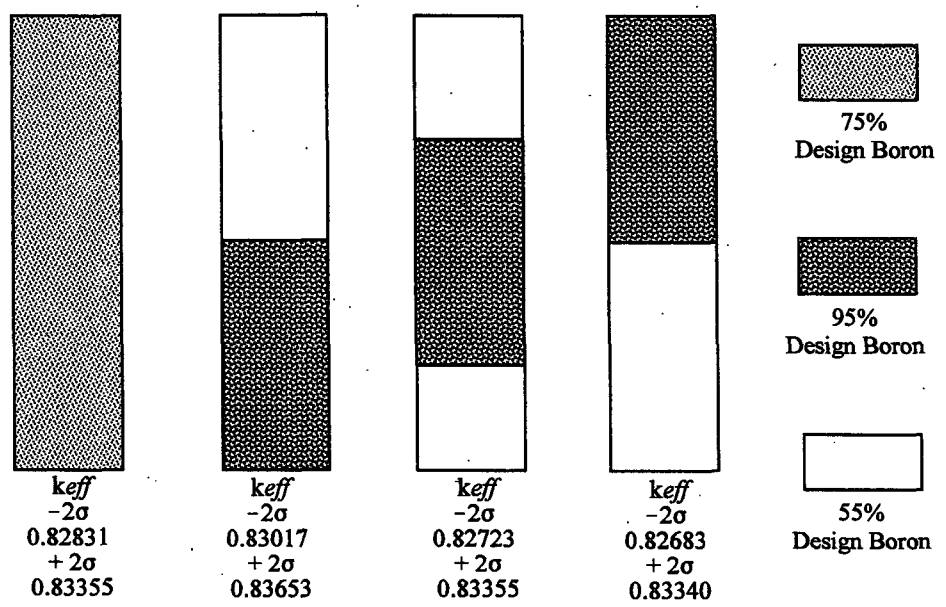

Fig. 6.9.3.3-3. Non-uniform region model for evaluation of non-homogeneity in the boron distribution.

In contrast to a Boral sheet application, the neutron absorber component of the ES-3100 package physically represents a significant fraction of the total container volume and is large in comparison to the potential fissile material volume. Furthermore, the neutron absorber component consists of boron dispersed throughout a hydraulic cement matrix with a high neutron scattering potential. The net result is that sensitivity to angular and spatial variations in the areal density of ^{10}B in the neutron absorber volume is eliminated.

The neutron absorbing material will be fabricated under strict quality control and accepted for use under an NQA-1 compliant QA program. The original equipment specification for the production of 277-4 neutron absorber material used a proprietary mixture from the Thermo Electron Corporation that combined high alumina cement and a boron grit (Cat 277-4). The manufacturing process for the neutron absorber was revised in order to obtain details necessary for material characterization and to achieve process control for ensuring consistency of absorber material among lots.

A two-part system of dry-blend components is now employed rather than relying on a single base material (a premixed powder of high alumina cement and boron grit). Thermo Electron Corporation's proprietary high-alumina cement without boron grit (Cat 277-0) is mixed on-site with boron carbide by the ES-3100 manufacturer under strict quality controls. A single batch is mixed on a per package basis. The boron carbide used in this process is strictly controlled. Boron carbide is specified per ASTM C 750-03, "Nuclear-Grade Boron Carbide Powder," in the Type 1 category. The grit size is controlled to ≤ 100 μm or a grit size of 120 per ANSI B74-12, with 100% passing a 120USS mesh.

The new formulation designated "277-4" is produced through a quality-controlled batch process of dry blending, wet mixing, vibration casting, and timed cure. (Equipment Specification JS-YMN3-801580-A005, Appendix 1.4.5) The plan is to control the purity, boron carbide particle size, chemistry, measurements, weights, mixing, recording, casting, and testing using one batch per each shipping package (and its two companion spacer cans). A design analysis calculation shows all of the calculations used in mixing and determines (from the minimum acceptable chemical purities) the volumetric densities in g/cm^3 and an areal density in g/cm^3 of ^{10}B. (DAC-PKG-801624-A001) These values will prove the acceptability of the mixing specifications.

An important part of this approach is a QA-approved 277-4 material verification and acceptance testing program. The applicant plans on performing 100% acceptance testing on the criticality safety significant properties of density, ^{10}B interaction (neutron absorption), and hydrogen content. The acceptance density shall be the as cast density in the drum to 105-5+10 lb/ft^3 and shall be determined as shown in Appendix 1.4.5. To test the other properties, two companion sample cans shall be cast from each batch used to cast a shipping container (the manufacturer will cast a fresh batch for each shipping container). The companion sample cans shall also have their density verified. The ^{10}B interaction will be tested in the manner described in Appendix A of the 277-4 specification (Appendix 1.4.5). Initially, a new set of 277-4–certified cans will be cast using the newly proposed casting specification with the QA plan described previously. Then, on a companion sample can for each batch pour, a Prompt Gamma-ray Neutron Activation Analysis (PGNAA) test will be used to neutronically test the ^{10}B for absorption. To pass the PGNAA test, the sample can results must be within the results obtained for the 277-4 certified standards, in units of Average Net Count rate (ANC/second) ±4 standard deviations. The second companion sample can will be used to test for hydrogen content using an LOD test as described in Appendix 1.4.5. Upon successful completion of the density, PGNAA, and LOD testing, the ES-3100 neutron absorber material will be accepted for use.

6.9.3.4 KAOLITE 1600

Kaolite 1600, manufactured by Thermal Ceramics of Augusta, Georgia [telephone number (404) 796-4200], is a super-lightweight, low thermal conductivity, castable material designed for backup insulation up to 1600°F. The material is obtained as a dry powder with the chemical composition given in Table 6.9.3.4-1. The powder is mixed with water in a water-to-powder ratio of 14.5 qt per 20-lb bag. The mixture is poured into the drum body weldment or top plug, vibrated to eliminate voids, and then dried and fired to form the finished product. (Rowland, 2001) The density of the fired material is ~25 lb/ft^3. It is assumed that the wet mixture contains the maximum water possible. This value (14.5 qt per 20 lb) is therefore used to determine the maximum water content of the fired product,

$$S.G._{max} = \frac{14.5\ qt}{20\ lb\ dry} \times \frac{25\ lb}{ft^3} \times \frac{0.946\ \ell}{1\ qt} \times \frac{998.2\ g}{\ell} \times \frac{35.32\ ft^3}{10^6\ cm^3} = \frac{0.6045\ g}{cm^3}$$

Table 6.9.3.4-1. Kaolite 1600 chemical composition, percent fired basis

Component	Weight percent	Component	Weight percent
Al_2O_3	9.6	CaO	30.7
SiO_2	36.7	MgO	13.1
Fe_2O_3	6.7	Na_2O	2.0
TiO_2	1.2		

Tables 6.9.3.4-2 and 6.9.3.4-3 provide detailed information regarding the weight measurements taken during the casting of Kaolite 1600 for the production of a series of drum body weldment and top plug parts for a similar package (the BWXT Y-12 Model ES-2100). The mean values for the amount of Kaolite and water present after baking are 107.08 lb of Kaolite and 4.8 lb of water in the drum body weldment, and 16.99 lb of Kaolite and 0.58 lb of water in the top plug. An ES-2100 package contains, on the average, 124.07 lb (56,276.91 g) of Kaolite and 5.38 lb (2,440.32 g) of water. Given that the average volume is 5.72 ft^3, the average density of Kaolite is 22.63 lb/ft^3 (0.3625 g/cm^3).

Table 6.9.3.4-2. Fabrication data, before and after baking the drum body weldment parts of the ES-2100 shipping package

								before baking			after baking		
Part Serial Number	clean & empty (lb)	filled with water (lb)	before baking (lb)	after baking (lb)	density after baking (lb/ft^3)	water conditions (lb)	volume (ft^3)	Kaolite and water (lb)	Kaolite (lb)	water (lb)	Kaolite and water (lb)	Kaolite (lb)	water (lb)
97	87.5	393.5	356.5	197.0	22.29	306.00	4.91	269.00	107.60	161.40	109.50	107.60	1.90
98	87.5	393.5	356.5	198.5	22.60	306.00	4.91	269.00	107.60	161.40	111.00	107.60	3.40
54	87.5	395.0	356.5	199.0	22.59	307.50	4.94	269.00	107.60	161.40	111.50	107.60	3.90
87	87.5	394.0	353.5	196.5	22.16	306.50	4.92	266.00	106.40	159.60	109.00	106.40	2.60
2	88.0	394.0	360.0	202.5	23.31	306.00	4.91	272.00	108.80	163.20	114.50	108.80	5.70
4	88.0	395.5	360.0	203.0	23.30	307.50	4.94	272.00	108.80	163.20	115.00	108.80	6.20
42	88.0	394.5	356.5	199.5	22.66	306.50	4.92	268.50	107.40	161.10	111.50	107.40	4.10
43	88.0	396.0	357.5	198.0	22.25	308.00	4.94	269.50	107.80	161.70	110.00	107.80	2.20
94	87.0	393.5	361.5	205.0	23.98	306.50	4.92	274.50	109.80	164.70	118.00	109.80	8.20
35	88.0	394.5	363.5	208.0	24.39	306.50	4.92	275.50	110.20	165.30	120.00	110.20	9.80
3	87.0	393.0	364.0	206.0	24.23	306.00	4.91	277.00	110.80	166.20	119.00	110.80	8.20
44	88.0	394.0	356.5	204.5	23.72	306.00	4.91	268.50	107.40	161.10	116.50	107.40	9.10
32	88.0	396.0	355.0	198.5	22.35	308.00	4.94	267.00	106.80	160.20	110.50	106.80	3.70
33	87.5	394.0	351.0	197.5	22.36	306.50	4.92	263.50	105.40	158.10	110.00	105.40	4.60
58	87.5	394.5	351.5	196.5	22.12	307.00	4.93	264.00	105.60	158.40	109.00	105.60	3.40
4	87.5	394.0	343.0	192.5	21.34	306.50	4.92	255.50	102.20	153.30	105.00	102.20	2.80
22	87.5	394.5	352.0	196.0	22.02	307.00	4.93	264.50	105.80	158.70	108.50	105.80	2.70
27	88.0	395.5	352.5	196.5	21.98	307.50	4.94	264.50	105.80	158.70	108.50	105.80	2.70
28	87.5	394.5	350.5	199.0	22.63	307.00	4.93	263.00	105.20	157.80	111.50	105.20	6.30
30	87.5	395.0	352.0	200.0	22.79	307.50	4.94	264.50	105.80	158.70	112.50	105.80	6.70
27	88.0	395.5	352.5	196.5	21.98	307.50	4.94	264.50	105.80	158.70	108.50	105.80	2.70
mean	87.67	394.50	355.36	199.55	22.72	306.83	4.93	267.69	107.08	160.61	111.88	107.08	4.80
std. dev.					0.8132						100%	95.71%	4.29%
computed on means					22.72	306.83	4.93	267.69	107.08	160.61	111.88	107.08	4.80

Table 6.9.3.4-3. Fabrication data, before and after baking the top plug parts of the ES-2100 shipping package

								before baking			after baking		
Part Serial Number	clean & empty (lb)	filled with water (lb)	before baking (lb)	after baking (lb)	density after baking (lb/ft^3)	water conditions (lb)	volume (ft^3)	Kaolite and water (lb)	Kaolite (lb)	water (lb)	Kaolite and water (lb)	Kaolite (lb)	water (lb)
97	10.5	60.0	53.5	28.5	22.65	49.50	0.79	43.00	17.20	25.80	18.00	17.20	0.80
83	10.5	59.0	50.5	27.0	50.50	27.00	50.50	27.00	16.00	24.00	16.00	24.00	16.00
86	10.5	60.0	50.5	27.5	21.40	49.50	0.79	40.00	16.00	24.00	17.00	16.00	1.00
87	10.5	59.0	53.0	28.5	23.12	48.50	0.78	42.50	17.00	25.50	18.00	17.00	1.00
28	11.0	59.0	53.0	28.5	22.71	48.00	0.77	42.00	16.80	25.20	17.50	16.80	0.70
23	10.5	59.5	52.5	28.0	22.25	49.00	0.79	42.00	16.80	25.20	17.50	16.80	0.70
24	10.5	59.0	53.5	28.5	23.12	48.50	0.78	43.00	17.20	25.80	18.00	17.20	0.80
25	10.5	58.5	54.0	29.0	24.01	48.00	0.77	43.50	17.40	26.10	18.50	17.40	1.10
26	10.5	59.0	54.0	29.0	23.76	48.50	0.78	43.50	17.40	26.10	18.50	17.40	1.10
27	10.5	60.0	54.5	29.0	23.28	49.50	0.79	44.00	17.60	26.40	18.50	17.60	0.90
0	10.5	60.0	52.0	27.0	20.77	49.50	0.79	41.50	16.60	24.90	16.50	16.60	-0.10[a]
20	10.5	60.0	53.5	28.0	22.03	49.50	0.79	43.00	17.20	25.80	17.50	17.20	0.30
22	10.5	60.0	54.0	28.5	22.65	49.50	0.79	43.50	17.40	26.10	18.00	17.40	0.60
21	10.5	61.0	53.0	28.0	21.59	50.50	0.81	42.50	17.00	25.50	17.50	17.00	0.50
19	10.5	60.0	53.0	27.5	21.40	49.50	0.79	42.50	17.00	25.50	17.00	17.00	0.00
11	10.5	60.0	52.5	28.0	22.03	49.50	0.79	42.00	16.80	25.20	17.50	16.80	0.70
14	10.5	60.0	52.5	27.5	21.40	49.50	0.79	42.00	16.80	25.20	17.00	16.80	0.20
15	10.5	60.5	54.0	28.0	21.80	50.00	0.80	43.50	17.40	26.10	17.50	17.40	0.10
16	10.5	59.0	52.0	27.5	21.84	48.50	0.78	41.50	16.60	24.90	17.00	16.60	0.40
17	10.5	60.5	54.5	28.5	22.43	50.00	0.80	44.00	17.60	26.40	18.00	17.60	0.40
mean	10.52	59.70	53.00	28.10	23.74	48.10	3.28	42.48	16.99	25.48	17.58	16.99	0.58
std. dev.					6.3565						100%	96.67%	3.33%
computed on means					22.27	49.18	0.79	42.48	16.99	25.48	17.58	16.99	0.58

[a] No explanation is given for the negative amount of water in Part 0. Also, the smaller percentage of water present in the top plug compared with to the drum body weldment is attributed to the larger surface-to-volume ratio, which results in better drying of the parts.

The volume of the Kaolite region in the KENO models is 1.63417 × 5 cm^3. For NCT, the density of Kaolite is 0.34438 g/cm^3, and the density of water is 0.01493 g/cm^3. The data in Tables 6.9.3.4-2 and 6.9.3.4-3 indicate that the Kaolite may have as little as 1.90 lb (861.82 g) of water after baking (Part Serial Number 97) such that the corresponding density of water is 0.00527 g/cm^3. For the water-flooded HAC, the amount of water is assumed not to exceed the amount present before baking. The package would contain on the average 186.10 lb (84,413.1 g) of water such that the corresponding density is 0.51655 g/cm^3. The full range of NCT and HAC conditions would be covered by a variation of water in the Kaolite from 0 g/cm^3 to 0.51655 g/cm^3 in a calculation model.

The Kaolite components of ES-3100 shipping package had not been manufactured at the time this criticality safety evaluation was performed. Given the lack of production data for ES-3100 Kaolite, a material specification (mass and density) was derived from data for ES-2100 production units. This specification, denoted "as-manufactured" (AM) Kaolite, was used for the ES-3100 criticality calculations. This ES-2100 shipping package is similar in design to the ES-3100 currently being evaluated.

The Kaolite production process was re-evaluated and improved following the production of ES-3100 units. (Y/DW-1890) Test samples were produced. These were classified into three groups: high density, medium density, and low density. The predominate number of samples fell into the medium density category (22.04 lb/ft^3), representing the expected, improved Kaolite production process. (Y/DW-1890, Appendix 2.10.4, Table 5) A material specification for use in criticality calculations was derived from the medium density "test sample" (TS) Kaolite data. However, the TS data are based on small sample volumes, whereas the AM data represents the entire package. Taking into consideration both the potential for scaling error and the uncertainty of how representative the test samples are of the manufactured ES-2100 units, the criticality safety packaging analysts chose to utilize the material specification derived from AM data rather than TS data in the criticality calculations for the ES-3100 safety analysis report.

A set of criticality calculations was performed for each of the packaging material specifications (i.e., the TS and the AM Kaolite) using three package water contents to represent the range of NCT and HAC. Y-12 statisticians were asked to determine whether or not the observed differences in neutronic performance are statistically significant for a package modeled with the TS specification versus one modeled with the AM specification. The purpose of this discussion is to summarize this comparison (DAC-FS-900000-A014) and draw conclusions.

Criticality Calculations. Each case is rerun using a different starting random number in order to produce computed k_{eff} values that are statistically independent. Table 6.9.3.4-4 presents the random starting number, the mean value (k_{eff}) and corresponding standard error (s_i) computed for 10 individual runs of each case.

Three sets of criticality calculations were run for both the AM Kaolite and TS Kaolite. One set of calculaitons is for dry Kaolite (i.e., low water content, IS = 1e-04 sp gr water); another set is for normal moisture Kaolite (i.e., NCT water content); and the third set is for flooded Kaolite (i.e., high water content, IS = 1.0 sp gr water). These conditions span the range of NCT and HAC addressed in the criticality evaluation. An infinite array of packages was evaluated in order to eliminate any biases arising from spectral leakage effects in the reflector of the finite array. Each package was modeled having 36 kg of 100% enriched uranium in the form of 3.24-in. diameter cylinder content. The k_{eff} values for each KENO V.a case are based on 500,000 neutron histories produced by running for 215 generations with 2,500 neutrons per generation and truncating the first 15 generations of data.

Statistical evaluation. A review of KENO V.a calculation results was made to determine if a statistically significant difference exists between the mean k_{eff} for the TS Kaolite specification and the AM Kaolite material specifications used in the criticality evaluation of the ES-3100 shipping package. Case results were classified into three groups (i.e., low water content, medium water content, or high water content) depending on the amount of water present in the ES-3100 shipping package. The symbol "T" is used to specify the

group. The mean difference and standard deviation for each of the three (3) sets of pair-wise differences was defined as follows:

(a) $d_i = (k_{effBi} - k_{effAi})/n$ and
(b) $s_{di} = \sqrt{[\, n\Sigma d_i^{\,2} - (\Sigma d_i)^2 \,] / n(n-1)}$ (conservatively defined for the t-test appropriate for small sample sizes).

where A_i denotes the TS by group classification, B_i the AM by group classification, and n the sample size of ten (10). It is reasonable to assume that the paired differences have been randomly selected from a normally distributed population of paired differences with mean μ_d and standard deviation σ_d. Therefore, the sampling distribution of

$$(d - \mu_d) / (s_d/\sqrt{n})$$

is a *t*-distribution having n-1 degrees of freedom.

The evaluation of the mean differences (d_i) for the 10 set of cases is accomplished through hypothesis testing, a statistical tool used to provide evidence that a difference exists or does not exist. The t_i values are 0.70, 10.0 and 0.95 for dry Kaolite, for NCT Kaolite, and for flooded Kaolite, respectively. A value of 3.25 is obtained from the standard table for critical values for the t distribution, from which the decision to accept or reject the null hypothesis H_0 is made with a Type I error probability (α) of 0.01. For $t < 3.25$, the H_o hypothesis is not rejected. Acceptance of the null hypothesis is the result of insufficient evidence to reject it. Thus, it can be concluded that the mean estimate of the difference of the AM Kaolite is not significantly different from the mean of the TS Kaolite for both dry and flooded Kaolite. For $t > 3.25$, the H_o hypothesis is rejected. Therefore, it can be concluded that the mean estimate of the difference of the AM Kaolite is significantly different from the mean of the TS Kaolite for the normal moisture Kaolite. The mean k_{eff} for AM Kaolite is significantly greater than the mean k_{eff} of the TS Kaolite; therefore, the use of the AM specification in the ES-3100 criticality calculations is conservative and bounding. Details of the statistical evaluation are documented in Reference DAC-FS-900000-A014.

Table 6.9.3.4-4. Data for the statistical evaluation of "as-manufactured"and "test sample" Kaolite

As-Manufactured Kaolite				Test Sample Kaolite			
Case name	Random number	k_{eff}	s_i	Case name	Random number	k_{eff}	s_i
Group 1 – Low water content							
esrandnum_01_01_in	109E77866CF	1.00274	0.00138	mdrandnum_01_01_in	109E77866CF	1.00170	0.00125
esrandnum_01_02_in	16AA4A58735	1.00224	0.00120	mdrandnum_01_02_in	16AA4A58735	1.00416	0.00116
esrandnum_01_03_in	1814171B652	1.00121	0.00107	mdrandnum_01_03_in	1814171B652	1.00208	0.00125
esrandnum_01_04_in	1A423B9472C	1.00367	0.00118	mdrandnum_01_04_in	1A423B9472C	1.00271	0.00131
esrandnum_01_05_in	20E876D8224	1.00290	0.00133	mdrandnum_01_05_in	20E876D8224	1.00406	0.00125
esrandnum_01_06_in	3F6E65CA744	1.00266	0.00137	mdrandnum_01_06_in	3F6E65CA744	1.00418	0.00124
esrandnum_01_07_in	479D21DB750	1.00393	0.00108	mdrandnum_01_07_in	479D21DB750	1.00193	0.00133
esrandnum_01_08_in	55D4371D3A2	1.00313	0.00113	mdrandnum_01_08_in	55D4371D3A2	1.00196	0.00105
esrandnum_01_09_in	6E1A14672B8	1.00343	0.00119	mdrandnum_01_09_in	6E1A14672B8	1.00503	0.00118
esrandnum_01_10_in	77A0308C0E4	1.00229	0.00113	mdrandnum_01_10_in	77A0308C0E4	1.00358	0.00108
Group 2 – NCT medium density							
esrandnum_06_01_in	109E77866CF	0.99025	0.00119	mdrandnum_06_01_in	109E77866CF	0.98323	0.00118
esrandnum_06_02_in	16AA4A58735	0.98863	0.00128	mdrandnum_06_02_in	16AA4A58735	0.98630	0.00108
esrandnum_06_03_in	1814171B652	0.98811	0.00120	mdrandnum_06_03_in	1814171B652	0.98328	0.00125
esrandnum_06_04_in	1A423B9472C	0.98933	0.00114	mdrandnum_06_04_in	1A423B9472C	0.98487	0.00112
esrandnum_06_05_in	20E876D8224	0.98869	0.00103	mdrandnum_06_05_in	20E876D8224	0.98559	0.00109
esrandnum_06_06_in	3F6E65CA744	0.98854	0.00117	mdrandnum_06_06_in	3F6E65CA744	0.98412	0.00106
esrandnum_06_07_in	479D21DB750	0.98900	0.00119	mdrandnum_06_07_in	479D21DB750	0.98395	0.00118
esrandnum_06_08_in	55D4371D3A2	0.98844	0.00113	mdrandnum_06_08_in	55D4371D3A2	0.98546	0.00114
esrandnum_06_09_in	6E1A14672B8	0.99007	0.00126	mdrandnum_06_09_in	6E1A14672B8	0.98424	0.00121
esrandnum_06_10_in	77A0308C0E4	0.99028	0.00122	mdrandnum_06_10_in	77A0308C0E4	0.98465	0.00118
Group 3 – High water content							
esrandnum_09_01_in	109E77866CF	0.92872	0.00118	mdrandnum_09_01_in	109E77866CF	0.92800	0.00123
esrandnum_09_02_in	16AA4A58735	0.92800	0.00110	mdrandnum_09_02_in	16AA4A58735	0.92817	0.00107
esrandnum_09_03_in	1814171B652	0.92844	0.00118	mdrandnum_09_03_in	1814171B652	0.92770	0.00115
esrandnum_09_04_in	1A423B9472C	0.92780	0.00123	mdrandnum_09_04_in	1A423B9472C	0.92763	0.00126
esrandnum_09_05_in	20E876D8224	0.92783	0.00134	mdrandnum_09_05_in	20E876D8224	0.92584	0.00105
esrandnum_09_06_in	3F6E65CA744	0.92809	0.00128	mdrandnum_09_06_in	3F6E65CA744	0.92853	0.00112
esrandnum_09_07_in	479D21DB750	0.92725	0.00111	mdrandnum_09_07_in	479D21DB750	0.92682	0.00111
esrandnum_09_08_in	55D4371D3A2	0.92622	0.00126	mdrandnum_09_08_in	55D4371D3A2	0.92706	0.00116
esrandnum_09_09_in	6E1A14672B8	0.92925	0.00132	mdrandnum_09_09_in	6E1A14672B8	0.92733	0.00110
esrandnum_09_10_in	77A0308C0E4	0.92757	0.00114	mdrandnum_09_10_in	77A0308C0E4	0.92886	0.00132

6.9.3.5 WATER

Water is used in various regions of the models to simulate HAC as an interstitial moderator and as a reflector. When used at full density, the density of water is 0.9982 g/cm^3. (SCALE, Vol. 3, Sect. M8)

6.9.3.6 CALCULATION OF EQUIVALENT WATER MASS FOR POLYETHYLENE

In the calculation models for evaluation of NCT, water may be substituted for the polyethylene composition of bags present in the package. Based on hydrogen density, 1285.14 g of water are equivalent to 1000 g of polyethylene for nuclear criticality safety calculations. The equivalent water mass is calculated as follows:

Hydrogen in 1 kg of polyethylene [$(CH_2)_2$, molecular weight = 28.0312; density = 0.92]:

$$\text{1 kg polyethylene} = \frac{1000\ \text{g}}{0.92\ \text{g/cm}^3} = 1087.0197\ \text{cm}^3$$

$$\text{H number density} = \frac{(0.92)(4)(6.02252\times10^{23})}{(28.0312)(10^{24})} = 7.906502\times10^{-2}\ \text{at/bn-cm}$$

$$\text{H in 1 kg} = (1087.0197\text{cm}^3)(7.906502\times10^{-2}) = 85.945234\ \text{at-cm}^2\text{/bn}$$

Grams of water [H_2O, molecular weight = 18.0110; density = 0.9982] with hydrogen content equivalent to 1 kg of polyethylene:

$$\text{equivalent g of } H_2O = \frac{(85.945234)(18.0110)(10^{24})}{(2)(6.02252\times10^{23})} = 1285.1427\ \text{g}$$

APPENDIX 6.9.4

QUALIFICATION OF A NEUTRON ABSORBER MATERIAL FOR THE ES-3100

APPENDIX 6.9.4

QUALIFICATION OF A NEUTRON ABSORBER MATERIAL FOR THE ES-3100

6.9.4.1 INTRODUCTION

277-4 is a formulation of Thermo Electron Corporation's Cat. 277-0, a boron carbide additive and water. 277-4 is a neutron radiation shielding product and is one of several materials in its class that have been evaluated as a candidate neutron absorber system for a variety of nuclear criticality safety applications by the Y-12 National Security Complex (Y-12). This class of materials is characterized as a dispersion of $^{nat}B_4C$ particulate* throughout a hardened hydraulic cement or binder, resulting in a high-hydrogen, borated material system. It offers many advantages for typical Y-12 applications over other classes of materials such as borated aluminum because a neutron moderator and neutron absorber are both integral to the solid material system itself. The separate addition of another neutron moderating material such as water or polyethylene is not required in order for it to function effectively.

Computational methods of analysis in simple geometry permit direct comparison of neutron absorber system performance for nuclear criticality safety applications. The measure of comparison is the neutron interaction potential between two parallel 0.745-cm-thick slabs of infinite extent of ^{235}U metal at a density of 18.81 g/cm^3. The slabs are separated by a variable thickness of material and reflected by a 60-cm thickness of the same material (Fig. 6.9.4.1-1). Each material is modeled as an idealized homogenous mixture of elements based on nominal density and constituent proportions (Table 6.9.4.1-1). The result is expressed in terms of calculated k_{eff} † as influenced by the thickness of the candidate material between the two parallel slabs (see Fig. 6.9.4.1-2).

The least effective neutron absorber material systems are those with low hydrogen content and low neutron absorption cross section (e.g., ordinary concrete). The performance of concrete that contains $^{nat}B_4C$ particulate (e.g., borated concrete) is improved, but it is still hindered by its low hydrogen content. This is a function of the proportion and type of cement in the typical concrete mixture (i.e., a low proportion of lime- and silica-based Portland cement). Ordinary water is also included for comparison because of its high hydrogen content, but its performance is also limited by a low total mass density and low neutron absorption cross section.

As expected, materials with high hydrogen content and high boron content (e.g., 277-4, borated ceramics, and borated polymers) are predicted to be the most effective neutron absorber systems. Although the mechanical and thermal properties of such systems can vary significantly, their nuclear properties are dictated almost exclusively by the relative proportion and content of ^{10}B and H and the total mass density of the material system. These things being equal, the nuclear performance of any material in this class (i.e., 277-4, borated ceramics, and borated polymers) is representative of the others.

*277-4 is an improved variant of the Cat 277 product ca. 2000 which was originally formulated as a dispersion of ^{nat}Borosilicate glass granules rather than the current practice of using $^{nat}B_4C$ particulate.

†SCALE 4.4a, CSAS25 code sequence for KENO V.a with the 238-group ENDF B-IV neutron cross-section library on the Y-12 SAE Hewlett-Packard J5600 workstation (CMODB).

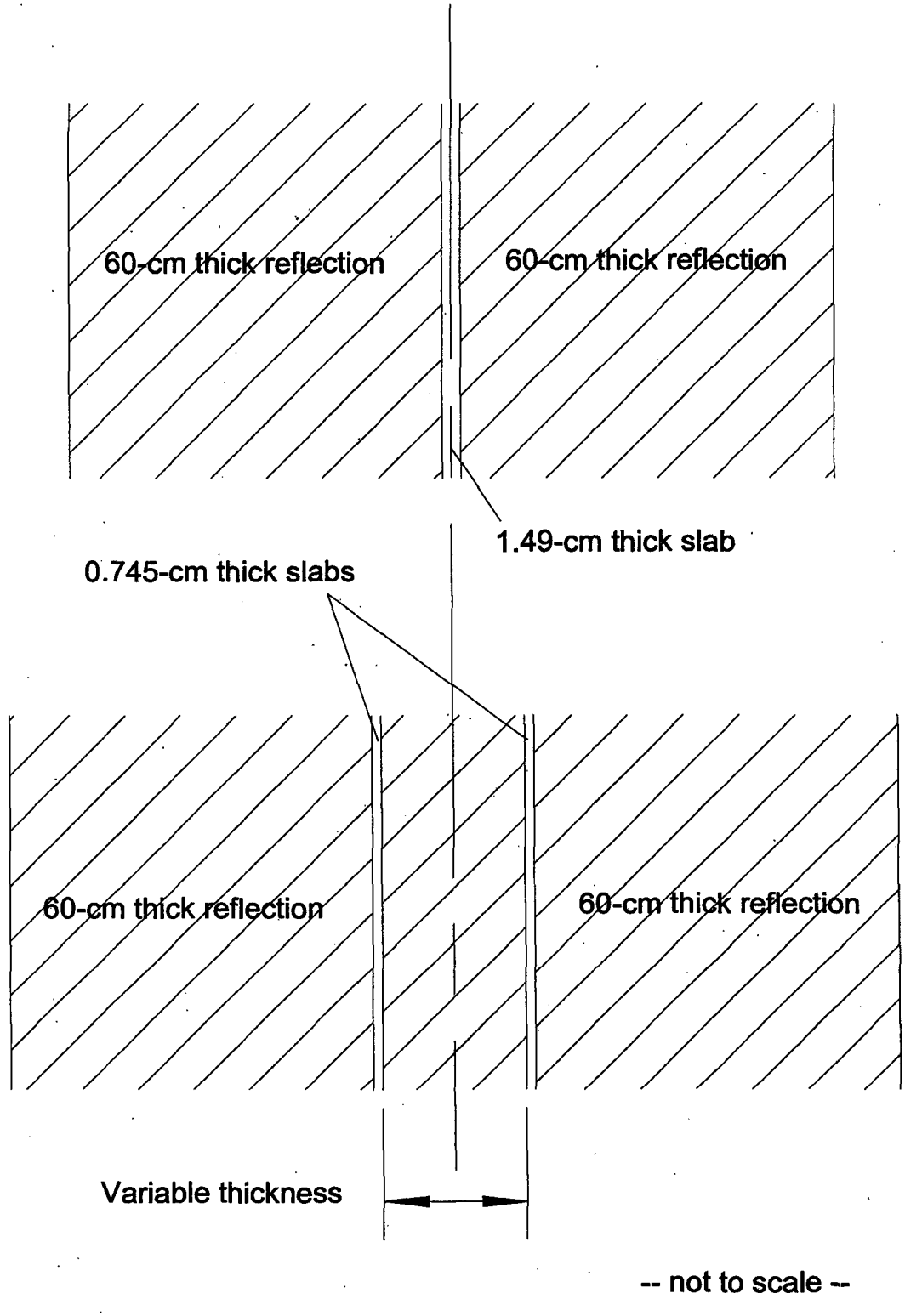

Fig. 6.9.4.1-1. Physical model of parallel ^{235}U metal slabs of infinite extent reflected and separated by various candidate neutron absorber materials.

Table 6.9.4.1-1. Nominal elemental and isotopic compositions of idealized material models for comparison of various neutron absorbers (atoms/barn·cm)

	Ordinary Concrete A 2.147 g/cm³	Ordinary Concrete B 2.299 g/cm³	Water 0.9982 g/cm³	Borated Concrete 2.563 g/cm³	Cat 277[a] 1.68 g/cm³	Borated Ceramic 1.91 g/cm³	Borated Polymer 1.717 g/cm³	^{235}U Metal 18.81 g/cm³
H	4.2581e-03	8.5010e-03	6.6751e-02	4.2900e-03	3.3800e-02	2.7200e-02	5.7600e-02	
B-10				1.7600e-04	2.8400e-04	2.6500e-03	9.4600e-04	
B-11				6.8100e-04	1.1800e-03	1.1000e-02	3.9200e-03	
C	1.1348e-02	2.0217e-02		9.0000e-04		4.2600e-03	2.3500e-02	
N							1.3800e-03	
O	4.0370e-02	3.5511e-02	3.3376e-02	4.2400e-02	3.7100e-02	3.2900e-02	2.5900e-02	
Na	7.9356e-05	1.6299e-05		6.7100e-05	2.6000e-04	7.9200e-05		
Mg	5.0111e-03	1.8602e-03		2.3000e-04	2.0800e-04	2.3300e-03		
Al	3.7660e-04	5.5580e-04		2.2900e-03	8.9700e-03	1.7400e-03	7.7000e-03	
Si	1.9382e-03	1.7000e-03		1.1800e-02	7.6700e-04	3.2300e-03		
P						2.1200e-03		
S	1.0013e-04			9.6300e-05	6.0000e-05	7.7800e-05		
Cl	1.9074e-05							
K	3.1231e-04	4.0300e-05		3.1600e-04		2.3100e-03		
Ca	7.3008e-03	1.1101e-02		3.1200e-03	2.2300e-03	2.4600e-04		
Ti	4.0183e-05					7.0800e-05		
Mn	1.2050e-05			1.4000e-04				
Fe	1.2954e-04	1.9301e-04		4.6200e-03	4.8900e-05	5.2000e-04		
U-235								4.8200e-02

[a] The ^{10}B content of this material model for Cat 277 is based on its ca. 2000 formulation using crushed borosilicate glass rather than the current practice of using $^{nat}B_4C$ particulate. This particular formulation is roughly equivalent to ~2% $^{nat}B_4C$ particulate (i.e., equivalent ^{10}B content, by weight). For otherwise identical H and B-10 content, this difference is unimportant relative to its nuclear performance as an idealized homogeneous mixture of elements. However, the current use of more than 5% $^{nat}B_4C$ particulate (by weight) is preferred due to reasons relating to the method of preparation, chemical reaction, and placement of 277-4 and uniformity of ^{10}B distribution in the cured product. As with all the materials in this class, the amount of H and ^{10}B in the finished product is determined by the relative proportions of its major constituents, which are tailored to the requirements of the specific application.

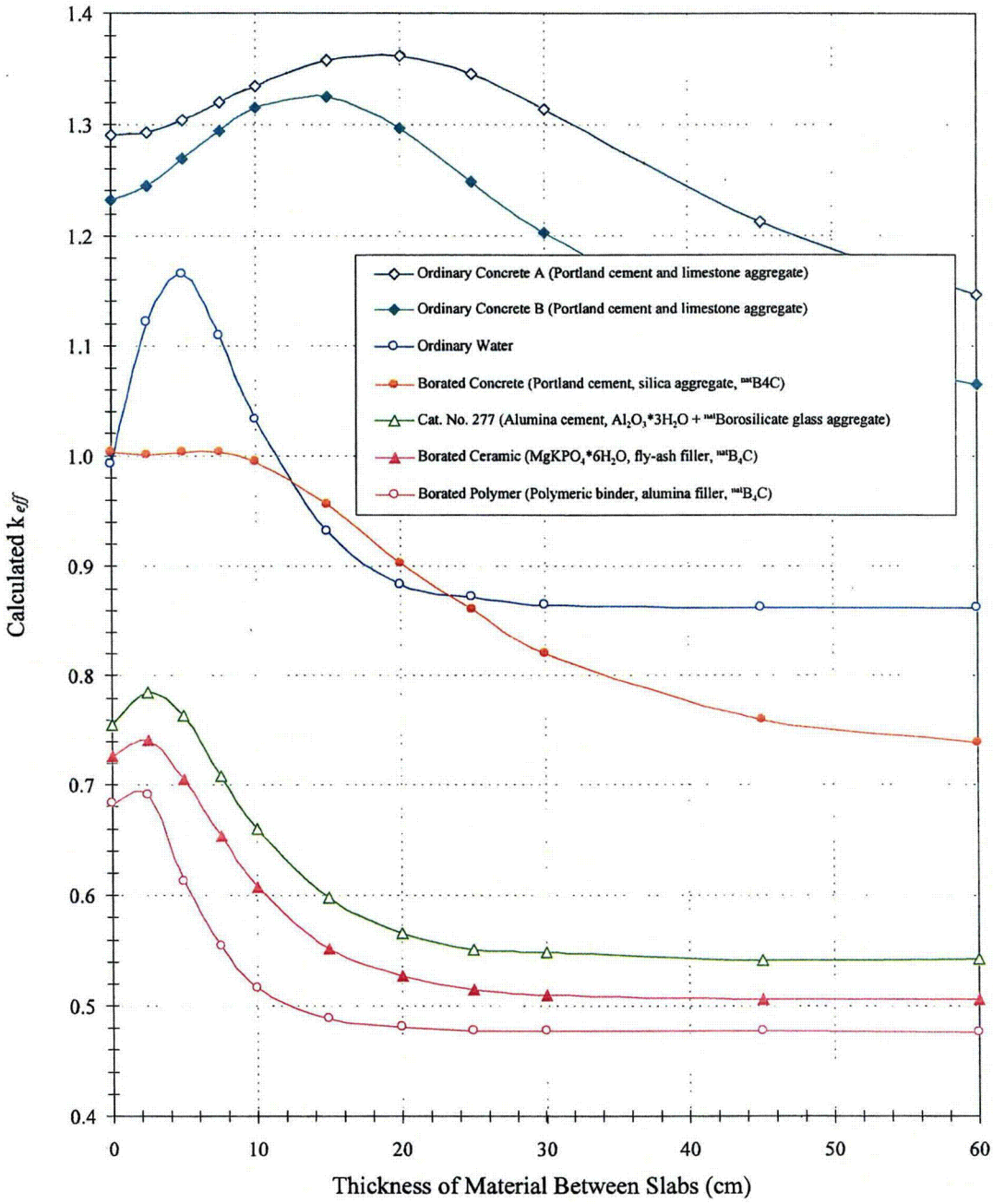

Fig. 6.9.4.1-2. The effect of various materials on neutron interaction between parallel slabs of ^{235}U metal of infinite extent.

6.9.4.2 PERFORMANCE TESTING

To investigate the performance of this class of neutron absorbing materials further, Y-12 has studied neutron radiography and neutron transmission measurements on several samples of a borated ceramic. Like 277-4, the borated ceramic is also a dispersion of $^{nat}B_4C$ particulate throughout a hardened hydraulic crystalline solid material matrix for which the binder phase is $MgKPO_4 \cdot 6H_2O$ rather than the hydrates of CaO and Al_2O_3. In fact, the more finely divided $^{nat}B_4C$ particulate specified for 277-4 is a slight advantage over the modestly coarser particulate in the borated ceramic. As shown below in Table 6.9.4.2-1, the relative proportion and content of H and ^{10}B and their total mass density are very similar. The small differences between the nuclear properties of their associated low- and intermediate-Z elements (i.e., oxides of Mg, Al, P, K, and Ca) are negligible. Thus, performance and the most significant factors affecting performance are nearly identical for both materials, so the results of neutron radiography and neutron transmission for the borated ceramic samples are judged applicable to 277-4 specimens of similar dimension.

Table 6.9.4.2-1. Comparison of nominal values for 277-4 and borated ceramic samples subjected to neutron radiography and neutron transmission testing.

Attribute	Cat 277 Original Formulation ca. 2000	277-4 ES-3100 Formulation as Cured	Borated Ceramic Samples for Testing
Principal Binder Phase(s)	Hydrates of CaO and Al_2O_3	Hydrates of CaO and Al_2O_3	$MgKPO_4 \cdot 6H_2O$
Neutron Absorber Particle Size	^{nat}Borosilicate glass granules 90 wt % <2360 μm 65 wt % <1180 μm 40 wt % <600 μm 15 wt % <102 μm 0 wt % <150 μm	$^{nat}B_4C$ particulate 100 wt % <102 μm	$^{nat}B_4C$ particulate 100 wt % <559 μm 90 wt % <356 μm 40 wt % <254 μm 3 wt % <122 μm 0 wt % <63 μm
Filler Material(s)	$Al_2O_3 \cdot 3H_2O$	$Al_2O_3 \cdot 3H_2O$	Class F Coal Fly-ash
Total Mass Density	1.68 g/cm^3	1.60 g/cm^3	1.91 g/cm^3
Total H_2O content	0.51 g/cm^3	0.51 g/cm^3	0.49 g/cm^3
Total ^{10}B content	0.005 g/cm^3	0.013 g/cm^3	0.012 g/cm^3

Samples were prepared from sectioned pieces of a single specimen from a vertically oriented mold measuring 10 × 10 × ~30 cm tall, as illustrated in Fig. 6.9.4.2-1 (nominally 4 × 4 × 12 in. tall). One specimen was prepared by the normal method of mixing and preparation for the borated ceramic material. Sectioning the first specimen resulted in two thick samples designated "1 of 2" and "2 of 2" which each measured 10-cm wide by ~30-cm long by ~2.4-cm thick (nominally 1-in. thick). A second specimen was prepared by abnormal methods intended to produce non-homogeneity (i.e., poorly mixed using retardants followed by excessive and extended vibration of the mold after installation). Sectioning this specimen resulted in two thin samples designated "062d1bc" and "062d1bd" which each measured 10-cm wide by ~30-cm long by ~1.2-cm thick (nominally 0.5-in. thick). The samples were delivered to the Breazeale Nuclear Reactor Building at Pennsylvania State University for inspection. Upon completion of inspection for all four samples as received, a thick sample "1 of 2" and a thin sample "062d1bc" were dehydrated by heating to 140°C to eliminate interference by hydrogen, and all four samples were tested again.

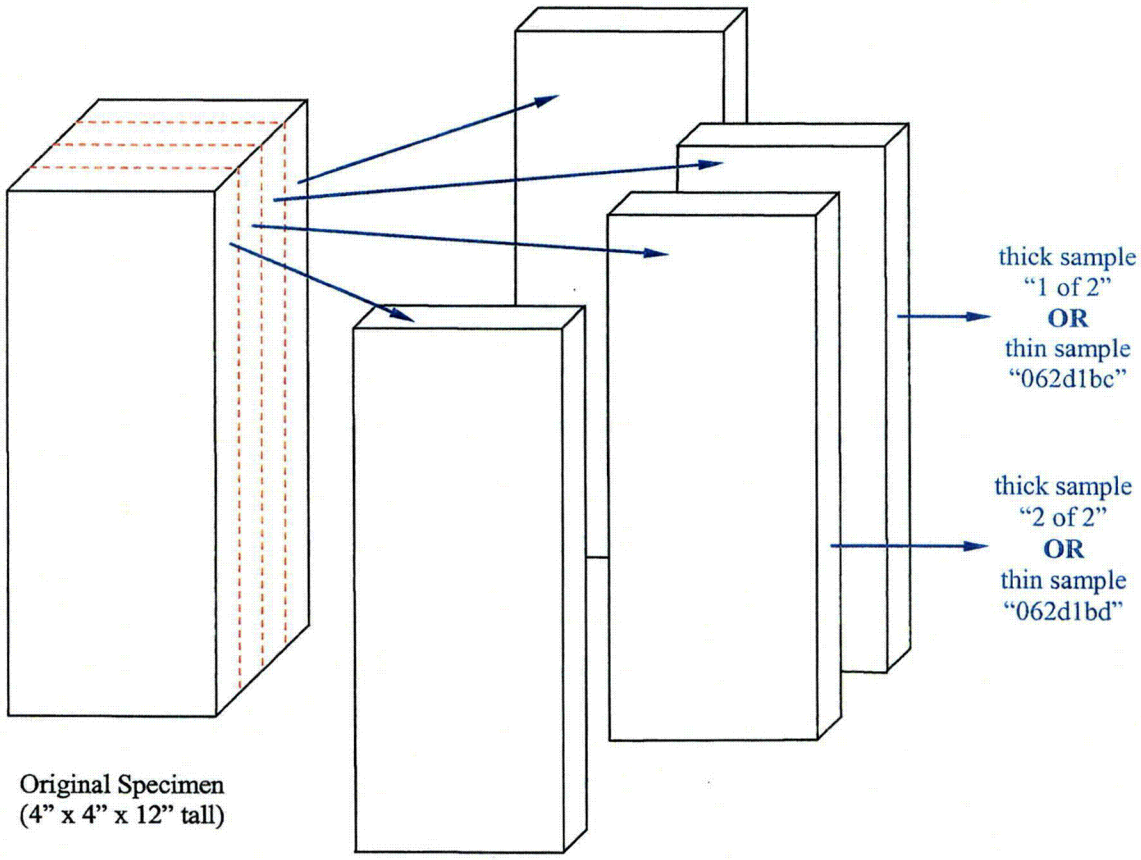

Fig. 6.9.4.2-1. Illustration of sectioning plan for borated ceramic samples for neutron radiography and neutron transmission measurements.

All four samples were qualitatively inspected for visual defects and subjected to neutron radiographic inspection. The inspections were intended to identify any variations in image luminance, which would indicate a variation in homogeneity and density. Neutron transmission measurements were calibrated to results for thin ZrB_2 reference coupons sandwiched with thick aluminum metal. The ^{10}B areal densities of the thin reference coupons ranged from 5.32 mg/cm^2 to 57.04 mg/cm^2 over a total ZrB_2 + Al reference thickness of 24.21–24.98 mm. By comparison, the thick samples contain an idealized ^{10}B areal density of 28.8 mg/cm^2 (i.e., 0.012 g/cm^3 over a 2.4-cm thickness), and the thin samples contain an idealized ^{10}B areal density of 14.4 mg/cm^2 (i.e., 0.012 g/cm^3 over a 1.2-cm thickness).

Radiographic examination of both thick samples "1 of 2" and "2 of 2" indicated uniformity of composition and density (see Fig. 6.9.4.2-2). Even after dehydration of thick sample "1 of 2," radioscopic examination indicated uniformity of composition and density. Initial neutron transmission results for both thick samples "1 of 2" and "2 of 2" indicated that neutron transmission was very low. In fact, the interference due to the hydrogen content implies an equivalent ^{10}B areal density measurement of ~67 ± 4 mg/cm^2. This is more than twice the actual physical value of 28.8 mg/cm^2. Only after thick sample of "1 of 2" is dehydrated and tested again do the results of neutron transmission measurements more accurately reflect the actual physical ^{10}B content. In fact, the average measured value of 27.419 mg/cm^2 at eleven points along the long axis of the dehydrated sample "1 of 2" is more than 95% of the actual physical value of 28.8 mg/cm^2 and varies no more than a few percent from one end to the other (see Tables 6.9.4.2-2 and 6.9.4.2-3).

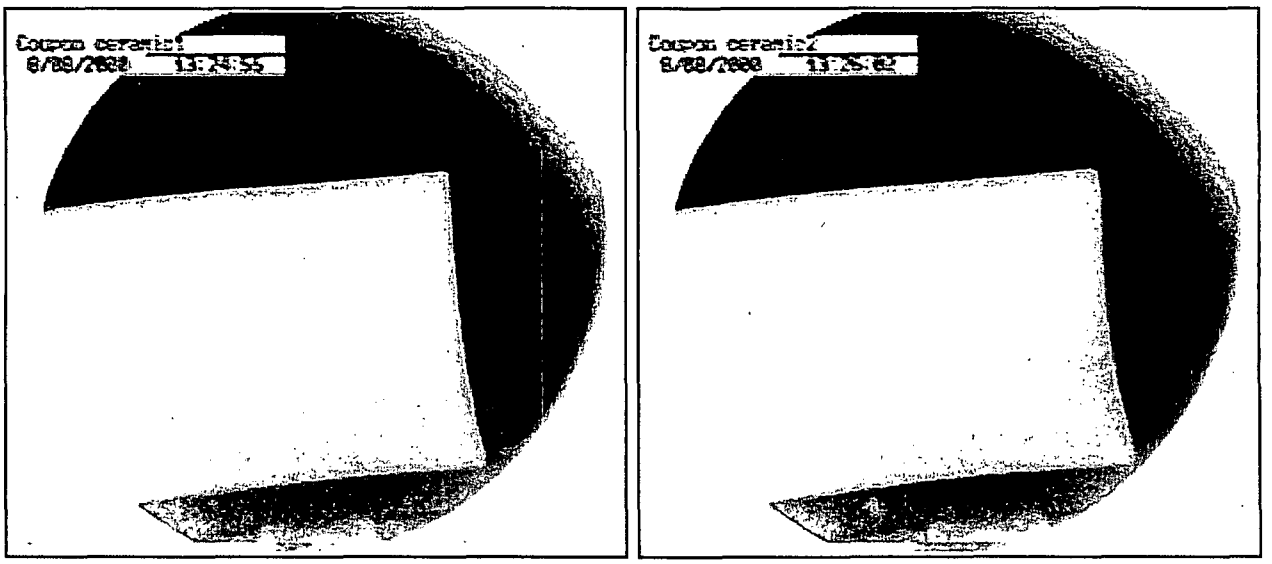

Fig. 6.9.4.2-2. Radiographic images of thick samples "1 of 2" (left) and "2 of 2" (right) indicating uniformity of composition and density.

Table 6.9.4.2-2. Results of neutron transmission measurements of thick samples

	Equivalent ^{10}B Areal Density (mg/cm^2)		
	End	**Center**	**End**
sample "1 of 2"	66.419	68.673	71.003
sample "2 of 2"	65.0	68.25	69.708
sample "1 of 2" (dehydrated)	27.586	27.191	28.555
sample "2 of 2" (re-test)	63.687	65.966	65.572

Table 6.9.4.2-3. Neutron transmission measurements of thick sample "1 of 2" after dehydration

Point of Measurement (uniform intervals from one end to the other)	Equivalent ^{10}B Areal Density (mg/cm^2)	Deviation from Average (%)
1	27.586	+0.6 %
2	26.909	-1.9 %
3	27.039	-1.4 %
4	27.358	-0.2 %
5	27.286	-0.5 %
6	27.191	-0.8 %
7	27.375	-0.2 %
8	27.179	-0.8 %
9	27.236	-0.7 %
10	27.897	-0.9 %
11	28.555	+4.1 %
Average	**27.419**	

Radiographic examination of both thin samples "062d1bc" and "062d1bd" indicates areas of nonuniformity and spots of lower neutron attenuation, along with greater dissimilarity between the samples themselves (see Fig. 6.9.4.2-3). Many of these areas and spots remained evident by radiographic examination even after dehydration of thin sample "062d1bc" and are attributed to physical voids revealed during visual inspection. Again, initial neutron transmission measurements implied a greater-than-actual equivalent ^{10}B areal density due to the interference of hydrogen (i.e., measured values averaged ~23.3 mg $^{10}B/cm^2$ rather than the actual value of 14.4 mg $^{10}B/cm^2$).

Measurements repeated after dehydration of sample "062d1bc" more correctly estimate the equivalent ^{10}B areal density to be ~11.1 mg/cm^2, which is ~77% of the actual physical ^{10}B content. Again, the relative values vary only a few percent from one end of the sample to the other (see Table 6.9.4.2-4). However, the measured values of a dehydrated sample in this case are known to be biased low. First, the total thicknesses of the ZrB_2 + Al reference coupons for calibration were ~24.21 to 24.98-mm compared to the 1.2-cm thickness of "062d1bc." Second, the total mass density of the sample is ~1.4 to 1.5 g/cm^3 after dehydration compared to an Al mass density of ~2.7 g/cm^3 for the ZrB_2 + Al reference coupons. This indicates that even the performance of the thin samples (i.e., 1.2-cm thickness) exhibiting non-uniformity of composition and density is only marginally reduced from that of the idealized, homogenous material model with respect to neutron absorber efficiency.

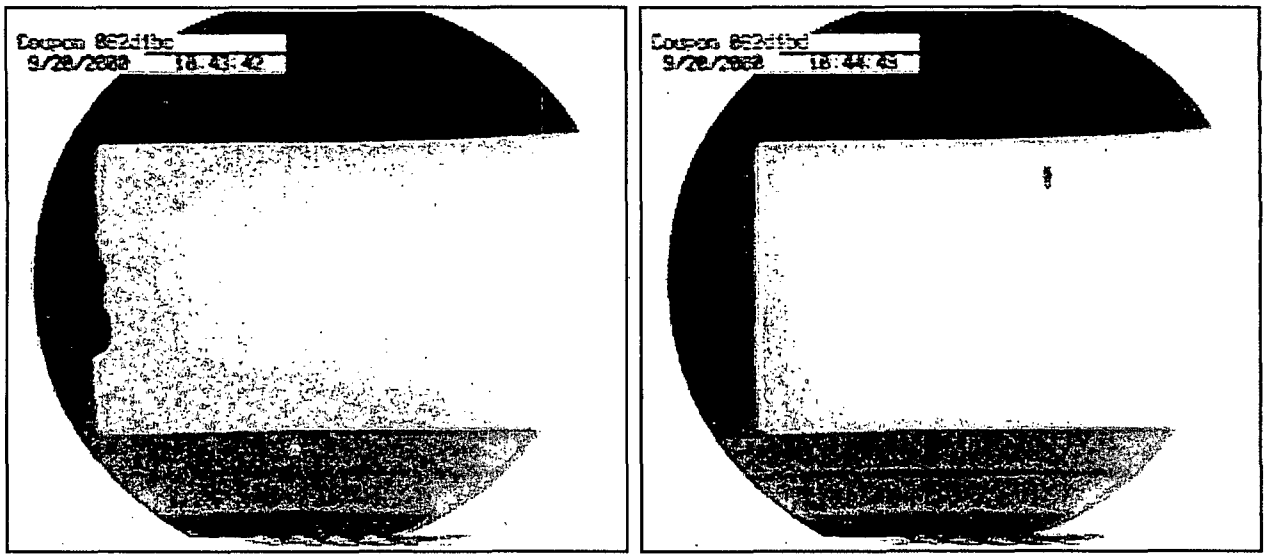

Fig. 6.9.4.2-3. Radiographic images of thin samples "062d1bc" (left) and "062d1bd" (right) indicating non-uniformity of composition and density and dissimilarity of samples.

Table 6.9.4.2-4. Neutron transmission results for dehydrated thin sample "062d1bc" and re-test of thin sample "062d1bd"

Position of Measurement (see Fig. 6.9.4.2-4)	Minimum Equivalent ^{10}B Areal Density (mg/cm^2)			
	Dehydrated Thin Sample "062d1bc"		Re-Test of Thin Sample "062d1bd"	
	Line A	Line B	Line A	Line B
1	12.227	11.781	25.909	25.154
2	11.776	11.462	24.390	25.344
3	11.388	11.252	24.257	24.645
4	10.554	10.462	25.341	24.885
5	10.432	10.528	24.646	25.483
6	10.754	11.728	25.450	25.712
7	10.396	11.534	25.761	23.063
8	11.166	10.221	24.522	25.257
9	10.875	10.459	23.113	23.882
10	11.051	10.676	25.270	23.724
11	11.258	11.214	24.922	25.355
Combined Average	11.1		24.8	

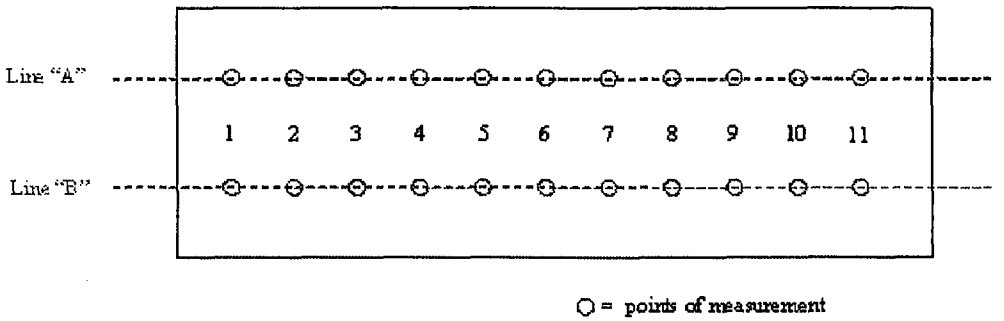

Fig. 6.9.4-6. Illustration of measurement plan for neutron transmission measurements of thin samples "062d1bc" and "062d1bd."

6.9.4.2.3 CONCLUSIONS

Provided that 277-4 is prepared in a controlled manner to ensure the proper specification and proportioning of batch constituents, thorough mixing of the wet slurry, and correct placement and installation to prevent large physical voids, a credible technical justification exists to credit no less than 75% f the $^{nat}B_4C$ particulate and its other constituents, by weight, as an idealized homogenous mixture for nuclear criticality safety analysis of the ES-3100. There is no evidence of non-homogeneity, neutron self-shielding effects, or neutron streaming effects in borated hydraulic cement or ceramic material systems for thicknesses of 2.4-cm or more. The qualification of 277-4 for use in the design and construction of the ES-3100 described herein is based on sound nuclear engineering principles and direct application of performance test results for such material systems.

APPENDIX 6.9.5

MISCELLANEOUS INFORMATION AND DATA

APPENDIX 6.9.5

MISCELLANEOUS INFORMATION AND DATA

Table 6.9.5.1 provides the atomic weights of the elements and isotopes of the materials used in this criticality safety evaluation. Atomic weights and isotopic weight percents of the naturally occurring materials are those taken from the Materials Information Processor in the SCALE Standard Composition Library.

Table 6.9.5.2 provides the molecular weights and weight percents of the corresponding elements and isotopes of the various compounds. The weight percents shown in this table are the input to KENO V.a. (SCALE, Vol. 2, Sect. F11)

Table 6.9.5.3 provides equations for determining atomic densities. These equations were derived based on the assumption that all constituents in the mixture are volume additive. Although these equations with their corresponding subscripts are for mixtures of elements, isotopes, or both, all except Equation (2) can be applied to compounds if the user substitutes certain subscript notations and meaning changes. For example, in Equations (1a) and (1b), the atomic weight becomes the molecular weight and the subscript for mixture (m) changes to the subscript for compound ©. Likewise, in Equations (3a) and (3b), the atomic weight becomes the molecular weight, and the atom fraction (n_i) becomes the stoichiometric proportion of the elements making up the molecule. In Equations (3)–(5), the atom fraction (n_i) becomes the stoichiometric proportion (the element number subscript in the molecular formula), whose sum does not equal unity. Equation (2) is applicable only to the theoretical density of mixtures; it does not apply to the density of compounds.

Table 6.9.5.1. Atomic weights

Element or isotope	Atomic weight
H	1.0078
C	12.0000
O	15.9954
N	14.0033
Na	22.9895
Mg	24.3051
Al	26.9818
Si	28.0853
Ca	40.0803
Ti	47.8789
Cr	51.9957
Mn	54.9380
Fe	55.8447
Ni	58.6868
Zr	91.2196
^{235}U	235.0442
^{238}U	238.0510

Table 6.9.5.2. Molecular weights

Compound	Molecular or atomic weight	Weight percent in compound	Stoichiometric composition
Kaolite 1600™			
Alumina	-	9.6	Al_2O_3
Al	26.9818	52.92507	
O	15.9954	47.07493	
Silica	-	36.7	SiO_2
Si	28.0853	46.74349	
O	15.9954	53.25651	
Ferric Oxide	-	6.7	Fe_2O_3
Fe	55.8447	69.94330	
O	15.9954	30.05670	
Titanium Oxide	-	1.2	TiO_2
Ti	47.8789	59.95084	
O	15.9954	40.04916	
Calcium Oxide	-	30.7	CaO
Ca	40.0803	71.47009	
O	15.9954	28.52991	
Magnesium Oxide	-	13.1	MgO
Mg	24.3051	60.30359	
O	15.9954	39.69641	
Alkalies	-	2.0	Na_2O
Na	22.9895	74.18575	
O	15.9954	25.81425	

Table 6.9.5.3. Useful equations

N_m	=	$\rho_m N_o / A_m$.	(1a)
N_i	=	$w_i \rho_m N_o / A_i$.	(1b)
ρ_m	=	$1/\Sigma w_i/\rho_i$.	(2)
A_m	=	$1/\Sigma w_i/A_i$.	(3a)
	=	$\Sigma n_i A_i$	(3b)
w_i	=	m_i/m_m .	(4a)
	=	$n_i A_i / \Sigma n_i A_i$.	(4b)
n_i	=	N_i/N_m .	(5a)
	=	$(w_i/A_i)/\Sigma(w_i/A_i)$.	(5b)

where

N_o	=	0.602252×10^{24} (atoms/mole) Avogadro's number,
N	=	atom density (atoms/cm^3), $N_m = \Sigma N_i$,
ρ	=	density (g/cm^3) ,
A	=	atomic mass (g-mole) ,
w	=	weight fraction, $\Sigma w_i = 1$,
n	=	atom fraction, $\Sigma n_i = 1$,
subscript "m"	=	of the mixture ,
subscript "i"	=	i^{th} component of the mixture ,
(atoms/cm^3)(1/10^{24})	=	atoms/barn-cm.